Chemotherapy induced intestinal mucositis: from bench to bed

Schade aan de darm door chemotherapie: van lab tot bed

ISBN: 978-90-8559-339-5

Cover design: Wim de Boer, Barendrecht
Lay-out: Margo Terlouw-Willebrand, Nieuwerkerk aan den IJssel
Printed by: Optima Grafische Communicatie, Rotterdam

This research was financially supported by Numico Research BV, Wageningen, the Sophia Foundation for Medical Research (SSWO), and the Sophia Foundation of Scientific Research (Kröger Foundation).

The printing of this thesis was financially supported by Stichting Kinderoncologisch Centrum Rotterdam, Numico Research, and Sanofi Aventis.

Chemotherapy induced intestinal mucositis: from bench to bed

Schade aan de darm door chemotherapie: van lab tot bed

Proefschrift

ter verkrijging van de graad van doctor
aan de Erasmus Universiteit Rotterdam
op gezag van rector magnificus
Prof.dr. S.W.J. Lamberts
en volgens besluit van het College voor Promoties

De openbare verdediging zal plaatsvinden op 9 januari 2008 om 09.45 uur

door

Barbara Anna Eleonora de Koning

geboren te Delft

Promotiecommissie

Promotoren:	Prof.dr. R. Pieters
	Prof.dr. H.A. Büller
Kleine commissie :	Prof.dr. J.B. van Goudoever
	Prof.dr. E.J. Kuipers
	Prof.dr. P. Sonneveld
Copromotor	Dr. A.W.C. Einerhand

CONTENTS

1

INTRODUCTION

Mucositis is one of the most severe and frequent side effects of chemotherapy. Mucositis refers to damage to the mucous membranes throughout the entire alimentary tract caused by anti-cancer treatment.[1] To date, despite an increasing amount of research there is no adequate prophylaxis. Research conducted on mucositis mainly focuses on oral mucositis in adult patients. Less attention however, is paid to mucositis located in the gastro-intestinal tract (GI-mucositis), especially in childhood cancer patients, whereas this forms a major complication in current anti-cancer therapies.[2] Therefore, the focus of this thesis is GI-mucositis in childhood cancer.

The main function of the intestine is digestion and absorption of harmless food and defense against various luminal noxious agents. To perform these two paradoxical tasks it is of utmost importance to maintain intestinal homeostasis. The maintenance of intestinal homeostasis during mucositis results from a dynamic process that includes damage induction, damage control and intestinal repair.

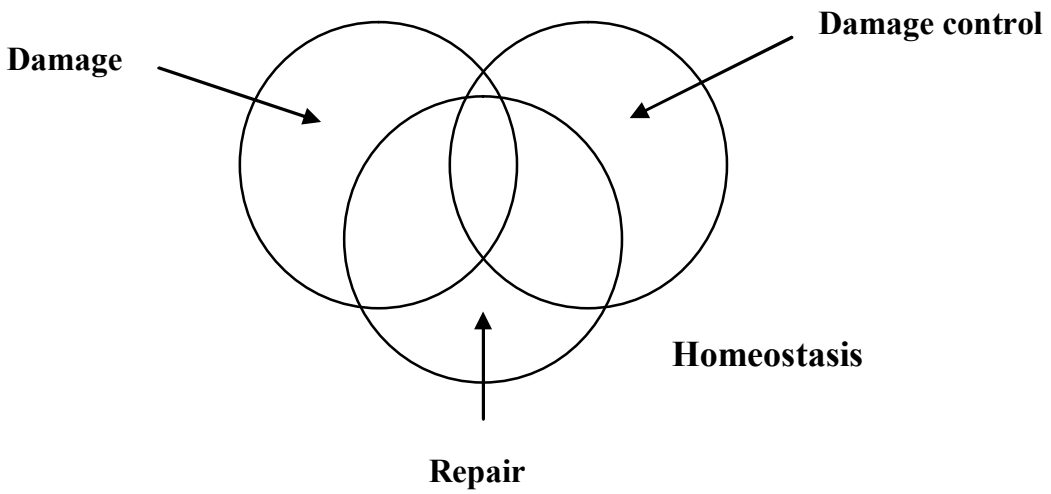

MUCOSITIS

Mucositis is characterized by edema, erythema and ulcerative lesions of the mucosa in the mouth, (small) intestine and anus. This causes severe pain, nausea, infections, bloating and diarrhea, which consequently leads to weight loss. Clinical symptoms of mucositis may present as early as day 3 - 5 after start of chemotherapy and peaks around day 7 - 14, followed by a phase of resolution.[3-8]

Incidence

Due to the introduction of hematopoietic growth factors and (peripheral) stem cell transplantation, high dose cytotoxic treatment is no longer limited by myelosuppressive toxicity.[9,10] Accordingly, mucositis has become the main primary dose limiting toxicity.[11] Moreover, the incidence of mucositis has increased due to the availability of increasingly aggressive single agent or multi-drug therapies and new radiation regimens.[12,13]

Oral mucositis develops in two thirds of all childhood cancer patients treated with chemotherapy.[14-17] Severe oral mucositis (grade 3-4) in children receiving mono- or combination chemotherapy ranges from 0 - 20%. Gastro-intestinal mucositis is scarcely reported in children but seems to range from 0 - 50%, depending on drug and dose.[18]

Myeloablative therapy, before stem cell transplantation, induces oral mucositis in 80% of childhood patients[19] while severe oral and gastro-intestinal mucositis develops in 30% and 10% of these patients, respectively.[18] These percentages increase to more than 40% and 30%, respectively, when total body irradiation is given in combination with chemotherapy.[18]

Clinical and economical burden

Patients report oral mucositis as the most severe side effect of anti-cancer treatment, significantly reducing their quality of life.[20-22] The most serious complications of mucositis are localized or disseminated infections resulting from opportunistic infections of oral and/or gastro-intestinal origin.[23,24] Patients suffering from severe mucositis[25] or myelosuppression[26] are more vulnerable to infection. As such, cancer patients with oral mucositis and neutropenia have a four times higher risk of septicemia than individuals without oral mucositis.[24,27] Consequently, cancer patients suffering from oral and gastro-intestinal mucositis display an enhanced probability to die from infectious complications.[25]

In addition to infections, oral and gastro-intestinal-mucositis predispose for impaired enteral intake and subsequent weight loss caused by physical pain, nausea and discomfort.[25] The total costs spend on extended hospitalization and intensified resource utilization are higher for patients suffering from mucositis and can be correlated with the increased degree of toxicity.[25,28] For example, oral ulceration increases utilization of narcotics, tube feeding, total parental nutrition and intravenous antibiotic treatment, in comparison to non ulceration.[25,28] Patients with severe oral and gastro-intestinal mucositis are hospitalized 4.3 and 8.2 days longer, respectively compared to patients not encountering mucositis[28] with consequent extra costs ranging from $ 3,000 - $ 43,000 per patient.[29] Finally, as mentioned earlier, mucositis is often dose limiting for current treatments.[11] More specifically, mucositis can seriously increase the risk on dose reduction or delay of the next chemotherapy cycle,[25,30,31] thereby reducing the probability of survival.[32,33]

CYTOSTATIC DRUGS

In experimental studies, the cytostatic drugs methotrexate (MTX) and doxorubicin (DOX) are used to induce mucositis because these drugs are known for this side effect in childhood cancer patients.[34-36] More than 20% of the children treated with MTX monotherapy or DOX combination therapy, suffer from severe oral mucositis (grade 3-4

on a 0-4 point scale formulated by the WHO).[18] The characteristics of MTX induced mucositis have been studied extensively.[37-39] Until recently, DOX-induced mucositis had not been thoroughly characterized. **Therefore, DOX induced mucositis was characterized as presented in chapter 2 of this thesis**.

Methotrexate[40]

The folate antagonist MTX is frequently used in treatment of childhood leukemia and osteosarcoma. MTX binds to dihydrofolate reductase (DHFR), which is responsible for the reduction of dihydrofolates to tetrahydrofolates. Tetrahydrofolates are involved in de novo synthesis of purines in reactions mediated by transformylases and in the thymidylate cycle. By binding of MTX to DHFR, a shortage of tetrahydrofolate is induced causing an inhibition of thymidylate biosynthesis, which in turn leads to a decreased synthesis of DNA. In addition, MTX, its metabolites and folate byproducts that are formed during the binding of MTX to DHFR can also directly inhibit the folate–dependent enzymes of thymidilate and purine biosynthesis. Therefore, MTX initially leads to the inhibition of DNA synthesis, and subsequently to inhibition of RNA and protein synthesis in all cells.

Doxorubicin[41]

DOX belongs to the anthracyclines class of chemotherapeutic agents and is the most widely used cytostatic drug in adult and childhood cancer. However, the mechanism of action has not been fully elucidated, but intercalation of DOX into the DNA double helix, and thereby reducing DNA elongation is important for its effect. Inhibition of DNA replication results in reduced RNA synthesis. Furthermore, DOX therapy induces formation of free radicals that lead to membrane- and DNA damage, thereby inducing damage to the cell surface and cell apoptosis.

Target cells

Research into drug-induced damage to the highly proliferating stem cells region and progenitor cells, located in the intestinal crypts of the intestine, revealed that different classes of cytostatic drugs affect specific epithelial crypt cells at different topographical (and hierarchical) locations.[42-44] MTX, 5-fluorouracil and vincristine, for example, induce damage high in the proliferative compartment, at crypt cell position 9-11. In contrast, DOX preferentially attacks cells at crypt cell position 4-6, which is just above, or at the same level as the intestinal stem cells.[43,45] DOX is therefore thought to induce more severe damage, especially to the proliferating compartment at the bottom of the crypts, as MTX. **This was the focus of our study described in chapter 2.**

PROLIFERATION AND DIFFERENTIATION

Our initial studies were based on the presumption that mucositis is solely caused by a strong inhibition of proliferation of the quickly dividing epithelial stem cells and an

increased apoptosis. This would result in a decreased epithelial replication followed by diminished cell migration and renewal leading to villus atrophy, breaching of the epithelial barrier and consequently ulceration.[7,46-48] Research in the past years revealed that mucositis may result from a more complex and dynamic cascade of events than initially proposed, involving DNA damage restricted to the rapidly dividing stem- and progenitor cells in the crypts, as well as DNA and non-DNA damage to other cell types of the gut mucosa.[49,50]

Signaling pathways

The balanced process of proliferation and differentiation is preserved by epithelial-mesenchymal interactions, which are critical for normal morphogenesis and maintenance of the crypt-villus axis.[51,52] Bone morphogenic protein (BMP)- and Wnt-signaling pathways are two of the main pathways involved in embryonic and adult intestinal development.[53] BMPs are morphogenes that constitute a large group of structurally and functionally related proteins to the TGF-β super family. BMP signaling pathways play a key role in organogenesis,[54,55] gastrointestinal development and intestinal homeostasis.[56-61] BMPs are intestinal 'landscapers', which are involved in crypt formation by mesenchymal-epithelial signaling. Disruption of these molecules may therefore lead to the formation of ectopic crypt-villus units, often perpendicular to the normal axis, resulting in a complex structure of branching villi and crypts.[59]

The absence of BMP4 in mice is associated with embryonic lethality.[62,63] In the developing intestine, BMP4 is expressed in the intravillus and intercrypt mesenchym, including the mesenchym adjacent to the intestinal stem cells.[57,59] The Wnt-signalling is also involved in the regulation and maintenance of the epithelial proliferation/differentiation balance.[64] TCF4 is one of the main Wnt pathway transcription factors in the intestinal epithelium.[65] In the intestine of mice lacking TCF-4, the proliferative compartments are lost and only differentiated epithelial cells are found,[65] suggesting that TCF4 is crucial in intestinal epithelial stem cell maintenance. In conclusion, both BMP and Wnt signaling pathways have been implicated in preserving a balanced control of intestinal stem cell self-renewal.[57] **In chapter 2 the role of epithelial-mesenchymal signaling in mucositis induction and epithelial regeneration was studied.**

Differentiation

Stem cells can differentiate into enterocytes that are specialized in nutrient degradation, absorption and transportation. The brush border is the highly folded apical membrane of these enterocytes, increasing their active surface area. Additionally, the brush border expresses a wide range of enzymes and proteins specific for nutrient degradation and subsequent transport across the apical membrane.

During MTX-induced mucositis carbohydrate digestion and absorption is severely deteriorated, characterized by down-regulation of enterocyte-specific gene expression, crucial for degradation and absorption of nutrients.[38,48,66-68] Degradation of complex

carbohydrates is primarily regulated by the brush border enzyme sucrase isomaltase (SI).[69] SI has shown to be expressed by enterocytes in a differentiation specific pattern.[70]

Transcription factors[71,72]

The expression pattern of intestinal genes is regulated by the combined effect of positive and negative regulatory elements. Although DNA regulatory elements, required to repeat the pattern of endogenous gene expression, are spread over relatively large genomic distances, promoters of several intestinal genes are sufficient to direct intestine-specific transcription. The promoter of the SI gene contains binding sides for the transcription factors GATA-4, Cdx2 and HNF-1α, which are also involved in intestinal development. These transcription factors are crucial for the expression of the SI gene[73] in addition to several other enterocyte-specific markers.[73-76] The transcriptional process is a rate-limiting step that regulates the abundance of proteins in the cell. The role of these transcription factors in the prevention of epithelial damage or promotion of intestinal repair is still unknown. **In chapter 3 it was hypothesized that the transcription factors involved in SI expression, are specifically down regulated during MTX-induced mucositis.**

Intestinal metabolism

The influence of chemotherapy on protein digestion and amino acid absorption is less addressed compared to the effects on carbohydrate digestion. The expression of peptide transporter 1 (PepT1), involved in absorption of dipeptides and tripeptides formed after digestion of dietary proteins,[77] appeared to be unaffected by 5'-flourouracil induced intestinal mucositis,[78] while the expression of several amino acid transporters (neutral basic transporter and high-affinity glutamate transporter) were decreased.[78] Enteral nutrients are of great importance for whole body metabolism as well as for intestinal homeostasis.[79,80] The small intestine controls the degradation and absorption of nutrients and consequently influences the systemic availability of these molecules for other organs.[79,81,82] In line with this, severe intestinal damage is believed to result in an increased energy demand by the intestine for epithelial regeneration. **The intestinal absorption of leucine during mucositis was studies in the clinical trial presented in chapter 7.**

INTESTINAL BARRIER

Mucus layer

The first line of defense in the intestine is the physical barrier. This barrier is formed by tightly bound epithelial cells regulating intestinal permeability that is reinforced with a thick gel-layer of mucus covering the epithelium. The major structural component of intestinal mucus is mucin. Mucus forms a barrier protecting against mechanical stress, noxious substances and microorganisms. On the other hand mucus is essential in colonization of bacteria by influencing their binding capacity.[83,84] Mucin 2 (Muc2), a

heavily glycosylated molecule stored in the apical granules of goblet cells,[85] is the most predominant secretory mucine in the small intestine.[86] Muc2 can be released rapidly when the epithelium needs to be protected.[87]

During mucositis the epithelium is severely damaged resulting in increased intestinal permeability[88,89] and eventually ulceration. In contrast to the enterocytes involved in nutrient digestion, goblet cell function appears to be preserved during MTX induced mucositis.[38] Although the total number of goblet cells decreases, goblet cells at the top of the villus seem selectively spared from extrusion from the tip of the villus.[38] In addition, Muc2 protein expression increases significantly during all phases of MTX induced mucositis, suggesting improved epithelial defense.[38,67] **The role of Muc2 during mucositis development was studied in chapter 4 of this thesis.**

Mucosal immune system[90,91]

The intestinal immune cells form a complex network that aims at eradication of pathogenic bacteria while maintaining mucosal homeostasis. The mucosal immune system comprises innate- and adaptive immune cells. Innate cells, such as neutrophils and macrophages are implicated in the first line of defense against invading microorganisms. At a later stage, cells of the adaptive immune system (B and T lymphocytes) proliferate and differentiate into specific effector cells with immunological memory for (microbial) antigens.[92] Subsets of T-lymphocytes producing specific sets of cytokines are produced upon antigen encounter.[93,94] During mucositis the epithelial barrier is disrupted and as a consequence the mucosal immune system encounters an increased amount of antigens. This increased exposure to microbial antigens could well lead to the activation of innate as well as adaptive immune cells. Indeed, mucositis is associated with an increased expression of pro-inflammatory cytokines,[49] of which tumor necrosis factor-α (TNF-α) is one of the most important cytokine. TNF-α is able to induce epithelial damage both in vitro and in vivo.[95, 96] In patients, increased local levels of TNF-α show high association with intestinal inflammation. The source for this pro-inflammatory cytokine during mucositis could be either intestinal innate cells (macrophages) and/or adaptive cells (T cells). Interestingly, inhibition of TNF-α was shown to diminish mucositis, and treatment of mucositis patients with anti-TNF-α antibodies resulted in a dramatic decrease of intestinal inflammation.[49,97,98] **The study described in chapter 5 analyzed the role of the immune system in mucositis pathogenesis.**

PROPHYLAXIS

Transforming growth factor-β

Different growth factors and cytokines have been proven to modify the vulnerability of the stem cells and progenitor cells in the small intestine.[99] One of these promising factors is transforming growth factor-β (TGF-β).

TGF-β is a member of the Transforming growth factor-β family of polypeptides, which consists of three isoforms, TGF-β1, 2, 3.[100] This paracrine growth factor plays a key role in cell proliferation and differentiation.[101] TGF-β is a negative growth factor for intestinal epithelial cells and protects clonogenic stem cells from the damaging effects of radiation and chemotherapy by inducing a cell cycle arrest in the G1 phase in cell-line and rodent models.[101,102] Reduction of the number of proliferating cells causes the cells to be less vulnerable to anti-cancer treatment. This effect is reversible once TGF-β is removed.[103] Consequently, it is hypothesized that prophylactic treatment with TGF-β, facilitates regeneration of crypts, thereby minimizing damage to the mucosal tissues and increasing intestinal repair.

In vitro TGF-β_3 protects epithelial cells against chemotherapy, specifically against cell-cycle specific chemotherapy.[104] In animal models, TGF-β_3 showed to be effective in protecting the oral epithelium against 5-Fluorouracil induced mucositis[47] and the intestinal epithelium against mucositis induced by radiotherapy.[99,105] In these rodent models, a decrease in mucositis was accompanied by decreased epithelial cell-proliferation, reduced weight loss and increased survival. In humans, TGF-β_3 enriched mouthwash was well tolerated and safe when administered to a small group of adult breast cancer patients.[106]

Recombinant TGF-β_2 showed the same promising results on ameliorating radiotherapy induced mucositis in a rodent model.[107] *In vitro* TGF-β_2 exhibited the same inhibitory effect on epithelial cell proliferation and protection against chemotherapy, as the recombinant TGF-β_3.[110] TGF-β_2, in a rodent model, was protective against methotrexate (MTX) induced mucositis. Rodents treated with a TGF-β_2 enriched feeding encountered less weight loss and significantly reduced villus atrophy in comparison to control rodents treated with MTX but not treated with TGF-β_2.[110] No studies however, have been performed on the prophylactic effect of TGF-β_2 on oral or gastro-intestinal-mucositis in humans. **In chapter 8 a clinical study is presented of the prophylactic value of TGF-β_2 in oral and gastro-intestinal-mucositis in childhood cancer patients.**

Interleukin-10

As mentioned above pro-inflammatory cytokines are involved in chemotherapy induced damage[49] of which the most prominent one is TNF-α.[95,96] Studies aiming for mucositis prophylaxis showed that down-regulation of pro-inflammatory cytokines ameliorates mucositis severity. IL-11 down-regulates the pro-inflammatory cytokines TNF-α and interleukine-1b (IL1b), thereby attenuating radiotherapy induced mucositis in hamsters.[111] Recombinant-IL11 also reduces gastrointestinal originated bacteraemia in patients receiving chemotherapy.[112] Recently, is was shown that keratinocyte growth factor (KGF) has great prophylactic potential in hematologic cancer patients.[113] One of the effects of KGF is up-regulation of IL-13, an anti-inflammatory cytokine that has the ability to down-regulate TNF-α.[114]

Both the innate and adaptive immune system produce anti-inflammatory cytokines upon stimulation.[92] IL-10 is one of the most important immunosuppressive and anti-inflammatory cytokine which plays a key role in intestinal homeostasis.[115] IL-10 is strongly implicated in protection against intestinal inflammatory processes such as inflammatory bowel disease.[116] Moreover, absence of IL-10 leads to spontaneous intestinal colitis in IL-10 deficient mice.[117] **In chapter 5 we describe the role of IL-10 in mucositis development.**

OUTLINE OF THE THESIS

Part 1 of this thesis focuses on gaining more insight into the pathophysiology of chemotherapy-induced mucositis in mouse models. In **chapter 2** the question is addressed whether doxorubicin induces mucositis in mice with the same characteristics as MTX induced mucositis. Secondly, we aim to gain insight in epithelial-mesenchymal crosstalk and progenitor compartment modulation during DOX-induced mucositis.

Previous studies showed that MTX-induced mucositis is characterized by a decreased expression of enterocyte-specific SI, crucial for degradation and absorption of nutrients. **Chapter 3** studies the relationship between the expression of SI and the specific transcription factors, GATA-4, Cdx2 and HNF-1α.

The next two chapters focus on the role of the intestinal barrier in mucositis development. The intestinal barrier is effective on different levels of defense. **Chapter 4** aims to gain insight into the mucositis protective role of the mucus layer covering the intestinal epithelium. During mucositis the epithelial barrier is severely deteriorated, thereby causing increased exposure of the mucosal immune-system to luminal antigens. The aim of **chapter 5** is to define the role of the innate and adaptive mucosal immune system in MTX-induced mucositis.

Part 2 of this thesis focuses on the intestinal metabolism during mucositis and clinical studies on mucositis prophylaxis. The aim of the study as described in **chapter 6** was to validate a more simple method for measuring CO_2 rate production, required to calculate whole body oxidation, in small children. Additionally, **chapter 7** describes a clinical study in childhood cancer patients aiming to determine whether splanchnic amino acid uptake is affected by mucositis. In **chapter 8** a clinical trial is presented, evaluating the efficacy and safety of a TGF-β_2-enriched feeding in reducing oral and gastro-intestinal mucositis in childhood cancer patients.

Finally, in **chapter 9 and 10** all studies presented in this thesis are summarized, and new insights for future studies are discussed.

REFERENCES

1. Sonis ST. Complications of cancer and their treatment: oral complications. In: Holland JF, Frei E, Bast RC, eds. Cancer Medicine, ed. 3 Philadelphia: Lea and Febiger, 1993:2381-2388.
2. Hockenberry M. Symptom management research in children with cancer. J Pediatr Oncol Nurs 2004;21:132-136.
3. Dreizen S. Description and incidence of oral complications. NCI Monographs 1991;9:11-15.
4. Loprinzi CL, Gastineau DA, Foote RL. Oral complications. In: M.D. A, Armitage JO, Lichter AS, Niederhuber JE, eds. Clinical Oncology New York: Churchill Livingstone, 1995:741-754.
5. Cheng KK, Molassiotis A, Chang AM, Wai WC, Cheung SS. Evaluation of an oral care protocol intervention in the prevention of chemotherapy-induced oral mucositis in paediatric cancer patients. Eur J Cancer 2001;37:2056-2063.
6. Keefe DM, Cummins AG, Dale BM, Kotasek D, Robb TA, Sage RE. Effect of high-dose chemotherapy on intestinal permeability in humans. Clin Sci (Lond) 1997;92:385-389.
7. Keefe DM, Brealey J, Goland GJ, Cummins AG. Chemotherapy for cancer causes apoptosis that precedes hypoplasia in crypts of the small intestine in humans. Gut 2000;47:632-637.
8. Blijlevens NM, Donnelly JP, de Pauw BE. Mucosal barrier injury: biology, pathology, clinical counterparts and consequences of intensive treatment for haematological malignancy: an overview. Bone Marrow Transplant 2000;25:1269-1278.
9. Dunn CJ, Goa KL. Lenograstim: an update of its pharmacological properties and use in chemotherapy-induced neutropenia and related clinical settings. Drugs 2000;59:681-717.
10. Hoekman K, Vermorken JB. Incidence and prevention of nonhaematological toxicity of high-dose chemotherapy. Ann Med 1996;28:175-182.
11. Sonis S, Clark J. Prevention and management of oral mucositis induced by antineoplastic therapy. Oncology (Huntingt) 1991;5:11-8; discussion 18-22.
12. Young A, Topham C, Moore J, Turner J, Wardle J, Downes M, Evans V, Kay S. A patient preference study comparing raltitrexed ('Tomudex') and bolus or infusional 5-fluorouracil regimens in advanced colorectal cancer: influence of side-effects and administration attributes. Eur J Cancer Care (Engl) 1999;8:154-161.
13. Trotti A, Bellm LA, Epstein JB, Frame D, Fuchs HJ, Gwede CK, Komaroff E, Nalysnyk L, Zilberberg MD. Mucositis incidence, severity and associated outcomes in patients with head and neck cancer receiving radiotherapy with or without chemotherapy: a systematic literature review. Radiother Oncol 2003;66:253-262.
14. Fayle SA, Curzon ME. Oral complications in pediatric oncology patients. Pediatr Dent 1991;13:289-295.
15. Childers NK, Stinnett EA, Wheeler P, Wright JT, Castleberry RP, Dasanayake AP. Oral complications in children with cancer. Oral Surg Oral Med Oral Pathol 1993;75:41-47.
16. Bonnaure-Mallet M, Bunetel L, Tricot-Doleux S, Guerin J, Bergeron C, LeGall E. Oral complications during treatment of malignant diseases in childhood: effects of tooth brushing. Eur J Cancer 1998;34:1588-1591.
17. Sonis ST, Sonis AL, Lieberman A. Oral complications in patients receiving treatment for malignancies other than of the head and neck. J Am Dent Assoc 1978;97:468-472.
18. Sonis ST, Elting LS, Keefe D, Peterson DE, Schubert M, Hauer-Jensen M, Bekele BN, Raber-Durlacher J, Donnelly JP, Rubenstein EB. Perspectives on cancer therapy-induced mucosal injury: pathogenesis, measurement, epidemiology, and consequences for patients. Cancer 2004;100:1995-2025.
19. Woo SB, Sonis ST, Monopoli MM, Sonis AL. A longitudinal study of oral ulcerative mucositis in bone marrow transplant recipients. Cancer 1993;72:1612-1617.

20. Bellm LA, Epstein JB, Rose-Ped A, Martin P, Fuchs HJ. Patient reports of complications of bone marrow transplantation. Support Care Cancer 2000;8:33-39.

21. Bellm LA, Cunningham G, Durnell L, Eilers J, Epstein JB, Fleming T, Fuchs HJ, Haskins MN, Horowitz MM, Martin PJ, McGuire DB, Mullane K, et al. Defining clinically meaningful outcomes in the evaluation of new treatments for oral mucositis: oral mucositis patient provider advisory board. Cancer Invest 2002;20:793-800.

22. Stiff P. Mucositis associated with stem cell transplantation: current status and innovative approaches to management. Bone Marrow Transplant 2001;27 Suppl 2:S3-S11.

23. Ruescher TJ, Sodeifi A, Scrivani SJ, Kaban LB, Sonis ST. The impact of mucositis on alpha-hemolytic streptococcal infection in patients undergoing autologous bone marrow transplantation for hematologic malignancies. Cancer 1998;82:2275-2281.

24. Elting LS, Bodey GP, Keefe BH. Septicemia and shock syndrome due to viridans streptococci: a case-control study of predisposing factors. Clin Infect Dis 1992;14:1201-1207.

25. Elting LS, Cooksley C, Chambers M, Cantor SB, Manzullo E, Rubenstein EB. The burdens of cancer therapy. Clinical and economic outcomes of chemotherapy-induced mucositis. Cancer 2003;98:1531-1539.

26. Rapoport AP, Miller Watelet LF, Linder T, Eberly S, Raubertas RF, Lipp J, Duerst R, Abboud CN, Constine L, Andrews J, Etter MA, Spear L, et al. Analysis of factors that correlate with mucositis in recipients of autologous and allogeneic stem-cell transplants. J Clin Oncol 1999;17:2446-2453.

27. Gonzalez-Barca E, Fernandez-Sevilla A, Carratala J, Granena A, Gudiol F. Prospective study of 288 episodes of bacteremia in neutropenic cancer patients in a single institution. Eur J Clin Microbiol Infect Dis 1996;15:291-296.

28. Sonis ST, Oster G, Fuchs H, Bellm L, Bradford WZ, Edelsberg J, Hayden V, Eilers J, Epstein JB, LeVeque FG, Miller C, Peterson DE, et al. Oral mucositis and the clinical and economic outcomes of hematopoietic stem-cell transplantation. J Clin Oncol 2001;19:2201-2205.

29. Avritscher EB, Cooksley CD, Elting LS. Scope and epidemiology of cancer therapy-induced oral and gastrointestinal mucositis. Semin Oncol Nurs 2004;20:3-10.

30. Vaughan WP, Kris E, Vose J, Bierman PJ, Gwilt P, Armitage JO. Phase I/II study incorporating intravenous hydroxyurea into high-dose chemotherapy for patients with primary refractory or relapsed and refractory intermediate-grade and high-grade malignant lymphoma. J Clin Oncol 1995;13:1089-1095.

31. Uziely B, Jeffers S, Isacson R, Kutsch K, Wei-Tsao D, Yehoshua Z, Libson E, Muggia FM, Gabizon A. Liposomal doxorubicin: antitumor activity and unique toxicities during two complementary phase I studies. J Clin Oncol 1995;13:1777-1785.

32. Fyles A, Keane TJ, Barton M, Simm J. The effect of treatment duration in the local control of cervix cancer. Radiother Oncol 1992;25:273-279.

33. Savarese DM, Hsieh C, Stewart FM. Clinical impact of chemotherapy dose escalation in patients with hematologic malignancies and solid tumors. J Clin Oncol 1997;15:2981-2995.

34. Kamps WA, Tamminga RYJ, Kimpen JLL. ondersteunenede behandeling, ed. 1. Houten/Diegem: Bohn Stafleu Van Loghum, 1997.

35. Pinkerton CR, Cameron CH, Sloan JM, Glasgow JF, Gwevava NJ. Jejunal crypt cell abnormalities associated with methotrexate treatment in children with acute lymphoblastic leukaemia. J Clin Pathol 1982;35:1272-1277.

36. Patte C, Laplanche A, Bertozzi AI, Baruchel A, Frappaz D, Schmitt C, Mechinaud F, Nelken B, Boutard P, Michon J. Granulocyte colony-stimulating factor in induction treatment of children with non-Hodgkin's lymphoma: a randomized study of the French Society of Pediatric Oncology. J Clin Oncol 2002;20:441-448.

37. Taminiau JA, Gall DG, Hamilton JR. Response of the rat small-intestine epithelium to methotrexate. Gut 1980;21:486-492.

38. Verburg M, Renes IB, Meijer HP, Taminiau JA, Buller HA, Einerhand AW, Dekker J. Selective sparing of goblet cells and paneth cells in the intestine of methotrexate-treated rats. Am J Physiol Gastrointest Liver Physiol 2000;279:G1037-1047.

39. Renes IB, Verburg M, Bulsing NP, Ferdinandusse S, Buller HA, Dekker J, Einerhand AW. Protection of the Peyer's patch-associated crypt and villus epithelium against methotrexate-induced damage is based on its distinct regulation of proliferation. J Pathol 2002;198:60-68.

40. Chu E, Allegra CJ. Antifolates. In: Chabner BA, Longo DL, eds. Cancer Chemotherapy and Biotherapy, ed. 2nd Philadelphia: Lippincott-Raven, 1996:109-148.

41. Doroshow JH. Anthracyclines and Anthracenediones. In: Chabner BA, Longo DL, eds. Cancer Chemotherapy and Biotherapy Philadelphia: Lippincott-Raven, 1996:409-434.

42. Ijiri K, Potten CS. Response of intestinal cells of differing topographical and hierarchical status to ten cytotoxic drugs and five sources of radiation. Br J Cancer 1983;47:175-185.

43. Ijiri K, Potten CS. Further studies on the response of intestinal crypt cells of different hierarchical status to eighteen different cytotoxic agents. Br J Cancer 1987;55:113-123.

44. Moore JV. Clonogenic response of cells of murine intestinal crypts to 12 cytotoxic drugs. Cancer Chemother Pharmacol 1985;15:11-15.

45. Potten CS, Owen G, Booth D. Intestinal stem cells protect their genome by selective segregation of template DNA strands. J Cell Sci 2002;115:2381-2388.

46. Lockhart PB, Sonis ST. Alterations in the oral mucosa caused by chemotherapeutic agents. A histologic study. J Dermatol Surg Oncol 1981;7:1019-1025.

47. Sonis ST, van Vugt AG, Brien JP, Muska AD, Bruskin AM, Rose A, Haley JD. Transforming growth factor-beta 3 mediated modulation of cell cycling and attenuation of 5-fluorouracil induced oral mucositis. Oral Oncol 1997;33:47-54.

48. Taminiau JA, Gall DG, Hamilton JR. Response of the rat small-intestine epithelium to methotrexate. Gut 1980;21:486-492.

49. Sonis ST. The pathobiology of mucositis. Nat Rev Cancer 2004;4:277-284.

50. Sonis ST. Mucositis as a biological process: a new hypothesis for the development of chemotherapy-induced stomatotoxicity. Oral Oncol 1998;34:39-43.

51. Montgomery RK, Mulberg AE, Grand RJ. Development of the human gastrointestinal tract: twenty years of progress. Gastroenterology 1999;116:702-731.

52. Kedinger M, Duluc I, Fritsch C, Lorentz O, Plateroti M, Freund JN. Intestinal epithelial-mesenchymal cell interactions. Ann N Y Acad Sci 1998;859:1-17.

53. de Santa Barbara P, van den Brink GR, Roberts DJ. Development and differentiation of the intestinal epithelium. Cell Mol Life Sci 2003;60:1322-1332.

54. Sukegawa A, Narita T, Kameda T, Saitoh K, Nohno T, Iba H, Yasugi S, Fukuda K. The concentric structure of the developing gut is regulated by Sonic hedgehog derived from endodermal epithelium. Development 2000;127:1971-1980.

55. Bitgood MJ, McMahon AP. Hedgehog and Bmp genes are coexpressed at many diverse sites of cell-cell interaction in the mouse embryo. Dev Biol 1995;172:126-138.

56. Itoh S, Itoh F, Goumans MJ, Ten Dijke P. Signaling of transforming growth factor-beta family members through Smad proteins. Eur J Biochem 2000;267:6954-6967.

57. He XC, Zhang J, Tong WG, Tawfik O, Ross J, Scoville DH, Tian Q, Zeng X, He X, Wiedemann LM, Mishina Y, Li L. BMP signaling inhibits intestinal stem cell self-renewal through suppression of Wnt-beta-catenin signaling. Nat Genet 2004;36:1117-1121.

58. Hardwick JC, van den Brink GR, Bleuming SA, Ballester I, van den Brande JM, Keller JJ, Offerhaus GJ, van Deventer SJ, Peppelenbosch MP. Bone morphogenetic protein 2 is expressed by, and acts upon, mature epithelial cells in the colon. Gastroenterology 2004;126:111-21.

59. Haramis AP, Begthel H, van den Born M, van Es J, Jonkheer S, Offerhaus GJ, Clevers H. De novo crypt formation and juvenile polyposis on BMP inhibition in mouse intestine. Science 2004;303:1684-1686.

60. Nishanian TG, Kim JS, Foxworth A, Waldman T. Suppression of Tumorigenesis and Activation of Wnt Signaling by Bone Morphogenetic Protein 4 in Human Cancer Cells. Cancer Biol Ther 2004;3.

61. Hogan BL. Bone morphogenetic proteins in development. Curr Opin Genet Dev 1996;6:432-438.

62. Lawson KA, Dunn NR, Roelen BA, Zeinstra LM, Davis AM, Wright CV, Korving JP, Hogan BL. Bmp4 is required for the generation of primordial germ cells in the mouse embryo. Genes Dev 1999;13:424-436.

63. Mishina Y, Suzuki A, Ueno N, Behringer RR. Bmpr encodes a type I bone morphogenetic protein receptor that is essential for gastrulation during mouse embryogenesis. Genes Dev 1995;9:3027-3037.

64. van de Wetering M, Sancho E, Verweij C, de Lau W, Oving I, Hurlstone A, van der Horn K, Batlle E, Coudreuse D, Haramis AP, Tjon-Pon-Fong M, Moerer P, et al. The beta-catenin/TCF-4 complex imposes a crypt progenitor phenotype on colorectal cancer cells. Cell 2002;111:241-250.

65. Korinek V, Barker N, Moerer P, van Donselaar E, Huls G, Peters PJ, Clevers H. Depletion of epithelial stem-cell compartments in the small intestine of mice lacking Tcf-4. Nat Genet 1998;19:379-383.

66. Naruhashi K, Nadai M, Nakao M, Suzuki N, Nabeshima T, Hasegawa T. Changes in absorptive function of rat intestine injured by methotrexate. Clin Exp Pharmacol Physiol 2000;27:980-986.

67. Verburg M, Renes IB, van Nispen DJ, Ferdinandusse S, Jorritsma M, Buller HA, Einerhand AW, Dekker J. Specific responses in rat small intestinal epithelial mRNA expression and protein levels during chemotherapeutic damage and regeneration. J Histochem Cytochem 2002;50:1525-1536.

68. Kralovanszky J, Prajda N. Biochemical changes of intestinal epithelial cells induced by cytostatic agents in rats. Arch Toxicol Suppl 1985;8:94-103.

69. van Beers EH, Buller HA, Grand RJ, Einerhand AW, Dekker J. Intestinal brush border glycohydrolases: structure, function, and development. Crit Rev Biochem Mol Biol 1995;30:197-262.

70. Rings EH, Krasinski SD, van Beers EH, Moorman AF, Dekker J, Montgomery RK, Grand RJ, Buller HA. Restriction of lactase gene expression along the proximal-to-distal axis of rat small intestine occurs during postnatal development. Gastroenterology 1994;106:1223-1232.

71. Hampsey M. Molecular genetics of the RNA polymerase II general transcriptional machinery. Microbiol Mol Biol Rev 1998;62:465-503.

72. van Wering HM. Complex interactions among tissue restricted transcription factors and cofactors are critical for intestine specific gene expression Rotterdam: ErasmusMC, 2002:11-37.

73. Boudreau F, Rings EH, van Wering HM, Kim RK, Swain GP, Krasinski SD, Moffett J, Grand RJ, Suh ER, Traber PG. Hepatocyte nuclear factor-1 alpha, GATA-4, and caudal related homeodomain protein Cdx2 interact functionally to modulate intestinal gene transcription. Implication for the developmental regulation of the sucrase-isomaltase gene. J Biol Chem 2002;277:31909-31917.

74. Clatworthy JP, Subramanian V. Stem cells and the regulation of proliferation, differentiation and patterning in the intestinal epithelium: emerging insights from gene expression patterns, transgenic and gene ablation studies. Mech Dev 2001;101:3-9.

75. Fang R, Olds LC, Santiago NA, Sibley E. GATA family transcription factors activate lactase gene promoter in intestinal Caco-2 cells. Am J Physiol Gastrointest Liver Physiol 2001;280:G58-67.

76. Fitzgerald K, Bazar L, Avigan MI. GATA-6 stimulates a cell line-specific activation element in the human lactase promoter. Am J Physiol 1998;274:G314-324.

77. Ganapathy V, Brandsch M, Leibach F. Intestinal transport of amino acids and peptides, ed. 3rd, vol. 2. New York: Raven, 1994.

78. Tanaka H, Miyamoto KI, Morita K, Haga H, Segawa H, Shiraga T, Fujioka A, Kouda T, Taketani Y, Hisano S, Fukui Y, Kitagawa K, et al. Regulation of the PepT1 peptide transporter in the rat small intestine in response to 5-fluorouracil-induced injury. Gastroenterology 1998;114:714-723.

79. Stoll B, Henry J, Reeds PJ, Yu H, Jahoor F, Burrin DG. Catabolism dominates the first-pass intestinal metabolism of dietary essential amino acids in milk protein-fed piglets. J Nutr 1998;128:606-614.

80. Deitch EA. Bacterial translocation: the influence of dietary variables. Gut 1994;35:S23-27.

81. Biolo G, Tessari P, Inchiostro S, Bruttomesso D, Fongher C, Sabadin L, Fratton MG, Valerio A, Tiengo A. Leucine and phenylalanine kinetics during mixed meal ingestion: a multiple tracer approach. Am J Physiol 1992;262:E455-463.

82. van Goudoever JB, Stoll B, Henry JF, Burrin DG, Reeds PJ. Adaptive regulation of intestinal lysine metabolism. Proc Natl Acad Sci U S A 2000;97:11620-11625.

83. Hecht G. Innate mechanisms of epithelial host defense: spotlight on intestine. Am J Physiol 1999;277:C351-358.

84. Strous GJ, Dekker J. Mucin-type glycoproteins. Crit Rev Biochem Mol Biol 1992;27:57-92.

85. Chang SK, Dohrman AF, Basbaum CB, Ho SB, Tsuda T, Toribara NW, Gum JR, Kim YS. Localization of mucin (MUC2 and MUC3) messenger RNA and peptide expression in human normal intestine and colon cancer. Gastroenterology 1994;107:28-36.

86. van Klinken BJ, Dekker J, Buller HA, de Bolos C, Einerhand AW. Biosynthesis of mucins (MUC2-6) along the longitudinal axis of the human gastrointestinal tract. Am J Physiol 1997;273:G296-302.

87. Tytgat KM, Buller HA, Opdam FJ, Kim YS, Einerhand AW, Dekker J. Biosynthesis of human colonic mucin: Muc2 is the prominent secretory mucin. Gastroenterology 1994;107:1352-1363.

88. Blijlevens NM, Donnelly JP, de Pauw BE. Prospective evaluation of gut mucosal barrier injury following various myeloablative regimens for haematopoietic stem cell transplant. Bone Marrow Transplant 2005;35:707-711.

89. Lifschitz CH, Mahoney DH. Low-dose methotrexate-induced changes in intestinal permeability determined by polyethylene glycol polymers. J Pediatr Gastroenterol Nutr 1989;9:301-306.

90. Sansonetti PJ. War and peace at mucosal surfaces. Nat Rev Immunol 2004;4:953-964.

91. Nagler-Anderson C. Man the barrier! Strategic defences in the intestinal mucosa. Nat Rev Immunol 2001;1:59-67.

92. Roit I, Brostoff J, Male D. Immunology. London: Mosby, 2000.

93. Mosmann TR, Coffman RL. TH1 and TH2 cells: different patterns of lymphokine secretion lead to different functional properties. Annu Rev Immunol 1989;7:145-173.

94. Mosmann TR, Sad S. The expanding universe of T-cell subsets: Th1, Th2 and more. Immunol Today 1996;17:138-146.

95. Abreu-Martin MT, Vidrich A, Lynch DH, Targan SR. Divergent induction of apoptosis and IL-8 secretion in HT-29 cells in response to TNF-alpha and ligation of Fas antigen. J Immunol 1995;155:4147-4154.

96. Guy-Grand D, DiSanto JP, Henchoz P, Malassis-Seris M, Vassalli P. Small bowel enteropathy: role of intraepithelial lymphocytes and of cytokines (IL-12, IFN-gamma, TNF) in the induction of epithelial cell death and renewal. Eur J Immunol 1998;28:730-744.

97. Sonis ST, Peterson RL, Edwards LJ, Lucey CA, Wang L, Mason L, Login G, Ymamkawa M, Moses G, Bouchard P, Hayes LL, Bedrosian C, et al. Defining mechanisms of action of interleukin-11 on the progression of radiation-induced oral mucositis in hamsters. Oral Oncol 2000;36:373-381.

98. Ricart E, Panaccione R, Loftus EV, Tremaine WJ, Sandborn WJ. Infliximab for Crohn's disease in clinical practice at the Mayo Clinic: the first 100 patients. Am J Gastroenterol 2001;96:722-729.

99. Booth D, Potten CS. Protection against mucosal injury by growth factors and cytokines. J Natl Cancer Inst Monogr 2001:16-20.

100. Barnard JA, Lyons RM, Moses HL. The cell biology of transforming growth factor beta. Biochim Biophys Acta 1990;1032:79-87.

101. Massague J. The transforming growth factor-beta family. Annu Rev Cell Biol 1990;6:597-641.

102. Koff A, Ohtsuki M, Polyak K, Roberts JM, Massague J. Negative regulation of G1 in mammalian cells: inhibition of cyclin E-dependent kinase by TGF-beta. Science 1993;260:536-539.

103. Roberts AB, Anzano MA, Wakefield LM, Roche NS, Stern DF, Sporn MB. Type beta transforming growth factor: a bifunctional regulator of cellular growth. Proc Natl Acad Sci U S A 1985;82:119-123.

104. McCormack ES, Borzillo GV, Ambrosino C, Mak G, Hamablet L, Qu GY, Haley JD. Transforming growth factor-beta3 protection of epithelial cells from cycle-selective chemotherapy in vitro. Biochem Pharmacol 1997;53:1149-1159.

105. Potten CS, Booth D, Haley JD. Pretreatment with transforming growth factor beta-3 protects small intestinal stem cells against radiation damage in vivo. Br J Cancer 1997;75:1454-1459.

106. Wymenga AN, van der Graaf WT, Hofstra LS, Spijkervet FK, Timens W, Timmer-Bosscha H, Sluiter WJ, van Buuren AH, Mulder NH, de Vries EG. Phase I study of transforming growth factor-beta3 mouthwashes for prevention of chemotherapy-induced mucositis. Clin Cancer Res 1999;5:1363-1368.

107. Zheng H, Wang J, Koteliansky VE, Gotwals PJ, Hauer-Jensen M. Recombinant soluble transforming growth factor beta type II receptor ameliorates radiation enteropathy in mice. Gastroenterology 2000;119:1286-1296.

108. Jin Y, Cox DA, Knecht R, Raschdorf F, Cerletti N. Separation, purification, and sequence identification of TGF-beta 1 and TGF-beta 2 from bovine milk. J Protein Chem 1991;10:565-575.

109. Rogers ML, Goddard C, Regester GO, Ballard FJ, Belford DA. Transforming growth factor beta in bovine milk: concentration, stability and molecular mass forms. J Endocrinol 1996;151:77-86.

110. van't Land B, Meijer HP, Frerichs J, Koetsier M, Jager D, Smeets RL, M'Rabet L, Hoijer M. Transforming Growth Factor-beta2 protects the small intestine during methotrexate treatment in rats possibly by reducing stem cell cycling. Br J Cancer 2002;87:113-118.

111. Sonis ST, Peterson RL, Edwards LJ, Lucey CA, Wang L, Mason L, Login G, Ymamkawa M, Moses G, Bouchard P, Hayes LL, Bedrosian C, et al. Defining mechanisms of action of interleukin-11 on the progression of radiation-induced oral mucositis in hamsters. Oral Oncol 2000;36:373-381.

112. Ellis M, Zwaan F, Hedstrom U, Poynton C, Kristensen J, Jumaa P, Wassell J, al-Ramadi B. Recombinant human interleukin 11 and bacterial infection in patients with [correction of] haematological malignant disease undergoing chemotherapy: a double-blind placebo-controlled randomised trial. Lancet 2003;361:275-280.

113. Spielberger R, Stiff P, Bensinger W, Gentile T, Weisdorf D, Kewalramani T, Shea T, Yanovich S, Hansen K, Noga S, McCarty J, LeMaistre CF, et al. Palifermin for oral mucositis after intensive therapy for hematologic cancers. N Engl J Med 2004;351:2590-2598.

114. Panoskaltsis-Mortari A, Taylor PA, Rubin JS, Uren A, Welniak LA, Murphy WJ, Farrell CL, Lacey DL, Blazar BR. Keratinocyte growth factor facilitates alloengraftment and ameliorates graft-versus-host disease in mice by a mechanism independent of repair of conditioning-induced tissue injury. Blood 2000;96:4350-4356.

115. Williams DA. Inflammatory cytokines and mucosal injury. J Natl Cancer Inst Monogr 2001;29:26-30.

116. Fuss IJ, Boirivant M, Lacy B, Strober W. The interrelated roles of TGF-beta and IL-10 in the regulation of experimental colitis. J Immunol 2002;168:900-908.

117. Kuhn R, Lohler J, Rennick D, Rajewsky K, Muller W. Interleukin-10-deficient mice develop chronic enterocolitis. Cell 1993;75:263-274.

Part I

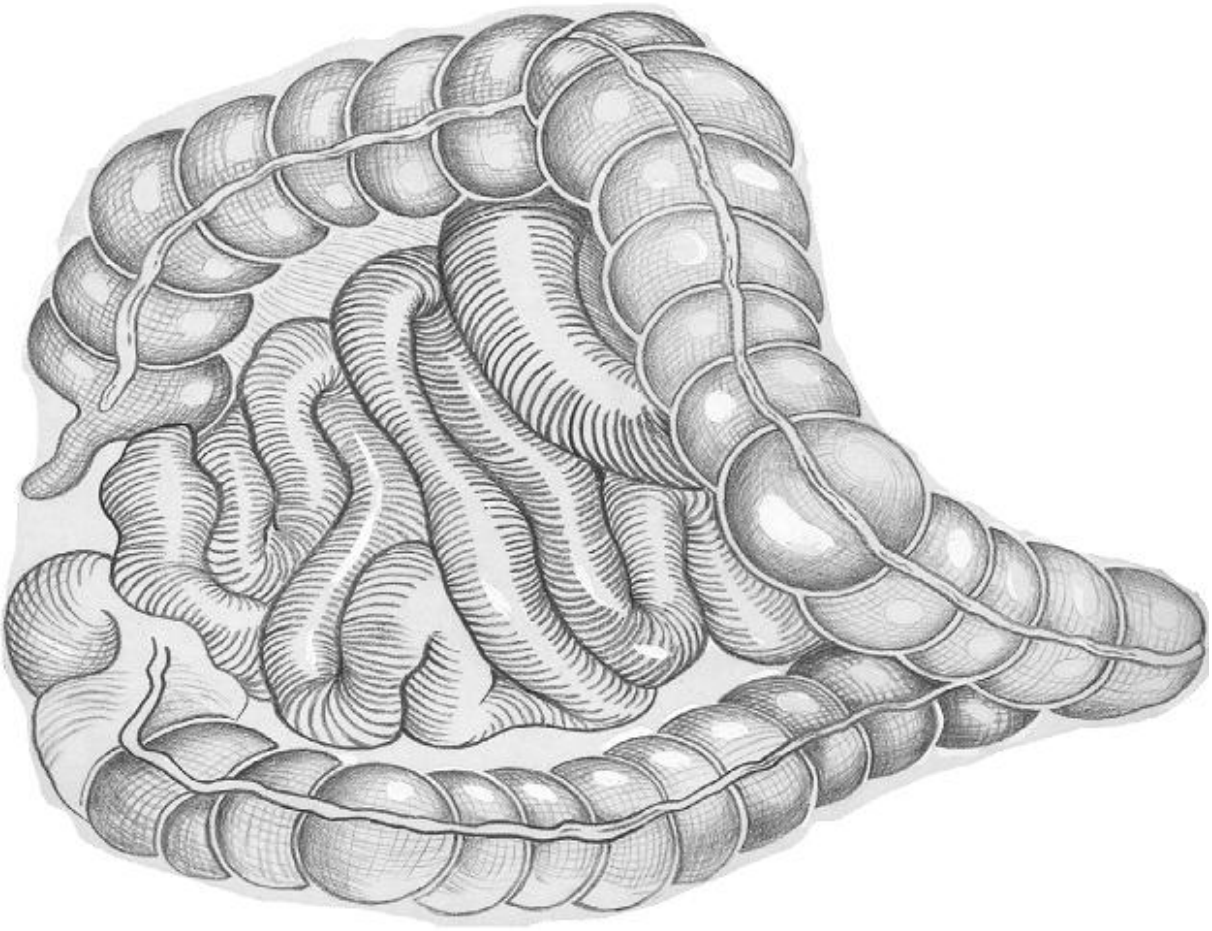

PATHOGENESIS OF CHEMOTHERAPY-INDUCED MUCOSITIS

2

ALTERATIONS IN EPITHELIAL AND MESENCHYMAL INTESTINAL GENE EXPRESSION DURING DOXORUBICIN-INDUCED MUCOSITIS IN MICE

Barbara A.E. de Koning, Dicky J. Lindenbergh-Kortleve, Rob Pieters, Hans A. Büller, Ingrid B. Renes, Alexandra W.C. Einerhand.

Digestive disease and Sciences 52:1814-1825 (2007).

ABSTRACT

In the current study we aimed to gain insight into epithelial-mesenchymal cross-talk and progenitor compartment modulation during doxorubicin (DOX)-induced mucositis in mice. Intestinal segments were collected on various days after DOX treatment. DOX-induced damage at day 1-2 was characterized by increased epithelial proliferation and apoptosis and a decrease in the expression of epithelial differentiation markers. Concurrently, T-cell factor-4 (TCF4) levels increased and the epithelial differentiation enhancing factor, bone morphogenic protein-4 (BMP4), decreased. During severe damage (day 3), BMP4 levels were significantly increased, which inversely correlated with epithelial proliferation. At the same time, the expression of the epithelial differentiation markers was increasing again. At day 7, BMP4 levels were down-regulated, while the levels of the epithelial differentiation markers and TCF4 were normalized again. These data suggest that in response to DOX-induced damage, BMP4 and TCF4 are modulated in such a way that homeostasis of the progenitor compartment is partly preserved.

INTRODUCTION

The highly proliferating small intestine is very susceptible to chemotherapy-induced damage.[1,2] This side effect, often referred to as mucositis, is very painful and can be life threatening due to the enhanced risk of bacterial translocation caused by loss of epithelial barrier function. Each year, around 500,000 patients worldwide suffer from this side effect[3] for which there is still no definitive prophylaxis or treatment.

Drug-induced damage to the highly proliferating stem cells and progenitors located in the crypts of Lieberkühn showed that different classes of cytostatic drugs affect epithelial crypt cells of different topographical and hierarchical status.[4-6] Methotrexate (MTX), 5-fluorouracil and vincristine for example, induce damage high in the proliferative compartment at crypt position 9 - 11. Damage induced by MTX is well characterized and shows severe morphological changes characterized by epithelial flattening, villus-atrophy, and specific de-differentiation of enterocytes. The last one is indicated by a decreased expression of the enterocytespecific enzymes but a maintained expression of goblet and Paneth cell-specific genes.[7-11] Doxorubicin (DOX) is a cytostatic drug that also frequently causes severe mucositis. However, DOX-induced damage is not well characterized.[12] DOX preferentially attacks cells at crypt position 4 - 6, which is just above or at the same level as the intestinal stem cells.[5,13] DOX is therefore thought to induce more severe damage, especially to the proliferating compartment at the bottom of the crypts, as for example MTX. In clinical practice, DOX is often used in treatment of solid tumors, leukemia, and lymphomas in both adult and childhood cancer patients.[12,14-16] Recent studies revealed a dynamic cascade of events leading to chemotherapy-induced mucositis.[17] Not only are the specialized epithelial cells affected by cytostatic-drug treatment, but also the underlying submucosal connective tissue. Under normal physiological circumstances, the epithelium maintains a cross-talk with the mesenchyme. Epithelial-mesenchymal interactions are critical for the normal morphogenesis and maintenance of the crypt-villus axis.[18,19]

Bone morphogenic protein (BMP)- and Wnt-signaling pathways are two of the main pathways involved in embryonic and adult intestinal development.[20,21] BMPs are morphogenes that constitute a large group of structurally and functionally related proteins of the TGF-beta superfamily. BMP signaling pathways have a key role in organo-genesis,[22,23] gastrointestinal development and intestinal homeostasis in adults.[24-29] After intestinal development, BMP4 is exclusively expressed in the intravillus and intracrypt mesenchymal cells, including those adjacent to the intestinal stem cells.[24,26] Paracrine BMP signaling occurs specifically in the villus from the mesenchyme to the adjacent epithelium,[24] suggesting involvement in epithelial-mesenchymal interactions as a mesenchymal signaling molecule.

The Wnt-signaling pathway also has been implicated in the regulation of the intestinal epithelial proliferation/differentiation balance *in vitro*.[30] In the intestine of mice deficient

for transcription factor TCF4, the main Wnt pathway transcription factor in the intestinal epithelium, loss of proliferative compartments and epithelial cell differentiation are found.[31] Interestingly, the BMP- and Wnt pathways appear to be linked, as was shown by the fact that BMP signaling suppresses Wnt signaling to ensure a balanced control of stem cell proliferation and subsequent epithelial differentiation.[24,26]

The objective of this study was to develop an experimental mucositis mouse model to characterize DOX-induced intestinal damage and subsequent repair. In addition, we aimed to correlate the alterations in morphology, epithelial homeostasis, and gene expression with changes in BMP4 and TCF4 expression. This, in order to gain insight into possible modulation of the epithelial-mesenchymal cross-talk and progenitor compartment during chemotherapy-induced intestinal damage and regeneration.

MATERIALS AND METHODS

Animals

Animal experiments were performed with permission of the Animal Ethics Committee of the Erasmus MC-Sophia. Upon arrival at our institute, 10-week-old male BALB/c mice (Harlan, Horst, The Netherlands) were housed individually during the whole experiment in micro-isolator cages under specific pathogen-free conditions with free access to a standard palletized diet (Hope farms, Woerden, The Netherlands) and water. After 1 week of adjustment to the new environment, the mice were divided into three groups and injected intravenously with doxorubicin (DOX) (Doxorubicin, Pharma Chemie, Haarlem, The Netherlands) on two subsequent days. At day -1 and 0, the first group of mice was injected with a low dose of DOX of 6 and 4 mg/kg (low dose) respectively, a second group was injected with a medium dose of 8 and 5 mg/kg (medium dose) and a third group was injected with a high dose of 10 and 6 mg/kg (high dose). Controls were given equivalent volumes of 0.9% NaCl. Mice in the low- and high-dose group were sacrificed at day 1, 2, 3 and 7 after the final DOX injection; mice in the medium dose group were only sacrificed at day 3 and 7. One hour before sacrifice, the mice were injected with 120 µl 10 mg/ml 5-Bromo-2'deoxyUridine (BrdU) (Sigma-Aldrich, Zwijndrecht, The Netherlands), an uridine analog, to locate the proliferating cells. Per time point 4 - 6 DOX-treated animals and 2 - 4 control animals were sacrificed. Segments of mid-jejunum were collected and either processed immediately for histological analyses or snap-frozen in liquid nitrogen for storage at 80 °C and subsequent protein isolation.

Histochemistry

Five-millimeter segments of mid-jejunum were fixed in 4% paraformaldehyde in phosphate-buffered saline (PBS), dehydrated and embedded in Paraplast Plus (Sherwood Medical, Den Bosch, The Netherlands) as previously described.[11] Four µm sections were routinely stained with hematoxylin (Vector Laboratories, Burlingame, CA) and eosin (Sigma-Aldrich) to study morphological alterations of the crypts and villi.

Immunohistochemistry was performed as described previously[11] with some minor modifications. The sections for BrdU staining required an extra adjustment to this protocol of HCL incubation, washing with borate buffer, and pepsin treatment as described before.[32] In short, the sections were blocked as described and incubated overnight with the following antibodies diluted in PBS: to visualize BrdU incorporation, mouse monoclonal anti-BrdU (1:250, Roche Applied Sciences, Indianapolis, IN) was used, as an enterocyte marker rabbit polyclonal anti-rat Sucrase-Isomaltase (SI) (1:9000 in PBS, kindly provided by Dr. K.Y. Yeh)[33] was used and as a goblet cell-specific marker rabbit polyclonal anti-rat trefoil factor family (TFF3: 1:3000, kindly provided by Prof. Dr. D.K. Podolsky) was used. Furthermore, BMP expression was visualized with anti-BMP4 (1:100, R&D Systems, Abingdon, UK). Immunoreactions were detected using Vectastain ABC Elite Kit (Vector Laboratories, Burlingame, CA) and 3,3'-diaminobenzidine tetrahydrochloride (Sigma-Aldrich, Zwijndrecht, The Netherlands).

Crypt and -villus length

Longitudinal sections of crypts and their corresponding villi were selected so that the base (marked by Paneth cells), middle and top of the crypt were all in the plane of section and thus well orientated. The depth of ten crypts and the length of ten villi were measured on three slides per animal, four animals per time point, with the use of a Nikon Eclipse E800 microscope and IM 500 software.

Protein dot blotting

The expression of enterocyte markers was detected and quantified as described previously.[10] Briefly, 5-mm segments of the mid-jejunum were homogenized and protein concentrations were measured using the BCA Protein Assay Reagent (Pierce, Rockford, IL) and 50 µg protein of each homogenate was dot-blotted on nitrocellulose (Protran BA83, 0.2 µm; Schleicher & Schuell, Dassel, Germany). Hereafter, blots were blocked for 1 h with blocking buffer containing 50 mM Tris, pH 7.8, 5% (wt/vol) nonfat dry milk powder (Campina Melkunie, Eindhoven, The Netherlands), 2 mM CaCl2, 0.05% (vol/vol) Nonidet P40 (BDH, Brunschwig Chemie, Amsterdam, The Netherlands) and 0.01% Antifoam B (Sigma-Aldrich). Blots were incubated overnight at 4 °C with rabbit polyclonal anti-rat SI (1:1000),[33] and rabbit polyclonal anti-rat trefoil factor family (TFF3: 1:1500) diluted in blocking buffer. After washing with blocking, the buffer blots were incubated with ^{125}I-labeled protein A (specific activity 30 mCi/mg, Amersham Biosciences, Roosendaal, The Netherlands) for 2 h at room temperature. Specific binding of ^{125}I-labeled protein A to the enterocyte marker antibodies was measured using PhosphorImager detection. The elicited signal was quantified by ImageQuant software (Molecular Dynamics, B&L systems, Zoetermeer, The Netherlands) and the expression of TFF3 and SI was expressed per 50 µg protein of tissue. Average expression levels of TFF3 and SI in the mid-jejunum were calculated per mouse, followed by calculation of the mean expression of TFF3 and SI per time point studied. Subsequently, the average expression of TFF3 and SI of control mice was set at 100%. The specificity of the above-described antibodies was previously confirmed by Western-blot analysis.[10]

Western-blot analysis

The same protein homogenate was used as described for protein dot blot analysis. Twenty µg of protein was loaded per lane and run on a 12.5% SDS-PAGE. The separated proteins were transferred to nitrocellulose membranes (Protran BA83, 0.2 µm) and blocked for 1 h at room temperature in blocking buffer as described above. The blots were incubated overnight at 4 °C with primary antibodies diluted in blocking buffer: mouse monoclonal anti-human PCNA, clone PC10 (1:250, Novo Castra Laboratories, Newcastle upon Tyne, UK) and mouse monoclonal anti-human BMP4, clone 3H2 (1:100), (Novocastra Laboratories, Newcastle upon Tyne, UK), rabbit polyclonal anti-human cleaved Caspase-3 antibody (1:1000, Cell Signaling, Beverly, MA), and mouse monoclonal anti-human TCF-4, clone 6H5-3 (1:250, Upstate, Waltham, MA). After washing with PBS, 0.2% Tween-20 blots bound antibodies were revealed using HRP conjugated goat anti-mouse or rabbit anti-goat secondary antibodies (1:1000) and SuperSignal West Femto Luminol Enhancer kit (Pierce, Rockford, IL). The signal was detected and quantified by the ChemiGenius gel documentation system (Syngene, Cambridge, UK) and the expression of the specific proteins analyzed was expressed per 20 µg protein of tissue. Average expression levels of PCNA, BMP4, TCF4, and caspase-3 in the mid-jejunum were calculated per mouse, followed by calculation of the mean expression of these specific proteins per time point studied. Subsequently, the average expression of PCNA, BMP4, TCF4, and caspase-3 in control mice was set at 100%.

Statistical analysis

Changes in protein expression levels during damage and regeneration were statistically analyzed using the Kruskal-Wallis H-test and the Mann-Whitney *U*-test. A $P < 0.05$ was considered statistically significant. Data are presented as the mean ± standard error of the mean (SEM).

RESULTS

Dose-response analysis of DOX-induced mucositis in an experimental mouse model

To optimize the dose of DOX necessary to induce severe intestinal damage (*i.e.*, villus atrophy, crypt loss and flattening of the epithelial cells) a dose-response curve was performed. Thereto, mice were divided in three treatment groups: low dose, medium dose, and high dose (see Materials and methods, section Animals for details). In the high-dose treatment group, two of the six mice died at day 4. Necropsy showed an excess of fluid in the abdominal cavity of unknown source. Because of the elapsed time after death, morphological evaluation could not be performed.

Morphological analysis of the low-dose treatment group at days 1 and 2 (data not shown), revealed only a slight increase in crypt length, which became more pronounced at day 3 (Figure 1B). An increase in crypt length was also seen in the medium dose group at day 3. (Note the medium-dose treatment group was not studied at days 1 and 2). No

other morphological changes were seen in the low dose- (days 1 - 3) and medium-dose group (day 3). In contrast, in the high-dose treatment group we did see severe morphological damage (Figures 1D-F). Specifically, severe villus atrophy, crypt lengthening, crypt loss, perturbation of crypt arrangement, flattening of crypt and villus epithelium and inflammation were observed at day 3 (Figure 1F). Moreover, the latter morphological damage was already seen, although in a milder degree, at days 1 and 2 after the high-dose DOX treatment (Figure 1D, day 1 and Figure 1E, day 2). At day 7, the intestinal morphology was completely restored in the low-dose and medium-dose group (data not shown), but was still affected in the high-dose group. As in the latter group, the crypt epithelium still showed signs of regeneration, like new crypt formation and less epithelial flattening (Figure 1G).

Quantitative analysis of crypt and villus length

To quantify the amount of morphological damage induced by the different doses of DOX, the length of the crypts and villi were measured (Figures 1H–I). In the high-dose group, but not in the low-dose or medium-dose group, a significant increase in crypt length was already observed at day 2 (data not shown). At day 3 the crypt length was significantly increased in each treatment group compared to the control group (Figure 1H). By day 7, the length of the crypts had returned to control levels in the low-dose and medium-dose group, but were still increased in the high-dose group. This increase in crypt length, however, showed a trend towards normal levels because the crypt length at day 3 was 41% above control level but at day 7 this was still only 13% above control level. The length of the villi did not change in the low-dose or the medium-dose treatment group on each day investigated. However, in the high-dose treatment group the length of the villi were significantly decreased on days 1 - 3 and 7 (Figures 1H, day 3 and 1I, day 7). Because severe intestinal mucositis (day 3) and morphological regeneration (day 7) were seen only in the high-dose treatment group, we continued our studies with the high-dose DOX treatment model.

Effects of high-dose DOX treatment on enterocyte-specific gene expression

To gain insight into the functional capacity of the intestinal epithelium after DOX treatment, a sucrase-isomaltase (SI) immunohistochemical staining was performed. SI is an enterocyte-specific disaccharidase responsible for sucrose degradation. SI is expressed in the brush border of differentiated villus enterocytes directly after weaning[34] and is considered an intestinal epithelial differentiation marker. At day 1 and 2 after DOX treatment SI was expressed in the brush border of enterocytes along the entire villi, comparable to the control epithelium (Figures 2A, control; B, day 1; C, day 2). At day 3, SI staining showed a patchy pattern with weak staining on less affected parts of the epithelium and even absence of staining on severely damaged epithelial parts of the sections (Figure 2D). At day 7, during the regenerative phase, the SI staining pattern was comparable to control again (Figure 2E).

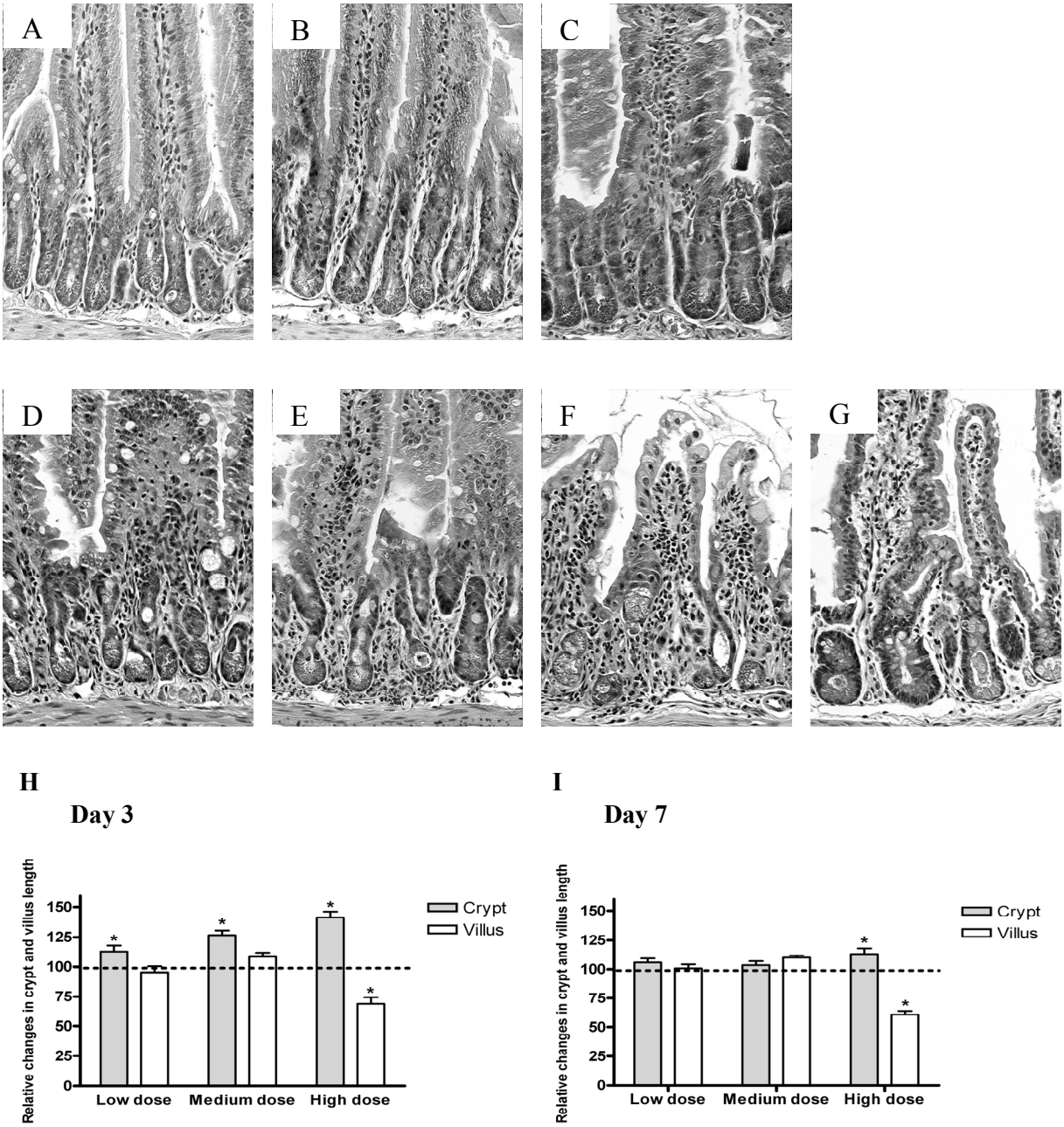

Figure 1 *Morphology of the murine small intestine after low, medium-or high-dose DOX treatment. Morphology of the jejunum of a control mouse (A), at day 3 after low-dose DOX (B) and at day 3 after medium-dose DOX (C), both were mildly affected by DOX treatment. Morphology of the jejunum at day 1(D) and day 2(E) after high-dose DOX treatment, which appeared progressively affected and severely deteriorated at day 3 (E). At day 7, the regenerative phase, the intestinal morphology of the mice in the low- and medium-dose group was completely restored to control situation (data not shown). The morphology at day 7 of the mice treated in the high-dose group was regenerating, showing new crypt formation but still villus atrophy. These photographs are representative examples of a group of four animals per time-point. To quantify the effect of these different doses of DOX treatment, crypt and villus lengths were measured. Crypt and villus lengths of control mice were set at 100%. At day 3 (A), the length of the crypts in all three DOX treatment groups was significantly increased in comparison to the control group. Villus length in the low- and medium-dose group remained at control level. The length of the villi of the high-dose group decreased significantly, indicating significant villus atrophy after high-dose DOX treatment. At day 7 (B) crypt and villus lengths of the low- and medium-dose DOX treatment groups showed complete restoration. The crypts of the high-dose treatment group were still significantly longer, but this increase in crypt length was declining compared to day 3 (day 341%, day 7 13%). The length of the villi was still significantly decreased at day 7, showing no signs of regeneration. $^{*}P < 0.05$ versus control. The bars are expressed in mean + SEM*

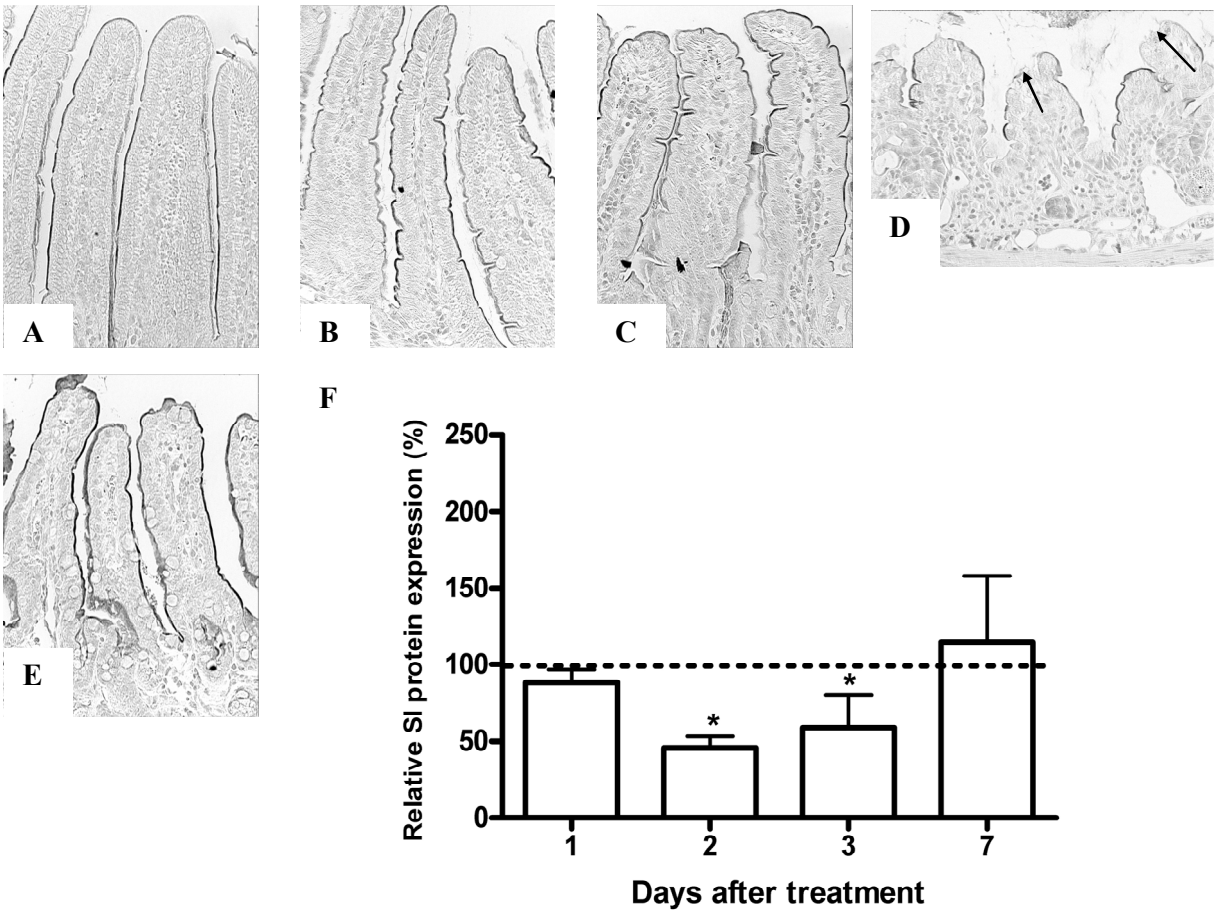

Figure 2 *Effect of high-dose DOX treatment on the enterocyte-specific SI expression in the small intestinal epithelium. SI expression of the jejunum of a control mouse (A), at day 1 (B) and at day 2 (C). The brush border staining at day 1 and 2 is comparable to control situation. At day 3 (D), SI staining showed a patchy pattern; some parts of the brush border showed SI expression, on some other parts of the brush border SI expression was absent (→). SI expression at day 7 (E) showed complete regeneration, and was equal to the control situation. SI protein expression levels were analyzed by dot-blot technique and the SI expression of control mice was set at 100% (F). The expression of SI remained stable at day 1, but decreased significantly at day 2 and 3. During the regenerative phase, at day 7, the SI expression reached control level again. *P < 0.05 day 2 and 3 versus control. The bars are expressed in mean + SEM*

To quantify SI protein expression, protein dot-blot analyses were performed using SI-specific antibodies (Figure 2F). The SI protein expression level at day 1 was similar to the control situation. At day 2, SI expression levels were significantly decreased and remained significantly decreased at day 3. At day 7, the SI expression levels regained to control levels.

Effects of DOX treatment on goblet cell-specific gene expression

Goblet cell-specific gene expression after high-dose DOX treatment was analyzed by the expression of trefoil factor family 3 (TFF3). TFF3 is a bioactive peptide, produced and secreted by goblet cells, that is involved in epithelial protection and repair.[35,36] Immunohistochemical staining of TFF3 showed TFF3 expression by goblet cells in crypts and villi of the jejunum (Figure 3).

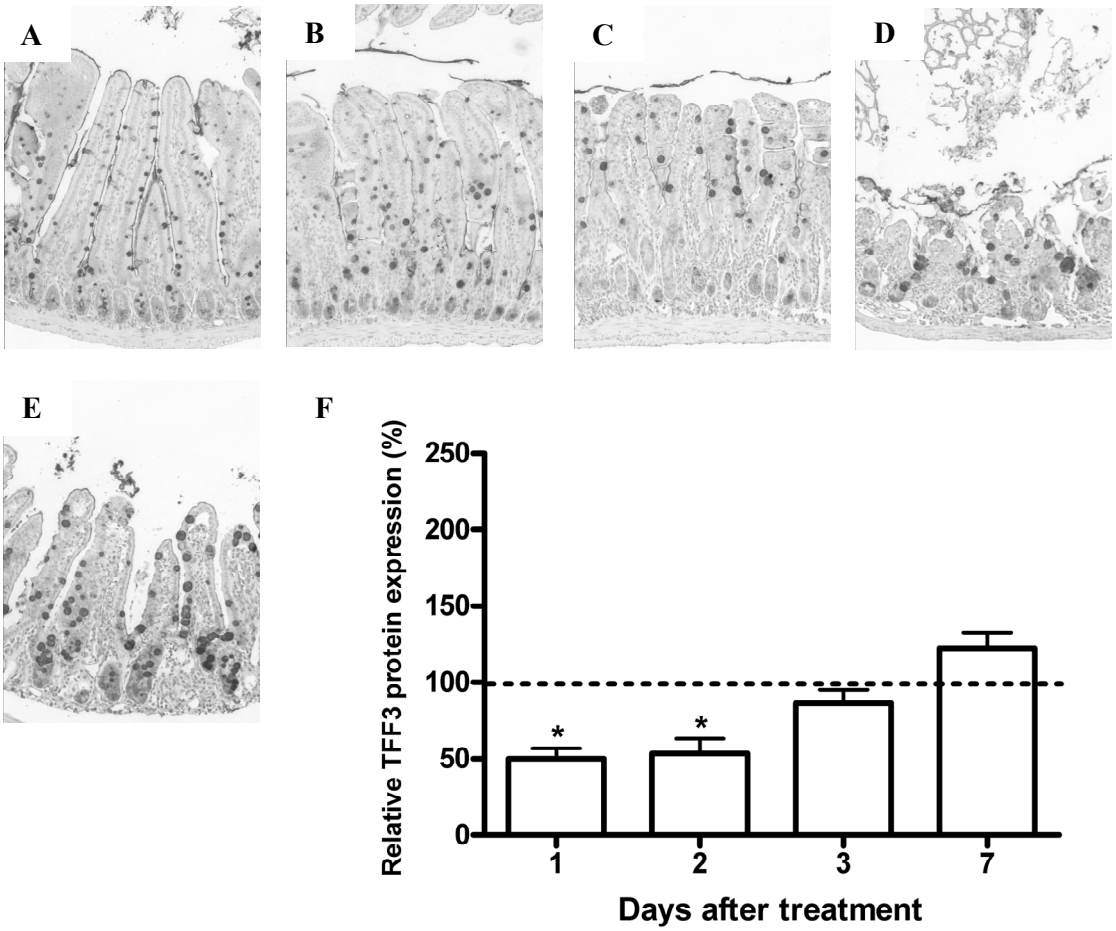

Figure 3 *Effect of high-dose DOX treatment on the goblet-specific TFF3 expression in the small intestine. Immunohistochemical staining of the goblet cell-specific protein TFF3 (A-E). TFF3 expression of the jejunum of a control mouse (A), at day 1 (B), at day 2 (C), at day 3 (D) and at day 7 (E). In the control situation, TFF3 was expressed in all goblet cells in the crypts and villi, at day 1 (B), the amount of goblet cells expressing TFF3 maintained at control level. At day 2 (C), TFF3 expression decreased visibly, the goblet cells localized in the crypts showed no staining. At day 3 (D), during severe morphological damage, TFF3 expression of goblet cells in the crypt was reconstituted. TFF3 expression at day 7 (E) was regenerated and comparable to control situation. TFF3 protein expression levels were analyzed by dot-blot technique, the TFF3 expression of control mice was set at 100% (F). TFF3 expression decreased significantly at day 1 and day 2, the expression was decreased to 50% of control level. During severe morphological damage at day 3, the TFF3 expression increased almost to control level. Day 7 showed TFF3 expression even above control level. *P < 0.05 day 1 and 2 versus control. The bars are expressed in mean + SEM*

At day 1, the TFF3 staining was not visibly altered compared to the control situation (Figure 3B). At day 2, the immunohistochemical detection of TFF3 decreased visibly, especially in the goblet cells localized in the crypts and lower part of the villi where TFF3 protein could hardly be detected/was absent (Figure 3C). At day 3, during most severe morphological damage, TFF3 staining by goblet cells in the crypt was reconstituted (Figure 3D). Day 7 showed complete regeneration of TFF3 (Figure 3E).

Subsequently, a protein dot-blot analysis was performed (Figure 3F) using TFF3-specific antibodies to quantify TFF3 levels. At day 1, the TFF3 expression was already significantly decreased to 50% of control level and maintained at this low level at day 2. At day 3,

concomitant with the most severe morphological damage, TFF3 expression returned to control level. TFF3 protein expression was again comparable to control situation at day 7.

Effect of high-dose DOX treatment on epithelial proliferation

Localization of proliferation was studied by immunohistochemical detection of incorporated BrdU (Figure 4). In controls (Figure 4A) BrdU was mainly localized in cells from the bottom of the crypt up to three quarter of the crypt length. At day 1 and 2 the proliferative zone broadened and progressively moved upwards to the crypt-villus junction. At day 3, during severe morphological damage, BrdU-positive cells formed a scattered pattern throughout the remaining crypt structures of the small intestine. In the regenerative phase, at day 7 BrdU-positive cells were located in the lower part of the crypts again.

The changes in proliferation induced by DOX were quantified by Western-blot analysis of PCNA protein expression[37,38] using a specific monoclonal PCNA antibody. PCNA protein expression after MTX treatment (Figures 4F, G) showed a trend of increased expression at days 1. At day 2, this increased expression was significant compared to control levels, indicating that high DOX treatment did not induce an arrest in proliferation at day 1 and 2. At day 3, PCNA expression was decreased to around 20% of the normal level and was still 50% of control level at day 7. The latter data indicate that the inhibition of epithelial proliferation sustained during the regenerative phase. Overall, the PCNA levels correlated with the immunohistochemical data (Figures 4A-E *vs.* 4G).

Effect of high-dose DOX treatment on enterocyte apoptosis

Besides proliferation, the influence of DOX treatment on apoptosis was quantified with a polyclonal antibody against cleaved Caspase-3 (Figures 4F, 5A). Caspase-3 is one of the key executioners of apoptosis.[39] The expression of cleaved Caspase-3 protein was significantly increased at day 1 and 2, at the beginning of DOX-induced morphological damage. At day 3, during severe morphological damage, and day 7, during regeneration, expression of cleaved caspase-3 was comparable to control level. Increased apoptosis at day 1 and 2 was primarily located along the crypt axis (Figure 5B showing day 1 after MTX treatment).

Effect of high-dose DOX treatment on TCF-4 protein expression

To gain insight into the effects of DOX on the epithelial stem cell compartment, the expression of TCF-4 was quantified. TCF-4 is a transcription factor of the Wnt-signaling pathway and is expressed in the gut epithelium in a gradient fashion that is highest at the base of the crypts.[40,41] TCF-4$^{-/-}$ mice lose the intestinal epithelial progenitor and stem cell population before crypt formation can be established.[31] Therefore, TCF-4 has a role in intestinal epithelial stem cell maintenance. The TCF-4 expression (Figures 4F and 6) remained very stable despite DOX treatment. Only at day 1 the TCF-4 expression increased significantly, although little in absolute sense. But at day 2, day 3 and day 7, the TCF4 protein expression remained at control level.

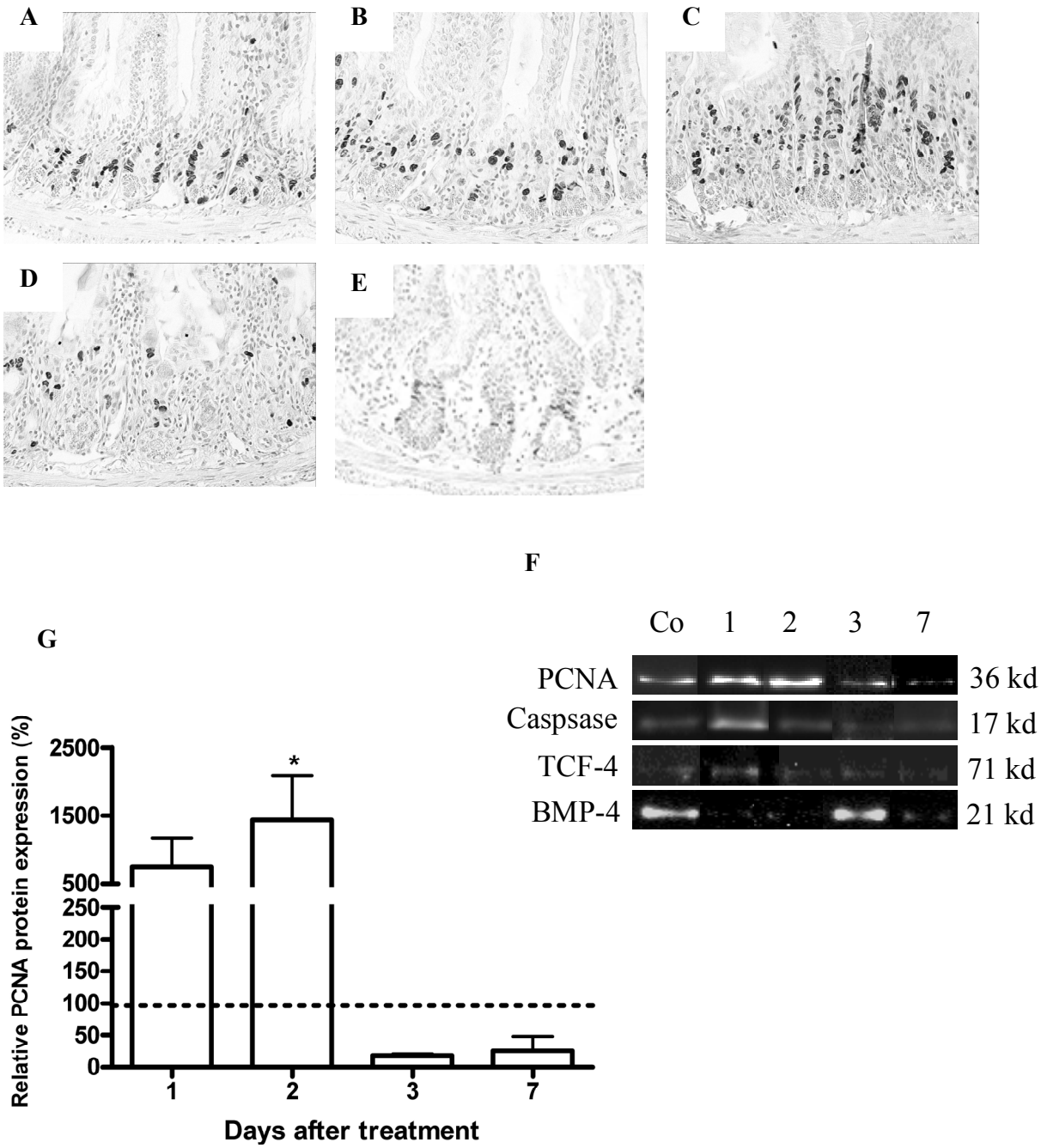

Figure 4 *Effect of high-dose DOX treatment on epithelial proliferation. The localization of epithelial proliferation was visualized by detection of BrdU incorporation. BrdU incorporation of the jejunum of a control mouse (A) and mice at day 1 (B), at day 2 (C), at day 3 (D) and at day 7 (E). At day 1, the BrdU-positive cells were slightly migrated upwards in the crypt, at day 2 the BrdU-positive cells were seen along the entire length of the crypts. At day 3 the BrdU expression decreased and showed a scattered pattern on some crypts and villi. The location of BrdU-positive cells at day 7 was confined again to the lower part of the crypts. PCNA, Caspase-3, TCF4 and BMP4 protein expression levels were analyzed by Western-blot technique (F), the PCNA expression of control mice was set at 100% (G). The expression of PCNA protein showed a non-significant trend of increased expression at day 1, and a significant increase at day 2. PCNA expression at day 3 and 7 showed a decreasing trend to around 20% of control level. $^{*}P < 0.05$ day 1 and 2 versus control. The bars are expressed in mean + SEM*

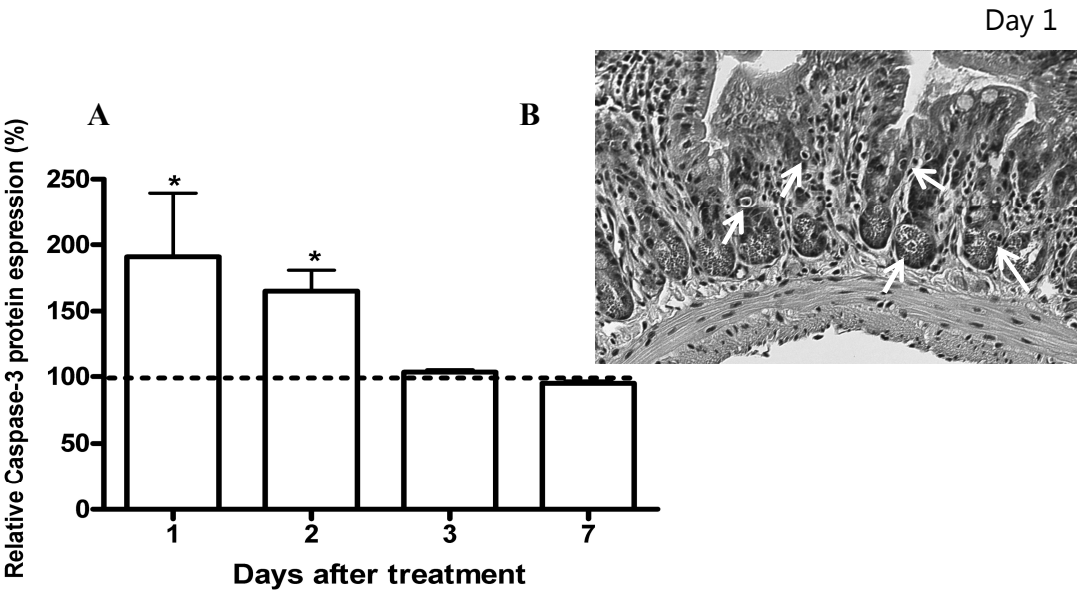

Figure 5 *Effect of high-dose DOX treatment on epithelial apoptosis. Caspase-3 protein expression of the control mice, analyzed by Western-blot technique (Fig 4F), was set at 100% (A). At day 1 and 2, the Caspase-3 levels increased significantly in comparison to the control levels. At day 3, during severe morphological damage the caspase-3 expression maintained at control level, the same was seen at day 7, during the regenerative phase. The increase in apoptosis at day 1 is primarily located in the crypt region (B). *P < 0.05 day 1 and 2 versus control. The bars are expressed in mean + SEM. → indicates apoptotic cells*

Effect of high-dose DOX treatment on expression of Bone morphogene 4 (BMP4)

To examine the role of BMP4 signaling in intestinal homeostasis the expression of BMP4 was quantified. BMP4 is crucial for epithelial-mesenchymal cross-talk and intestinal homeostasis. BMP4 is expressed in the intravillus and intracrypt mesenchymal cells,[24,26] inhibition of BMP signaling causes intestinal architectural abnormalities[24] and decreased differentiation as seen in tumorigenesis.[29]

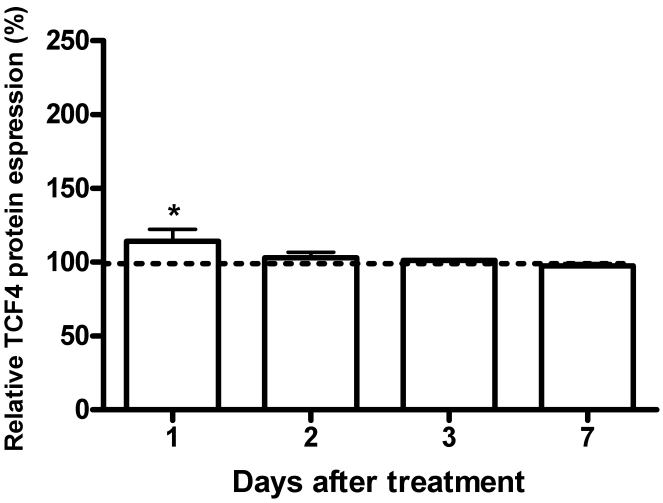

Figure 6 *Effect of high-dose DOX treatment on TCF-4 protein expression. TCF-4 protein expression of control mice, analyzed by Western-blot technique (Figure 4F), was set at 100%. At day 1, TCF-4 protein expression increased significantly. At day 2, day 3, and day 7, the TCF4 protein expression remained stable at control level. ∗P < 0.05 day 1 versus control. The bars are expressed in mean + SEM*

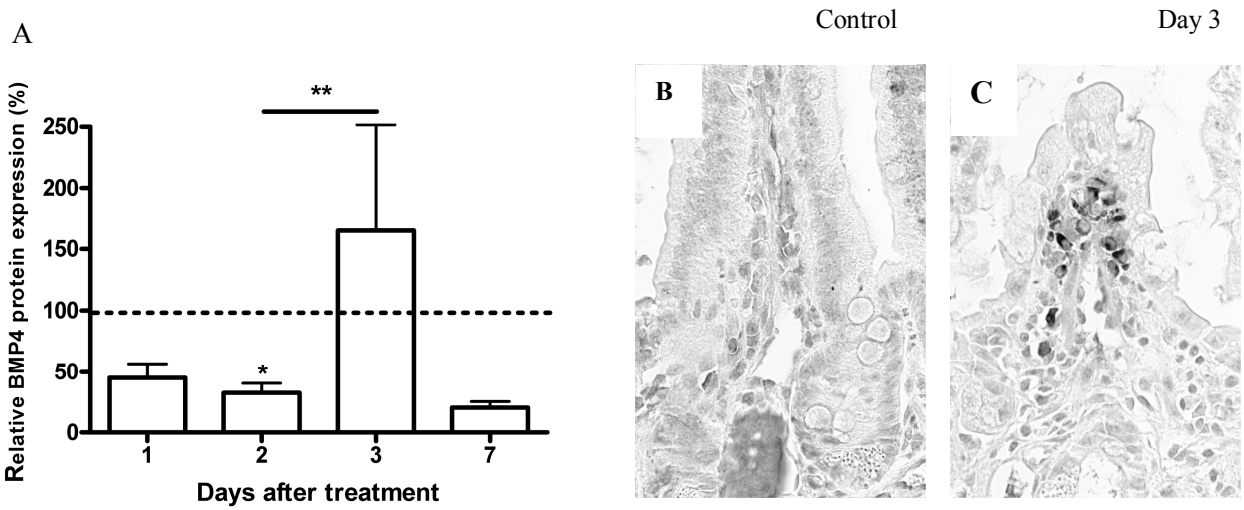

Figure 7 *Effect of high-dose DOX treatment on expression of the morphogen BMP4. The BMP4 protein expression of the control mice, analyzed by Western-blot technique (Fig. 4F), was set at 100% (A). Expression of the morphogen BMP4 protein showed a decreasing trend at day 1, which was at the brink of significance (P = 0.05) at day 2 in comparison to control expression. At day 3, the BMP4 expression showed an increasing trend. This increase in expression was significant in comparison to day 2. Day 7 showed a decrease in expression again beneath the level of control expression. The localization of BMP4 expression did not change at day three (C) in comparison to control situation (B). $^{*}P < 0.05$ day 2 versus control, $^{**}P < 0.05$ day 2 versus day 3. The bars are expressed in mean + SEM*

BMP4 protein expression showed a mild decrease in expression level at day 1 after DOX treatment (Figures 4F, 7A). At day 2, this decrease in BMP4 expression level progressed and was almost significant (P = 0.05) in comparison to the control level. Thereafter, BMP4 day 2 but not to control. Day 7 showed a non-significant decrease in expression compared to control mice. BMP4 was predominantly expressed in the intravillus mesenchym as shown by immuno-histochemistry (Figures 7B, C), both in control as in MTX-treated mice.

DISCUSSION

This study revealed that DOX, in a dose of 10 and 6 mg/kg induced severe morphological damage to the small intestine of mice within 3 days, which was almost completely regenerated by day 7. Moreover, it revealed that the intestine was virtually not or much less affected by lower doses of DOX. Mucositis induced by the chosen dose of DOX was characterized by an increasing degree of intestinal morphological damage at day 1 and 2, which correlated with a significant increase in both apoptosis and proliferation. During this phase of epithelial hyper-proliferation, the epithelial cells lost their highly differentiated status as measured by a significant down-regulation of epithelial-specific SI at days 2 - 3. The decreased expression of TFF3 at days 1 - 2 could be caused by a decrease in goblet cell differentiation, but on the other hand, could also be the result of increased TFF3 secretion. At day 3, the time-point when intestinal damage was most severe, the morphology was characterized by severe villus atrophy, a significant rise in crypt length, epithelial flattening, crypt loss, inhibition of proliferation and impaired

epithelial differentiation. During morphological regeneration, at day 7, proliferation started to return to control level, and SI and TFF3 expression levels were normalized again.

In order to be able to prevent or treat chemotherapy-induced mucositis, it is essential to know if different cytostatic drugs induce the same or different kinds of intestinal damage. Potten *et al.* demonstrated that there is a general tendency for antibiotics, like DOX, and radiation to damage the lower cell positions in the crypt near or at the position of the stem cells (position 4 - 6).[5] Alkylating agents on the other hand mainly damage cells at position 6 - 8. Anti-metabolites like MTX and a microtubule dissociating agents act on higher cell positions (9 - 11). It is, however, unclear if cytostatic drugs attacking at the lowest positions in the crypts cause a different kind of damage than drugs damaging cells at higher positions. If we compare the DOX-induced mucositis as studied presently with the well-characterized MTXinduced mucositis,[8,10,11,32,42,43] then it is clear that there are many similarities and few discrepancies between the two. Although the two drugs affected cells of different hierarchical height,[5] they both caused apoptosis, villus atrophy, epithelial flattening, crypt loss and a temporary loss of SI expression and TFF3 expression.[10,11,43] Since SI is involved in carbohydrate metabolism and TFF3 is involved in mucosal repair,[34-36,44] these data suggest impaired absorption and mucosal repair after DOX as well as after MTX treatment. In contrast, both MTX[11] and DOX hardly affect the expression of lysozyme by Paneth cells in the crypts (data not shown).

Decreased levels of TFF3 after both DOX and MTX was at the same time as epithelial hyper-proliferation,[11,43] but changes in proliferation, induced by MTX treatment followed a different time-line compared to DOX treatment. MTX causes proliferation inhibition within 1 day, followed by a period of hyper-proliferation during severe intestinal damage.[11,32] DOX treatment leads to immediate hyper-proliferation (day 1 and 2) with subsequent inhibition of proliferation during severe morphological damage (day 3). Moreover, the cell-fate specific affect of MTX on goblet cells causing goblet cells to accumulate in the crypt and at the top of the villus[10,11] was not seen after DOX treatment. The reason for these discrepancies remains to be further investigated, but might be directly related to the difference in topographical height (and thus status) of the cells vulnerable to the two different drugs. Overall, however, the similarities in intestinal responses after DOX or MTX treatment are striking. This suggests that there may be common pathways involved in intestinal damage and repair.

Historically, chemotherapy- or radiation-induced mucositis was believed to be solely due to damage to dividing epithelial cells at the bottom of the crypts.[45] However, recently it has become clear that other parts of the intestinal mucosa and submucosa might also be involved.[17,46] Here we provide evidence for a mesenchymal contribution to the damage by showing that BMP4, a very important lamina propria derived-morphogen in the small intestine,[24,26] is affected by DOX treatment. BMP4 was modulated by DOX during the onset of damage at days 1 and 2. BMP4 expression decreased almost significant at day 2,

which correlated well with an increasing degree of morphological damage, increased proliferation, and loss of epithelial differentiation as measured by the decreased SI and likely TFF3 expression. Very recently, a link between the BMP and the Wnt pathways has been demonstrated. It was shown that BMP signaling suppresses Wnt signaling to ensure a balanced control of stem cell proliferation and subsequent epithelial differentiation.[24,26] Here we show that there indeed might be a close relationship between BMP and Wnt pathways, because at day 1 when BMP4 expression is decreased, expression of TCF4, a Wnt effector, increased significantly, which correlated well with increased proliferation and inhibited epithelial differentiation. At day 2, BMP4 remained low, whereas TCF4 returned to a normal level and remained at control level during the following days. At day 3, when damage was most severe, BMP4 was increased, which inversely correlated with proliferation, and correlated with epithelial differentiation, as suggested by the recovery of TFF3 expression level.

BMP is involved in epithelial-mesenchymal signaling[24] and therefore we conclude that the data presented in this study indicate that epithelial-mesenchymal cross-talk is modulated during onset of DOX-induced damage in order to stimulate proliferation instead of differentiation and during severe intestinal damage to induce differentiation and inhibit proliferation. During the regenerative phase, at day 7, BMP4 expression level was down-regulated again, which could be a response to the shortage in number of crypts, since a blockage of BMP4 has been shown to cause stem cells to divide, leading to newly formed crypts.[24,26] Therefore, our findings are in line with the roles of the BMP and Wnt/TCF pathway in epithelial homeostasis/morphogenesis. Furthermore, the decrease in BMP4 might also indirectly cause the observed decrease in SI expression, because inhibition of BMP4 stimulates Wnt signaling, and Wnt signaling itself induces SOX9, a negative regulator of Cdx2, which is a SI transcriptional activator.[26,47,48] In addition, BMP4 has been shown to be directly involved in HNF-1α expression, also a well-known activator of SI transcription.[49] Thus, the decrease in BMP4 might result in a decrease in Cdx2 and HNF-1α expression, two of the most important activators of SI transcription.[48] Currently, it is not known whether the Wnt or BMP4 signaling pathways regulate TFF3 gene expression.

In conclusion, high-dose DOX induces severe damage to the epithelium, which closely resembles damage induced by MTX, indicating that general mechanisms of damage and repair are involved. We show that signaling pathways involving BMP4 and TCF4 and thus epithelial-mesenchymal cross-talk are modulated by DOX-induced damage in such a way that homeostasis of the progenitor compartment is restored by initially inducing cell proliferation and inhibiting differentiation and subsequently inducing differentiation, inhibiting proliferation and promoting crypt fission. Understanding these mechanisms is essential to develop clinical strategies to prevent chemotherapy-induced mucositis.

ACKNOWLEDGEMENTS

We thank Dr. K.Y. Yeh for kindly providing the rabbit polyclonal anti-rat sucrase-isomaltase antiserum and Prof. Dr. D.K. Podolsky for kindly providing the rabbit polyclonal anti-rat trefoil factor family-3 antiserum. This work was supported by a grant from Numico Research BV, Wageningen, the Netherlands and from the Sophia Foundation for Medical Research (SSWO).

REFERENCES

1. Potten CS, Loeffler M. Stem cells: attributes, cycles, spirals, pitfalls and uncertainties. Lessons for and from the crypt. Development 1990;110:1001-1020.
2. Wright NA, Irwin M. The kinetics of villus cell populations in the mouse small intestine. I. Normal villi: the steady state requirement. Cell Tissue Kinet 1982;15:595-609.
3. Duncan M, Grant G. Oral and intestinal mucositis: causes and possible treatments. Aliment Pharmacol Ther 2003;18:853-874.
4. Ijiri K, Potten CS. Response of intestinal cells of differing topographical and hierarchical status to ten cytotoxic drugs and five sources of radiation. Br J Cancer. 1983;47:175-185.
5. Ijiri K, Potten CS. Further studies on the response of intestinal crypt cells of different hierarchical status to eighteen different cytotoxic agents. Br J Cancer 1987;55:113-123.
6. Moore JV. Clonogenic response of cells of murine intestinal crypts to 12 cytotoxic drugs. Cancer Chemother Pharmacol 1985;15:11-15.
7. Pinkerton CR, Cameron CH, Sloan JM, et al. Jejunal crypt cell abnormalities associated with methotrexate treatment in children with acute lymphoblastic leukaemia. J Clin Pathol 1982;35:1272-1277.
8. Taminiau JA, Gall DG, Hamilton JR. Response of the rat small-intestine epithelium to methotrexate. Gut 1980;21:486-492.
9. Trier JS. Morphologic alterations induced by methotrexate in the mucosa of human proximal intestine. I. Serial observations by light microscopy. Gastroenterology 1962;42:295-305.
10. Verburg M, Renes IB, Van Nispen DJ, et al. Specific responses in rat small intestinal epithelial mRNA expression and protein levels during chemotherapeutic damage and regeneration. J Histochem Cytochem 2002;50:1525-1536.
11. Verburg M, Renes IB, Meijer HP, et al. Selective sparing of goblet cells and paneth cells in the intestine of methotrexatetreated rats. Am J Physiol Gastrointest Liver Physiol 2000;279:G1037-1047.
12. Patte C, Laplanche A, Bertozzi AI, et al. Granulocyte colony-stimulating factor in induction treatment of children with non-Hodgkin's lymphoma: a randomized study of the French Society of Pediatric Oncology. J Clin Oncol 2002;20:441-448.
13. Potten CS, Owen G, Booth D. Intestinal stem cells protect their genome by selective segregation of template DNA strands. J Cell Sci 2002;115:2381-2388.
14. Kushner BH, Kramer K, LaQuaglia MP, et al. Reduction from seven to five cycles of intensive induction chemotherapy in children with high-risk neuroblastoma. J Clin Oncol 2004;22:4888-4892.
15. Martin M, Garcia-Donas J, Casado A, et al. Phase II study of pegylated liposomal doxorubicin plus vinorelbine in breast cancer with previous anthracycline exposure. Clin Breast Cancer 2004;5:353-357.
16. Kelly KM, Hutchinson RJ, Sposto R, et al. Feasibility of upfront dose-intensive chemotherapy in children with advanced-stage Hodgkin's lymphoma: preliminary results from the Children's Cancer Group Study CCG-59704. Ann Oncol 13 Suppl 2002;1:107-111.
17. Sonis ST. The pathobiology of mucositis. Nat Rev Cancer 2004;4:277-284.
18. Montgomery RK, Mulberg AE, Grand RJ. Development of the human gastrointestinal tract: twenty years of progress. Gastroenterology 1999;116:702-731.
19. Kedinger M, Duluc I, Fritsch C, et al. Intestinal epithelial-mesenchymal cell interactions. Ann NY Acad Sci 1998;859:1-17.
20. de Santa Barbara P, van den Brink GR, Roberts DJ. Development and differentiation of the intestinal epithelium. Cell Mol Life Sci 2003;60:1322-1332.

21. Radtke F, Clevers H. Self-renewal and cancer of the gut: two sides of a coin. Science 2005;307:1904-1909.

22. Sukegawa A, Narita T, Kameda T, et al. The concentric structure of the developing gut is regulated by Sonic hedgehog derived from endodermal epithelium. Development 2000;127:1971-1980.

23. Bitgood MJ, McMahon AP. Hedgehog and Bmp genes are coexpressed at many diverse sites of cell-cell interaction in the mouse embryo. Dev Biol 1995;172:126-138.

24. Haramis AP, Begthel H, van den Born M, et al. De novo crypt formation and juvenile polyposis on BMP inhibition in mouse intestine. Science 2004;303:1684-1686.

25. Hardwick JC, Van Den Brink GR, Bleuming SA, et al. Bone morphogenetic protein 2 is expressed by, and acts upon, mature epithelial cells in the colon. Gastroenterology 2004;126:111-121.

26. He XC, Zhang J, Tong WG, et al. BMP signaling inhibits intestinal stem cell self-renewal through suppression of Wnt-betacatenin signaling. Nat Genet 2004;36:1117-1121.

27. Hogan BL. Bone morphogenetic proteins in development. Curr Opin Genet Dev 1996;6:432-438.

28. Itoh S, Itoh F, Goumans MJ, et al. Signaling of transforming growth factor-beta family members through Smad proteins. Eur J Biochem 2000;267:6954-6967.

29. Nishanian TG, Kim JS, Foxworth A, et al. Suppression of tumorigenesis and activation of Wnt signaling by bone morphogenetic protein 4 in human cancer cells. Cancer Biol Ther 2004;3:667-675.

30. van de Wetering M, Sancho E, Verweij C, et al. The betacatenin/TCF-4 complex imposes a crypt progenitor phenotype on colorectal cancer cells. Cell 2002;111:241-250.

31. Korinek V, Barker N, Moerer P, et al. Depletion of epithelial stem-cell compartments in the small intestine of mice lacking Tcf4. Nat Genet 1998;19:379-383.

32. Renes IB, Verburg M, Bulsing NP, et al. Protection of the Peyer's patch-associated crypt and villus epithelium against methotrexate-induced damage is based on its distinct regulation of proliferation. J Pathol 2002;198:60-68.

33. Yeh KY, Yeh M, Montgomery RK, et al. Cortisone and thyroxine modulate intestinal lactase and sucrase mRNA levels and activities in the suckling rat. Biochem Biophys Res Commun 1991;180:174-180.

34. Van Beers EH, Buller HA, Grand RJ, et al. Intestinal brush border glycohydrolases: structure, function, and development. Crit Rev Biochem Mol Biol 1995;30:197-262.

35. Dignass A, Lynch-Devaney K, Kindon H, et al. Trefoil peptides promote epithelial migration through a transforming growth factor beta-independent pathway. J Clin Invest 1994;94:376-383.

36. Mashimo H, Wu DC, Podolsky DK, et al. Impaired defense of intestinal mucosainmice lacking intestinal trefoil factor. Science 1996;274:262-265.

37. Theon AP, Metzger L, Griffey S. In situ analysis of cellular proliferation in canine, feline and equine tumors by immunohistochemistry: a comparison of bromodeoxyuridine, proliferating cell nuclear antigen, and interchromatin-associated antigen immunostaining techniques. J Vet Diagn Invest 1994;6:453-457.

38. Bromley M, Rew D, Becciolini A, et al. A comparison of proliferation markers (BrdUrd, Ki-67, PCNA) determined at each cell position in the crypts of normal human colonic mucosa. Eur J Histochem 1996;40:89-100.

39. Nicholson DW, Ali A, Thornberry NA, et al. Identification and inhibition of the ICE/CED-3 protease necessary for mammalian apoptosis. Nature 1995;376:37-43.

40. Lee YJ, Swencki B, Shoichet S, et al. A possible role for the high-mobility group box transcription factor Tcf-4 in vertebrate gut epithelial cell differentiation. J Biol Chem 1999;274:1566-1572.

41. Barker N, Huls G, Korinek V, et al. Restricted high-level expression of Tcf-4 protein in intestinal and mammary gland epithelium. Am J Pathol 1999;154:29-35.

42. Verburg M, Renes IB, Einerhand AW, et al. Isolation-stress increases small intestinal sensitivity to chemotherapy in rats. Gastroenterology 2003;124:660-671.

43. Xian CJ, Howarth GS, Mardell CE, et al. Temporal changes in TFF3 expression and jejunal morphology during methotrexateinduced damage and repair. Am J Physiol 1999;277:G785-795.

44. Playford RJ, Marchbank T, Chinery R, et al. Human spasmolytic polypeptide is a cytoprotective agent that stimulates cell migration. Gastroenterology 1995;108:108-116.

45. Lockhart PB, Sonis ST. Alterations in the oral mucosa caused by chemotherapeutic agents. A histologic study. J Dermatol Surg Oncol 1981;7:1019-1025.

46. Sonis ST, Elting LS, Keefe D, et al. Perspectives on cancer therapy-induced mucosal injury: pathogenesis, measurement, epidemiology, and consequences for patients. Cancer 2004;100:1995-2025.

47. Blache P, van de Wetering M, Duluc I, et al. SOX9 is an intestine crypt transcription factor, is regulated by the Wnt pathway, and represses the CDX2 and MUC2 genes. J Cell Biol 2004;166:37-47.

48. Taylor JK, Boll W, Levy T, et al. Comparison of intestinal phospholipase A/lysophospholipase and sucrase-isomaltase genes suggest a common structure for enterocyte-specific promoters. DNA Cell Biol 1997;16:1419-1428.

49. Nastos A, Pogge von Strandmann E, Weber H, et al. The embryonic expression of the tissue-specific transcription factor HNF1 alpha in Xenopus: rapid activation by HNF4 and delayed induction by mesoderm inducers. Nucleic Acids Res 1998;26:5602-5608.

3

THE EFFECT OF CYTOSTATIC DRUG TREATMENT ON INTESTINE-SPECIFIC TRANSCRIPTION FACTORS CDX2, GATA-4 AND HNF-1α IN MICE

Barbara A.E. de Koning, Dicky J. Lindenbergh-Kortleve, Rob Pieters, Edmond H.H.M. Rings, Hans A. Büller, Ingrid B. Renes, Alexandra W.C. Einerhand.

Cancer Chemotherapy and Pharmacology 57:801-810 (2006).

ABSTRACT

Chemotherapy-induced intestinal damage is a very important dose-limiting side effect for which there is no definitive prophylaxis or treatment. This is in part due to the lack of understanding of its pathophysiology and impact on intestinal differentiation. The objective of this study was to investigate the gene expression of the small intestinal transcription factors HNF-1α, Cdx2, GATA-4 in an experimental model of methotrexate (MTX)-induced intestinal damage, and to correlate these alterations with histological damage, epithelial proliferation and differentiation. HNF-1α, Cdx2 and GATA-4 are critical transcription factors in epithelial differentiation, and in combination they act as promoting factors of the sucrase-isomaltase (SI) gene, an enterocyte-specific differentiation marker which is distinctly downregulated after MTX treatment. Mice received two doses of MTX i.v. on two consecutive days and were sacrificed 1, 3 and 7 or 9 days after final injection. Segments of the jejunum were taken for morphological, immunohistochemical and quantitative analyses. Intestinal damage was most severe at day 3 and was associated with decreased expression of the transcriptional factors HNF-1α, Cdx2 and GATA-4, which correlated well with decreased expression of SI, and seemed inversely correlated with enhanced proliferation of epithelial crypt cells. During severe damage, the epithelium was preferentially concerned with proliferation rather than differentiation, most likely in order to restore the small intestinal barrier function rather than maintaining its absorptive function. Since HNF-1α, Cdx2 and GATA-4 are critical for intestine-specific gene expression and therefore crucial in epithelial differentiation, these results may explain, at least in part, why intestinal differentiation is compromised during MTX treatment.

INTRODUCTION

One of the most severe side effects of chemotherapy is damage of the gastrointestinal tract often referred to as mucositis. Especially, the epithelium in the small intestine is extremely sensitive to cytostatic drug treatment,[1] since it is proliferating rapidly. The loss of intestinal epithelial integrity causes symptoms of malabsorption, like pain and diarrhea, and an enhanced risk on septic bacteraemia. Mucositis is therefore a serious side effect that is often dose-limiting,[2] and influences the quality of life. It is estimated that this disorder affects around 500,000 patients worldwide annually.[3] Despite a great amount of research, there is currently no definitive prophylaxis or treatment for this chemotherapy-induced side effect. This is in part due to the lack of understanding of its pathophysiology.

Methotrexate (MTX) is frequently used in the treatment of leukemia, osteosarcoma and other malignancies. Especially in childhood, cancer patients receiving high dose treatments, MTX is known to cause this severe side effect.[4] MTX is a folate antagonist and a strong inhibitor of dihydrofolate reductase (DHFR), which is a key enzyme in the thymidylate cycle. Because of an arrest in thymidylate biosynthesis, the replication of DNA will be inhibited. Therefore, in the small intestine MTX primarily targets the proliferating cells in the crypts of Lieberkühn.[5]

In animal models, the effects of MTX on the small intestinal epithelium in time are well described and characterized by an inhibition of proliferation, loss of crypts, flattening of the epithelium and atrophy of the villi.[1,6,7] We along with others demonstrated a down-regulation of enterocyte-specific gene expression crucial for degradation and absorption of nutrients.[6-9] Goblet and Paneth cells seem to be selectively spared.[7] Furthermore, the epithelium surrounding the Peyers' patches also seems to be spared from MTX-induced damage, whereas isolation stress seems to aggravate the intestinal damage.[10]

At present, the molecular mechanisms underlying the dynamic processes of intestine-specific gene expression, cell fate determination, cellular differentiation and intestinal development are poorly understood. However, the influence of specific transcription factors is beginning to be unraveled. The epithelial specific transcription factors Cdx2, GATA-4 and HNF-1α are important for intestinal development, differentiation and gene expression. Cdx2, a member of a homeobox gene family related to Drosophila caudal, is expressed in all epithelial cells in the small and large intestine of the adult mouse.[11,12] Cdx2 modulates proliferation, apoptosis, cell-adhesion and columnar morphology.[13-15] Cdx2 is also necessary for the expression of a number of intestine-specific genes.[13,16-18] By targeting these processes and genes, Cdx2 promotes the appearance of a mature intestinal cell phenotype. GATA-4, a member of the GATA gene family, is expressed in heart, ovary, testis, lung, liver and the small intestine, but not the colon.[19] GATA-4 is important for development since GATA-4 knockout mice die at embryonic day 9.5 lacking a primitive heart and foregut. Hepatocyte nuclear factor-1 alpha (HNF-1α) is a homeodomain-containing transcription factor that plays an important role in regulation of

gene expression in pancreatic beta-cells, intestine, kidney and liver.[20] In combination Cdx2, GATA-4 and HNF-1α have been shown to be crucial for developmentally regulated expression of the sucrase– isomaltase (SI) gene[16] as several other enterocyte-specific markers.[12,16,21,22]

Sucrase–isomaltase is a brush border enzyme with an important function in degradation of disaccharides[23] and is specifically expressed by enterocytes in a differentiation-specific pattern and therefore is a widely used marker for intestinal differentiation.[24] SI is almost undetectable at birth and increases to adult levels during the suckling-weaning transition. Its expression is characterized by a strong expression at the crypt-villus junction and mid-villus, and a decreased intensity towards the tips of the villi.[24] The expression of SI is affected by MTX-induced intestinal damage.[9,25]

Cells respond to external stimuli by changes in gene expression, which are largely dependent on transcription factors. In this study we investigated the role of the SI gene transcriptional activators, Cdx2, GATA-4 and HNF-1α, during MTX-induced intestinal damage and repair.

MATERIALS AND METHODS

Animals

Animal experiments were performed with permission of the Animal Ethics Committee of the Erasmus MC-Sophia. Upon arrival at our institute, 10-week-old male BALB/c mice (Charles River, Les Oncins, France) were housed individually in micro-isolator cages under specific pathogen-free conditions with free access to a standard palletized diet (Hope farms, Woerden, The Netherlands) and water. After 1 week of adjustment to the new environment, MTX [Emthrexate (PF) Pharma Chemie, Haarlem, The Netherlands] was injected intravenously. To determine the optimal MTX dose to induce severe intestinal damage and allow regeneration within 7 - 9 days, a dose-response curve was performed with increasing concentrations of MTX (data not shown), ranging from 20 mg/kg in a single dose (which induced mild intestinal damage) to a final concentration of 120 and 60 mg/kg on two subsequent days. The latter dose was chosen in the studies described here.

At day 1 and 0 mice were injected with 120 and 60 mg/kg, respectively. Controls were given equivalent volumes of 0.9% NaCl. Mice were sacrificed at day 1, 3 and 7 or 9 after final MTX injection. Day 1 represents the early phase of the induced intestinal damage, day 3 the phase of severe intestinal damage, day 7 and 9 both represent the regenerative phase in which day 7 is considered as the middle and day 9 the end of intestinal regeneration. Histological, immunohistochemical and protein data were derived from intestinal segments collected at day 9. The quantification of PCNA, HNF-1α, Cdx2 and GATA-4 were performed on nuclear extracts collected at day 7. Per time-point 4-6 MTX-treated animals and 2 control animals were sacrificed. One hour before sacrifice the mice

were injected with 120 μl 10 mg/ml 5-bromo-2¢deoxyuridine (BrdU), a uridine analog, to locate the proliferating cells. Segments of mid-jejunum were collected and either processed immediately for histological analysis or snap-frozen in liquid nitrogen for storage at -80 °C and subsequent protein isolation.

Histochemistry

Five millimeter segments of mid-jejunum were fixed in 4% paraformaldehyde in phosphate-buffered saline (PBS), dehydrated and embedded in Paraplast Plus (Sherwood Medical, Den Bosch, The Netherlands) as previously described.[7] Four micrometer sections were routinely stained with hematoxylin (Vector Laboratories, Burlingame, CA, USA) and eosin (Sigma-Aldrich, Zwijndrecht, The Netherlands) to study morphological alterations of the crypts and villi. Immunohistochemistry (IHC) was performed as described previously[7] with some minor modifications. The sections for BrdU staining required an extra adjustment to this protocol of HCl incubation, washing with borate buffer and pepsin treatment, as described before.[25] In short, sections were blocked as described and incubated overnight with the following antibodies diluted in 1% BSA, 0.1% Triton X-100 in PBS: mouse monoclonal anti-BrdU (1:250, Roche Applied Sciences, Indianapolis, IN, USA), goat polyclonal anti-mouse GATA-4 (1:2,500, sc-1237X, Santa Cruz Biotechnology), goat polyclonal anti-human HNF-1α (1:2,500, sc-6547X, Santa Cruz Biotechnology). For the enterocyte marker SI and transcription factor Cdx2 sections were blocked for 30 min with 1% blocking reagent (Roche, Almere, The Netherlands) in PBS and incubated overnight with rabbit polyclonal anti-rat SI (1:9,000 in PBS, kindly provided by Yeh),[26] or rabbit polyclonal anti-mouse Cdx2 (1:500 in PBS).[14] Immunoreactions were detected using Vectastain ABC Elite Kit (Vector Laboratories) and 3,3'-diaminobenzidine tetrahydrochloride (Sigma-Aldrich, Zwijndrecht, The Netherlands).

Protein dot blotting

The expression of enterocyte markers was detected and quantified as described previously.[9] Briefly, 5 mm segments of the mid-jejunum were homogenized, protein concentration was measured and 50 μg protein of each homogenate was dot-blotted on nitrocellulose (Protran BA83, 0.2 μm; Schleicher & Schuell, Dassel, Germany). Hereafter blots were blocked for 1 h with blocking buffer containing 50 mM Tris, pH 7.8, 5% (wt/vol) nonfat dry milk powder (Campina Melkunie, Eindhoven, The Netherlands), 2 mM $CaCl_2$, 0.05% (vol/vol) Nonidet P40® (BDH, Brunschwig Chemie, Amsterdam, The Netherlands) and 0.01% Antifoam B (Sigma-Aldrich, Zwijndrecht, The Netherlands). Blots were incubated overnight at 4 °C with rabbit polyclonal anti-rat SI (1:1,000)[26] diluted in blocking buffer. After washing with blocking buffer blots were incubated with ^{125}I-labeled protein A (specific activity 30 mCi/mg, Amersham Biosciences, Roosendaal, The Netherlands) for 2 h at room temperature. Specific binding of ^{125}I-labeled protein A to the enterocyte marker antibodies was measured using PhosphorImager detection. The elicited signal was quantified by ImageQuant software (Molecular Dynamics, B&L systems, Zoetermeer, The Netherlands) and the expression of the enterocyte markers was expressed per microgram protein.

Western blot analysis nuclear extracts

Nuclear extracts were prepared as described by Van Seuningen et al.[27] with minor modifications. Immediately after isolation of the intestine, the epithelial cell layer was scraped off from an 8 cm segment of the proximal jejunum and suspended in freshly prepared lysis buffer containing 10 mM HEPES, pH 7.9, 10 mM KCl, 1.5 mM $MgCl_2$, 0.5 mM DTT, 0.5 mM PMSF, 10 μg/ml leupeptin, 10 μg/ml aprotinin, 100 μM sodium molybdate, 10 mM β-glycerophosphate, 10 mM Nafluoride, 100 μM Na-orthovanadate, 13.84 mg/ml p-nitro-phenylphosphate. After centrifugation for 1 min at 9,000 rpm at 4 °C the supernatant was discarded and the pellet resuspended in 150 μl lysis buffer plus 0.1% NP-40 and gently homogenized on ice, vortexed and centrifuged for 10 min at 14,000 rpm at 4 °C. The supernatant containing the cytosol fraction was diluted with 225 μl dilution buffer containing 20 mM HEPES, pH 7.9, 50 mM KCl, 0.2 mM EDTA, 20% glycerol, 0.5 mM DTT, 0.5 mM PMSF and stored at -80 °C. The obtained pellet was resuspended in 125 μl extraction buffer containing 20 mM HEPES, pH 7.9, 420 mM NaCl, 1.5 mM $MgCl_2$, 0.2 mM EDTA, 25% glycerol, 0.5 mM DTT, 0.5 mM PMSF, 10 μg/ml leupeptin, 10 μg/ml aprotinin, 100 μM sodium molybdate, 10 mM β-glycerophosphate, 10 mM sodium fluoride, 100 μM sodium orthovanadate, 13.84 mg/ml *p*-nitro-phenylphosphate. The suspension was gently homogenized, vortexed and centrifuged for 10 min at 14,000 rpm at 4 °C. The supernatant containing the nuclear fraction was diluted with 187.5 μl dilution buffer, centrifuged for 5 min at 14,000 rpm at 4 °C, transferred to a new tube and stored at -80 °C until further processing. Protein concentration was measured using the BCA Protein Assay Reagent (Pierce, Rockford, IL, USA) following the manufacturer's protocol.

Twenty microgram of nuclear extract was loaded per lane and run on a 10% SDS-PAGE. The separated proteins were transferred to nitrocellulose membranes (Protran BA83, 0.2 μm; Schleicher & Schuell) and blocked for 1 h at room temperature in blocking buffer containing 50 mM Tris, pH 7.8, 5% (wt/vol) nonfat dry milk powder (Campina Melkunie, Eindhoven, The Netherlands), 2 mM $CaCl_2$, 0.01% Antifoam B (Sigma-Aldrich, Zwijndrecht, The Netherlands), 0.05% Triton X-100. Blots were incubated overnight at 4 °C with primary antibodies diluted in blocking buffer: goat poly-clonal anti-mouse GATA-4 (1:5,000, sc-1237X, Santa Cruz Biotechnology), goat polyclonal anti-human HNF-1α (1:5,000, sc-6547X, Santa Cruz Biotechnology), mouse monoclonal anti-human Cdx2 (1:1,000, BioGenex, San Ramon, CA, USA), or mouse monoclonal anti-human PCNA, clone PC10 (1:250, Novo Castra Laboratories, Newcastle upon Tyne, UK). After washing with PBS, 0.2% Tween-20 blots bound antibodies were revealed using horseradish peroxidase (HRP) conjugated goat anti-mouse or rabbit anti-goat (1:1,000) and SuperSignal® West Femto Luminol Enhancer kit (Pierce, Rockford, IL, USA). The signal was detected and quantified by the ChemiGenius gel documentation system (Syngene, Cambridge, UK). If necessary blots were stripped by incubating twice for 30 min with 0.2 M glycine, pH 2.2, 0.1% SDS, 1% Tween-20. TCF4, [mouse monoclonal anti-human TCF4, clone 6H5-3 (1:250, Upstate, Waltham, MA, USA)] was used as internal control in the Western blot analysis since the expression of TCF4 was preserved during MTX treatment.

Statistical analysis

Changes in protein expression levels during damage and regeneration were statistically analyzed using the Kruskal-Wallis *H* test followed by the Mann-Whitney *U* test. A $P < 0.05$ was considered statistically significant. Data are presented as the mean ± standard error of the mean (SEM).

RESULTS

MTX damages the epithelial structure and function of the small intestinal epithelium

To ascertain the effect of cytostatic drugs on small intestinal morphology, epithelial proliferation, differentiation and function, we developed a mouse model. The mice were injected i.v. at day 1 with 120 mg/kg MTX and at day 0 with 60 mg/kg MTX, creating a window in the MTX administration similar to the previously described rat MTX model.[32,33] and in a more severe phase at day 3. The subsequent regeneration of the intestinal epithelium was studied at day 7 or 9. Days 7 and 9 represent the regenerative phase in which day 7 is considered as mid-regenerative phase and day 9 as the end of the regenerative phase. The histological, immunohistochemical and protein data were collected at day 9. Data derived from nuclear extracts were obtained at day 7. Histological evaluation of the jejunum revealed progressive loss of structure characterized by flattening of villus and crypt epithelial cells, progressive villus atrophy, crypt loss and crypt abscesses, starting at day 1 (Figure 1). Intestinal damage was most severe at day 3, thereafter the jejunal epithelium regenerated and was virtually normal at day 9.

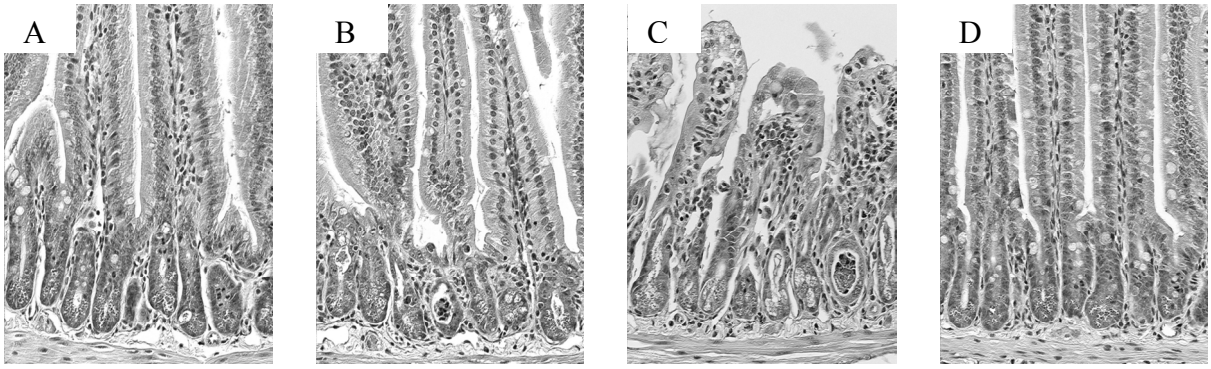

Figure 1 *Morphology of the murine small intestine after MTX treatment. BALB/c mice were treated with 120 and 60 mg/kg MTX i.v. at day 1 and 0. Segments of the small intestine were collected at day 1, representing early damage; at day 3, representing severe intestinal damage; and at day 7 or 9, representing the regenerative phase. The intestinal segments were stained with hematoxiin and eosin for morphological evaluation. Morphology of the jejunum of control mouse (A), at day 1 (B), day 3 (C) and day 9 (D). The morphology was mildly affected at day 1 (B), characterized by mild flattening of crypt epithelium and development of a few crypt-abcesses. At day 3 (C) the morphology was severely affected: extensive flattening of crypt epithelium, villus atrophy and progressive deterioration of the lamina propria. At day 9 (D) the morphology was virtually normal again. These photographs are representative examples of a group of four to six animals per time-point*

To gain insight in the expression of an intestine-specific brush border enzyme after MTX-treatment, a SI immunohistochemical staining was performed. At day 1 SI was expressed at the brush border along the whole villi, which was comparable with the expression of SI in the control epithelium (Figures 2A, B). SI expression was virtually absent at day 3, when morphological damage was most severe (Figure 2C). Only weak staining was still detectable on small parts of the villi where the epithelium was less affected. During the regenerative phase at day 9 the expression of SI was back to the control level again (Figure 2D).

To quantify these observed histological changes, protein dot blotting analyses were performed using an enterocyte-specific SI antibody (Figure 3). This revealed in essence the same results as the immunohistological data. The SI protein expression at day 1 was similar to the control situation. The expression decreased significantly at day 3, concomitant with the most severe epithelial damage and returned to control level at day 9.

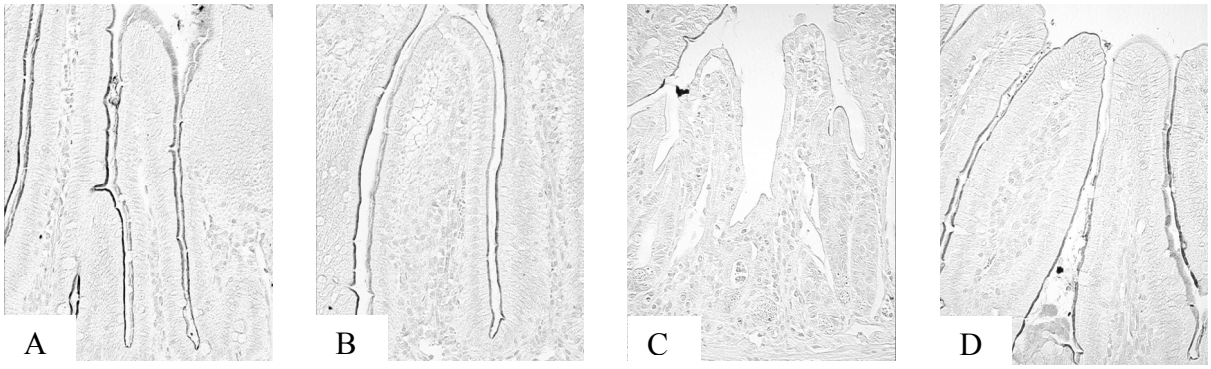

Figure 2 *Effect of MTX treatment on the enterocyte-specific sucrase–isomaltase (SI) expression in the small intestinal epithelium. SI expression in the jejunum of a control mouse (A) and mice at day 1 (B), 3 (C) and 9 (D), detected by immunohistochemistry. Brush border staining of SI was readily detectable in the control mouse (A) at day 1 (B), was virtually absent at day 3 (C) and was normal again at day 9 (D)*

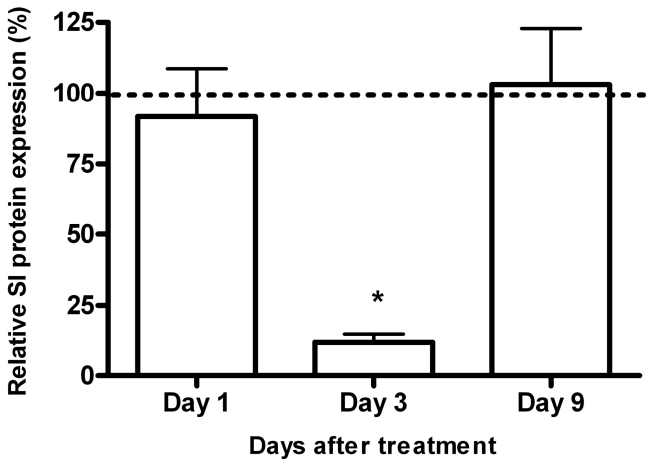

Figure 3 *The relative SI protein expression of the small intestine. Protein expression was quantified by protein dot blotting analysis using a specific polyclonal SI antiserum. The SI protein expression of the control mice was set at 100%. SI expression remained almost stable at day 1, but decreased significantly at day 3. The SI expression returned to normal levels at day 9. *P < 0.05 day 3 versus control*

Increase of epithelial proliferation during severe MTX-induced damage

Loss of epithelial structure and SI expression were most pronounced at day 3. To determine the rate of epithelial proliferation during the period of MTX-induced damage and subsequent regeneration, two proliferation assays were performed. Proliferation was localized by detection of incorporated BrdU, injected 1 h before the mice were sacrificed, and quantified by determining the expression of the proliferation cell nuclear antigen (PCNA) in jejunal epithelium at several time-points similar as described previously.[28,29] At day 1, BrdU incorporation was localized to the lower part of the crypts, virtually the same as in the control situation (Figure 4A). The epithelial proliferation zone increased dramatically at day 3 and was localized almost along the entire length of the crypts. During the regenerative phase at day 9 proliferation decreased again, but was still slightly higher than control.

The quantitative PCNA data showed similar changes in the intestinal proliferation after MTX treatment (Figure 4B). PCNA expression decreased to 65% of control level at day 1, but this decrease did not reach statistical significance. PCNA expression increased significantly (almost sixfold) at day 3, a time-point at which morphological damage was most severe. During regeneration at day 7 epithelial PCNA expression decreased, but was still elevated in comparison to the PCNA expression in the control situation. In Figure 4C, a representative Western blot demonstrating the expression of PCNA and the internal control TCF-4 are shown.

Down-regulation of the intestine-specific transcription factors

The intestine-specific transcription factors Cdx2, GATA-4 and HNF-1α are important in intestinal development, differentiation and morphogenesis. Moreover, the combination of these three transcription factors specifically activate the transcription of SI.[16] Therefore, the current study was extended to determine whether the down-regulation of intestinal differentiation illustrated by the decrease in SI expression was preceded by alterations in expression of these three transcription factors. To study the effect of MTX on the localization and expression of these three specific transcription factors, immunohistochemical staining was performed on sections of the collected intestine. All three transcription factors were detectable in the nuclei of jejunal epithelial cells along the crypt-villus axes (Figure 5). Staining was not detectable in the Paneth cells at the bottom of the crypts. At day 1 the expression of Cdx2, GATA-4 and HNF-1α was similar to the control situation. At day 3 the expression of these transcription factors was virtually absent in the crypt cells and the number of villus cells expressing them was drastically decreased (Figure 5). The nuclear expression of Cdx2 completely disappeared, however, there was some cytoplasmatic staining of Cdx2 visible at the base of the villi. At day 9 expression and localization of all three transcription factors were similar to control (data not shown).

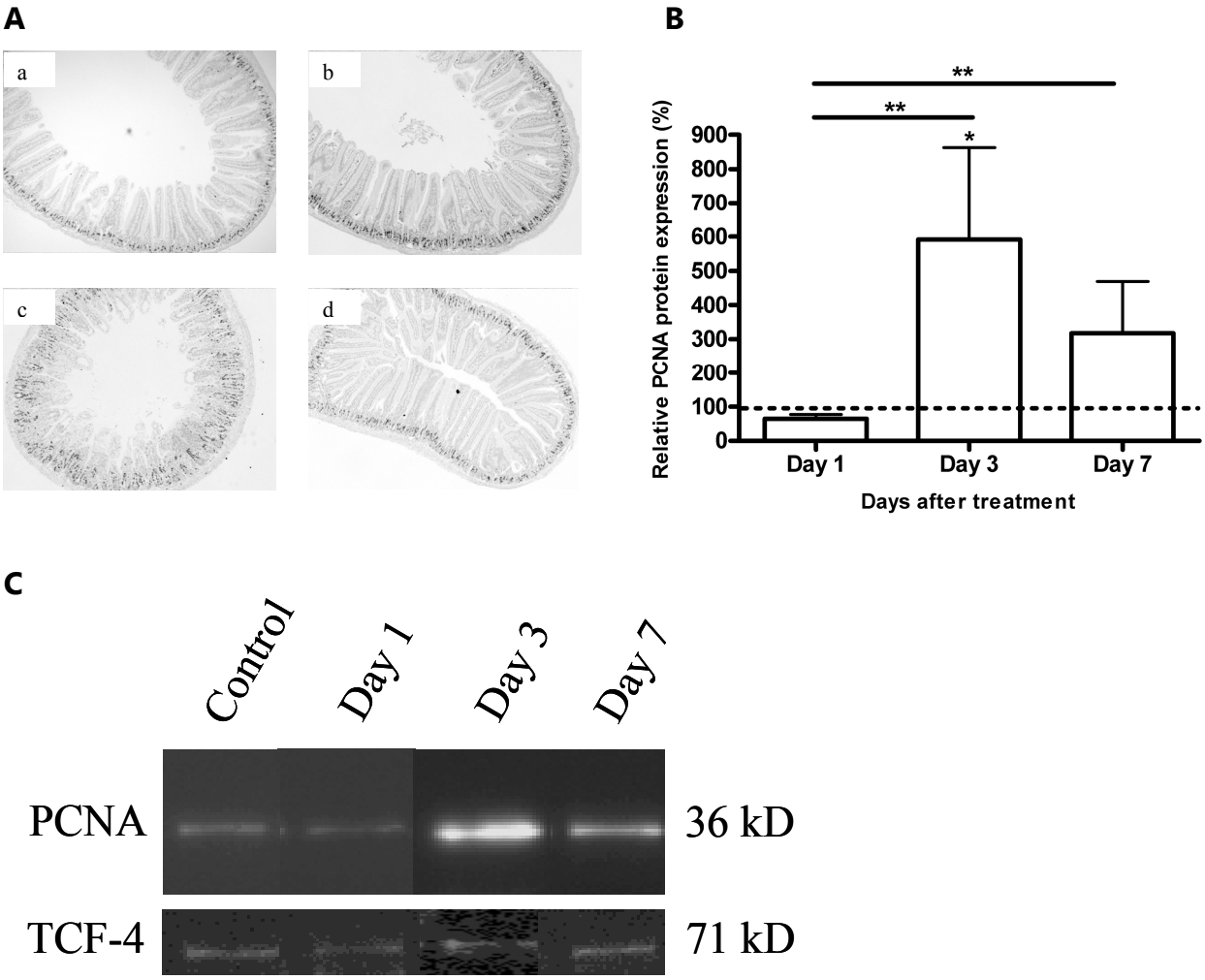

Figure 4 *Effect of MTX treatment on epithelial proliferation. Localization of epithelial proliferation was visualized by detection of BrdU incorporation (A). BrdU incorporation of the jejunum of a control mouse (a) and mice at day 1 (b), day 3 (c) and day 9 (d). At day 1 (b), BrdU incorporation was still localized to the lower part of the crypts matching the control situation. At day 3 (c), epithelial proliferation increased and was localized almost along the entire length of the crypts. At day 9 (d) the crypts showed still some hyper-proliferation compared to control. PCNA expression was quantified by Western blot analysis using a PCNA-specific monoclonal antibody (B). The PCNA protein expression of the control mice was set at 100%. PCNA protein expression was unchanged at day 1, and increased significantly at day 3 in comparison to control situation and expression at day 1. Thereafter the expression decreased during regenerative phase at day 7, but was still relatively elevated to the control situation and even significantly increased in comparison to day 1. *P < 0.05 day 3 versus control. **P < 0.05 day 1 versus day 3 and day 1 versus day 7. Representative Western blot demonstrating PCNA and TCF4 expression which was used as internal control (C). All results are shown for one mouse at each time point. To the right the size of the proteins are given*

The expression of the intestine-specific transcription factors Cdx2, GATA-4 and HNF-1α before and after MTX treatment was quantified by Western blot analyses of nuclear extracts derived from the jejunal segments. All measured transcription factors showed a similar pattern of expression after MTX treatment (Figure 6). Strikingly, at day 1 all three transcription factors showed (a trend towards) increased expression; Cdx2 expression was 25-fold higher, HNF-1α 1.6-fold higher, and GATA-4 was twofold higher than in controls. At day 3 Cdx2 expression decreased to virtually nondetectable levels, HNF-1α decreased to 50% and GATA-4 to 20% of control level. The regenerative phase (day 7) was

characterized by a significant increase in expression of all three transcription factors relative to day 3, Cdx2 and HNF-1α were also significantly increased in comparison to control situation. Cdx2 expression was 14-fold higher, HNF-1α. 3.8-fold and GATA-4 threefold higher than control levels (Figure 6).

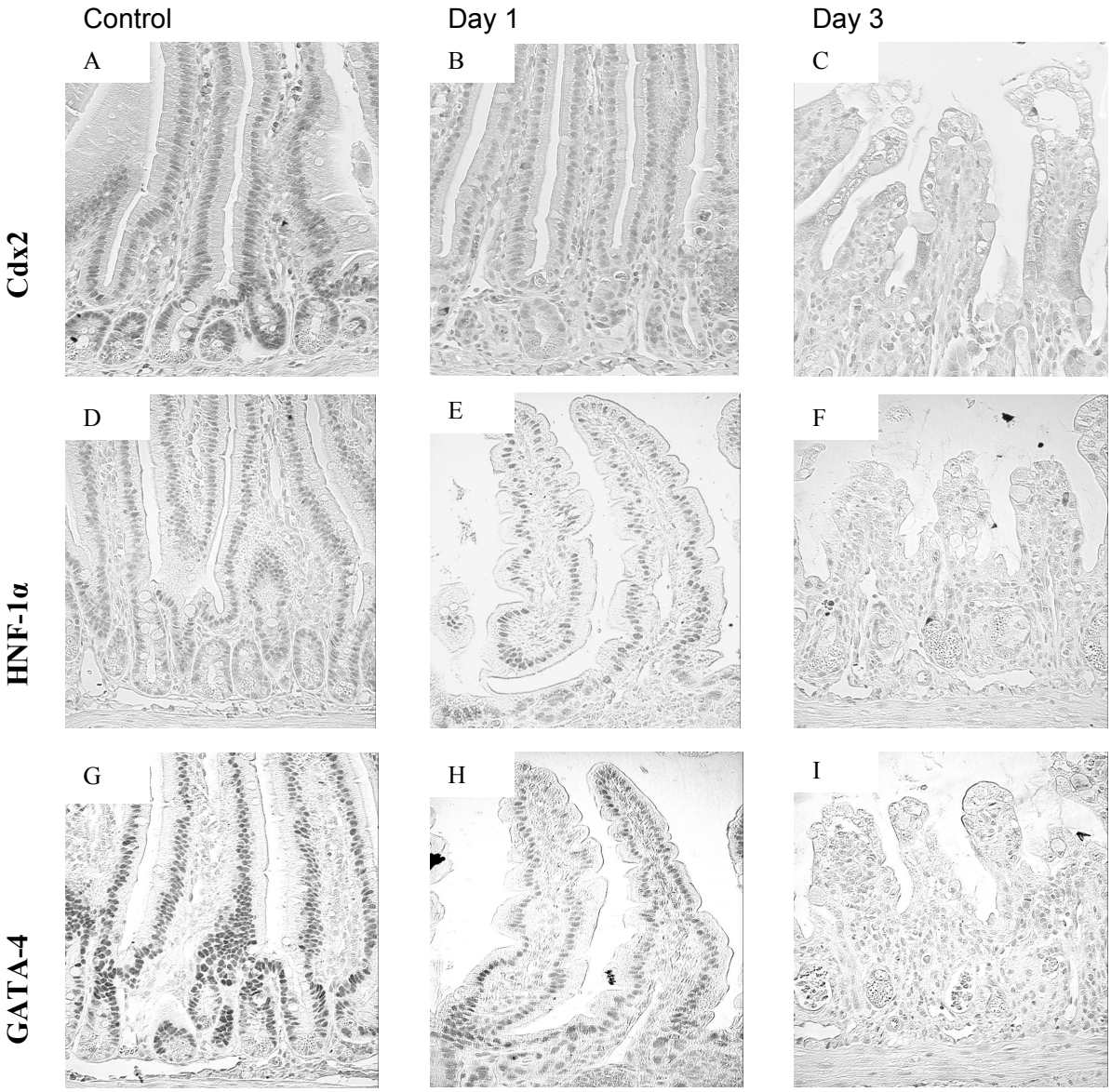

Figure 5 *Effect of MTX treatment on the enterocyte-specific transcription factors in the small intestinal epithelium. Immunohistochemical staining of Cdx2 (A), HNF-1α. (D) and GATA-4 expression (G) in control mice. At day 1, Cdx2 (B), HNF-1α. (E) and GATA-4 (H) showed no changes in expression, but at day 3, the expression of Cdx2 (C), HNF-1α. (F), GATA-4 (I) was down regulated. At day 7 (data not shown) the same pattern of expression was seen as in control mice*

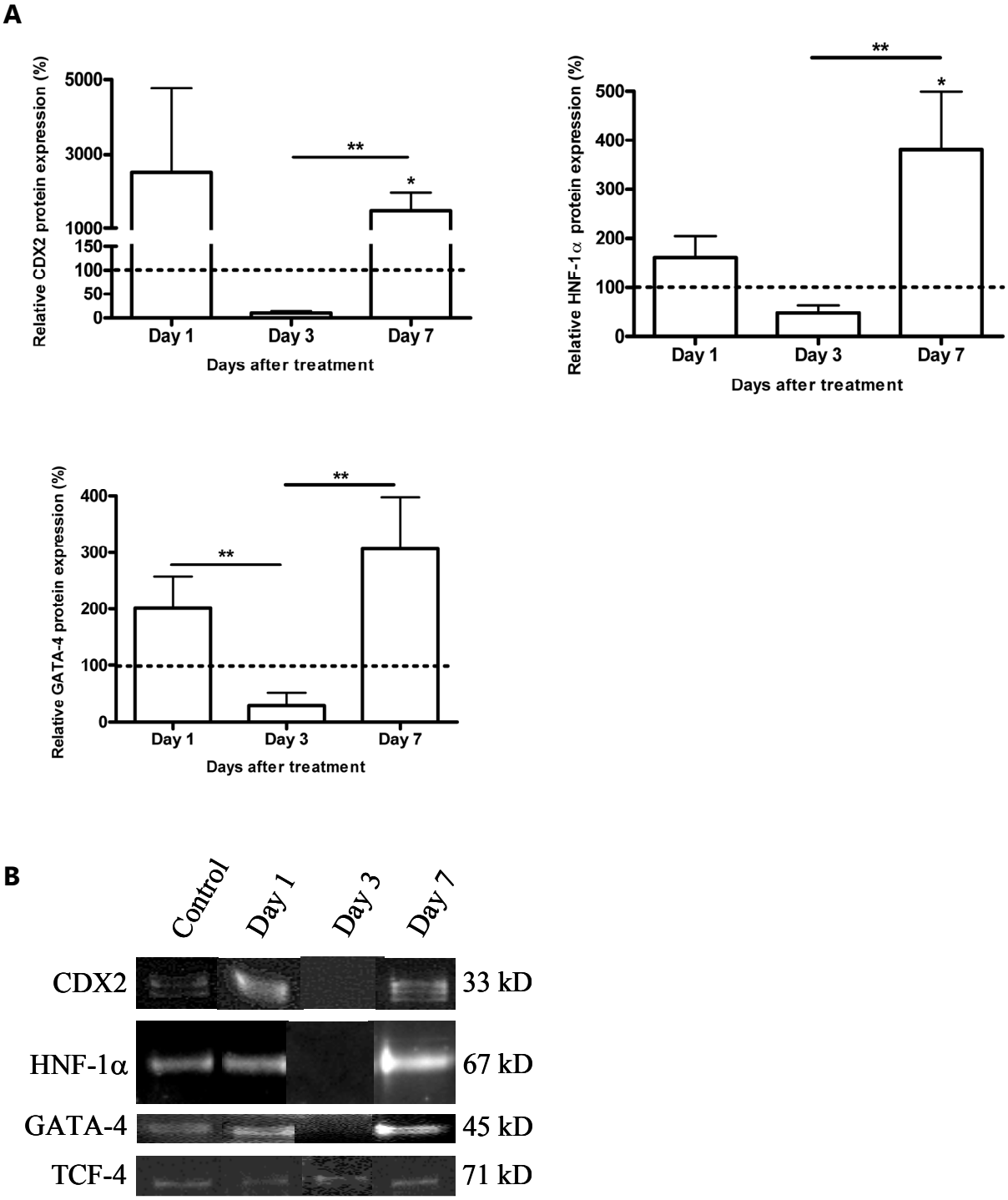

Figure 6 *Expression of the intestine-specific transcription factors Cdx2, HNF-1α, GATA-4. Protein expression of Cdx2, HNF-1α and GATA-4 was determined by Western blot analysis using a Cdx2-specific monoclonal antibody and HNF-1α-specific and GATA-4-specific antisera. Representative Western blots demonstrating the expression of the selected intestine-specific transcription factors (A). All results are shown for one mouse at each time-point. To the right the size of the proteins are indicated. For quantification the protein expression of the control mice was set at 100% (B). The expression of Cdx2, HNF-1α and GATA-4 showed a trend toward an increased expression at day 1, and a decreased expression at day 3. Both increases were not significant. At day 7 the expression of Cdx2 and HNF-1α was significantly increased in comparison to the controls, GATA-4 expression showed a trend toward increased expression. All three transcription factors were significantly increased at day 7 in comparison to the expression at day 3. *P < 0.05, day 7 of Cdx2 and HNF-1α versus control, **P < 0.05, day 3 of Cdx2, HNF-1α and GATA-4 versus day 7, and GATA-4 day 1 versus day 3*

DISCUSSION

The objective of this study was to investigate the gene expression of the transcription factors Cdx2, GATA-4 and HNF-1α. in an experimental mouse model of MTX-induced mucositis, and to correlate these alterations with histological damage, epithelial proliferation and SI expression as a marker of enterocyte differentiation. To the best of our knowledge, this is the first time that the changes of these transcription factors were studied in a damage and regeneration model.

In the present study, we observed severe mucosal damage characterized by crypt loss, crypt abscesses, flattening of epithelial cells and villus atrophy at day 3. At day 9, during the regenerative phase, epithelial morphology was virtually normal again. This mouse model therefore was ideal to study responses during damage and subsequent regeneration.

The data presented here show that the cytostatic drug MTX has a time-dependent effect on the small intestinal epithelial proliferation. The epithelium responded by an initial slight decrease in proliferation at day 1, but at day 3 during severe epithelial damage a subsequent significant increase in the rate of proliferation was observed. In the regenerative phase, at day 7, proliferation decreased again, but was still significantly higher than control levels. It is of note that, although the induced morphological damage at day 3 was very severe, the degree of proliferation inhibition at day 1 was very limited. This could suggest that complete inhibition of proliferation did not take place or, with the time-points taken, we might have missed the complete inhibition. However, in the light of recent findings it is perhaps more likely that the induced damage is due to a multi-factorial process and not only depending on inhibition of stem cell proliferation.[30] Other cells in the intestinal mucosa also seem to be involved in the induction of mucositis by producing pro-inflammatory cytokines and reactive oxygen radicals.[30] This might explain why a drastic inhibition of proliferation at day 1 was not observed.

Here, we demonstrated a significant down-regulation of the enterocyte marker SI at day 3 after MTX treatment which is similar to what has been described for the rat model.[6,7,9,25] The clinical consequence of SI down-regulation is dysfunction of degradation and uptake of sugars by the intestine during villus atrophy. In the rat, other enterocyte markers like lactase, I-FABP, L-FABP, SGLT1 and GLUT5 were also downregulated after MTX treatment similarly to SI, indicating that SI is a good marker for enterocyte gene expression after MTX. At day 3, when morphological damage was most severe and the epithelial SI expression was drastically downregulated, a significant increase in epithelial proliferation was observed compared to control levels. This suggests that during severe intestinal damage, epithelial differentiation was compromised and not epithelial proliferation, as earlier studies also showed.[6,7,25]

Quantification of Cdx2, GATA-4 and HNF-1α after MTX treatment resulted in a trend towards increased expression at day 1, and a decreased expression at day 3, during severe morphological damage. Besides stimulating the SI promoter the transcription factors Cdx2, GATA-4 and HNF-1α are all involved in intestinal differentiation. [11,12,14-18,21,31] This suggests that the observed alterations in expression of these transcription factors during severe MTX-induced damage may lead to changes in the epithelial differentiation.

Previously, it has been shown that cytostatic drugs induce oxidative stress and activation of NFκB as early events in pathways leading to intestinal damage.[30] NFκB is considered a primary regulator of stress response, and activates a number of transcription factors such as Cdx2.[32,33] Therefore, the initial increase of transcription factor expression at day 1 after MTX treatment could be explained by the induction of NFκB by MTX. The subsequent decreased Cdx2, HNF-1α and GATA-4 expression occurred at the same time as the decreased SI expression and significantly increased the proliferation, suggesting that the epithelium is more involved in proliferation rather than maintaining its absorptive function and fully differentiated status. This switch from differentiation to proliferation could be caused by the decrease in Cdx2 expression, because Cdx2 plays a key role in both proliferation and differentiation.[15] On the one hand Cdx2 upregulates P21 (WAF/CIP),[13,34] a cyclin-dependent kinase inhibitor and an active inhibitor of cell proliferation, for the benefit of cell differentiation and maturation. On the other hand Cdx2 stimulates a number of intestine-specific cell fate and differentiation markers like carbonic anhydrase I, intestinal mucin MUC2, IPAL, lactase-phlorizin hydrolase, Math1, and Notch.[31] Thus, the decrease of Cdx2 observed at day 3 might result in a decrease of differentiation markers directly and/or indirectly via down-regulation of p21 expression. The down-regulation in p21 expression in its turn might lead to stimulation of proliferation and loss of differentiation. The mechanism by which MTX down-regulates Cdx2 in this model has not been elucidated. However, we speculate that, as in colon cancer, Cdx2 expression may be downregulated as a result of defects in its transcriptional activation, decreased mRNA synthesis or by gene silencing via DNA hypermethylation and/or histone modifications.[35]

This study provides new insight in the pathophysiology of mucositis. The presumed cytotoxic mechanism of MTX, inhibition of DNA replication, is only partially responsible for the MTX-induced intestinal damage. Especially, loss of differentiation and intestinal function, in particular absorption, seemed at least in part to be caused by an inhibition of Cdx2, HNF-1α and GATA-4 expression during severe MTX-induced intestinal damage. Therefore these transcription factors are possible targets in mucositis therapy.

In summary, we report here that after MTX treatment of mice expression of transcription factors Cdx2, HNF-1α and GATA-4, involved in epithelial differentiation, were temporarily and regionally modulated in a way that correlated well with the intestinal morphology and with the expression of SI, and seemed to be inversely correlated with proliferation of epithelial crypt cells. During severe damage, the epithelium was preferentially involved

with proliferation rather than differentiation, most likely in order to restore the small intestinal barrier function rather than maintaining its absorptive function. Since HNF-1α, Cdx2 and GATA-4 are critical for intestine-specific gene expressions and therefore crucial in epithelial differentiation, these results may explain, at least in part, why intestinal differentiation is compromised during MTX treatment.

ACKNOWLEDGEMENTS

We thank Dr. K.Y. Yeh for kindly providing the rabbit polyclonal anti-rat sucrase–isomaltase antiserum. This work was supported by a grant from Numico Research BV, Wageningen, The Netherlands and from the Sophia Foundation for Medical Research (SSWO). E.H.H.M.R. is supported by a fellowship of the Royal Netherlands Academy of Arts and Sciences.

REFERENCES

1. Potten CS, Merritt A, Hickman J, Hall P, Faranda A. Characterization of radiation-induced apoptosis in the small intestine and its biological implications. Int J Radiat Biol 1994;65:71-78.
2. Sonis ST, Elting LS, Keefe D, Peterson DE, Schubert M, Hauer-Jensen M, Bekele BN, Raber-Durlacher J, Donnelly JP, Rubenstein EB. Perspectives on cancer therapy-induced mucosal injury: pathogenesis, measurement, epidemiology, and consequences for patients. Cancer 2004;100:1995-2025.
3. Duncan M, Grant G. Oral and intestinal mucositis-causes and possible treatments. Aliment Pharmacol Ther 2003;18:853-874.
4. Pinkerton CR, Cameron CH, Sloan JM, Glasgow JF, Gwevava NJ. Jejunal crypt cell abnormalities associated with methotrexate treatment in children with acute lymphoblastic leukaemia. J Clin Pathol 1982;35:1272-1277.
5. Ijiri K, Potten CS. Further studies on the response of intestinal crypt cells of different hierarchical status to eighteen different cytotoxic agents. Br J Cancer 1987;55:113-123.
6. Taminiau JA, Gall DG, Hamilton JR. Response of the rat small-intestine epithelium to methotrexate. Gut 1980;21:486-492.
7. Verburg M, Renes IB, Meijer HP, Taminiau JA, Buller HA, Einerhand AW, Dekker J. Selective sparing of goblet cells and paneth cells in the intestine of methotrexate-treated rats. Am J Physiol Gastrointest Liver Physiol 2000;279:G1037-G1047.
8. Naruhashi K, Nadai M, Nakao M, Suzuki N, Nabeshima T, Hasegawa T. Changes in absorptive function of rat intestine injured by methotrexate. Clin Exp Pharmacol Physiol 2000;27:980-986.
9. Verburg M, Renes IB, Van Nispen DJ, Ferdinandusse S, Jorritsma M, Buller HA, Einerhand AW, Dekker J. Specific responses in rat small intestinal epithelial mRNA expression and protein levels during chemotherapeutic damage and regeneration. J Histochem Cytochem 2002;50:1525-1536.
10. Verburg M, Renes IB, Einerhand AW, Buller HA, Dekker J. Isolation-stress increases small intestinal sensitivity to chemotherapy in rats. Gastroenterology 2003-124:660-671.
11. Freund JN, Domon-Dell C, Kedinger M, Duluc I. The Cdx-1 and Cdx-2 homeobox genes in the intestine. Biochem Cell Biol 1998;76:957-969.
12. Clatworthy JP, Subramanian V. Stem cells and the regulation of proliferation, differentiation and patterning in the intestinal epithelium: emerging insights from gene expression patterns, transgenic and gene ablation studies. Mech Dev 2001;101:3-9.
13. Bai YQ, Miyake S, Iwai T, Yuasa Y. CDX2, a homeobox transcription factor, upregulates transcription of the p21/ WAF1/CIP1 gene. Oncogene 2003;22:7942-7949.
14. Rings EH, Boudreau F, Taylor JK, Moffett J, Suh ER, Traber PG. Phosphorylation of the serine 60 residue within the Cdx2 activation domain mediates its transactivation capacity. Gastroenterology 2001;121:1437-1450.
15. Suh E, Traber PG. An intestine-specific homeobox gene regulates proliferation and differentiation. Mol Cell Biol 1996;16:619-625.
16. Boudreau F, Rings EH, van Wering HM, Kim RK, Swain GP, Krasinski SD, Moffett J, Grand RJ, Suh ER, Traber PG. Hepatocyte nuclear factor-1 alpha, GATA-4, and caudal related homeodomain protein Cdx2 interact functionally to modulate intestinal gene transcription. Implication for the developmental regulation of the sucrase-isomaltase gene. J Biol Chem 2002;277:31909-31917.
17. Mesquita P, Jonckheere N, Almeida R, Ducourouble MP, Serpa J, Silva E, Pigny P, Silva FS, Reis C, Silberg D, Van Seuningen I, David L. Human MUC2 mucin gene is transcriptionally regulated by Cdx homeodomain proteins in gastrointestinal carcinoma cell lines. J Biol Chem 2003;278:51549-51556.
18. Uesaka T, Kageyama N, Watanabe H. Identifying target genes regulated downstream of Cdx2 by microarray analysis. J Mol Biol 2004;337:647-660.

19. Molkentin JD. The zinc finger-containing transcription factors GATA-4, -5, and -6. Ubiquitously expressed regulators of tissue-specific gene expression. J Biol Chem 2000;275:38949-38952.

20. Ryffel GU. Mutations in the human genes encoding the transcription factors of the hepatocyte nuclear factor (HNF)1 and HNF4 families: functional and pathological consequences. J Mol Endocrinol 2001;27:11-29.

21. Fang R, Olds LC, Santiago NA, Sibley E. GATA family transcription factors activate lactase gene promoter in intestinal Caco-2 cells. Am J Physiol Gastrointest Liver Physiol 2001;280:G58-G67.

22. Fitzgerald K, Bazar L, Avigan MI. GATA-6 stimulates a cell line-specific activation element in the human lactase promoter. Am J Physiol 1998;274:G314-G324.

23. Van Beers EH, Buller HA, Grand RJ, Einerhand AW, Dekker J. Intestinal brush border glycohydrolases: structure, function, and development. Crit Rev Biochem Mol Biol 1995;30:197-262.

24. Rings EH, Krasinski SD, van Beers EH, Moorman AF, Dekker J, Montgomery RK, Grand RJ, Buller HA. Restriction of lactase gene expression along the proximal-todistal axis of rat small intestine occurs during postnatal development. Gastroenterology 1994;106:1223-1232.

25. Renes IB, Verburg M, Bulsing NP, Ferdinandusse S, Buller HA, Dekker J, Einerhand AW. Protection of the Peyer's patch-associated crypt and villus epithelium against methotrexate-induced damage is based on its distinct regulation of proliferation. J Pathol 2002;198:60-68.

26. Yeh KY, Yeh M, Montgomery RK, Grand RJ, Holt PR. Cortisone and thyroxine modulate intestinal lactase and sucrase mRNA levels and activities in the suckling rat. Biochem Biophys Res Commun 1991;180:174-180.

27. Van Seuningen I, Ostrowski J, Bustelo XR, Sleath PR, Bomsztyk K. The K protein domain that recruits the interleukin 1-responsive K protein kinase lies adjacent to a cluster of c-Src and Vav SH3-binding sites. Implications that K protein acts as a docking platform. J Biol Chem 1995;270:26976-26985.

28. Theon AP, Metzger L, Griffey S. In situ analysis of cellular proliferation in canine, feline and equine tumors by immunohistochemistry: a comparison of bromodeoxyuridine, proliferating cell nuclear antigen, and interchromatin-associated antigen immunostaining techniques. J Vet Diagn Invest 1994;6:453-457.

29. Bromley M, Rew D, Becciolini A, Balzi M, Chadwick C, Hewitt D, Li YQ, Potten CS. A comparison of proliferation markers (BrdUrd, Ki-67, PCNA) determined at each cell position in the crypts of normal human colonic mucosa. Eur J Histochem 1996;40:89-100.

30. Sonis ST. The pathobiology of mucositis. Nat Rev Cancer 2004;4:277-284.

31. Taylor JK, Boll W, Levy T, Suh E, Siang S, Mantei N, Traber PG. Comparison of intestinal phospholipase A/lysophospholipase and sucrase-isomaltase genes suggest a common structure for enterocyte-specific promoters. DNA Cell Biol 1997;16:1419-1428.

32. Carlsen H, Alexander G, Austenaa LM, Ebihara K, Blomhoff R. Molecular imaging of the transcription factor NFkappaB, a primary regulator of stress response. Mutat Res 2004;551:199-211.

33. Kim S, Domon-Dell C, Wang Q, Chung DH, Di Cristofano A, Pandolfi PP, Freund JN, Evers BM. PTEN and TNFalpha regulation of the intestinal-specific Cdx-2 homeobox gene through a PI3K, PKB/Akt, and NF-kappaB-dependent pathway. Gastroenterology 2002;123:1163-1178.

34. Gartel AL, Tyner AL. Transcriptional regulation of the p21(WAF1/CIP1) gene. Exp Cell Res 1999;246:280-289.

35. Hinoi T, Loda M, Fearon ER. Silencing of CDX2 expression in colon cancer via a dominant repression pathway. J Biol Chem 2003;278:44608-44616.

4

METHOTREXATE-INDUCED MUCOSITIS IN MUCIN 2-DEFICIENT MICE

Barbara A.E. de Koning, Maria van der Sluis, Dicky J. Lindenbergh-Kortleve, Anna Velcich, Rob Pieters, Hans A. Büller, Alexandra W.C. Einerhand, Ingrid B. Renes.
(Barbara A.E. de Koning and Maria van der Sluis participated equally in this study)

Journal of Cellular Physiology 210:144-152 (2007).

ABSTRACT

The mucin Muc2, which is the main structural component of the protective mucus layer, has shown to be upregulated during chemotherapy-induced mucositis. As Muc2 has shown to have protective capacities, upregulation of Muc2 may be a counter reaction of the intestine protecting against mucositis. Therefore, increasing Muc2 protein levels could be a therapeutic target in mucositis prevention or reduction. Our aim was to determine the role of Muc2 in chemotherapy-induced mucositis. Mucositis was induced in Muc2 knockout ($Muc2^{-/-}$) and wild type ($Muc2^{+/+}$) mice by injecting methotrexate (MTX). Animals were weighed and sacrificed on days 2 - 6 after MTX treatment and jejunal segments were analyzed. Before MTX treatment, the small intestine of $Muc2^{+/+}$ and $Muc2^{-/-}$ mice were similar with respect to epithelial morphology and proliferation. Moreover, sucrase-isomaltase and trefoil factor-3 protein expression levels were comparable between $Muc2^{+/+}$ and $Muc2^{-/-}$ mice. Up to day 3 after MTX treatment, percentages of weight-loss did not differ. Thereafter, $Muc2^{+/+}$ mice showed a trend towards regaining weight, whereas $Muc2^{-/-}$ mice continued to lose weight. Surprisingly, MTX-induced intestinal damage of $Muc2^{-/-}$ and $Muc2^{+/+}$ mice was comparable. Prior to MTX-injection, tumor necrosis factor-α and interleukin-10 mRNAs were upregulated in $Muc2^{-/-}$ mice, probably due to continuous exposure of the intestine to luminal antigens. Muc2 deficiency does not lead to an increase in chemotherapy-induced mucositis. A possible explanation is the mechanism by which Muc2 deficiency may trigger the immune system to release interleukin-10, an anti-inflammatory cytokine before MTX-treatment.

INTRODUCTION

Mucositis is one of the most frequent and severest side effects of anti-cancer chemotherapy, for which there is still no definitive prophylaxis. Around 500,000 patients worldwide suffer from mucositis annually.[1] The disorder causes considerable oral and abdominal pain, diarrhea, and weight-loss. Moreover, patients suffering from mucositis are predisposed to life-threatening infections.[2-4] All together, this could lead to forced reduction of chemotherapy intensity, thereby potentially reducing the efficacy of anti-cancer treatment.[4,5]

The intestinal mucus layer plays an important role in epithelial defense against mechanical stress, luminal pathogens, enzymes, and toxins.[6-8] Goblet cells secrete molecules, such as mucins and trefoil factors that serve protective roles in the gut. Mucins are the most important structural component of mucus layer covering the epithelial cells. The intestine abundantly expresses the secretory mucin, Mucin 2 (Muc2).[9,10] Abnormalities of secreted products of goblet cells could affect the physical barrier function of the mucus layer in the intestine.

Recent research, supporting the hypothesis that Muc2 might contribute to epithelial defense against chemotherapy-induced damage, showed a halving of the number of goblet cells on days 1 - 2 after treatment with methotrexate (MTX).[11,12] Remarkably, Muc2 protein expression was significantly increased during all phases of MTX-induced damage.[11,12]

The role of Muc2 in the protection against mucositis is still unclear, but if its protective capacities could be demonstrated, increasing Muc2 protein levels could be a therapeutic target in mucositis prevention or reduction. We used an experimental Muc2-deficient ($Muc2^{-/-}$) mice model[13,14] to analyze the role of Muc2 in epithelial protection against MTX-induced intestinal damage.

MATERIALS AND METHODS

Animals

The previously described $Muc2^{-/-}$ mice of mixed genetic background, were backcrossed onto a 129SV (Charles River, Maastricht, the Netherlands) genetic background for nine generations followed by intercrosses to generate mice homozygous for the Muc2 disruption. Throughout the backcrossing procedure, the targeted Muc2 gene was monitored as previously described.[13]

All mice were housed in micro-isolator cages under specific pathogen-free conditions with free access to standard rodent pellets (Special Diets Services, Witham, Essex, UK) and acidified tap water. Animal experiments were performed with permission of the Erasmus MC Animal Ethics Committee (Rotterdam, the Netherlands).

Clinical symptoms

Groups of Muc2$^{+/+}$ and Muc2$^{-/-}$ mice were monitored from 5 until 12 weeks of age. Weekly, weight and clinical signs such as softness of the stool and appearance of fecal occult blood[15] were assessed. At ages 5, 8, and 12 weeks, four mice per group were sacrificed.

MTX-induced mucositis

Mice, (n = 16, each group) 8 weeks of age, were injected intraperitoneally with MTX (Emthrexate (PF); Pharmacie B.V., Haarlem, the Netherlands) using dosages of 50 and 25 mg/kg body-weight respectively on day-1 and 0. The concentration of MTX required to induce severe mucositis, was based on a dose-response-curve experiment we previously performed using 129SV Muc2$^{+/+}$ mice (B.A.E. de Koning, unpublished observations). The induced mucositis in the pilot experiment was characterized by villus atrophy, crypt loss, and morphological regeneration within 6 days. Controls (n = 4, both groups) were given equivalent volumes of 0.9 % NaCl. Mice were weighed daily and groups of four were sacrificed on respective days 2, 3, 4, and 6 after the final MTX injection.

Tissue collection

One hour before sacrifice, the mice were injected with 120 µl 10 mg/ml 5-Bromo 2'deoxyUridine (BrdU; Sigma-Aldrich, Zwijndrecht, the Netherlands), to locate proliferating cells. Segments of the duodenum, mid-jejunum, ileum, proximal, and distal colon were collected and processed for histological analyses, stored in RNA later (Qiagen, Venlo, the Netherlands) at -20 °C, or snap-frozen in liquid nitrogen for storage at -80 °C and subsequent protein isolation.

(Immuno)histochemistry

Segments of mid-jejunum were fixed in 4% paraformaldehyde in phosphate-buffered saline (PBS), dehydrated, and embedded in Paraplast Plus (Sherwood Medical, Den Bosch, the Netherlands). Sections were stained with hematoxylin (Vector Laboratories, Burlingame, CA) and eosin (Sigma-Aldrich) (H&E) to study morphological alterations of the crypts and villi. Immunohistochemistry was performed as previously described.[14,16] To detect incorporated BrdU, anti-BrdU (1:250 in PBS; Roche Applied Sciences, Indianapolis, IN) was used. Expression of Muc2 was detected using a goat polyclonal anti-human Muc2 antibody (H-300; 1:1,000 in PBS, SC-15334, Santa Cruz, SanverTech, Heerhugowaard, the Netherlands). As a marker for goblet cell-specific protein expression, a rabbit polyclonal anti-rat trefoil factor family (Tff3; 1:3,000 in PBS, kindly provided by Prof. Dr. D.K. Podolsky)[17] was used, and to determine enterocyte-specific protein expression, a rabbit polyclonal anti-rat sucrase-isomaltase (SI; 1:9,000 in PBS, kindly provided by Dr. K.Y. Yeh)[18] was used. An anti-human CD3 antibody (DAKO, Heverlee, Belgium; 1:800 diluted in 1% BSA, 0.1% Triton X100 in PBS) was used to detect CD3^{+} T-cells. Additionally, non-specific binding was reduced by blocking with TENG-T (10 mM Tris-HCl, 5 mM EDTA, 150 mM NaCl, 0.25% (w/v) gelatin, 0.05% (w/v) Tween-20). Appropriate positive and negative controls were included in each immunohistochemical assay.

Morphological analysis

The following intestinal histological parameters were studied: morphology of the epithelium, degree of inflammation, villus atrophy, crypt loss, crypt abscess, and mucosal bleedings. All scores were obtained in a blinded fashion by two independent investigators.

Crypt and villus length

Lengths of 10 well-orientated crypts and villi of each individual animal were measured with the use of a Nikon Eclipse E800 microscope and Leica Image Manager 500 software (Leica Microsystems B.V, Rijswijk, the Netherlands). However, in cases of severe disease, crypts could not be measured in all slides, due to extensive crypt loss; then, several slides within the jejunal region were combined in order to measure 10 whole crypts and villi.

Intraepithelial lymphocytes

Number of intraepithelial lymphocytes (IELs) in the villi of the small intestine were determined by counting the number of CD3-positive cells per 10 villi of each individual animal. This was done by two independent investigators in a blinded fashion.

Protein dot blotting

The expression of epithelial markers was detected and quantified as previously described.[12] Blots were incubated with anti-SI (1:1,000) or anti-Tff3 (1:1,500). Bound antibodies were detected using HRP-conjugated goat anti-rabbit secondary antibodies (1:1,000 in PBS), and SuperSignal® West Femto Luminol Enhancer kit (Pierce, Rockford, IL). The signal was detected and quantified by the ChemiGenius gel documentation system (Syngene, Cambridge, UK).

Western-blot analysis

The same protein homogenate was used as described for protein dot-blot analysis. Twenty micrograms of protein was loaded per lane and run on a 12.5% SDS–PAGE. The separated proteins were transferred to nitrocellulose membranes (Protran BA83, 0.2 μm) which were subsequently blocked.[12] Blots were incubated overnight at 4 °C with mouse monoclonal anti-human proliferative cell nuclear antigen (PCNA); clone PC10 (1:250 in blocking buffer; Novo Castra Laboratories, Newcastle upon Tyne, UK). After washing with PBS-0.2% Tween-20, bound antibodies were revealed using HRP-conjugated goat anti-mouse secondary antibodies (1:1,000 in PBS) and detected and quantified as described above.

Quantitative real-time PCR (Sybergreen technology)

Total RNAs from mouse small intestine were prepared using the QIAamp RNA midi-kit (Qiagen), following the manufacturer's protocol, and treated with DNase (Qiagen). Total RNA (1.5 μg) was used to prepare first-strand cDNA (AdvantageTM RT-for-PCR kit; BD Biosciences, Clontech, Alphen aan den Rijn, the Netherlands). The mRNA expression levels of tumor necrosis factor alpha (TNF-α) and interleukin-10 (IL-10) as well as the endogenous

housekeeping gene β-actin were quantified using real-time PCR analysis (Sybergreen chemistry) based upon the intercalation of SYBR® Green on an ABI Prism 7700 sequence detection system (PE Applied Biosystems) as described previously.[14] Primer combinations for β-actin (5′-GGGACCTGACGGACTAC-3′ and 5′-TGCCACAGGATTCCATAC-3′), IL-10 (5′-CAAGCCTTATCGGAAATG-3′ and 5′-CATGGCCTTGTAGACACC-3′), and TNF-α (5′-TGGCCTCCCTCTCATC-3′ and 5'-GGCTGGCACCACTAGTT-3') were designed using the OLIGO 6.22 software (Molecular Biology Insights, Cascade, CO) and purchased from Invitrogen (Breda, the Netherlands).

Statistical analysis

The Mann–Whitney *U*-test was used to analyze changes in protein and mRNA expression levels. Results were considered statistically significant at $P < 0.05$. Data are presented as the mean ± standard error of the mean (SEM).

RESULTS

Clinical symptoms

To characterize the phenotype of $Muc2^{-/-}$ mice, we monitored their weight in relation to $Muc2^{+/+}$ litter-mates (Figure 1). From the start, at week 5 of age, $Muc2^{-/-}$ mice had significantly lower body-weight ($P < 0.0001$) and showed growth retardation compared to $Muc2^{+/+}$ littermates. At 6 weeks of age, $Muc2^{-/-}$ mice exhibited diarrhea and occult blood loss, which occasionally progressed to gross bleeding as of 8 weeks of age.

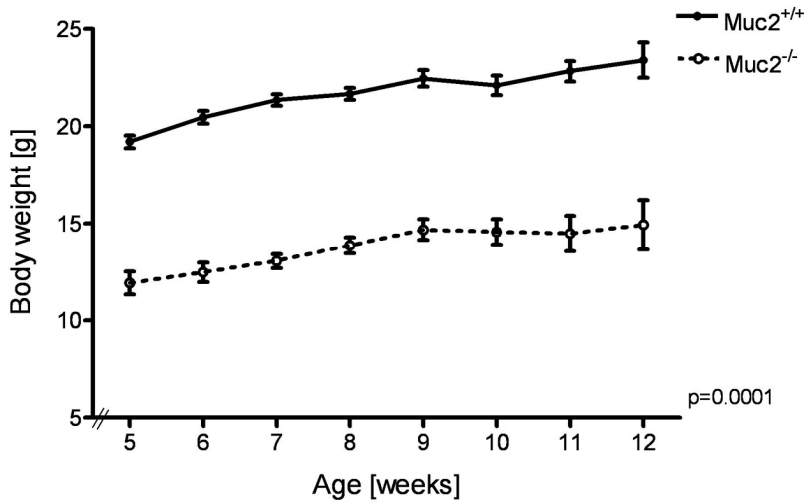

Figure 1 *Body-weight of $Muc2^{+/+}$ and $Muc2^{-/-}$ mice between 5 and 12 weeks of age. As from the start at week 5, $Muc2^{-/-}$ mice weighed significantly less and showed growth retardation compared to their $Muc2^{+/+}$ littermates. Groups follow similar growth curves, but at a different level. Weight per group is expressed as mean ± SEM.*

Morphological analyses

In order to study morphological changes in the small intestine, H&E-stained slides of the duodenum, jejunum, and ileum of $Muc2^{-/-}$ and $Muc2^{+/+}$ mice were compared (Figures 2A,B jejunum, duodenum, and ileum are not shown). The main characteristic difference was the lack of recognizable goblet cells along the crypt-villus axis in the $Muc2^{-/-}$ mice throughout the small intestine. There were no further pronounced differences in epithelial morphology up to 12 weeks of age. There were no differences in number of apoptotic bodies along the crypt-villus axis between the $Muc2^{-/-}$ and $Muc2^{+/+}$ mice. Similarly, there were no significant differences in villus and crypt lengths between $Muc2^{-/-}$ and $Muc2^{+/+}$ mice at any time investigated (Figures 2G,H, Week 8, jejunum).

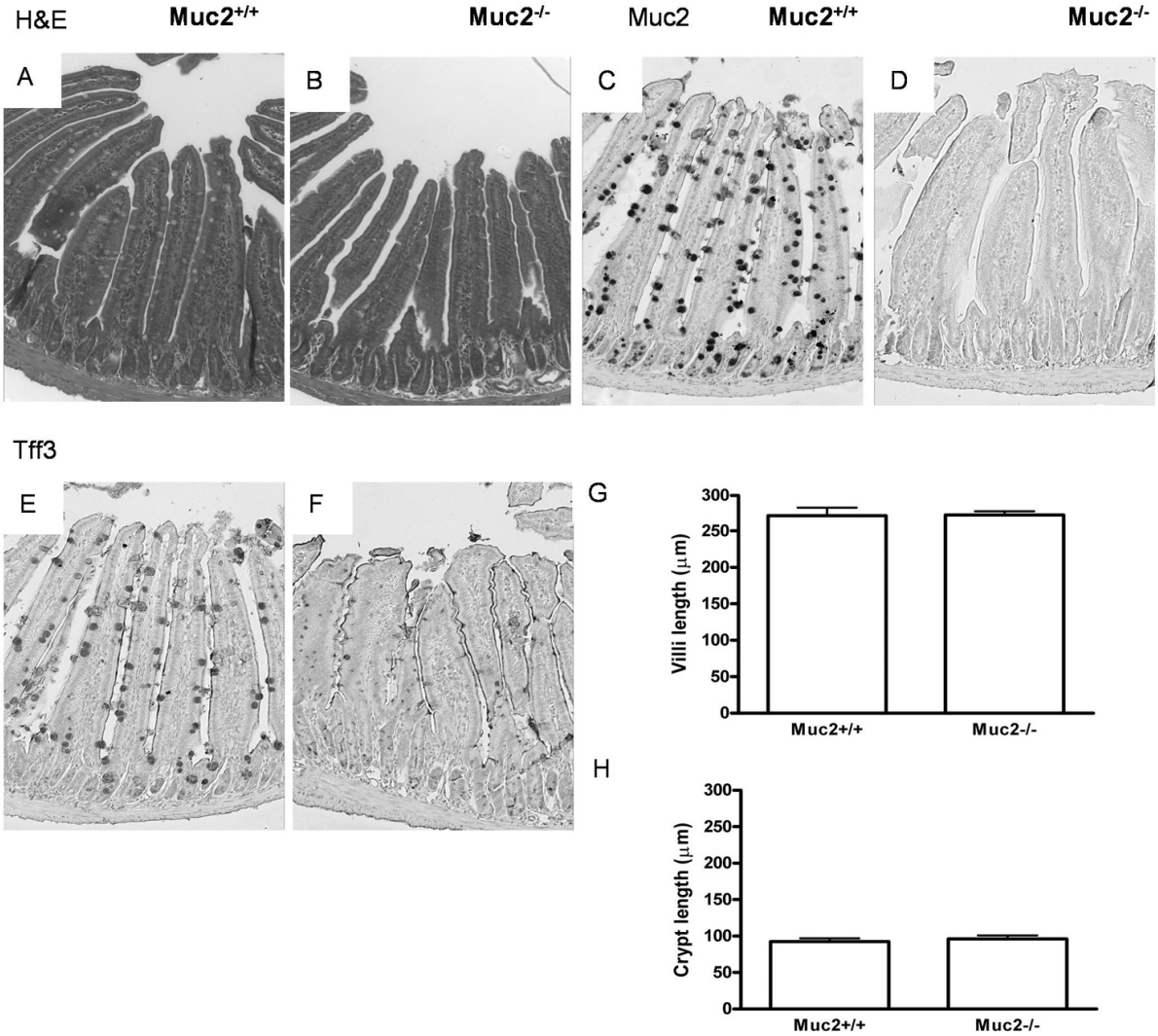

Figure 2 *Absence of Muc2 does not affect small intestinal morphology. Representative sections of a hematoxilin eosin (A-B) , Muc2 (C-D), and Tff3 (E-F) staining of the small intestine of $Muc2^{+/+}$ (A, C, E) and $Muc2^{-/-}$ (B, D, F) mice at 8 weeks of age. The most characteristic difference between the $Muc2^{-/-}$ and $Muc2^{+/+}$ mice was the lack of recognizable goblet cells along the crypt-villus axis of the small intestine in the $Muc2^{-/-}$ mice (B, D). The goblet cells in the small intestine of $Muc2^{-/-}$ mice showed the same expression pattern for Tff3, concentrating on the villi, similar as seen in the small intestine of the $Muc2^{+/+}$ (E), but showed a distinct change in morphology of the goblet cells (F). Vili and crypt length (G, H) of $Muc2^{+/+}$and $Muc2^{-/-}$ littermates 8 weeks of age. Villi and crypt lengths per group are expressed as mean ± SEM.*

Two markers for goblet cells were analyzed: Muc2, which is stored in apical granules of the goblet cells determining the goblet cell morphology[9,13,14] and Tff3, a bioactive peptide which is involved in epithelial protection and repair.[17,19,20] In the small intestine of $Muc2^{+/+}$ mice, Muc2 was expressed in goblet cells from the crypt bottom to the tips of the villi (Figure 2C). Tff3 was also expressed in goblet cells located in the crypts, but was more predominant in goblet cells located on the villi (Figure 2E). Goblet cells in the small intestine of the $Muc2^{-/-}$ mice were negative for Muc2 (Figure 2D), but remained positive for Tff3 (Figure 2F) with an expression pattern similar to that seen in the small intestine of $Muc2^{+/+}$ mice. The goblet cells of the $Muc2^{-/-}$ mice showed distinctly altered morphology as previously described.[13,14] Specifically, the goblet cells of the $Muc2^{+/+}$ mice were round and bell shaped, whereas those of the $Muc2^{-/-}$ mice were smaller, flatter, and more condensed.

Methotrexate-induced mucositis model

MTX-treated $Muc2^{+/+}$ mice showed significant weight-loss compared to the $Muc2^{+/+}$ controls on days 1, 2, 3, and 5 (Figure 3A) (P = 0.003, P = 0.002, P = 0.004, P = 0.045, respectively). After day 3, the treated $Muc2^{+/+}$ mice started to regain weight, almost equalizing control weights by day 6 (Figure 3A). A significant weight-loss was also seen in MTX-treated $Muc2^{-/-}$ compared to $Muc2^{-/-}$ controls, on day 1 and 3 after treatment (Figure 3B) (P = 0.008, P = 0.021, respectively). In addition, weight-loss on day 2 almost reached significance (P = 0.052). In contrast to $Muc2^{+/+}$ mice, $Muc2^{-/-}$ mice continued to lose weight during MTX-treatment. Between days 5 and 6, three of four MTX-treated $Muc2^{-/-}$ mice died, whereas all treated $Muc2^{+/+}$ mice survived. The three non-surviving mice had suffered severe weight-loss (25%) prior to death. On account of the elapsed time after death, morphological evaluation could not be performed. The clinical symptoms displayed by $Muc2^{-/-}$ mice before MTX-treatment, that is, diarrhea and occult blood, did not aggravate after MTX-treatment.

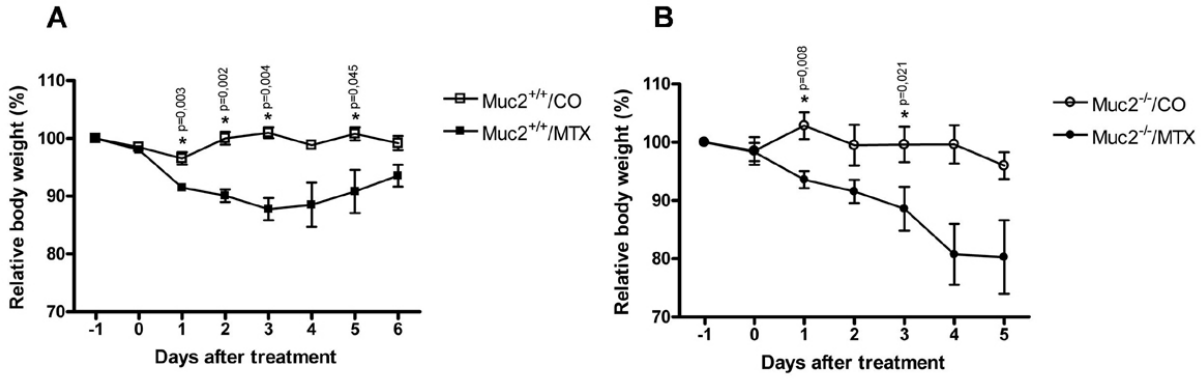

Figure 3 *Weight-loss of MTX-treated $Muc2^{+/+}$ and $Muc2^{-/-}$ mice. Weight of the mice on day-1, before start of the experiment, was set at 100%. A significant decrease in weight versus the saline-treated (i.e., control) mice was seen on days 1, 2, 3, and 5 for the MTX-treated $Muc2^{+/+}$ (A) mice and on days 1 and 3 for the MTX-treated $Muc2^{-/-}$ (B) mice. Weight of the MTX-treated $Muc2^{-/-}$ mice differed at the brink of significance versus that of the control mice on day 2. Weight per group is expressed as mean ± SEM.*

The effect of MTX-treatment on intestinal morphology

MTX-induced changes in small intestinal morphology of $Muc2^{+/+}$ and $Muc2^{-/-}$ mice were examined on days 2, 3, and 4 after treatment (Figures 4A-F). On day 2, both MTX-treated $Muc2^{+/+}$ and $Muc2^{-/-}$ mice showed affected intestinal morphology (Figures 4A,B). The degree of intestinal damage increased with time, indicated by severe villus atrophy, epithelial flattening and extensive crypt loss in both $Muc2^{+/+}$ and $Muc2^{-/-}$ mice by day 3 (Figures 4C,D). Although the mucosa was still severely damaged on day 4, both groups showed the presence of newly formed crypts (Figures 4E,F). On day 6, the intestinal morphology of the $Muc2^{+/+}$ mice had started to regenerate as evidenced by higher numbers of well-formed crypts and villi (Figure 4G), and regeneration corresponded with improvement in body-weight. The one surviving $Muc2^{-/-}$ mice by day 6 was not considered representative of the whole group and was therefore excluded from further analyses.

To exclude death by intestinal failure, we analyzed the proximal and distal colon segments of both the MTX-treated $Muc2^{+/+}$ and $Muc2^{-/-}$ mice. Apart from lack of recognizable goblet cells in the crypts of the $Muc2^{-/-}$ mice, the proximal segment showed no distinct changes in morphology (data not shown). In contrast, microscopic analysis of the distal colon of untreated $Muc2^{-/-}$ mice, showed mucosal thickening, increased proliferation, and superficial erosions in addition to lack of recognizable goblet cells,[14] compared to $Muc2^{+/+}$ mice (Figures 5A,B). MTX-treatment did not affect colonic morphology in the $Muc2^{+/+}$ mice, and the pathology of the $Muc2^{-/-}$ mice did not deteriorate (Figures 5C,D, respectively).

Crypt and villus length after MTX-treatment

After MTX-treatment, crypt length in both $Muc2^{+/+}$ and $Muc2^{-/-}$ mice progressively increased with time (Figure 4H). On day 2, $Muc2^{+/+}$ mice showed a significant increase in crypt length compared to control mice (P = 0.004). $Muc2^{-/-}$ mice responded similarly 1 day later. On days 2 and 3, a significant difference (P = 0.003 and P = 0.025 respectively) in crypt length was observed between the $Muc2^{+/+}$ and $Muc2^{-/-}$ mice, with crypts of $Muc2^{+/+}$ mice longer than those of $Muc2^{-/-}$ mice. However, on day 4, the increase in crypt length was similar in both groups of mice.

In addition, after MTX-treatment, a significant villus shortening was observed both in $Muc2^{+/+}$ mice and in $Muc2^{-/-}$ mice (Figure 4I). A significant decrease in villus length was seen in $Muc2^{-/-}$ mice on days 2 and 3, and in $Muc2^{+/+}$ mice on days 3 and 4. Subsequent regeneration of villus length was seen in the $Muc2^{-/-}$ mice on day 4, but in the $Muc2^{+/+}$ mice not until day 6. MTX-induced changes in villus length between the two types of mice were significantly different on day 2 only (P = 0.0001).

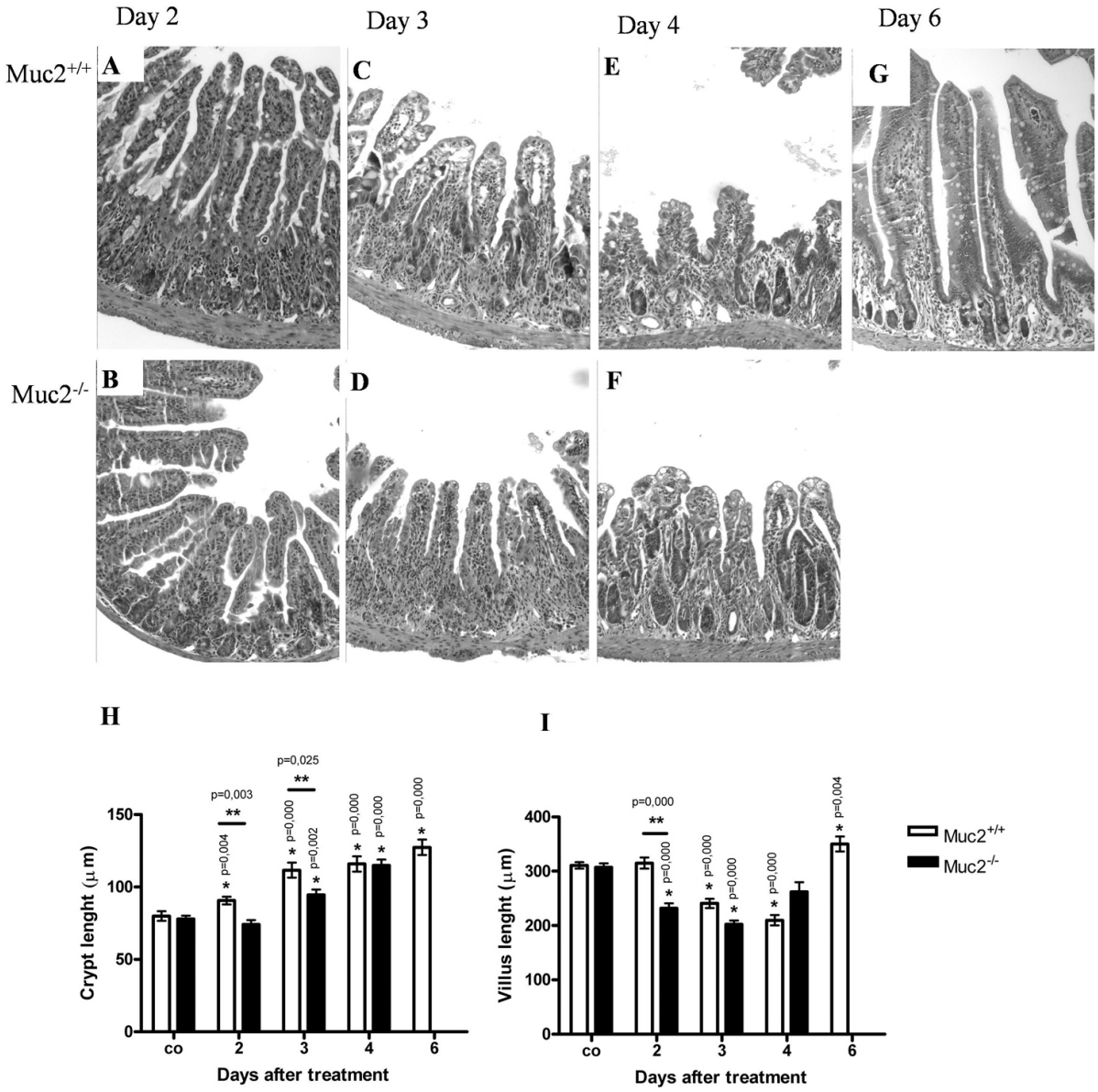

Figure 4 *MTX-induced changes in the small intestine in Muc2$^{+/+}$ and Muc2$^{-/-}$ mice. Morphology of the jejunum of Muc2$^{+/+}$ (A, C, E, G) and Muc2$^{-/-}$ (B, D, F) mice on days 2 (A, B), 3 (C, D), 4 (E, F), and 6 (G) after MTX-treatment. On day 2, morphology of Muc2$^{+/+}$ and Muc2$^{-/-}$ mice was mildly affected and characterized by mild crypt loss and epithelial flattening. On days 3 and 4, intestinal damage was more severe, showing increased crypt loss on day 3 and epithelial flattening and villus atrophy on days 3 and 4. Crypt regeneration was seen on day 4, but was more pronounced in the Muc2$^{-/-}$ mice compared to Muc2$^{+/+}$ mice. On day 6, the intestinal morphology of the Muc2$^{+/+}$ mice had started to regenerate as evidenced by higher numbers of well-formed crypts and villi. Crypt (H) and villus (I) lengths of Muc2$^{+/+}$ and Muc2$^{-/-}$ littermates before and after MTX-treatment. Both groups showed significant villus atrophy and crypt elongation after MTX-treatment. Significant differences were seen on day 2; Muc2$^{-/-}$ mice showed more villus atrophy, but less elongation of crypt length compared to Muc2$^{+/+}$ mice. On day 3, villus atrophy was comparable in both groups, but still minimal differences were seen in crypt length. In the regenerative phase, day 6, Muc2$^{+/+}$ mice showed an increase in villus and crypt length compared to control littermates. Bars are expressed in mean ± SEM.*

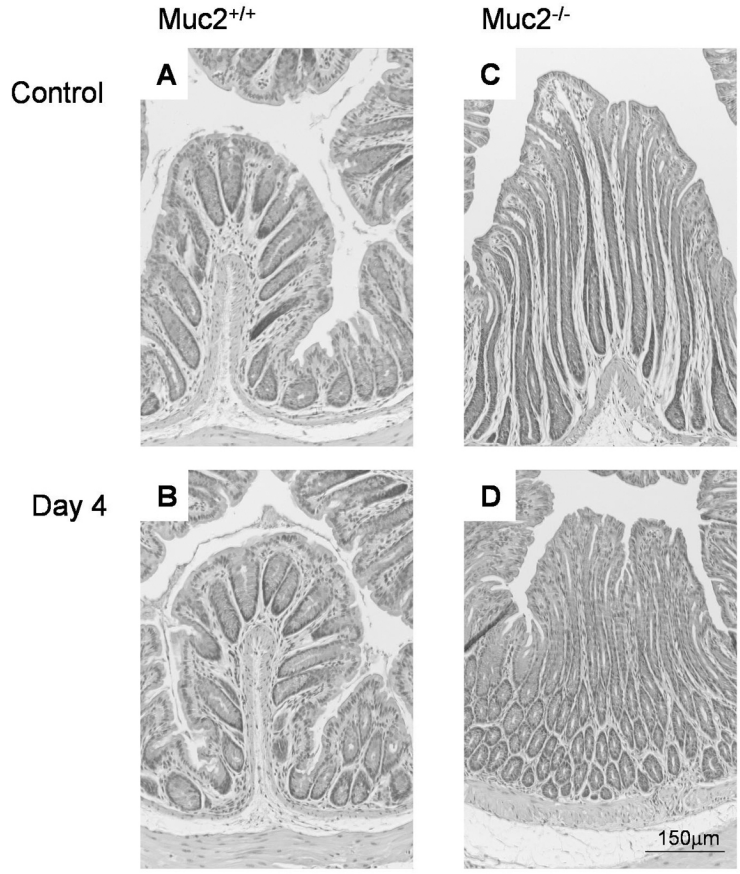

Figure 5 *Morphology of the distal colon before and after MTX-treatment. Morphology of the distal colon of (A, B) Muc2$^{+/+}$ mice and (C, D) Muc2$^{-/-}$ mice, untreated (A and C) and day 4 after MTX-treatment (B and D). Untreated Muc2$^{-/-}$ mice showed mucosal thickening and superficial erosions in addition to lack of recognizable goblet cells, compared to Muc2$^{+/+}$mice. MTX-treatment did not affect the colonic morphology in the Muc2$^{+/+}$ mice, and the pathology of the Muc2$^{-/-}$ mice did not deteriorate as determined by the parameters described above.*

Effect of MTX-treatment on epithelial proliferation

In Muc2$^{+/+}$ and Muc2$^{-/-}$ saline-treated (control) mice BrdU-positive cells were seen from the bottom of the crypt up to three quarters of the crypt height, showing no distinct differences in location or number of BrdU positive cells (Figures 6A,B). On day 2, the proliferative zone in Muc2$^{+/+}$ mice moved progressively upwards in the crypts towards the crypt-villus junction (Figure 6C). At the same time, the proliferative zone in the Muc2$^{-/-}$ mice was only mildly affected, showing a slight shift upwards within the crypts (Figure 6D). On days 3 and 4, the proliferative zone in both groups had broadened and moved upwards along the crypt-villus axis (Figure 6E,F showing day 3). Subsequently, proliferation was quantified by Western blot analysis, using a monoclonal antibody specific for PCNA, a marker for proliferation[21,22] (Figure 6G). PCNA expression in the small intestine of the Muc2$^{+/+}$ mice decreased significantly (P = 0.01) on day 2 compared to their controls, while the Muc2$^{-/-}$ animals only showed a non-significant decrease. During severe intestinal damage, on days 3 and 4, PCNA expression in both Muc2$^{+/+}$and Muc2$^{-/-}$ mice had returned to control levels. On day 6, PCNA expression in the intestine of the Muc2$^{+/+}$ mice was similar to control level. Overall, PCNA expression levels did not significantly differ between Muc2$^{+/+}$ and Muc2$^{-/-}$ mice at any time.

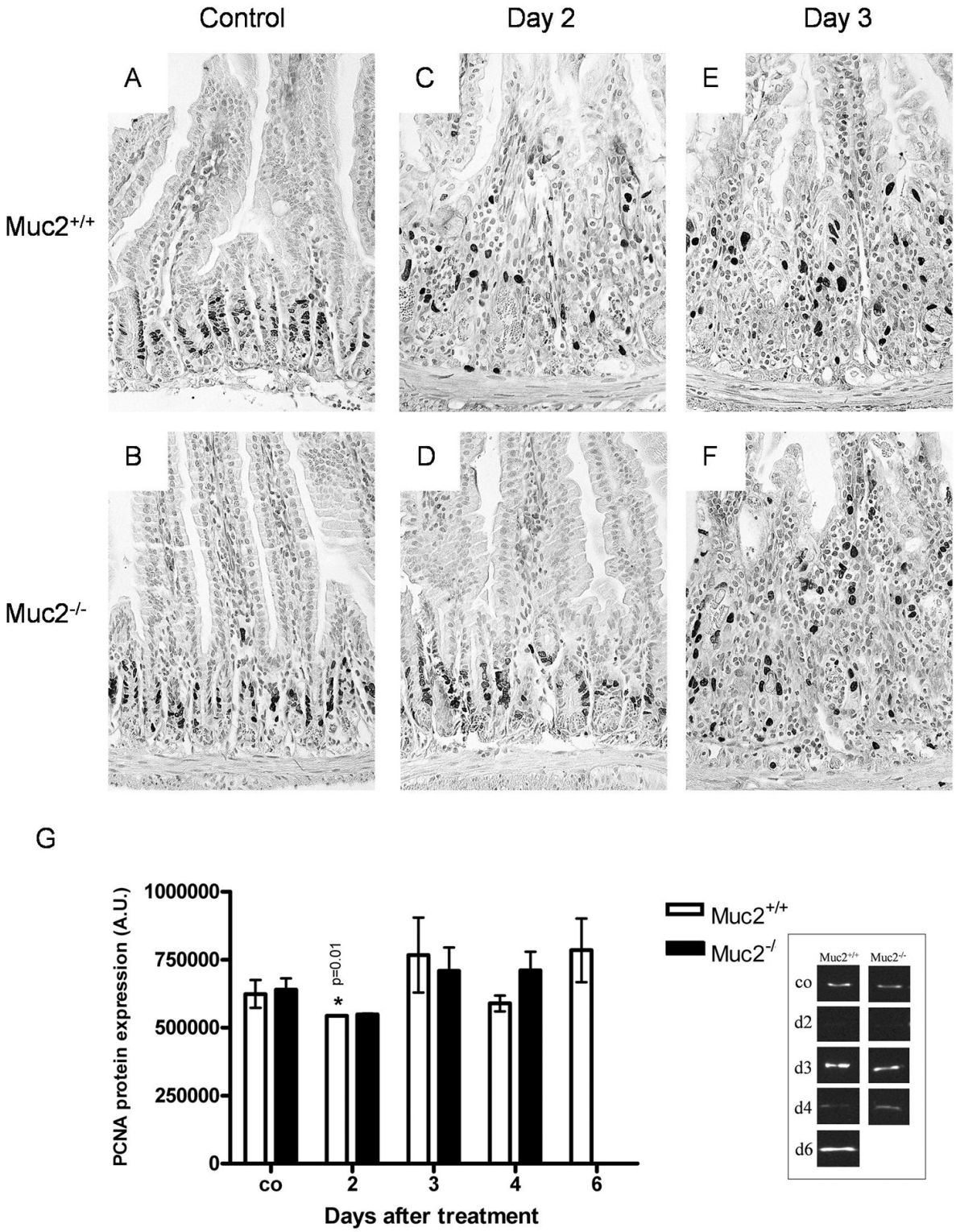

Figure 6 *Effect of MTX-treatment on epithelial proliferation. BrdU stainingof the jejunum of saline-treated (i.e., control) Muc2$^{+/+}$ (A) and Muc2$^{-/-}$ (B) mice on day 2 (C-D) and 3 (E-F) after MTX-treatment (BrdU was injected 1 h before sacrificing the mice). On day 2, the BrdU-positive cells in the Muc2$^{-/-}$ mice were located higher in the crypt. The BrdU-positive cells in the Muc2$^{+/+}$ mice were seen along the entire length of the crypts. A similar pattern was seen in both groups on day 3; BrdU-positive cells were not restricted to the crypts and showed a scattered pattern along the entire length of the crypts. G: Western blot analysis, using a monoclonal antibody specific for PCNA. Representative Western blots for each day are shown. The expression of PCNA protein decreased significantly on day 2 in the Muc2 mice. PCNA expression on days 3 and 4 showed mild, non-significant changes in MTX-treated Muc2$^{+/+}$ and Muc2$^{-/-}$ mice versus control mice. Bars are expressed in mean ± SEM.*

Effects of MTX-treatment on enterocyte- and goblet cell-specific protein expression

To gain insight in the functional capacity of the intestinal epithelium after MTX-treatment, we analyzed the expression pattern of SI (Figures 7A–D). SI is considered a marker for intestinal epithelial differentiation.[18,23] Control $Muc2^{-/-}$ and $Muc2^{+/+}$ mice showed a clear SI staining at the brush border along the entire villi (Figures 7A,B). On day 3, during severe mucositis, SI expression was undetectable in the intestine of both $Muc2^{+/+}$ and $Muc2^{-/-}$ mice (data not shown). However, on day 4, SI expression in $Muc2^{-/-}$ mice had partly regenerated and was detected at the villus tips, in contrast to $Muc2^{+/+}$ mice (Figures 7C,D) in which expression of SI was still virtually absent.

SI dot-blot analysis revealed no significant difference in SI expression levels between $Muc2^{-/-}$ and $Muc2^{+/+}$ control mice (Figure 7E). SI expression in the MTX-treated $Muc2^{+/+}$ mice was significantly decreased on days 2, 3, and 4, (P = 0.0001, P = 0.002, and P = 0.0001, respectively) and returned to control levels by day 6, corresponding to the results described for immunohistochemical detection of SI. SI expression in $Muc2^{-/-}$ mice had significantly decreased on days 2 and 3 (P = 0.046, P = 0.001 respectively) and was re-established by day 4, in line with the immunohistochemical data.

To quantify Tff3 expression levels, protein dot-blot analyses were performed using a Tff3-specific antibody (Figure 7F). Interestingly, even though the goblet cells of the $Muc2^{-/-}$ mice showed a distinct change in morphology as detected by the immunohistochemical staining of Tff3 (Figure 2F), there were no significant differences in Tff3 expression levels between $Muc2^{+/+}$ and $Muc2^{-/-}$ control mice. On day 2, Tff3 expression increased significantly in MTX-treated $Muc2^{+/+}$ mice only, compared to $Muc2^{+/+}$ control mice (P = 0.00 1) and MTX-treated $Muc2^{-/-}$ mice (P = 0.008) and returned to control levels by day 3. In MTX-treated $Muc2^{-/-}$ mice, Tff3 expression levels remained stable at control level throughout the entire experiment.

Release of IL-10 and TNF-α in $Muc2^{-/-}$ intestine prior to MTX-treatment

So far, these data in conjunction suggest $Muc2^{-/-}$ and $Muc2^{+/+}$ mice have similar intestinal sensitivity to MTX, or even that $Muc2^{-/-}$ mice are less sensitive to MTX-treatment, up to day 4. Absence of Muc2 in $Muc2^{-/-}$ mice may lead to a continuous exposure to luminal antigens, which might have resulted in disbalance in cytokine production prior to MTX-treatment. IELs are one of the first immune cells to encounter antigens that have entered the body via the epithelial surface.[24] Therefore, IELs play an important role in mediating local immune responses in the intestine.[24-26] In order to evaluate two major cytokines involved in anti-inflammatory (IL-10) and pro-inflammatory (TNF-α) responses, we performed quantitative real-time PCR. Prior to MTX-treatment, $Muc2^{-/-}$ mice showed a non-significant increase in mRNA expression of TNF-α (Figure 8A), but a significant increase (P = 0.003) in mRNA expression of the anti-inflammatory cytokine IL-10 compared to $Muc2^{+/+}$ mice (Figure 8B). The presence of IELs was determined by staining with anti-CD3, which detects both $CD4^+$ and $CD8^+$ T cells. There was an increase of IELs in

the Muc2$^{-/-}$ mice before MTX-treatment compared to Muc2$^{+/+}$mice (Figure 8C), with a difference at the brink of significance (*P* = 0.0571).

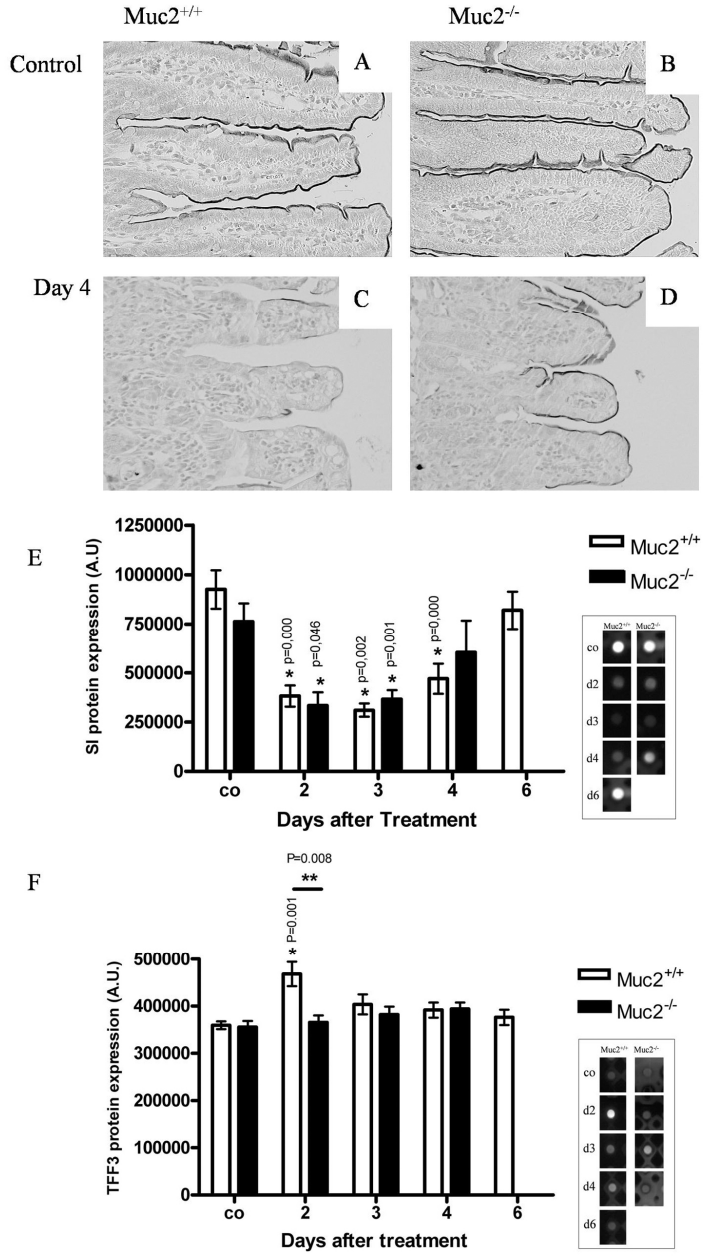

Figure 7 *Effect of MTX-treatment on the SI and Tff3 protein expression in the small intestine. Representative sections of SI staining of the small intestine after MTX treatment (A-D). Saline-treated (i.e., control) Muc2$^{+/+}$ (A) and Muc2$^{-/-}$ (B) mice showed a clear SI staining at the brush border along the entire villi. C: On day 4, SI expression in the Muc2$^{+/+}$ mice was virtually absent in contrast to (D) the Muc2$^{-/-}$ mice, in which SI expression was partly regenerated and expressed at the tips of the villi. Dot-blot analysis was performed to quantify SI (E) and Tff3 (F) in the small intestine during MTX-treatment. Representative spot blots for each antibody are shown. There was no significant difference in SI and Tff3 expression levels between the Muc2$^{-/-}$mice and Muc2$^{+/+}$ controls. SI expression in the MTX-treated Muc2$^{+/+}$ mice was significantly decreased on days 2, 3, and 4, and returned to control levels on day 6. In contrast, SI expression in Muc2$^{-/-}$ mice was significantly decreased on days 2 and 3 only and showed regeneration on day 4. On day 2, Tff3 expression of the Muc2$^{+/+}$ mice significantly increased compared to Tff3 expression of the Muc2$^{-/-}$ mice, which maintained at control level. On days 3 and 4, no significant changes were seen in either of the MTX-treated groups. Bars are expressed in mean ± SEM.*

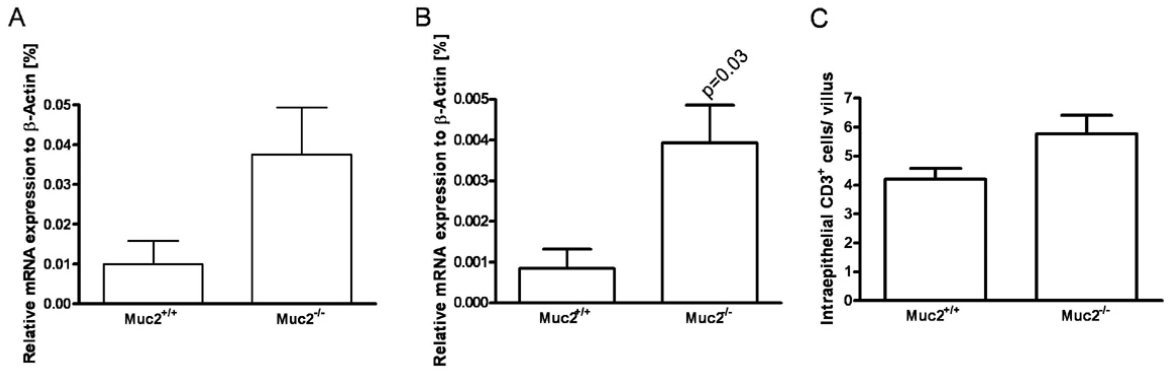

Figure 8 *Increased release of IL-10 and TNF-α mRNA in the small intesine of Muc2$^{-/-}$ mice, prior to MTX-treatment. Real-time PCR data of TNF-α (A) and IL-10 (B) on RNA isolated from the small intestine of both Muc2$^{+/+}$ and Muc2$^{-/-}$ control, untreated mice. The results were normalized for the housekeeping gene β-actin. The Muc2$^{-/-}$ mice showed a non-significant increase in mRNA expression of TNF-α, but a significant increase in mRNA expression of the anti-inflammatory cytokine IL-10 compared to Muc2$^{+/+}$. C: Quantification of CD3^{+} IELs in the villi of both types of mice. Control, untreated Muc2$^{-/-}$ mice showed an increase in IELs compared to Muc2$^{+/+}$ mice, which was at the brink of significance (P = 0.057 1) Bars are expressed in mean ± SEM*

DISCUSSION

We addressed the question whether Muc2 is involved in epithelial protection against chemotherapy-induced mucositis in the small intestine by challenging Muc2-deficient mice with the cytostatic drug MTX. As chemotherapy increases the permeability of the intestinal epithelium, we hypothesized that the deficiency of Muc2, and resultant major changes of the mucus layer, would sensitize the intestine to chemotherapy-induced damage.

The Muc2$^{-/-}$ mice weighed significantly less than the Muc2$^{+/+}$ mice and showed growth retardation. In addition, they showed diarrhea, occult blood loss, and even occasional gross bleeding, caused by a distinct pathology in the distal colon.[14] We cannot explain the significant difference in weight at an early age, especially as there was no difference in birth-weight (our unpublished data). There is no indication that the small intestine contributes to any of the described symptoms above, as histological analysis showed no distinct pathology. The only telling difference between the Muc2$^{+/+}$ and the Muc2$^{-/-}$ mice was the lack of recognizable goblet cells in the Muc2$^{-/-}$ mice, in line with findings from previous studies.[13,14,27] Quantification of Tff3 and SI, important markers of the functionality of goblet cells and enterocytes, respectively, showed no difference in expression levels in the small intestine between Muc2$^{+/+}$ and Muc2$^{-/-}$ mice. Neither did crypt and villus lengths differ between the Muc2$^{-/-}$ and Muc2$^{+/+}$ mice. Taken together, these data suggest that under unchallenged conditions, Muc2 is not essential for normal epithelial morphology and function in the small intestine. However, this hypothesis is undermined by the fact that the Muc2$^{-/-}$ mice showed significant growth retardation.

Mucositis was induced in both $Muc2^{+/+}$ and $Muc2^{-/-}$ animals by injecting MTX. Up to day 3, there were no differences in percentage of weight-loss compared to initial body-weights between $Muc2^{+/+}$ and $Muc2^{-/-}$ mice. Thereafter, however, $Muc2^{+/+}$ mice showed a trend towards regaining their initial body-weights, whereas $Muc2^{-/-}$ mice continued to lose weight, which may have led to the death of three of four mice on day 5. The intestine of the $Muc2^{-/-}$ mice already had started to regenerate on day 4, as indicated by an earlier regeneration of crypts, restoration of villus length (on day 4), and restoration of enterocyte-specific SI levels in $Muc2^{-/-}$ mice compared to $Muc2^{+/+}$ mice. Furthermore, the proliferative zone in the $Muc2^{-/-}$ mice seemed to be less affected by MTX-treatment compared to that in $Muc2^{+/+}$ mice. These results are contradictive to our hypothesis, and do not explain why the mice died during the experiment. We, therefore, have no indication that death of the $Muc2^{-/-}$ animals could be caused by intestinal failure. This is supported by data showing that the pathology of the distal colon of the $Muc2^{-/-}$ mice did not deteriorate during MTX-treatment, and by the fact that clinical symptoms such as diarrhea and occult blood loss did not aggravate. Since the $Muc2^{-/-}$ mice were significantly lighter than the $Muc2^{+/+}$ mice before MTX treatment, the same percentage of weight-loss after MTX could have had a bigger impact on the $Muc2^{-/-}$ mice and resulting in the sudden death of these mice. We have now learned, from continuing experiments, that lighter $Muc2^{+/+}$ mice are also predisposed to death during MTX treatment compared to heavier littermates (B.A.E. de Koning, unpublished observations).

Mucositis is the result of a dynamic cascade of events, in which the release of pro-inflammatory cytokines, activated by transcription-factors and invading bacteria, plays an important role.[28] Mucositis toxicity is correlated with the release of the pro-inflammatory cytokine TNF-α, which is involved in intestinal damage induction.[28-31] Furthermore, TNF-α was shown to play a pivotal role in the pathogenesis of inflammatory bowel disease.[32,33] In contrast, the anti-inflammatory cytokine IL-10, has protective capacities in the intestine, and studies have shown that $IL\text{-}10^{-/-}$ mice are predisposed to develop chronic mucosal inflammation.[34-36] As described previously, local expression of (anti-)inflammatory cytokines might be able to modulate local immune responses.[25] Local immune responses are mediated by e.g. the IELs.[24] IELs are instrumental in mediating tolerance and driving immune regulation and could be activated in the $Muc2^{-/-}$ mice by an increased stimulation caused by the absence of Muc2, the structural component of the mucus layer. Our data reveal a trend towards increased numbers of IELs present in the villi of the $Muc2^{-/-}$ mice before MTX-treatment. Apart from IELs, we also investigated IL-10 and TNF-α production in the intestine of $Muc2^{-/-}$ mice prior to MTX-treatment. Untreated $Muc2^{-/-}$ mice showed a non-significant increase in TNF-α mRNA levels, but a significant increase in IL-10 mRNA levels compared to $Muc2^{+/+}$ mice. These data suggest an opposite TNF-α release in which IL-10 restricts the damage-inducing capacity of TNF-α under unchallenged condition (i.e., not treated with MTX) in the small intestine of $Muc2^{-/-}$ mice. Further support for this hypothesis is the observation that $IL\text{-}10^{-/-}$ mice develop more severe mucositis after MTX-treatment than their $IL\text{-}10^{+/+}$ littermates and that IELs from $IL\text{-}10^{-/-}$ mice were unable to control Th1-induced gut inflammation.[24,37]

Thus, Muc2 deficiency may have led to an altered immune-response prior to MTX challenge. This might explain why the MTX-induced damage was similar, or even less severe in the $Muc2^{-/-}$ mice. This mechanism however, needs further investigation.

In conclusion, our data do not provide evidence that Muc2 deficiency leads to an increase in chemotherapy-induced mucositis. A possible explanation is the mechanism by which Muc2 deficiency triggers the immune system to release IL-10, an anti-inflammatory cytokine, prior to MTX-treatment.

ACKNOWLEDGMENTS

We thank A.C.J.M. de Bruijn for his excellent technical assistance. Y. Simons-Oosterhuis is gratefully acknowledged for the careful design and validation of the IL-10 primers. We thank J. Hagoort for an excellent review of this manuscript. The current address of A.W.C. Einerhand is Lipid Nutrition, Loders Croklaan, Wormerveer, the Netherlands.

Contract grant sponsor: Numico Research BV, Wageningen, the Netherlands; Contract grant sponsor: The Sophia Foundation for Scientific Research Rotterdam, the Netherlands; Contract grant number: SSWO 406; Contract grant sponsor: The Foundation "De Drie Lichten," the Netherlands; Contract grant sponsor: Netherlands Organization for Scientific Research, Den Haag, the Netherlands.

REFERENCES

1. Duncan M, Grant G. Oral and intestinal mucositis - causes and possible treatments. Aliment Pharmacol Ther 2003;18:853-874.
2. Ruescher TJ, Sodeifi A, Scrivani SJ, Kaban LB, Sonis ST. The impact of mucositis on alpha-hemolytic streptococcal infection in patients undergoing autologous bone marrow transplantation for hematologic malignancies. Cancer 1998;82:2275-2281.
3. McGuire DB. Mucosal tissue injury in cancer therapy. More than muscositis and mouthwash. Cancer Pract 2002;10:179-191.
4. Elting LS, Cooksley C, Chambers M, Cantor SB, Manzullo E, Rubenstein EB. The burdens of cancer therapy. Clinical and economic outcomes of chemotherapy-induced mucositis. Cancer 2003;98:1531-1539.
5. Sonis ST, Elting LS, Keefe D, Peterson DE, Schubert M, Hauer-Jensen M, Bekele BN, Raber-Durlacher J, Donnelly JP, Rubenstein EB. Perspectives on cancer therapy-induced mucosal injury: pathogenesis, measurement, epidemiology, and consequences for patients. Cancer 2004;100:1995-2025.
6. Strous GJ, Dekker J. Mucin-type glycoproteins. Crit Rev Biochem Mol Biol 1992;27:57-92.
7. Forstner JF, GG. gastrointestinal mucus, ed. 3, vol. 2. New York: Raven, 1994.
8. Hecht G. Innate mechanisms of epithelial host defense: spotlight on intestine. Am J Physiol 1999;277:C351-358.
9. Tytgat KM, Buller HA, Opdam FJ, Kim YS, Einerhand AW, Dekker J. Biosynthesis of human colonic mucin: Muc2 is the prominent secretory mucin. Gastroenterology 1994;107:1352-1363.
10. Van Klinken BJ, Dekker J, Buller HA, de Bolos C, Einerhand AW. Biosynthesis of mucins (MUC2-6) along the longitudinal axis of the human gastrointestinal tract. Am J Physiol 1997;273:G296-302.
11. Verburg M, Renes IB, Meijer HP, Taminiau JA, Buller HA, Einerhand AW, Dekker J. Selective sparing of goblet cells and paneth cells in the intestine of methotrexate-treated rats. Am J Physiol Gastrointest Liver Physiol 2000;279:G1037-1047.
12. Verburg M, Renes IB, Van Nispen DJ, Ferdinandusse S, Jorritsma M, Buller HA, Einerhand AW, Dekker J. Specific responses in rat small intestinal epithelial mRNA expression and protein levels during chemotherapeutic damage and regeneration. J Histochem Cytochem 2002;50:1525-1536.
13. Velcich A, Yang W, Heyer J, Fragale A, Nicholas C, Viani S, Kucherlapati R, Lipkin M, Yang K, Augenlicht L. Colorectal cancer in mice genetically deficient in the mucin Muc2. Science 2002;295:1726-1729.
14. van der Sluis M, de Koning BAE, de Bruijn ACJM, Velcich A, Meijerink JPP, van Goudoever JB, Büller HA, Dekker J, van Seuningen I, Renes IB, Einerhand AWC. Muc2-deficient mice spontaneously develop colitis, indicating that Muc2 is critical for colonic protection. Gastroenterology 2006; *in press*.
15. Wahba N. An ortho-tolidine hydrochloride test for the detection of occult blood in faeces without dietary restrictions. J Clin Pathol 1965;18:687-688.
16. Renes IB, Verburg M, Van Nispen DJ, Taminiau JA, Buller HA, Dekker J, Einerhand AW. Epithelial proliferation, cell death, and gene expression in experimental colitis: alterations in carbonic anhydrase I, mucin MUC2, and trefoil factor 3 expression. Int J Colorectal Dis 2002;17:317-326.
17. Mashimo H, Wu DC, Podolsky DK, Fishman MC. Impaired defense of intestinal mucosa in mice lacking intestinal trefoil factor. Science 1996;274:262-265.
18. Yeh KY, Yeh M, Montgomery RK, Grand RJ, Holt PR. Cortisone and thyroxine modulate intestinal lactase and sucrase mRNA levels and activities in the suckling rat. Biochem Biophys Res Commun 1991;180:174-180.
19. Dignass A, Lynch-Devaney K, Kindon H, Thim L, Podolsky DK. Trefoil peptides promote epithelial migration through a transforming growth factor beta-independent pathway. J Clin Invest 1994;94:376-383.

20. Mashimo H, Wu DC, Podolsky DK, Fishman MC. Impaired defense of intestinal mucosa in mice lacking intestinal trefoil factor. Science 1996;274:262-265.

21. Theon AP, Metzger L, Griffey S. In situ analysis of cellular proliferation in canine, feline and equine tumors by immunohistochemistry: a comparison of bromodeoxyuridine, proliferating cell nuclear antigen, and interchromatin-associated antigen immunostaining techniques. J Vet Diagn Invest 1994;6:453-457.

22. Bromley M, Rew D, Becciolini A, Balzi M, Chadwick C, Hewitt D, Li YQ, Potten CS. A comparison of proliferation markers (BrdUrd, Ki-67, PCNA) determined at each cell position in the crypts of normal human colonic mucosa. Eur J Histochem 1996;40:89-100.

23. Van Beers EH, Buller HA, Grand RJ, Einerhand AW, Dekker J. Intestinal brush border glycohydrolases: structure, function, and development. Crit Rev Biochem Mol Biol 1995;30:197-262.

24. Cheroutre H. IELs: enforcing law and order in the court of the intestinal epithelium. Immunol Rev 2005;206:114-131.

25. De Winter H, Elewaut D, Turovskaya O, Huflejt M, Shimeld C, Hagenbaugh A, Binder S, Takahashi I, Kronenberg M, Cheroutre H. Regulation of mucosal immune responses by recombinant interleukin 10 produced by intestinal epithelial cells in mice. Gastroenterology 2002;122:1829-1841.

26. Chen Y, Chou K, Fuchs E, Havran WL, Boismenu R. Protection of the intestinal mucosa by intraepithelial gamma delta T cells. Proc Natl Acad Sci U S A 2002;99:14338-14343.

27. Yang W, Velcich A, Lozonschi I, Liang J, Nicholas C, Zhuang M, Bancroft L, Augenlicht LH. Inactivation of p21WAF1/cip1 enhances intestinal tumor formation in Muc2-/- mice. Am J Pathol 2005;166:1239-1246.

28. Sonis ST. The pathobiology of mucositis. Nat Rev Cancer 2004;4:277-284.

29. Abreu-Martin MT, Vidrich A, Lynch DH, Targan SR. Divergent induction of apoptosis and IL-8 secretion in HT-29 cells in response to TNF-alpha and ligation of Fas antigen. J Immunol 1995;155:4147-4154.

30. Hall PD, Benko H, Hogan KR, Stuart RK. The influence of serum tumor necrosis factor-alpha and interleukin-6 concentrations on nonhematologic toxicity and hematologic recovery in patients with acute myelogenous leukemia. Exp Hematol 1995;23:1256-1260.

31. Guy-Grand D, DiSanto JP, Henchoz P, Malassis-Seris M, Vassalli P. Small bowel enteropathy: role of intraepithelial lymphocytes and of cytokines (IL-12, IFN-gamma, TNF) in the induction of epithelial cell death and renewal. Eur J Immunol 1998;28:730-744.

32. Strober W, Fuss IJ, Blumberg RS. The immunology of mucosal models of inflammation. Annu Rev Immunol 2002;20:495-549.

33. Bouma G, Strober W. The immunological and genetic basis of inflammatory bowel disease. Nat Rev Immunol 2003;3:521-533.

34. Kuhn R, Lohler J, Rennick D, Rajewsky K, Muller W. Interleukin-10-deficient mice develop chronic enterocolitis. Cell 1993;75:263-274.

35. Löhler J, Kühn R, Rennick D, Rajewsky K, Müller W. Interleukin-10-deficient mice: a model of chronic mucosal inflammation. In: Tytgat GNJ, Bartelsman MFWM, van Deventer SJH, eds. Inflammatory Bowel Diseases Dordrecht: Kluwer Academic Publishers, 1995:410-417.

36. Sellon RK, Tonkonogy S, Schultz M, Dieleman LA, Grenther W, Balish E, Rennick DM, Sartor RB. Resident enteric bacteria are necessary for development of spontaneous colitis and immune system activation in interleukin-10-deficient mice. Infect Immun 1998;66:5224-5231.

37. de Koning BA, van Dieren JM, Lindenbergh-Kortleve DJ, van der Sluis M, Matsumoto T, Yamaguchi K, Einerhand AW, Samsom JN, Pieters R, Nieuwenhuis EE. Contributions of mucosal immune cells to methotrexate-induced mucositis. Int Immunol 2006;18:941-949.

5

CONTRIBUTIONS OF MUCOSAL IMMUNE CELLS TO METHOTREXATE-INDUCED MUCOSITIS

Barbara A.E. de Koning, Jolanda M. van Dieren, Dicky J. Lindenbergh-Kortleve, Maria van der Sluis, Tetsuya Matsumoto, Keizo Yamaguchi, Alexandra W. Einerhand, Janneke N. Samsom, Rob Pieters, Edward E.S. Nieuwenhuis.

International Immunology, 18:941-949 (2006).

ABSTRACT

The use of high doses of the anti-cancer drug methotrexate (MTX) is associated with intestinal damage. As a result, mucosal immune cells become increasingly exposed to a vast amount of microbial stimuli. We aimed at determining whether these cells are still functional during MTX treatment. Furthermore, we assessed if activation of the mucosal immune system would play a role in the pathogenesis of mucositis. A contributive role to mucositis for the adaptive immune system was established by showing that mucosal lymphocytes from MTX-treated mice secreted enhanced amounts of cytokines upon *ex vivo* polyclonal stimulation. Next, *in vitro* experiments revealed that macrophages were not affected by MTX in the capacity to produce tumor necrosis factor-α (TNF-α) and IL-10 after LPS exposure. Moreover, peritoneal macrophages from MTX-treated mice produced more IL-10 and TNF-α upon LPS stimulation, compared with cells derived from control mice. These data indicate a persistence of both innate and adaptive immune responses in this model. The clinical relevance of these findings was further established by the fact that LPS exposure prior to MTX-treatment aggravated the course of mucositis. Furthermore, LPS-responsive mice recovered more slowly compared with LPS-unresponsive mice from MTX treatment. Finally, we found an increase in weight loss and intestinal damage upon MTX treatment in IL-10-deficient mice in comparison to wild-type controls, suggesting a protective role for IL-10 in mucositis. We conclude that mucosal immune responses remain resilient during MTX-induced mucositis. Whereas TNF-α production may contribute to mucosal damage, IL-10 may regulate by restricting excessive mucositis.

INTRODUCTION

One of the most severe side effects of chemotherapy is the damage induced to the gastrointestinal mucosa, often referred to as mucositis.[1] Mucositis is characterized by severe pain, diarrhea and weight loss. Patients suffering from mucositis experience a decreased quality of life[2] and an enhanced risk on developing infections with micro-organisms originating from the oral cavity and intestinal lumen.[3-6] These side effects may lead to delays in scheduled chemotherapy courses, thereby potentially reducing the efficacy of anti-cancer treatment.[1,3] Thus far, there is no definitive prophylaxis or treatment for mucositis, partly caused by a lack of insight into the complex pathophysiology.

Besides digestive absorption of dietary nutrients, the main task of the intestine is to form a barrier against micro-organisms and food antigens that are present within the lumen. Methotrexate (MTX) damages rapidly dividing cells, such as epithelial cells in the intestinal crypts, thereby causing diminished cell renewal and decreased cell replacement. Ultimately, this leads to ulceration and a decreased barrier function.[7-9] As a consequence, the mucosal immune system is exposed to an increased amount of microbial stimuli.

In healthy individuals, the homeostasis at the mucosal surfaces of the gastrointestinal tract is maintained by a balanced release of anti- and pro-inflammatory cytokines. Emerging knowledge on mucosal immune regulation comes from animal models of colitis.[10] As such, it has been established that the pro-inflammatory cytokine tumor necrosis factor-α (TNF-α) is associated with epithelial damage.[11,12] Furthermore, chronic intestinal inflammation is highly associated with increased mucosal TNF-α production. A causative role for TNF-α in the pathogenesis of intestinal inflammation is further confirmed by the fact that these patients experience dramatic improvement upon anti-TNF-α treatment.[13] Under physiological conditions these pro-inflammatory responses are under the control of anti-inflammatory processes. As such, IL-10 knockout (IL-10 KO) mice develop spontaneous intestinal inflammation. Corolarily, treatment with an IL-10-producing Lactococcus appears to exert a potent anti-inflammatory effect both in mice models as well as in man.[14,15] In parallel with the expanding knowledge on the pathogenesis of chronic inflammatory diseases, recent data suggest that pro-inflammatory cytokines may also play a role in the pathophysiology of mucositis.[16] In adult leukemia patients receiving chemotherapy, mucositis development is correlated with increased serum levels of TNF-α.[17] Moreover, various interventions that limit mucositis are frequently found to result from direct or indirect inhibition of the TNF-α release.[16,18,19]

Thus far, it is not known to what extent the mucosal immune system is still functional despite therapy with MTX. Subsequently, it is not clear whether the mucosal immune cells actively contribute to the course of mucositis. To address these questions, we analyzed the effects of MTX treatment on various components of the mucosal immune system.

METHODS

Animals

Specific pathogen-free (SPF) 10-week-old female BALB/c mice were purchased from Charles River (Saint Aubin Leés Elbeuf, France). SPF 10-week-old female LPS-unresponsive C3H/HeJ mice and LPS-responsive C3H/HeN mice[20,21] were purchased from CLEA Japan, Inc. (Tokyo, Japan). SPF 8- to 10-week old IL-10-deficient C57BL/6 mice, formally designated 'IL-10^{tm1Cgn}' (I.J. Bristol, M. Mähler, E.H. Leiter, J.P. Sundberg: IL-10tm1Cgn, an IL-10 gene-targeted mutation; JAX notes 471, The Jackson Laboratory, Bar harbor, ME, USA, 1997) (obtained from M. Mähler, Hanover, Germany), and their wild-type (WT) littermates were bred at the animal facility of the Erasmus MC (Rotterdam, the Netherlands) and maintained in isolator cages with water and a standard pellet diet (Hope Farms, Woerden, the Netherlands) *ad libitum*.

Induction of mucositis by MTX in different mouse models

All animal procedures and protocols were performed with the approval of local institutional animal studies ethics committee. For the *in vivo* studies, we have adapted a rat MTX-induced mucositis model to a mouse system.[22,23] The dosages of MTX (Emthrexate (PF) Pharmacie B.V., Haarlem, the Netherlands) used in this model were optimized for each mouse strain in order to obtain full recovery after severe damage of the small intestine (characterized by villus atrophy, crypt loss and epithelial flattening). All mice were weighed daily and euthanized by CO_2 administration at indicated time points.

LPS pre-treated mice

BALB/c mice were treated with an intra-peritoneal (i.p.) injection of 5 μg LPS (from Escherichia coli serotype 055: B5, Sigma-Aldrich, Zwijndrecht, the Netherlands) or saline on day -2. Subsequently, on day -1 and day 0, mice were injected i.p. with MTX dosages of 100 and 50 mg/kg body weight, respectively, or equivalent volumes of saline for controls. Mid-jejunum segments were collected on days 3 and 5 from 4 to 5 animals per treatment group (described in Histology).

LPS-responsive versus -unresponsive mice

On days -1, 0 and 4, C3H/HeJ and C3H/HeN mice were injected i.p. with MTX dosages of 200, 100 and 100 mg/kg body weight, respectively, or equivalent volumes of saline for controls. Each treatment group consisted of 8 animals per group. All mice were sacrificed on day 7 after MTX treatment.

Treatment of mice for isolation of lymphocytes and peritoneal macrophages

BALB/c mice were injected i.p. with a single MTX dose of 100 mg/kg body weight or an equivalent volume of saline for controls. At 42 h after injection, mononuclear cells from lamina propria (LPMCs), mesenteric lymph nodes (MLNs) and Peyer's patches (PPs) were isolated (described in Isolation of Lymphocytes). Each study group consisted of at least 4 mice.

IL-10-deficient C57BL/6 (IL-10 KO) versus WT littermates

On day -1 and day 0, mice were treated i.p. with MTX dosages of 100 and 50 mg/kg body weight, respectively, or equivalent volumes of saline for controls. On days 1, 3 and 7, segments of mid-jejunum were collected from 6 MTX-treated animals and 3 controls of both WT and KO mice (described in Histology).

Isolation and culture of macrophages

Macrophage cell line

Cells of a murine macrophage cell line (RAW264.7) were obtained from the American Type Culture Collection. Cells were grown in DMEM (Life technologies, Breda, the Netherlands) supplemented with 10% heat-inactivated fetal bovine serum (FBS; Integro, Leuvenheim, the Netherlands), 1% non-essential amino acids (Bio Whittaker, Verviers, Belgium), 100 U/ml penicillin and 100 μg/ml streptomycin (Life technologies) and incubated in a humified incubator at 37 °C with 5% CO_2. Cells were exposed to LPS in the presence of various quantities of MTX as indicated. A total of 1 x 10^5 cells per well were seeded in 96-well plates in the presence of 0 and 1 ng/ml LPS. Serial dilutions of MTX ranging from 0 to 12.5 μg/ml were added per well. After 24 h of incubation, supernatants were assayed by ELISA for IL-10 and TNF-α (described in Immunoassays for Cytokines).

In vitro MTX treatment of peritoneal macrophages

Naive 10-week-old female BALB/c mice were sacrificed. Resident peritoneal macrophages were collected by flushing the peritoneal cavity with 5 ml of RPMI 1640 medium (Life technologies) containing 10% FBS, 0.015 mol/l HEPES, 0.002 mol/l L-glutamine (BioWhittaker), 100 U/ml penicillin and 100 μg/ml streptomycin. Cells were centrifuged for 10 min at 1400 revolutions per minute (r.p.m.) and re-suspended in medium. Next, macrophages were counted with Türk solution and 1 x 10^5 macrophages per well were seeded in 96-well plates in the presence of 10 ng/ml LPS. After 24 h of incubation, supernatants were assayed by ELISA for IL-10 and TNF-α.

In vivo MTX treatment of peritoneal macrophages

Ten-week-old female BALB/c mice were injected i.p. with a single MTX dose of 100 mg/kg body weight or an equivalent volume of saline for controls. At 42 h after injection, peritoneal macrophages were isolated and cultured as described above. Peritoneal macrophages were stimulated with 0, 1 or 10 ng/ml LPS and supernatants were assayed by ELISA for IL-10 and TNF-α at 24 h.

Isolation of lymphocytes

The small intestine from stomach to the ileocecal valve was resected for the isolation of LPMCs, PPs lymphocytes and MLN lymphocytes. Viability of the isolated lymphocytes was determined by trypan blue exclusion.

LPMCs

Mononuclear cells from the small intestinal lamina propria were isolated according to the procedures described by Coligan *et al.*[24] with some minor modifications.

The intestine was cut open longitudinally, thoroughly washed in Ca^{2+}- and Mg^{2+}-free (CMF) HBSS (Life technologies) with 0.015 mol/l HEPES (Merck/VWR, Amsterdam, the Netherlands) pH 7.2 and cut into small pieces. To remove epithelial cells and intra-epithelial lymphocytes, the intestinal pieces were incubated twice for 20 min in a shaker (250 r.p.m.) at 37 °C in 20 ml HBSS-CMF-HEPES supplemented with 10% FBS, 0.005 mol/l dithiothreitol (DTT; Sigma-Aldrich), 0.005 mol/l EDTA (Merck/VWR), 100 U/ml penicillin and 100 μg/ml streptomycin. LPMCs were isolated by incubating the remaining intestinal pieces during two subsequent periods of 1 h at 37 °C in a shaker (250 r.p.m.) in 20 ml complete RPMI pH 7.2, containing RPMI 1640 (Life technologies), 10% FBS, 0.005 mol/l DTT, 0.015 mol/l HEPES, 0.002 mol/l L-glutamine (Bio Whittaker), 100 U/ml penicillin and 100 μg/ml streptomycin supplemented with 100 U/ml collagenase type VIII (Sigma-Aldrich) and 10 μg/ml DNAse I (Sigma-Aldrich). Mononuclear cells were harvested by sieving the cell suspension through a 70 μM cell strainer (Micronic, Lelystad, the Netherlands), washed with HBSS-CMF-HEPES and purified by Percoll (Amersham Biosciences, Roosendaal, the Netherlands) density gradient centrifugation (40/90%) at the interface.After washing, cells were suspended in complete Iscove's Modified Dulbecco's Medium (IMDM) containing 50 μM β-mercaptoethanol (Merck/VWR).

PPs lymphocytes

The small intestine segment from the stomach to the ileocecal valve was isolated and PPs were excised. Excised PPs were incubated in HBSS-CMF-HEPES supplemented with FBS, EDTA, DTT, penicillin and streptomycin for 20 min in a shaker at 250 r.p.m. at 37 °C to remove epithelial cells. Lymphocytes were recovered in HBSS-CMF-HEPES by sieving the PP through a 70 μM cell strainer. After washing with HBSS-CMF-HEPES, lymphocytes were suspended in complete IMDM containing 50 μM β-mercaptoethanol.

MLN lymphocytes

MLNs were placed in HBSS-CMF-HEPES and sieved through a 70 μM cell strainer. After washing with HBSS-CMF-HEPES, lymphocytes were suspended in complete IMDM containing 50 μM β-mercaptoethanol.

Culture and stimulation of lymphocytes

Lymphocyte suspensions were stimulated with hamster anti-mouse CD3ε-chain mAbs and hamster anti-mouse CD28 mAb (145-2C11 and 37.51, respectively, BD Pharmingen, Alphen a/d Rijn, the Netherlands). A 96-well plate was pre-coated overnight with 100 μl anti-CD3ε (2 μg/ml) in PBS. Hundred microliters of lymphocyte suspension (10^6 cells/ml) in complete IMDM containing 50 μM β-mercaptoethanol was added to the wells combined with 100 μl anti-CD28 (4 μg/ml) in complete IMDM containing 50 μM

β-mercaptoethanol. Cell cultures were maintained in a humified incubator at 37 °C with 5% CO_2. After 48 h of incubation, the supernatant was collected for further analysis.

Immunoassays for cytokines

Supernatants of macrophage cultures were assayed by ELISA using the mouse IL-10 BD OptEIA™ ELISA Set (BD Biosciences, Alphen a/d Rijn, the Netherlands) and the mouse TNF-α (Mono/Poly) BD OptEIA™ ELISA Set (BD Biosciences). Measurements were analyzed by a VERSAmax Microplate reader (Molecular Devices Ltd, Wokingham, UK).

Supernatants of LPMCs, PP lymphocytes and MLN lymphocytes were assayed using a Cytometric Bead Array kit for IL-10, TNF-α and IFN-γ according to instructions of the manufacturer (BD Biosciences). IL-2 levels were determined with ELISA (BD Biosciences).

Fluorescent antibody staining of isolated LPMCs

After polyclonal stimulation, cytospins of 25000 LPMCs per slide were prepared according to standard procedures. After fixation in methanol, slides were blocked for 1 h at room temperature with 10% normal mouse serum in Teng-T (0.01 M Tris, 0.005 M EDTA, 0.15 M NaCl, 0.25% gelatin, 0.05% Tween-20), rinsed with PBS and incubated overnight in the dark at 4 °C with antibodies diluted in PBT (1% BSA, 0.1% Triton-X100 in PBS): anti-CD3ε-FITC, 1:50 (clone 145-2C11); anti-CD11b-FITC, 1:50 (clone M1/70) (Biolegend, San Diego, CA, USA) and anti-TNF-α, 1:200 (Santa Cruz Biotechnology, Santa Cruz, CA, USA). Texas Red-labeled donkey anti-goat was applied for 1 h at room temperature to detect TNF-α. All slides were mounted with a 4,6-diamidino-2-phenylindole, dihydrochloridehydraat/Mowiol solution. As a control, double and single incubations of the antibodies were included.

Histology

For histology, 5-mm segments of mid-jejunum were fixed in 4% PFA in PBS and paraffin embedded. 4-μm sections were routinely stained with hematoxylin (Vector Laboratories, Burlingame, CA, USA) and eosin (Sigma-Aldrich) to study morphological alterations in crypts and villi. We have developed a histology score in order to quantitate the severity of mucositis. The histology score ranged from 0 to 13 and was subdivided in the following categories: villus aspect (0 = normal, 1 = short, 2 = extremely short), villus tops (0 = normal, 1 = damaged, 2 = severely damaged), epithelium (0 = normal, 1 = flattened, 2 = damaged, 3 = severely damaged), inflammation (0 = no infiltration, 1 = mild infiltration, 2 = severe infiltration), crypts (0 = normal, 1 = mild crypt loss, 2 = severe crypt loss), cryptabcesses (0 = none, 1 = present) and bleeding (0 = none, 1 = present).

Finally, villus lenghts were measured (10 villi per histology section). Histology was scored blinded by an independent pathologist.

Statistical analysis

Changes in weight and levels of cytokines were statistically analyzed using the Student's *t*-test. A $P < 0.05$ was considered statistically significant. Data are presented as the mean 6 ± standard error of the mean and n = 4 to 8 mice per group as indicated. All experiments have been performed at least twice. One representative experiment is shown. The IL-10 KO versus WT experiment (as shown in Figure 5) was performed once (n = 6 mice per treatment group for each selected time point).

RESULTS

LPS pre-treatment is associated with enhanced weight loss and increased signs of mucositis

We sought to determine whether microbial stimuli contribute to MTX-induced mucositis. BALB/c mice, pre-treated with LPS prior to MTX treatment, showed a more profound weight loss compared with saline pre-treated mice. These differences reached statistical significance on days 3 and 4 (Figure 1A). The severity of weight loss upon MTX treatment corresponded with the intestinal damage as determined by histological analysis on days 3 and 5. Morphological analysis of saline pre-treated mice that were treated with MTX revealed mild epithelial flattening in the crypt and mild crypt loss but no villus atrophy on day 3 (Figures 1B and C). In contrast, LPS pre-treated mice showed enhanced intestinal damage compared with saline pre-treated mice at this time point as characterized by severe villus atrophy, massive crypt loss and increased cellular infiltration of the lamina propria (Figures 1B and C). Finally, regeneration occurred in saline pre-treated MTX-treated mice on day 5. However, LPS pre-treated mice regenerated less well since they still displayed villus atrophy and a higher histology score compared with controls on day 5 (Figures 1 B and C). Notably, no morphological changes on any of the assessed days were found in control mice that were treated with LPS or saline only (Figures 1 B and C).

To further elucidate the role of LPS in the pathogenesis of MTX-induced mucositis, we exposed LPS-responsive and LPS-unresponsive mice to MTX. In general, mice with the C3H background appeared to be less susceptible for the MTX-induced mucosal damage when compared with the previously tested mouse strains. In this set of experiments, LPS-responsive mice recovered more slowly compared with LPS-unresponsive mice, which reached significance on days 2, 5, 6 and 7 (Figure 2). These experiments establish a contributive role for LPS to the severity of MTX-induced mucositis.

MTX does not inhibit LPS-induced TNF-α- and IL-10 release by macrophages

To elucidate the nature of the innate immune responses upon MTX treatment, we exposed a macrophage cell line to increasing concentrations of MTX and LPS (1 ng/ml). Upon LPS stimulation, these cells release both TNF-α and IL-10. As depicted in Figure 3(A), increasing concentrations of MTX did not affect LPS-induced TNF-α and IL-10 release.

Next, we stimulated peritoneal macrophages from naive mice with LPS (10 ng/ml) in the presence of increasing concentrations of MTX. Again, MTX did not suppress LPS-induced TNF-α and IL-10 production (Figure 3B). To establish whether *in vivo* MTX treatment would affect cytokine production by macrophages, peritoneal macrophages from MTX-treated mice were stimulated ex vivo with LPS (at 1 and 10 ng/ml). After 24 h of LPS stimulation, peritoneal macrophages that were isolated from MTX-treated mice produced a significantly higher amount of both TNF-α and IL-10 in comparison to peritoneal macrophages isolated from untreated mice (Figure 3C). Notably, no differences were found in the viability of macrophages after MTX treatment either *in vivo* or *in vitro*.

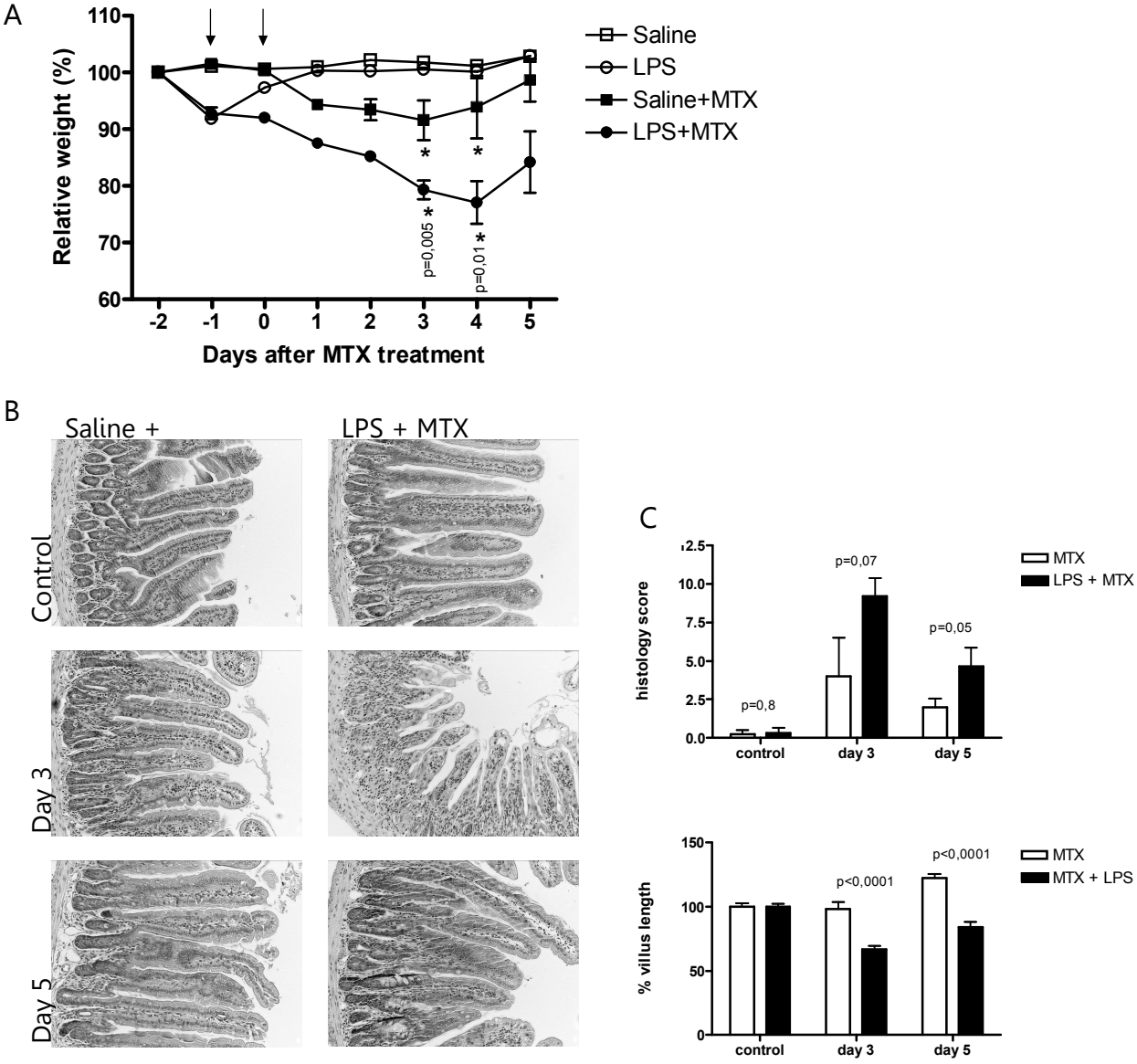

Figure 1 *LPS pre-treatment is associated with enhanced weight loss and increased severity of MTX-induced mucositis. (A) Mice pretreated with LPS i.p. 1 day prior to MTX injection (= 4day -2) display significantly enhanced weight loss compared with mice receiving only MTX. (Arrows indicate MTX or saline treatment i.p. and asterisks indicate statistically significant difference). (B) Increase of histological changes of intestinal samples (more severe villus atrophy, massive crypt loss and increased cellular infiltration of the lamina propria) derived from LPS pre-treated mice in comparison to saline pre-treated mice. (C) Increase of histological score and reduced villus lengths in LPS pre-treated mice in comparison to saline pre-treated mice (P-values are indicated).*

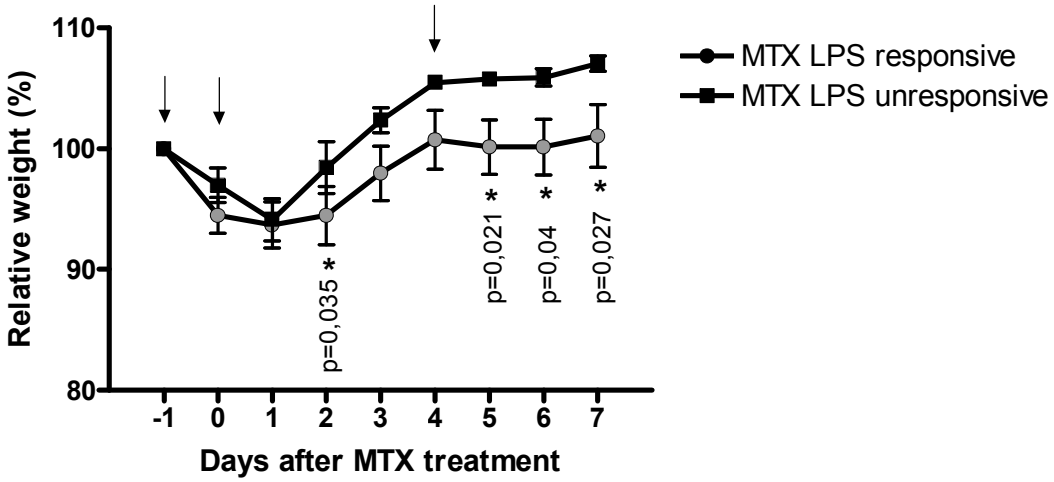

Figure 2 *LPS-responsive mice show a sub-optimal weight gain after MTX treatment compared with LPS-unresponsive mice. LPS-responsive and LPS-unresponsive mice were exposed to MTX. LPS-responsive mice recovered more slowly compared with LPS-unresponsive mice upon MTX treatment. (Arrows indicate MTX or saline treatment i.p. and asterisks indicate statistically significant difference).*

Alterations in cytokine production by lymphocytes from lamina propria, MLNs and PPs derived from MTX-treated mice

Responses of the adaptive intestinal immune system were assessed by determining the production of TNF-α, IFN-γ, IL-2 and IL-10 by re-stimulated mononuclear cells derived from various intestinal locations. Upon polyclonal stimulation with anti-CD3ε and anti-CD28 mAb, lymphocytes from MLN, PP and LPMCs from both MTX-treated and untreated mice produced TNF-α, IFN-γ, IL-10 and IL-2. The production of none of the cytokines studied was significantly inhibited by *in vivo* MTX treatment (Figure 4A). Moreover, LPMCs from MTX treated mice produced significantly more TNF-α, IFN-γ and IL-10 versus LPMCs from non-treated mice. Also, there was a significant increase in TNF-α production in MLN cultures of MTX-treated mice compared with untreated controls. PP lymphocytes from MTX-treated mice produced significantly more IL-2 than PP lymphocytes from untreated controls (Figure 4). The fact that lymphocytes from all intestinal locations produce IL-2 confirms that adaptive immune cells are functional despite MTX treatment since IL-2 is specifically produced by lymphocytes. However, within LPMCs it is possible that non-lymphocytes contribute to the cytokine production observed. To address this question TNF-α/CD3 and TNF-α/CD11b immuno-histochemistry of polyclonally stimulated LPMCs was performed. These stainings show that both CD3+ lymphocytes as well as CD11b+ monocytes/macrophages are the source of the TNF-α (Figure 4B).These experiments show that both innate and adaptive mucosal immune cells are still capable of producing pro-inflammatory cytokines such as TNF-α and IFN-γ as well as the anti-inflammatory cytokine IL-10 during mucositis.

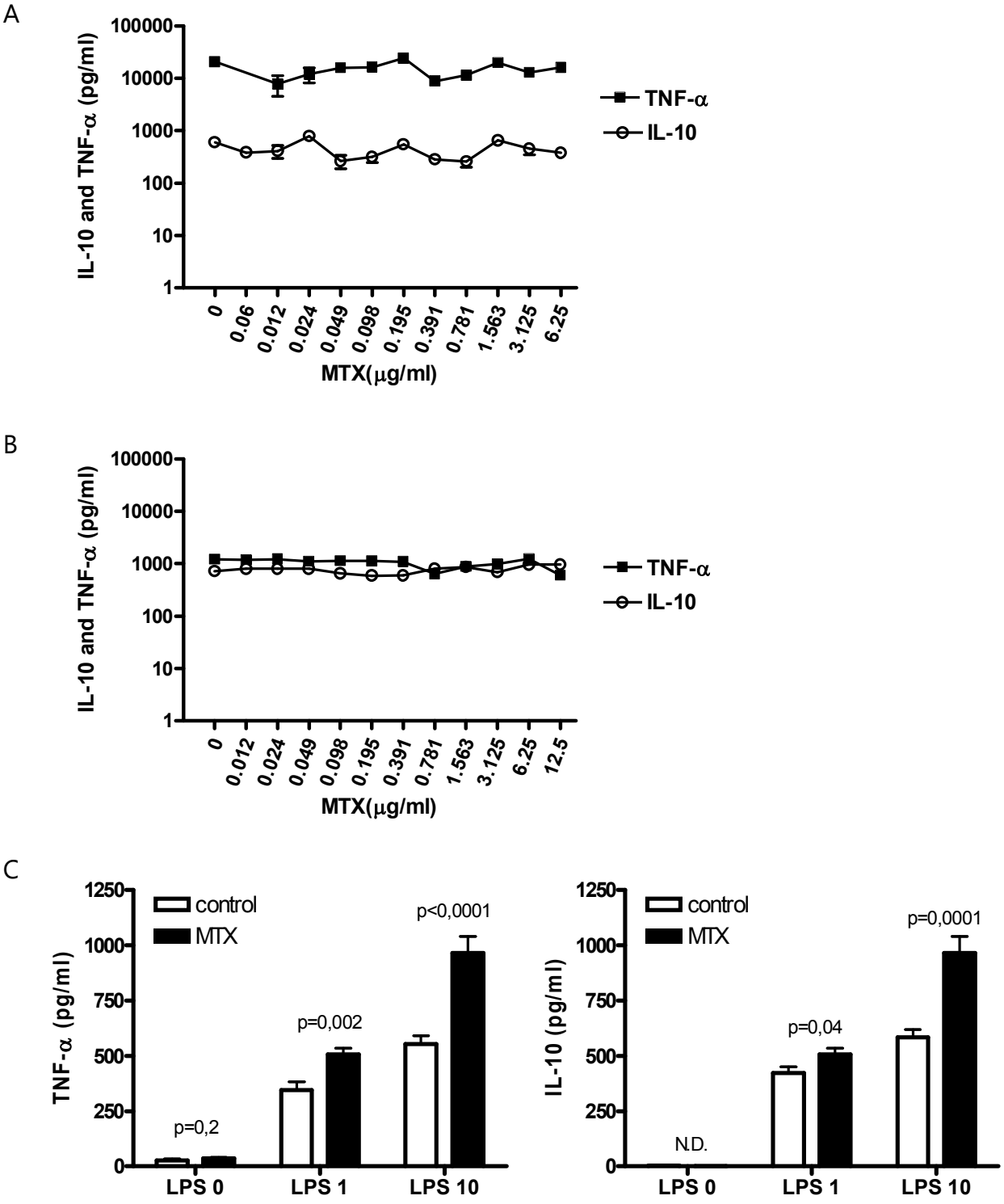

Figure 3 *Treatment of macrophages with MTX either in vivo or in vitro does not inhibit in vitro LPS-induced TNF-α and IL-10 release. (A) A macrophage cell line was exposed simultaneously to increasing concentrations of MTX and LPS (1 ng/ml). Upon LPS stimulation, macrophages released both TNF-α and IL-10. Increasing concentrations of MTX did not suppress LPS-induced TNF-α and IL-10 release. (B) Peritoneal macrophages were isolated from naive mice and stimulated ex vivo with LPS (10 ng/ml). Macrophages were exposed simultaneously to increasing concentrations of MTX. Upon LPS stimulation, macrophages released both TNF-α and IL-10. Increasing concentrations of MTX did not suppress LPS-induced TNF-α and IL-10 release. (C) Peritoneal macrophages were isolated from MTX-treated and untreated mice and stimulated ex vivo with LPS (1 and 10 ng/ml). Macrophages from MTX-treated mice produced significantly more TNF-α and IL-10 upon LPS stimulation compared with macrophages from untreated mice (P-values are indicated). N.D., not detectable*

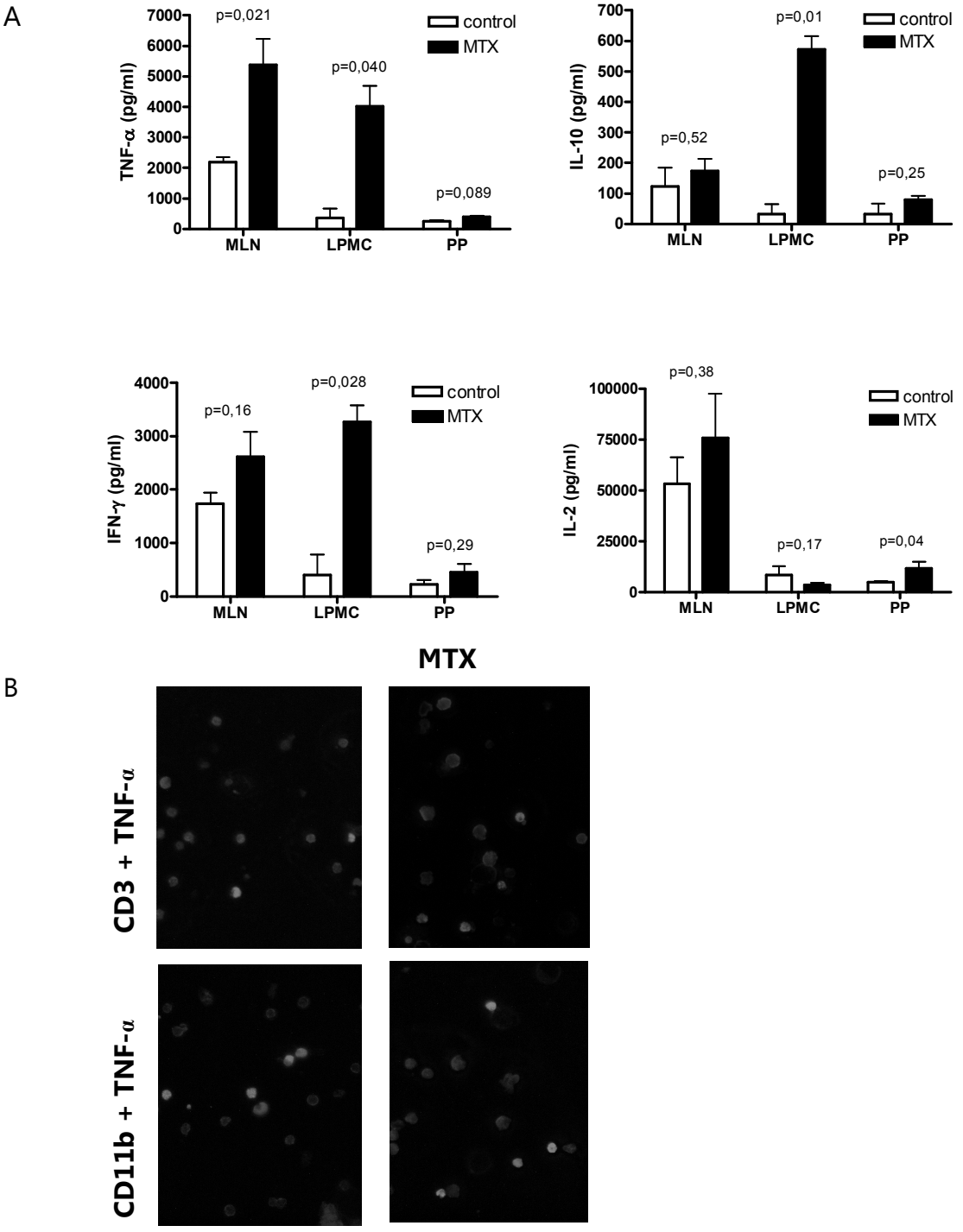

Figure 4 *Increased cytokine release ex vivo, by re-stimulated LPMCs, cells from MLNs and cells from PPs derived from MTX-treated mice in comparison to controls. (A) We determined the production of TNF-α , IFN-γ, IL-10 and IL-2 by stimulated T cells derived from various intestinal locations. Upon polyclonal stimulation (anti-CD3/anti-CD28), LPMCs from MTX-treated mice produced significantly more TNF-α , IFN-γ and IL-10 versus LPMCs from non-treated mice. MLN-derived lymphocytes from MTX-treated mice produced significantly more TNF-α and PP-derived lymphocytes from MTX-treated mice produced significantly more IL-2 compared with lymphocytes derived from untreated mice (P-values are indicated). (B) TNF-α/CD3 and TNF-α/CD1 1b double stainings of polyclonally stimulated LPMCs from MTX-treated (right panel) or untreated (left panel) mice. Red-stained cells are TNF-α-producing cells. Green-stained cells are either CD3+ (upper panel) or CD11b+ (lower panel). Yellow cells indicate double positivity for CD3 and TNF-α (upper panel) or CD11b and TNF-α (lower panel). These figures indicate that both innate (CD11b+) and adaptive (CD3+) immune cells within the lamina propria are capable of producing TNF-α despite MTX treatment.*

IL- 10 restricts MTX-induced mucositis

To gain further insight into the role of IL-10 in mucositis development *in vivo*, we treated IL-10 KO mice and their WT littermates with MTX. MTX-treated IL-10 KO mice lost profoundly more weight in comparison to MTX-treated WT controls that reached significance on days 1 and 2 (Figure 5A). On days 1 and 3 after MTX treatment, analysis of the intestinal morphology of IL-10 KO mice revealed strongly increased symptoms of mucositis in comparison to WT mice (Figures 5B and C). On day 7, both groups appeared to regenerate equally well (Figures 5B and C). Notably, at this age, we did not detect any pathological change in the intestinal morphology of non-treated IL-10 KO mice, which has been described in IL-10 KO mice at later time points (Figures 5B and C).

DISCUSSION

In this study, we showed that during MTX-induced mucositis the mucosal immune system is still able to respond to bacterial stimuli, which is remarkable considering the immunosuppressive capacity of MTX. In healthy individuals, mucosal homeostasis of the gastrointestinal tract requires the involvement of innate cells, such as macrophages, and adaptive cells, such as B and T cells. The typical innate responsiveness of macrophages to LPS is not suppressed either by *in vivo* or *in vitro* MTX treatment. Notably, in our experimental set-up these cells expressed an enhanced susceptibility to LPS stimulation that indicates that MTX treatment may rather prime instead of suppress these cells. The adaptive immune responses are also intact as reflected by the capacity of lamina propria, MLN and PP lymphocytes from MTX-treated mice to respond to anti-CD3ε and anti-CD28 mAb stimulation.

MTX is effective as chemotherapy through the inhibition of cellular proliferation. As a result, rapidly dividing intestinal epithelial cells are strongly affected, leading to severe intestinal barrier dysfunction. Subsequently, the innate immune cells are increasingly exposed to microbial immunogens such as LPS that is associated with activation of the mucosal immune system. We have established a contributive role for LPS in the pathogenesis of mucositis by showing that LPS pre-treatment enhances MTX-induced intestinal damage. These data are substantiated by our observations that LPS-responsive mice regained weight more slowly compared with LPS-unresponsive mice after MTX treatment.

In order to establish whether disruption of the intestinal barrier would also lead to activation of adaptive immune responses, we isolated LPMCs, PP lymphocytes and MLN lymphocytes of mice treated with MTX. Indeed, upon ex vivo re-stimulation, these cells produced enhanced levels of cytokines. This finding indicates that instead of MTX-induced immune suppression, endogenous priming of these lymphocytes may have occurred as a consequence of MTX-induced mucositis.

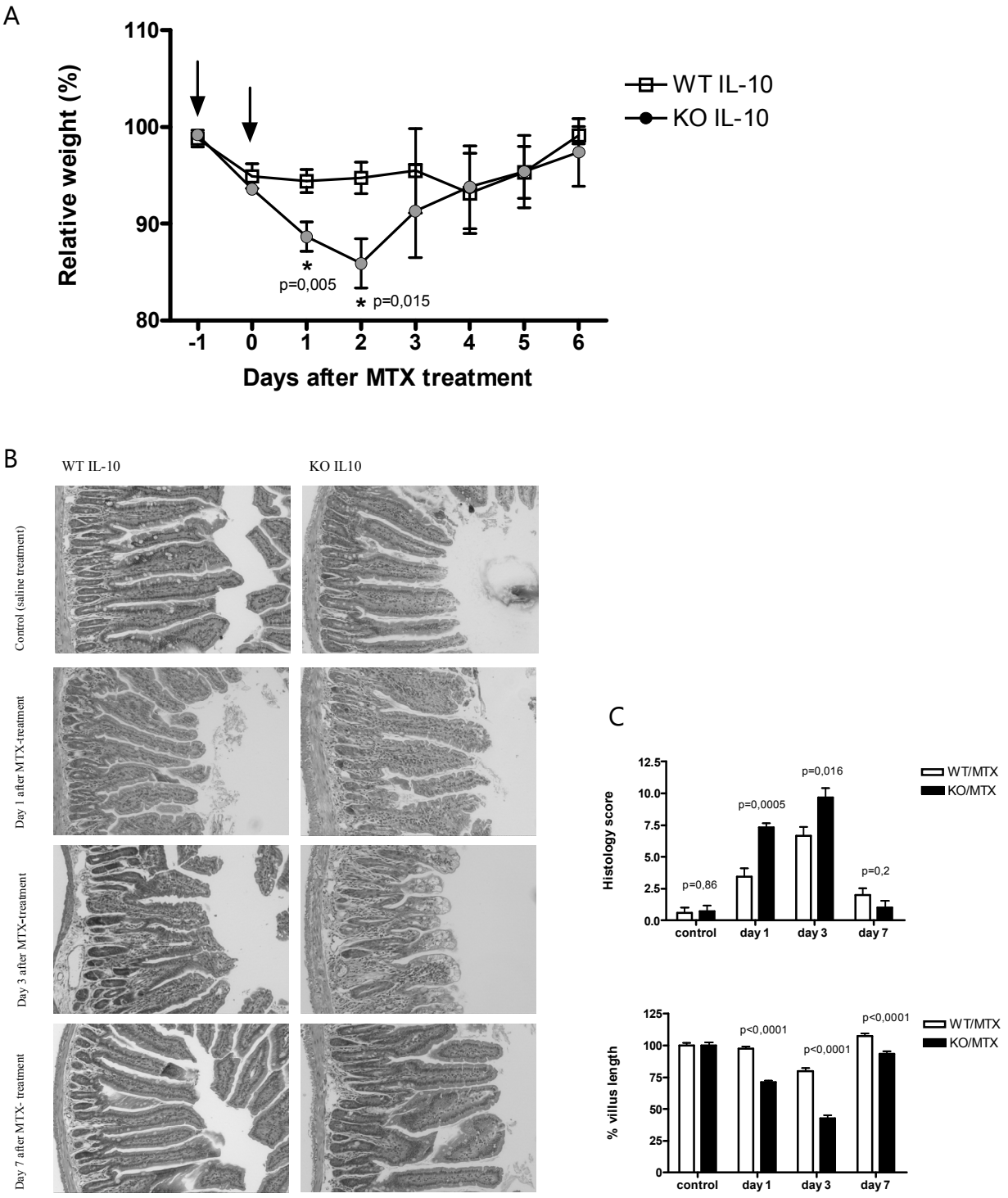

Figure 5 *IL-10 restricts severity of MTX-induced mucositis. (A) IL-10 KO mice and their WT littermates were treated with MTX. MTX-treated IL-10 KO mice lost more weight in comparison to MTX-treated WT controls. (Arrows indicate the timing of MTX or saline treatment i.p. and asterisks indicate statistically significant difference). (B) Increase of histopathological changes in intestinal samples (increased crypt and epithelial loss and complete villus atrophy) derived from IL-10 KO mice in comparison to samples from their WT littermates on day 3. (C) Increase of histopathological score and reduced villus lengths displayed by IL-10 KO mice in comparison to WT littermates on days 1 and 3 (P-values are indicated).*

As activation of the mucosal immune system can lead to pro-inflammatory as well as anti-inflammatory processes, we determined the production of TNF-α and IL-10 by these mucosal T cells.

Intriguingly, besides the anticipated pro-inflammatory TNF-α response, we also detected a robust IL-10 release by LPMCs. As IL-10 is strongly implicated in protection from intestinal inflammatory processes such as IBD, this prompted us to specifically investigate the potential protective role for IL-10 in MTX-induced mucositis. Indeed, we established that mice deficient in IL-10 experience more weight loss and enhanced intestinal damage on histology compared with WT controls. To a certain extent, these data imply that the pathogenesis of mucositis has strong similarities to that of inflammatory bowel diseases.

The pivotal finding of this study is that both innate and adaptive immune responses remain intact during MTX treatment. In response to enhanced exposure to microbial-derived stimuli, a combined pro- and counter-inflammatory response is elicited. How and to what extent these responses contribute to the damage and repair that is associated with mucositis is difficult to establish.

Based on these data, we support that selective targeting of the pro-inflammatory response during mucositis may become a beneficial strategy.[18,19,25] As such, this may facilitate ongoing protective anti-inflammatory responses. In line with this view, other strategies such as the use of antibiotics aiming at neutralizing specific microbial stimuli (*i.e.* LPS) appear crucial. Finally, novel experimental therapies for IBD patients such as the application of IL-10-producing *Lactococci* may provide attractive means to prevent mucositis.[14, 15]

ACKNOWLEDGEMENTS

We thank Prof. H.A. Büller for critically reading the manuscript. This work was supported by a grant from Numico Research BV, Wageningen, the Netherlands.

REFERENCES

1. Sonis ST, Elting LS, Keefe D. et al. Perspectives on cancer therapy-induced mucosal injury: pathogenesis, measurement, epidemiology, and consequences for patients. Cancer 2004;100:1995-2025
2. Bellm LA, Epstein JB, Rose-Ped A, Martin P, Fuchs HJ. Patient reports of complications of bone marrow transplantation. Support. Care Cancer 2000;8:33-39.
3. Elting LS, Cooksley C, Chambers M, Cantor SB, Manzullo E, Rubenstein EB. The burdens of cancer therapy. Clinical and economic outcomes of chemotherapy-induced mucositis. Cancer 2003;98:1531-1539.
4. Ruescher TJ, Sodeifi A, Scrivani SJ, Kaban LB, Sonis ST. The impact of mucositis on alpha-hemolytic streptococcal infection in patients undergoing autologous bone marrow transplantation for hematologic malignancies. Cancer 1998;82:2275-2281.
5. McGuire DB. Mucosal tissue injury in cancer therapy. More than muscositis and mouthwash. Cancer Pract. 2002;10:179-191.
6. Meurman JH, Pyrhonen S, Teerenhovi L, Lindqvist C. Oral sources of septicaemia in patients with malignancies. Oral Oncol. 1997;33:389-397.
7. Sonis ST. Mucositis as a biological process:a new hypothesis for the development of chemotherapy-induced stomatotoxicity. Oral Oncol. 1998;34:39-43.
8. Keefe DM, Brealey J, Goland GJ, Cummins AG. Chemotherapy for cancer causes apoptosis that precedes hypoplasia in crypts of the small intestine in humans. Gut 2000;47:632-637.
9. Anilkumar TV, Sarraf CE, Hunt T, Alison MR. The nature of cytotoxic drug-induced cell death in murine intestinal crypts. Br. J. Cancer 1992;65:552-558.
10. Strober W, Fuss IJ, Blumberg RS. The immunology of mucosal models of inflammation. Annu. Rev. Immunol. 2002;20:495-549.
11. Abreu-Martin MT, Vidrich A, Lynch DH, Targan SR. Divergent induction of apoptosis and IL-8 secretion in HT-29 cells in response to TNF-alpha and ligation of Fas antigen. J. Immunol. 1995;155:4147-4154.
12. Guy-Grand D, DiSanto JP, Henchoz P, Malassis-Seris M, Vassalli P. Smallbowel enteropathy:role of intraepithelial lymphocytes and of cytokines (IL-12, IFN-gamma, TNF) in the induction of epithelial cell death and renewal. Eur. J. Immunol. 1998;28:730-744.
13. Ricart E, Panaccione R, Loftus EV, Tremaine WJ, Sandborn WJ. Infliximab for Crohn's disease in clinical practice at the Mayo Clinic:the first 100 patients. Am. J. Gastroenterol. 2001;96:722-729.
14. Steidler L, Hans W, Schotte L. et al. Treatment of murine colitis by Lactococcus lactis secreting interleukin-10. Science 2000;289:1352-1355.
15. Braat H, Rottiers P, Huyghebaart N et al. Interleukin-10 producing Lactococcus lactis for the treatment of Crohn's disease. Gastroenterology 2005;128(suppl 2):A-104 (abstract 685).
16. Sonis ST. The pathobiology of mucositis. Nat. Rev. Cancer 2004;4:277-284.
17. Hall PD, Benko H, Hogan KR, Stuart RK. The influence of serum tumor necrosis factor-alpha and interleukin-6 concentrations on nonhematologic toxicity and hematologic recovery in patients with acute myelogenous leukemia. Exp. Hematol. 1995;23:1256-1260.
18. Sonis ST, Peterson RL, Edwards LJ. et al. Defining mechanisms of action of interleukin-11 on the progression of radiation-induced oral mucositis in hamsters. Oral Oncol. 2000;36:373-381.
19. Spielberger R, Stiff P, Bensinger W. et al. Palifermin for oral mucositis after intensive therapy for hematologic cancers. N. Engl. J. Med. 2004;351:2590-2598.
20. Sultzer BM. Genetic factors in leucocyte responses to endotoxin:further studies in mice. J. Immunol. 1969;103:32-38.
21. Glode LM, Rosenstreich DL. Genetic control of B cell activation by bacterial lipopolysaccharide is mediated by multiple distinct genes or alleles. J. Immunol. 1976;117:2061-2066.

22. Taminiau JA, Gall DG, Hamilton JR. Response of the rat small-intestine epithelium to methotrexate. Gut 1980;21:486-492.

23. Verburg M, Renes IB, Meijer HP. et al. Selective sparing of goblet cells and paneth cells in the intestine of methotrexate-treated rats. Am. J. Physiol. Gastrointest. Liver Physiol. 2000;279:G1037-1047.

24. Coligan CE, Kruisbeek AM, Marqulies DH, Shevach EH, Strober W. Current Protocols in Immunology. Green Publishing and Wiley-Interscience, New York. 2002

25. Nemzek JA, Ebong SJ, KimJ, Bolgos GL, Remick DG. Keratinocyte growth factor pretreatment is associated with decreased macrophage inflammatory protein-2alpha concentrations and reduced neutrophil recruitment in acid aspiration lung injury. Shock 2002;18:501-506.

Part II

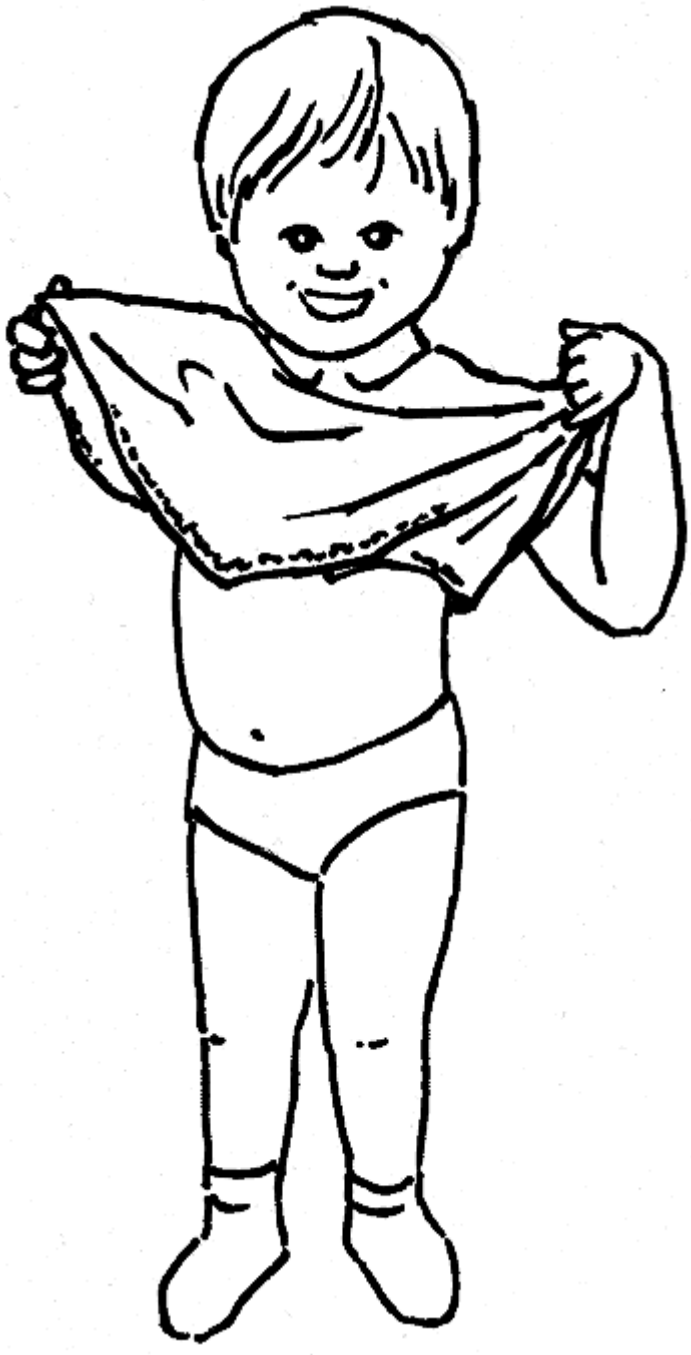

CLINICAL ASPECTS AND INTERVENTION

6

VALIDATION OF THE DIRECT NASOPHARYNGEAL SAMPLING METHOD FOR COLLECTION OF EXPIRED AIR IN PRETERM NEONATES

Sophie R.D. van der Schoor, Barbara A.E. de Koning, Darcos L. Wattimena, Dick Tibboel, Johannes B. van Goudoever

Pediatric Research 55:50-54 (2004).

ABSTRACT

In clinical studies, the oxidation of ^{13}C-labeled substrates to $^{13}CO_2$ and the measurement of the appearance of excess $^{13}CO_2$ in expiratory air has progressed to an increasingly common method as it is noninvasive and lacks the radiation exposure associated with the use of ^{14}C. The collection of respiratory CO_2 currently used occurs via trapping of CO_2 in sodium hydroxide (trapping method), sometimes in conjunction with indirect calorimetry. The aim of the present study was to determine the accuracy of our direct nasopharyngeal sampling method for the collection of breath samples in preterm infants compared with the currently used trapping method. We present a method that simplifies the collection of breath samples in preterm infants. Seven preterm infants with a gestational age of 26 - 29 wk were studied on different postnatal days (range, 8 - 52 d) while receiving full enteral feeding. A primed constant 3-h intragastric infusion of [^{13}C]bicarbonate was given, and breath samples were collected by means of direct nasopharyngeal sampling and by a sodium hydroxide trap simultaneously. Breath CO_2 isotopic enrichments rose rapidly to reach a plateau by 120 min with < 5% variation of plateau in both methods. $^{13}CO_2$ breath isotopic enrichments obtained by the direct nasopharyngeal sampling method correlated highly (r^2 = 0.933; P < 0.0001) with the trapping method. The Bland-Altman analysis showed no significant variability between the two methods and demonstrated that the 95% confidence interval is within ± 4.68 δ‰. These findings validate the simple method of direct nasopharyngeal sampling of expired air in neonates.

INTRODUCTION

During the last three decades, stable isotopes have been used extensively to investigate whole-body protein metabolism in adults, children, and newborns.[1-3] To determine the rate of substrate oxidation, the excretion of $^{13}CO_2$ in expired air must be quantified. The rate of oxidation is calculated by multiplying the isotopic enrichment of CO_2 in breath by the total rate of CO_2 excreted, correcting for the incomplete recovery of ^{13}C during an infusion of [^{13}C]bicarbonate.[1] This correction factor has to be used to adjust for the fractional recovery of CO_2.[4,5] In addition, the VCO_2 needs to be measured.

Several methods are used to quantify VCO_2, but closed-circuit indirect calorimetry is the most commonly performed method and serves as gold standard for the estimation of VCO_2. This procedure requires the patient to breathe via a mouthpiece with the nares occluded or via a hood that catches all expired CO_2.[6] However, interpretation of the results obtained from indirect calorimetry may be difficult in particular. For instance, results are difficult to interpret when there is an unmeasured loss of expired gasses because of the use of uncuffed leaking endotracheal tubes in mechanically ventilated neonates.[7] In addition, there is an increased possibility of error in the indirect calorimeter determination of oxygen consumption and VCO_2 with the low volumes of respiratory gas exchanged in small neonates[8] and the higher fraction of inspired oxygen used in critically ill patients.[9] This error is of such a significant degree that the use of indirect calorimetry is not recommended in patients receiving more than 0.60 fraction of inspired oxygen.[10]

Another method for measuring VCO_2 involves the infusion of a ^{14}C-labeled substrate and the measurement of its specific activity and the rate of excretion of $^{14}CO_2$ in breath for a period at isotopic steady-state.[11] However, the use of radioactive isotopes in children is prohibited.

Numerous studies described the use of dilution of $^{13}CO_2$ during the infusion of [^{13}C]bicarbonate to calculate CO_2 production, which avoids the quantification of total expired air.[4,12] However, this tracer technique uses a relatively complicated method to collect expired air. Breath samples must be collected using a closely fitted facemask and an inlet-outlet system with a low dead volume. Thereafter, the collected expired air has to pass through an all-glass spiral condenser containing sodium hydroxide. After liberating CO_2 by adding phosphoric acid to the solution, the CO_2 can be stored in a septum-capped tube until analysis.[13] During all these procedures to liberate CO_2, the fraction of $^{13}CO_2$ might be decreased, resulting in an underestimation of the substrate oxidation.

To collect breath samples from preterm infants in a suitable manner, we applied the direct nasopharyngeal sampling technique previously described by Perman *et al.*[14] This method has been used in older children for the noninvasive diagnosis of sucrose or lactose malabsorption by a hydrogen breath test, and in preterm infants for the

collection of expiratory air after administration of ^{13}C-labeled substrates.[14-16] However, in preterm infants, the direct nasopharyngeal sampling method has never been validated for the use in substrate oxidation studies. The direct sampling approach offers the advantage of being simple and not time-consuming, making it appropriate for use in preterm infants in combination with [^{13}C]bicarbonate stable isotope dilution technique to estimate the CO_2 production. Validation of such a method would provide a technique that could be used in a variety of clinical investigations in neonates and children.

The purpose of this study was to determine whether the direct nasopharyngeal sampling technique for the collection of expired air could be used to estimate CO_2 production in preterm infants. We validated this technique against the method using CO_2 trapping in sodium hydroxide for collection of expiratory air after [^{13}C]bicarbonate infusion in preterm infants.

METHODS

Subjects

Subjects included seven preterm infants admitted to the neonatal intensive care unit of the Erasmus MC-Sophia Children's Hospital. The study protocol was reviewed and approved by the Erasmus-MC Institutional Review Board, and written and informed consent was obtained from the parents of the preterm infants.

Direct nasopharyngeal sampling method and trapping method

The collection of expired air was obtained by two different methods, *i.e.* the direct nasopharyngeal sampling method and the trapping method. In the direct nasopharyngeal sampling technique for the collection of expired air, we used a 6F gastric tube (6 Ch Argyle; Sherwood Medical, Tullamore, Ireland) as a collection device, which was placed carefully for 1 to 1.5 cm into the nasopharynx. When the infant received supplemental oxygen by nasal prong, the oxygen air had to pass a soda-lime filter (Erich Jaeger GmbH & Co. KG, Wurzburg, Germany) before entering the nasopharynx to supply CO_2-free air. While observing the patient's normal breathing pattern, the examiner repeatedly aspirated 1 mL of each tidal volume late in the expiratory phase from the nasal prong connected to a 10-mL plastic syringe until 10 mL was obtained. Aliquots were transferred by syringe to a 1 0-mL Vacutainer (Van Loenen Instruments, Zaandam, The Netherlands).

The trapping method has been described for VCO_2 measurements in neonates.[13,17] In this method, breath samples are collected via a closely fitted facemask or canopy, which is placed around the head and chest of the neonate. The baby's head and neck were placed under the transparent Perspex canopy, and a partial seal is created by tucking the attached flexible material beneath the body and mattress to prevent any air leaks. We used a canopy as is used for indirect calorimetry studies in infants.[18] An inlet-outlet

system with a low dead volume is used to avoid dilution of the carbon dioxide < 1.5 - 2.0%. Next, the collected expired air has to pass a sample of air leaving the ventilated hood through an all-glass spiral condenser, containing 10 mL of 1 M sodium hydroxide (Merck, Darmstadt, Germany). After liberating CO_2 by adding phosphoric acid (Merck) to the solution, the CO_2 can be stored in septum-capped tubes until analysis.

Validation of the collection method

To demonstrate that the isotopic enrichment in the expired air collected by the direct nasopharyngeal sampling method showed a consistent relationship and to show that this collection of expired air is a reliable technique, comparison with the trapping method was performed. Validation of direct nasopharyngeal sampling technique and the trapping method was achieved by simultaneously obtaining duplicate paired samples of expired air according to both methods in seven clinically stable preterm infants without ventilatory support.

Tracer protocol

After baseline expired breath samples were obtained according to both methods (Figure 1), a primed (10.02 μmol/kg), 3-h continuous intragastric infusion (10.02 μmol/kg/h) of sterile pyrogen-free sodium [1-^{13}C]bicarbonate (99 mol% ^{13}C; Cambridge Isotopes, Woburn, MA, U.S.A.) was administered. Five sets of duplicate CO_2 breath samples were collected at 15-min intervals during the last hour of infusion by using both sampling techniques. Breath CO_2 isotopic enrichment was plotted against time, and the plateau defined according to the convention of taking four or more consecutive points with a coefficient of variation of < 5%.

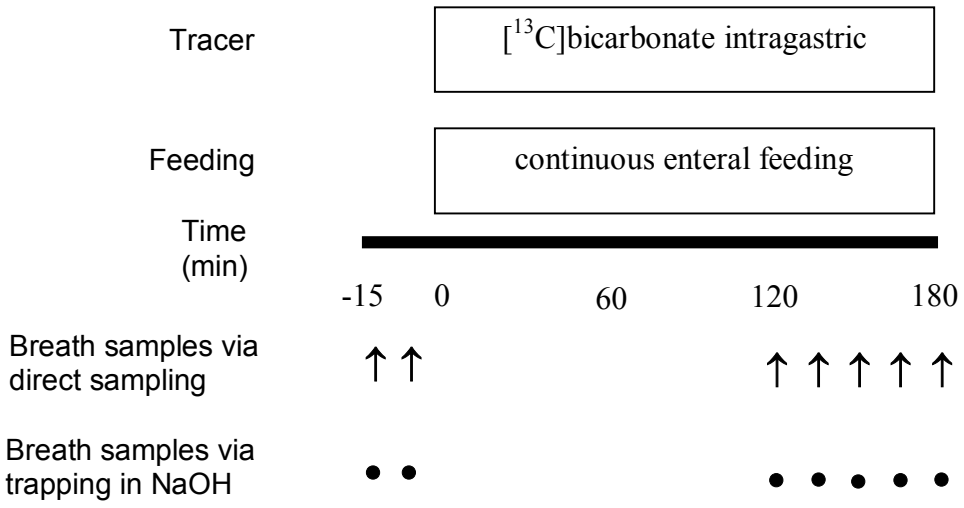

Figure 1 *Schematic overview of study protocol.*

Analytical methods

Isotopic enrichment of expired CO_2 was measured by monitoring ions at m/e 44 and 45 with a continuous flow isotope ratio mass spectrometer (ABCA; Europa Scientific, Van Loenen Instruments, Leiden, The Netherlands).[19] The ratio of the signals from the ionized species $^{13}CO_2$ and $^{12}CO_2$ each focused on one of the dual spectrometers is recorded and compared with the natural abundance of CO_2 gas of known isotopic composition relative to the standard Pee Dee Belemnite (PDB). The results of this differential measurement are expressed as the delta per mille (δ‰) difference between the $^{13}CO_2/^{12}CO_2$ ratio of the sample and standard.[20]

$$\delta^{13}C\ (‰) = \frac{R_u - R_s}{R_s} \times 1{,}000 \qquad (1)$$

where R_u is the difference between the $^{13}CO_2/^{12}CO_2$ ratio of the sample, and R_s is the difference between the $^{13}CO_2/^{12}CO_2$ ratio of the standard.

Steady-state values were obtained by determining the average CO_2 isotopic enrichment after reaching plateau as previously described.[21] $RaCO_2$ was calculated using the standard steady-state equation:[22]

$$RaCO_2 = i_B \times [(IE_I/IE_B) - 1] \qquad (2)$$

where i_B is the infusion rate of sodium [^{13}C]bicarbonate (μmol/kg/h), IE_I is the enrichment (mole percent excess) of [^{13}C]bicarbonate in the bicarbonate infusate, and IE_B is the $^{13}CO_2$ enrichment in expiratory air at plateau during the sodium [^{13}C]bicarbonate infusion (mole percent excess).

Statistics

All values are expressed in mean ± SD. Statistical analyses were performed by ANOVA, *t* test, and Pearson correlation. Significance was determined as $P < 0.05$. Bland-Altman analysis was performed to test the variability between the two sampling methods.[23]

RESULTS

All infants were appropriate for gestational age (median gestational age, 28 wk; range, 26 - 29 wk; Table 1). Seven patients who breathed spontaneously were studied; six of them received supplemental oxygen by a nasal prong. All infants were clinically stable at the time of the study. The median body weight at the time of study period was 1.2 kg (range, 1.0 - 1.5 kg), and the median postnatal age was 28 d (range, 8 - 52 d).

Table 1 Clinical characteristics

Patient	Gender	Birth weight (kg)	Gestational age (wk)	Study weight (g)	Postnatal age (d)	Ventilation
1	F	0.62	29	1.06	52	none
2	M	0.96	26	1.48	52	nasal prong
3	F	1.11	28	1.38	29	nasal prong
4	F	0.46	27	0.60	18	nasal prong
5	F	0.88	28	0.98	21	nasal prong
6	M	1.29	28	1.19	16	nasal prong
7	M	0.99	27	1.35	36	nasal prong
Median		1.01	28	1.18	28	

The estimated CO_2 production was 37.04 ± 5.99 mmol/kg/h). Isotopic steady-state was achieved during sodium [^{13}C]bicarbonate infusion with a coefficient of variation of 4.1% in the direct sampling method and 4.8% in the trapping method (Figure 2). More importantly, the delta per mille difference determined from the direct nasopharyngeal sampling method correlated highly (r^2 = 0.933; P < 0.0001) with the delta per mille difference obtained by the trapping technique.

Furthermore, Bland-Altman analysis (Figure 3) demonstrated agreement between the two methods to within ± 4.68 δ‰, *i.e.* 95% confidence interval.

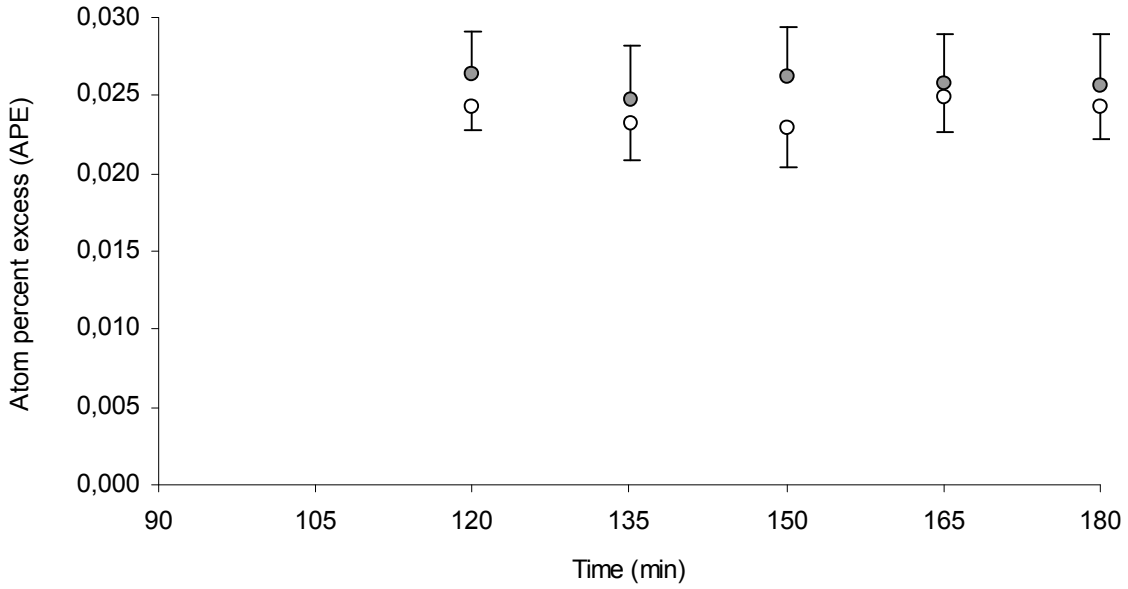

Figure 2 *Steady-state isotopic enrichment of CO_2 in breath collected by the direct nasopharyngeal sampling method (dark circles) and collected by the trapping method (white circles) after a primed-constant intragastric [^{13}C]bicarbonate infusion. An isotopic steady-state was achieved by 120 min with less than 5% variation of the plateau in both methods.*

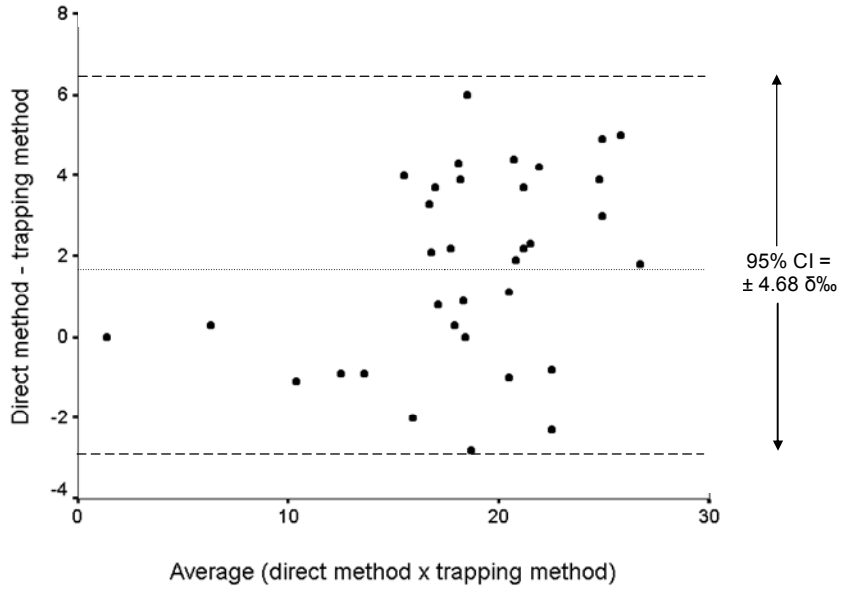

Figure 3 *Bland-Altman analysis showing the difference between the direct nasopharyngeal sampling method and the trapping method measurements of $^{13}CO_2$ enrichment in breath is in agreement to within ± 4.68 δ‰. CI indicates confidence interval.*

DISCUSSION

The present study describes a methodology for the collection of expired air in preterm infants after administration of ^{13}C-labeled material. In preterm neonates, isotopic steady-state of $^{13}CO_2$ in breath obtained by our direct nasopharyngeal sampling technique during a [^{13}C]bicarbonate infusion agreed closely with the isotopic steady-state obtained with the trapping technique during a [^{13}C]bicarbonate infusion. This is demonstrated by the highly significant correlation between the measured values acquired from both methods. Therefore, in neonates the direct nasopharyngeal sampling technique can be used for the measurement of CO_2 isotopic enrichment, which is necessary for estimation of VCO_2 and the quantification of oxidation of labeled substrates.

To determine the accuracy and precision of our technique in each individual subject in comparison with the trapping method we used the Bland-Altman analysis. Furthermore, by using this analysis we could assess the variability between the two methods.[23] As shown in Figure 3, the 95% confidence interval of the two methods vary within an acceptable ± 4.68 δ‰. In other words, there is less then 5% probability that the two methods differ more than this amount.

Although we validated our direct sampling method only in nonventilated infants, we speculate that this technique will work in ventilated infants. Instead of sampling directly from the nasopharynx, expired air has to be withdrawn from the ventilation tube. The clinical applications of the direct sampling technique for the collection of breath are extensive, because whole-body flux and oxidation rates of nutrients can be quantified in adults and infants from primed constant infusion studies using ^{13}C-labeled substrates

with the collection of expired air.[1-3] The methodology for measuring *in vivo* oxidation of substrates with the use of ^{13}C-labeled material in clinical studies has been developed with the use of isotope ratio mass spectrometry analysis. The direct sampling method can also be used in breath tests for the noninvasive diagnosis of sucrose or lactose malabsorption and gastric emptying.

The excretion of labeled CO_2 in breath after administration of ^{13}C-labeled substrates is a function of the physical variables involved in CO_2 metabolism, the kinetics of metabolism, and the delay associated with the passage through the whole-body bicarbonate pool before its expiration in the breath.[24] For example, the labeled CO_2 is temporarily retained in the bicarbonate pool of the bone, in larger organic molecules, and in smaller amounts in feces, sweat, and urine.[24] That this bicarbonate pool is limited is shown by an almost complete recovery of CO_2 during an extended infusion (24 - 48 h) and collection of expired air.[25] In short-lasting studies in neonates, the CO_2 retention varies between 70 and 84% and is correlated with the energy intake, metabolic rate, and VCO_2.[5] Therefore, to determine the rate of oxidation of a labeled substrate, a correction factor is commonly used in the calculations.[5] However, in previous studies in preterm infants without signs of infection or respiratory distress, we have shown that the correction factor can be left out assuming a constant VCO_2 for a few hours and by the use of a sequential [^{13}C]bicarbonate and ^{13}C-labeled substrate infusion.[13,17] Therefore, our direct sampling technique can be used very well to collect expired CO_2 for mass spectrometric analysis.

CONCLUSIONS

We conclude that the presently described direct nasopharyngeal sampling method for the collection of expired air in preterm neonates is as good as other previously described breath collection methods for the calculation of substrate oxidation. This method is simple to use, and should provide new opportunities to study metabolism of various substrates in preterm infants, children, and adults.

ACKNOWLEDGMENTS

The authors thank Prof. dr. H.A. Büller for helpful comments and review of the manuscript. We also thank the parents who consented for their babies to participate in the study.

REFERENCES

1. Matthews DE, Motil KJ, Rohrbaugh DK, Burke JF, Young VR, Bier DM. Measurement of leucine metabolism in man from a primed, continuous infusion of L-[1-^{13}C]leucine. Am J Physiol 1980;238:E473-E479.
2. Denne SC, Kalhan SC. Leucine metabolism in human newborns. Am J Physiol 1987;253:E608-E615
3. Van Goudoever JB, Sulkers EJ, Halliday D, Degenhart HJ, Carnielli VP, Wattimena JL, Sauer PJ. Whole-body protein turnover in preterm appropriate for gestational age and small for gestational age infants: comparison of [^{15}N]glycine and [1-^{13}C]leucine administered simultaneously. Pediatr Res 1995;37:381-388.
4. Kien CL. Isotopic dilution of CO_2 as an estimate of CO_2 production during substrate oxidation studies. Am J Physiol 1989;257:E296-E298.
5. Van Aerde JE, Sauer PJ, Pencharz PB, Canagarayar U, Beesley J, Smith JM, Swyer PR. The effect of energy intake and expenditure on the recovery of $^{13}CO_2$ in the parenterally fed neonate during a 4-hour primed constant infusion of $NaH^{13}CO_3$. Pediatr Res 1995;19:806-810.
6. Ferrannini E. The theoretical bases of indirect calorimetry: a review. Metabolism 1988;37:287-301.
7. Forsyth JS, Crighton A. Low birthweight infants and total parenteral nutrition immediately after birth. I. Energy expenditure and respiratory quotient of ventilated and non-ventilated infants. Arch Dis Child Fetal Neonatal Ed 1995;73:F4-F7.
8. Bauer K, Pasel K, Uhrig C, Sperling P, Versmold H. Comparison of face mask, head hood, and canopy for breath sampling in flow-through indirect calorimetry to measure oxygen consumption and carbon dioxide production of preterm infants < 1500 grams. Pediatr Res 1997;41:139-144.
9. Ultman JS, Bursztein S. Analysis of error in the determination of respiratory gas exchange at varying FiO_2. J Appl Physiol 1981;50:210-216.
10. Mayfield SR. Technical and clinical testing of a computerized indirect calorimeter for use in mechanically ventilated neonates. Am J Clin Nutr 1991;54:30-34.
11. Classic KL, Schenk WF, Haymond MW. Radiobiological half-lives for carbon-14 and hydrogen-3 leucine in man. Proc 4th Int Radiopharm Dosimetry Sym 1986;681-687.
12. Spear ML, Darmaun D, Sager BK, Parsons WR, Haymond MW. Use of [^{13}C]bicarbonate infusion for measurement of CO_2 production. Am J Physiol 1995;268:E1123-E1127.
13. Van Goudoever JB, Sulkers EJ, Kalhan SC, Sauer PJ. Glucose metabolism in a term infant with transient hyperinsulinism and high carbohydrate intake. Eur J Pediatr 1993;152:343-347.
14. Perman JA, Barr RG, Watkins JB. Sucrose malabsorption in children; a noninvasive diagnosis by interval breath hydrogen determination. J Pediatr 1978;93:17-22.
15. Veereman-Wauters G, Ghoos Y, Van der Schoor S, Maes B, Hebbalkar N, Devlieger H, Eggermont E. The ^{13}C-octanoic acid breath test: a noninvasive technique to assess gastric emptying in preterm infants. J Pediatr Gastroenterol Nutr 1996;23:111-117.
16. Van Dijk-Van Aalst K, Van den Driessche M, Van der Schoor S, Schiffelers S, van't Westeinde T, Ghoos Y, Veereman-Wauters G. ^{13}C mixed triglyceride breath test: a noninvasive method to assess lipase activity in children. J Pediatr Gastroenterol Nutr 2001;32:579-585.
17. Van Goudoever JB, Colen T, Wattimena JL, Huijmans JG, Carnielli VP, Sauer PJ. Immediate commencement of amino acid supplementation in preterm infants: effect on serum amino acid concentrations and protein kinetics on the first day of life. J Pediatr 1995;127:458-465.
18. Kingdon CC, Mitchell F, Bodamer OA, Williams AF. Measurement of carbon dioxide production in very low birth weight babies. Arch Dis Child Fetal Neonatal Ed 2000;83:F50-F55.
19. Zuijdgeest-van Leeuwen SD, Van den Berg JW, Wattimena JL, Van der Gaast A, Swart GR, Wilson JH, Dagnelie PC. Lipolysis and lipid oxidation in weight-losing cancer patients and healthy subjects. Metabolism 2000;49:931-936.

20. Craig H. Isotopic standards for C and O and correction factors for mass-spectrometric analysis of CO_2. Geochim Cosmochim Acta 1957;12:133-149.

21. Jahoor F, Burrin DG, Reeds PJ, Frazer M. Measurement of plasma protein synthesis rate in infant pig: an investigation of alternative tracer approaches. Am J Physiol 1994;267:R221-R227.

22. Tserng K, Hay WJ. Calculation of substrate turnover rate in stable isotope tracer studies. Am J Physiol 1983;245:E308-E311.

23. Bland JM, Altman DG. Statistical methods for assessing agreement between two methods of clinical measurement. Lancet 1986;1:307-310.

24. Winchell HS, Wiley K. Considerations in analysis of breath $^{14}CO_2$ data. J Nucl Med 1970;11:708-710.

25. Elia M, Fuller NJ, Murgatroyd PR. Measurement of bicarbonate turnover in humans: applicability to estimation of energy expenditure. Am J Physiol 1992;263:E676-E687.

7

CHEMOTHERAPY DOES NOT INFLUENCE INTESTINAL AMINO ACID UPTAKE IN CHILDREN

Barbara A. de Koning, Sophie R. van der Schoor, Darcos L. Wattimena, Peter C. de Laat, Rob Pieters, Johannes B. Van Goudoever.
(Rob Pieters, Johannes B. Van Goudoever participated equally in this study)

Pediatric Research 62:195-199 (2007).

ABSTRACT

Chemotherapy will frequently induce intestinal damage (mucositis). Enteral nutrition is then often withheld for fear of impaired intestinal absorption as shown in animal models. There is no clinical evidence, however, that absorption is indeed compromised during chemotherapy-induced mucositis. The aim of this study was to evaluate systemic availability of dietary amino acids (leucine) during chemotherapy-induced mucositis. We studied eight childhood cancer patients (age 1.5 - 16 years) on 2 days, *i.e.* the day before chemotherapy and 3 - 5 days after. Chemotherapy-induced oral mucositis and diarrhea were scored on a World Health Organization toxicity scale. Stable isotope tracers were used to measure first-pass splanchnic leucine uptake and whole-body leucine kinetics. Patients showed increased mucositis and/or diarrhea toxicity scores ($P < 0.0001$) after chemotherapy. Systemic availability of enterally administered leucine was not significantly affected by chemotherapy (before 60%, after 90%, $P = 0.46$). Interestingly, five patients already showed a negative leucine balance before chemotherapy. In conclusion, most children receiving chemotherapy are already catabolic before start of a new cycle of chemotherapy. Amino acid transport as measured by leucine uptake in the intestine is not affected by chemotherapy-induced mucositis.

INTRODUCTION

Chemotherapy may severely damage the intestinal mucosa, resulting in a condition referred to as mucositis.[1,2] Mucositis is characterized by major morphologic changes of the intestinal epithelium, such as epithelial flattening, villus atrophy, and specific down-regulation of the enterocytespecific gene expression that is crucial for degradation and absorption of nutrients.[3-5] It is unknown how this condition effects digestion and absorption of enteral nutrition.

Normally, the intestine itself metabolizes a substantial part of the nutrients absorbed from the intestinal lumen in first-pass splanchnic uptake.[6,7] Animal and human studies have shown that 20 - 80% of dietary essential amino acids are used within the intestine.[8-10] The more nutrients are used by the small intestine, the fewer essential amino acids are systemically available for whole-body energy metabolism and protein synthesis. It is unknown whether chemotherapy-induced mucositis affects first-pass splanchnic amino acid uptake. We hypothesized, first, that chemotherapy-induced mucositis will lead to lower nutrient uptake by the intestine and, second, that it will lead to a higher intestinal utilization rate due to mucosal regeneration. The combined result would be a lower systemic availability of dietary amino acids.

To test these hypotheses we determined first-pass splanchnic uptake of dietary leucine, an essential amino acid, in pediatric patients before and after receiving mucotoxic chemotherapy.

METHODS

Subjects

The ethics review board of the Erasmus MC-Sophia Children's Hospital approved the study. Informed consent was obtained from parents and patients, as appropriate. Eligible subjects were patients aged between 1 and 18 years, admitted for a cycle of chemotherapy in their drug regimen with known high risk of severe intestinal side effects. Patients diagnosed with acute myeloid leukemia (AML) and B cell–non-Hodgkin lymphoma (B-NHL) fulfilled these criteria already at diagnosis. Acute lymphoid leukemia (ALL) patients were eligible if they had developed mucositis during a previous chemotherapy cycle. Exclusion criteria were cow's milk allergy and abdominal radiotherapy.

Protocol

Each subject was studied on 2 d, *i.e.* the day before start of chemotherapy and 3 - 5 days after chemotherapy. The study protocol was similar on these days, as illustrated in Figure 1. The degree of oral mucositis and diarrhea were scored according to the World Health Organization (WHO) criteria (Table 1).

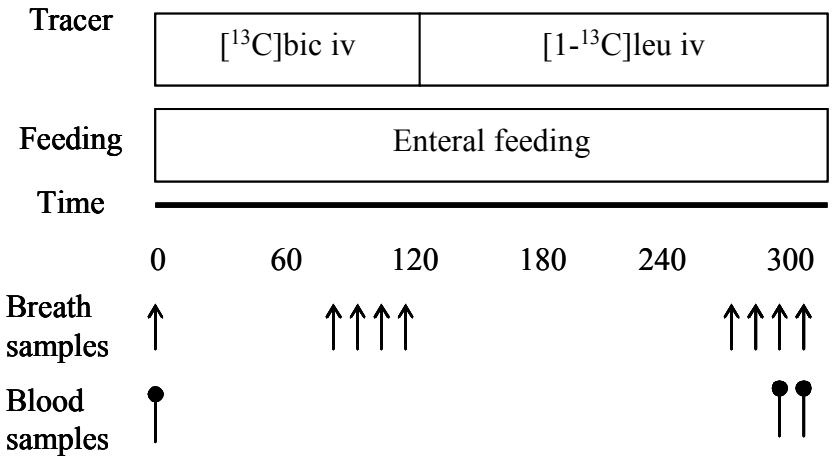

Figure 1 *Schematic overview of study day before and after chemotherapy. [^{13}C] bic, [^{13}C] sodium bicarbonate; [1-^{13}C] leu, [1-^{13}C] leucine.*

All patients had a central venous catheter already in place, which was used to infuse stable isotopes. Blood samples were collected by capillary blood puncture. Breath samples of patients younger than 5 years were collected as described before.[11] Older patients were asked to exhale into a vacutainer through a straw. After a 4-h fast, patients who were capable of drinking received a formula diet (Tentrini, Nutricia, Zoetermeer, The Netherlands), every hour for 5 h. Others were continuously fed this formula through a nasogastric tube. Nutrient intake was similar on both study days. Three different stable isotopes were infused. First, a primed, continuous 2-h i.v. infusion (4.7 μmol/kg and 4.7 μmol/kg/h) of [^{13}C]sodium bicarbonate (99.0 mol% ^{13}C; Cambridge Isotopes, Woburn, MA) dissolved in sterile saline was administered at a constant rate. This was immediately followed by a primed, continuous i.v. infusion (11.3 μmol/kg prime and 11.3 μmol/kg/h) of 1-^{13}C leucine (98.0 mol% ^{13}C; Cambridge Isotopes) and an intragastric infusion (11.0 μmol/kg and 11 μmol/kg/h) of $^{2}H_3$ leucine (98.0 mol% $_2H^3$; Cambridge Isotopes), both for 3 h.

Baseline blood and breath samples were collected just before start of tracer infusion. Breath samples were also taken every 15 min during the last 45 min of sodium bicarbonate infusion and during the last hour of leucine infusion. Two blood samples were collected during the last 15 min of leucine infusion (T 285, 300 min.). The heparinized blood was directly put on melting ice, centrifuged, and stored at -80 °C until further analysis.

Table 1 WHO grading scale of oral mucositis and diarrhea

	Oral mucositis	**Diarrhea**
0	None	none
1	soreness/erythema	transient, < 2days
2	erythema, ulcers, can eat solids	tolerable, but > 2days
3	ulcers require liquid diet only	intolerable, requires therapy
4	oral alimentation impossible	hemorrhagic dehydration

Calculations

The assessment of amino acid kinetics by stable isotope technique is based on the following model:[12]

Turnover or Flux (Q) = Intake + Breakdown = Synthesis + Oxidation

Amino acids enter a metabolic pool *via* diet (Intake) and protein breakdown (Breakdown), and are withdrawn from this pool by protein synthesis (Synthesis) or amino acid oxidation (Oxidation). During steady state, tracer enters and leaves the pool at equal rate. This process of replacement or renewal of a given substance is referred to as turnover or flux.

All calculations used were previously described by van der Schoor *et al.*[13]

Equation 1 is the above-mentioned model modified for leucine: leucine entering the pool equals leucine leaving the pool. Leucine enters the pool *via* intake (I) and through leucine release from protein breakdown (LRP) and leaves the pool *via* NOLD, a measure of protein synthesis rate, and through leucine oxidation (OX).

(1) $Q = I + LRP = NOLD + OX$

Q, flux of leucine tracer (μmol/kg/h); I, LRP, NOLD, and OX (μmol/kg/h).

The rate of leucine flux was calculated by measuring the dilution of its intracellular representation KICA at steady state as modified for stable isotope tracers.[14,15]

Equation 2a calculates the leucine flux of the i.v. tracer.

(2a) $Qiv = IL \times [(Ei/Ep)/Ep]$

Qiv, flux of intravenous leucine tracer [1-^{13}C] leucine (μmol/kg/h); i_L, leucine infusion rate (μmol/kg/h); Ei and Ep are the enrichments in mole percent excess (MPE) of [1-^{13}C] leucine in the leucine infusate and [1-^{13}C] KICA in plasma during steady state, respectively.

Equation 2b calculates the leucine flux of the intragastric tracer.

(2b) $Qig = IL \times [(Ei/Ep)/Ep]$

Qig, flux of intragastric leucine tracer [$^2H_3$] leucine (μmol/kg/h); i_L, leucine infusion rate (μmol/kg/h); Ei and Ep are the enrichments (MPE) of [$^2H_3$] leucine in the leucine infusate and [$^2H_3$] KICA in plasma at steady state, respectively.

After determining both i.v. and intragastric tracer flux, first-pass splanchnic uptake can be calculated.

Equation 3 calculates first-pass up-take fraction (%).

(3) $First\ Pass\ Uptake = [(Qig - Qiv)/Qig]$

Equation 4 calculates the absolute first-pass leucine uptake in μmol/kg/h.

(4) Absolute First Pass Uptake = [(Qig - Qiv)/Qig] x I

I, enteral leucine intake (μmol/kg/h).

Equation 5 calculates the fraction of leucine oxidized.

(5) Fraction of leucine oxidized = [IEL x iB]/[IEB x iL]

IE_L and IE_B, $^{13}CO_2$ enrichment at steady state during i.v. [1-^{13}C] leucine and [^{13}C] sodium bicarbonate infusion, respectively; i_L and i_B, infusion rate (μmol/kg/h) of leucine and bicarbonate, respectively, as described previously.[16]

Equation 6 is calculated by multiplying the outcome of Equation 5 with the flux of the i.v. leucine tracer as calculated in Equation 2a (although this does not take first-pass oxidation into account).

(6) Whole-Body Leucine Oxidation = [Eq 5.] x [Qiv]

Equation 7 calculates leucine balance.

(7) Balance = NOLD - LRP (Leucine Used for Synthesis - Leucine Used for Breakdown)

Leucine balance (μmol/kg/h).

Analytical methods

$^{13}CO_2$ enrichment in the breath samples was measured on an isotope ratio mass spectrometer (ABCA; Europa Scientific, Van Loenen Instruments, Leiden, the Netherlands).[17] Plasma enrichment of [1-^{13}C] and [$^2H_3$] KICA in small aliquots of plasma was determined by gas chromatography/ mass spectrometry.[18]

Statistics

All data are expressed in median (25^{th} percentile - 75^{th} percentile) values obtained from the breath or blood samples taken at the end of each tracer infusion. The distribution of the differences in direction and magnitude between the two related values (before and after chemotherapy) was compared by Wilcoxon signed-ranks tests. A value of $P < 0.05$ was considered statistically significant.

RESULTS

Patients, treatment, and toxicity

Eight patients participated in the study; age at diagnosis and type of chemotherapy are listed in Table 2. Seven patients were measured both before and after chemotherapy. In one patient, baseline measurements are lacking for logistic reasons. All patients showed good clinical health, with no or only moderate signs of diarrhea or oral mucositis on the

first study day (Table 2). Following chemotherapy, however, the clinical condition of seven patients had deteriorated. They showed increased mucositis and/or diarrhea WHO-toxicity scores ($P < 0.0001$). Two patients demonstrated weight loss and two other patients suffered from severe abdominal pain. Four patients already received tube feeding before the study days, and were given formula through this tube; the other four received a normal diet (although characterized by a reduced intake). Table 3 shows the individual intake of all patients on both study days.

Table 2 Patient characteristics

	1	**2**	**3**	**4**	**5**	**6**	**7**	**8**
Patient	1.8	1.7	2.4	11.9	13.1	6.7	7.0	15.8
Diagnosis	ALL	AML	AML	AML	AML	BNH	BNH	BNH
Cycle	MD-MTX	MAE	ADE	ADE	ADE	COPADM	COPADM	COPADM
Oral mucositis (WHO grade)								
Before chemotherapy	1	0	0	0	0	0	1	0
After chemotherapy	2	0	0	2	0	2	3	1
Diarrhea (WHO grade)								
Before chemotherapy	0	0	0	0	2	0	0	0
After chemotherapy	2	0	1	2	3	3	3	1

Median mucositis and diarrhea scores are shown.
Cycle, chemotherapy cycle; ALL, acute lymphoid leukemia; AML, acute myeloid leukemia; B-NHL, B-non-Hodgkin lymphoma; MD-MTX, medium dose methotrexate; MAE, ara-C, mitoxantrone, and etoposide; ADE, ara-C, daunorubicin, and etoposide; COPADM, vincristine, cyclophosphamide, doxorubicin, and high-dose MTX.

Leucine kinetics

Table 4 shows the $^{13}CO_2$ enrichment expressed in MPE of breath-samples collected during steady state at the end of [^{13}C] bicarbonate and leucine infusion. It also shows the enrichment of [1-^{13}C] and [$^{2}H_3$] KICA (MPE) of serum collected at steady state. There are no significant differences in enrichment before and after chemotherapy.

Table 3 Calorie (kcal/kg/h) and protein (mg/kg/h) intake during study day 1 and 2

	study day 1		**study day 2**	
Patient	Calorie	protein	calorie	protein
1	1,5	60	1.5	60
2	2,5	100	2.5	100
3			4.6	184
4	1,1	44	1.4	56
5	0,4	16	0.4	16
6	1,3	52	1.4	56
7	1,5	60	1.8	72
8	1,5	60	1.7	68

Table 4 MPE CO_2 and leucine plasma isotopic enrichments (%) before and after chemotherapy

	Breath samples		Serum samples	
Patient	**$^{13}CO_2$ enrichment (MPE) (after [^{13}C] bicarnonate iv)**	**$^{13}CO_2$ enrichment (MPE) (after [^{13}C] leucine iv)**	**1-^{13}C KICA (MPE)**	**$^{2}H_3$ KICA (MPE)**
Before chemotherapy				
1	0.0149	0.0138	3.59	2.03
2	0.0240	0.0126	3.86	2.35
3				
4	0.0260	0.0136	2.67	3.80
5	0.0161	0.0145	2.65	1.30
6	0.0221	0.0102	3.76	2.37
7	0.0154	0.0882	6.81	3.22
8	0.0326	0.0354	2.78	2.68
Median	0.0161	0.0138	3.59	2.37
P25	0.0149	0.0123	2.67	2.03
P75	0.0240	0.0354	3.86	3.22
After chemotherapy				
1	0.0140	0.0160	2.97	3.20
2	0.0109	0.0140	2.80	2.30
3	0.0157	0.0139	2.54	5.36
4	0.0351	0.0241	2.66	3.03
5	0.0238	0.0235	3.68	1.65
6	0.0224	0.0254	2.44	2.36
7	0.0168	0.0165	4.61	3.15
8	0.0371	0.0319	4.03	0.88
Median	0.0196	0.0200	2.89	2.70
P25	0.0144	0.0145	2.57	1.81
P75	0.0323	0.0251	3.94	3.19
p	0.31	0.50	0.31	0.5

Leu, leucine; p25, 25th percentile; p75, 75th percentile; P-value, Wilcoxon signed-rank test.

The influence of chemotherapy-induced mucositis on first-pass splanchnic uptake and whole-body leucine kinetics is shown in Table 5. Before chemotherapy, there was a first-pass uptake of leucine as shown by the difference in turnover of the enterally and intravenously-administered tracer. Inasmuch as, before chemotherapy, a median of 40% of the dietary leucine was used in first pass or not absorbed, 60% was systemically available. Following chemotherapy, only 10% of the ingested leucine was used in first pass or not absorbed, so that 90% (median) was systemically available. However, this difference in intestinal utilization does not reach statistical significance. Both LRP (an indication of proteolysis) and leucine oxidation increased following chemotherapy. These differences did not reach statistical significance. NOLD (an indication of protein synthesis) was not affected by chemotherapy. Interestingly, five patients were found to be already in negative leucine balance (the equation NOLD – LRP has a negative result) before start of chemotherapy, indicating a catabolic leucine metabolism already before start of chemotherapy. This negative balance almost doubled following chemotherapy, although this difference was not statistically significant.

Table 5 Leucine kinetics before and after chemotherapy

	Before chemotherapy		After chemotherapy		
	Median	**percentile (25-75)**	**Median**	**percentile (25-75)**	***P***
Total leucine intake	42.8	(37.9-43.8)	44.9	(34.9-61.5)	0.46
Enteral leucine intake	31.5	(23.6-32.6)	33.7	(23.7-50.3)	0.17
Turnover iv	300.0	(278.0-407.0)	378.0	(272.5-436.8)	0.61
Turnover ig	451.0	(329.0-528.0)	460.5	(339.5-634.5)	0.61
First-pass uptake fraction (%)	40.0	(2.0-50)	10.0	(0.0-50)	0.46
Absolute first-pass uptake	8.6	(0.0-17.0)	4.6	(0.0-11.5)	0.60
Oxidation	88.6	(54.7-149.3)	124.0	(100.3-204.5)	0.31
NOLD	217.3	(150.7-281.2)	215.3	(170.9-275.9)	0.61
LRP	256.4	(214.2-366.3)	323.7	(230.5-401.9)	0.40
Balance	-47.9	(-109.5-3.1)	-92.0	(-150.9-54.7)	0.31

All values are expressed in, μmol/kg/h. P-Value, Wilcoxon signed-rank test; ig, intragastric; Oxidation, whole-body leucine oxidation; Balance, NOLD - LRP.

DISCUSSION

We studied leucine kinetics in children treated with chemotherapy as a means to evaluate the effect of chemotherapy-induced mucositis on intestinal amino acid absorption. Our data demonstrate that childhood cancer patients have at least a similar systemic availability of leucine just before receiving chemotherapy compared with healthy children.[19] The systemic availability of leucine after chemotherapy during a period of mucositis did not change significantly, indicating that chemotherapy treatment does not affect amino acid transport in the intestine. On the other hand, in contrast to our hypothesis, it demonstrates that the intestinal mucosa does not use more amino acids during intestinal mucositis. These are unexpected results seeing that almost all patients showed a distinct increase in mucositis toxicity score. We would have expected that leucine availability from the intestinal lumen should be impaired. Surprisingly, too, we found almost all patients to be in negative leucine balance already before start of chemotherapy, representing catabolic metabolism. We would have expected that the children should be in an anabolic state at the start of a new cycle of chemotherapy. We conclude that in our study amino acid (leucine) absorption in children with cancer was not compromised during chemotherapy-induced mucositis.

However, our study may have had some limitations. First, it might have been underpowered to detect possible differences in the systemic availability of leucine: the study group was fairly small and the overall incidence of very severe mucositis (grade 3 or 4) was low. Second, the results on isotopic enrichment and consequent leucine kinetics showed great variability. This could be explained by the heterozygosis of our study group. Patient characteristics showed a wide range in age, diagnosis, and treatment differences, which could cause variability in clinical condition. Third, we are

well aware of the limitations of the described amino acid tracer studies. Intestinal absorption of only one essential amino acid was studied and not the entire cascade of digestion and absorption following a protein-containing meal. The transport of amino acids into the cytoplasm and through the basolateral membrane is facilitated by highly regulated transporter systems defined on the kinetic properties of the specific amino acid.[20,21] Transport of amino acids such as leucine in the intestinal brush border is regulated by the L and $B^{0,8}$ system[21,22] and is predominantly Na^+-dependent.[22]. In contrast, dietary components need to be digested before absorption by specific tightly regulated metabolic enzymes expressed in the brush border at the apical membrane of villus enterocytes.

From previous animal studies we know that different kinds of chemotherapy affect intestinal digestion and absorption processes dissimilar. Conflicting reports on protein digestion and amino acid absorption have been published. The expression of peptide transporter 1 (PepT1), involved in absorption of dipeptides and tripeptides formed after digestion of dietary proteins,[23] appeared unchanged during 5'-flourouracil induced intestinal mucositis,[24] whereas several amino acid transporters (neutral basic transporter and high-affinity glutamate transporter) showed decreased expression.[24] On the other hand, glutamine supplementation seems to ameliorate chemotherapy induced toxicity.[25-27] Although conflicting results are published, this could indicate that glutamine transport is not affected by chemotherapy. *In vivo* data available for glutamine transporters are lacking. Other macronutrients such as carbohydrates might be less well absorbed. Expression of sucrase isomaltase and lactase, two glycohydrolases responsible for degradation of complex carbohydrates into absorbable monosaccharide, is strongly down-regulated during mucositis.[5,28,29] Also, the monosaccharide transporters sodium glucose co-transporter 1 and glucose transporter 5, harbored at the apical enterocyte membrane and glucose transporter 2 at the basolateral membrane, are distinctly down-regulated during mucositis.[5] Although not clinically tested, these findings suggest that carbohydrates might be less properly absorbed during mucositis. Only a few data are available on the third macronutrient in the diet, lipids. Transport of fatty acid in the enterocyte by fatty acid binding protein seems to be less affected during severe mucositis.[5]

So, in contrast to leucine absorption, we don't know whether the digestion of whole proteins in a regular meal is disturbed during a period of mucositis. An intrinsically labeled protein diet could be used to investigate whether digestion is impaired in children with mucositis following chemotherapy. Our data on leucine absorption and findings from previous animal studies[24] suggest a role for an elementary diet consisting of small peptides and free amino acids during mucotoxic treatment. Considering that most of our patients already showed catabolic state before start of chemotherapy, there is a definite need for the development of such elementary feeding. The more so since a major positive effect of proper nutrition in critically ill patients was demonstrated in recent years.[30-32]

In conclusion, we found that after mucotoxic chemotherapy in pediatric patients the intestinal mucosa is still capable of absorbing leucine efficiently. Additionally, most children receiving chemotherapy are already catabolic before start of a new cycle of chemotherapy. Therefore, all efforts should be directed at initiating enteral feeding even before start of chemotherapy to reduce catabolic state. Moreover, our data imply that this might be accomplished best by hydrolyzed formula.

REFERENCES

1. Sonis ST. The pathobiology of mucositis. Nat Rev Cancer 2004;4:277-284.
2. Sonis ST, Elting LS, Keefe D, Peterson DE, Schubert M, Hauer-Jensen M, Bekele BN, Raber-Durlacher J, Donnelly JP, Rubenstein EB. Perspectives on cancer therapy-induced mucosal injury: pathogenesis, measurement, epidemiology, and consequences for patients. Cancer 2004;100:1995-2025.
3. Hyams JS, Batrus CL, Grand RJ, Sallan SE. Cancer chemotherapy-induced lactose malabsorption in children. Cancer 1982;49:646-650.
4. Naruhashi K, Nadai M, Nakao M, Suzuki N, Nabeshima T, Hasegawa T. Changes in absorptive function of rat intestine injured by methotrexate. Clin Exp Pharmacol Physiol 2000;27:980-986
5. Verburg M, Renes IB, Van Nispen DJ, Ferdinandusse S, Jorritsma M, Buller HA, Einerhand AW, Dekker J. Specific responses in rat small intestinal epithelial mRNA expression and protein levels during chemotherapeutic damage and regeneration. J Histochem Cytochem 2002;50:1525-1536.
6. McNurlan MA, Garlick PJ. Contribution of rat liver and gastrointestinal tract to whole-body protein synthesis in the rat. Biochem J 1980;186:381-383.
7. Lobley GE, Milne V, Lovie JM, Reeds PJ, Pennie K. Whole body and tissue protein synthesis in cattle. Br J Nutr 1980;43:491-502.
8. Biolo G, Tessari P, Inchiostro S, Bruttomesso D, Fongher C, Sabadin L, Fratton MG, Valerio A, Tiengo A. Leucine and phenylalanine kinetics during mixed meal ingestion: a multiple tracer approach. Am J Physiol 1992;262:E455-E463.
9. van Goudoever JB, Stoll B, Henry JF, Burrin DG, Reeds PJ. Adaptive regulation of intestinal lysine metabolism. Proc Natl Acad Sci USA 2000;97:11620-11625.
10. Stoll B, Henry J, Reeds PJ, Yu H, Jahoor F, Burrin DG. Catabolism dominates the first-pass intestinal metabolism of dietary essential amino acids in milk protein-fed piglets. J Nutr 1998;128:606-614.
11. Perman JA, Barr RG, Watkins JB. Sucrose malabsorption in children: noninvasive diagnosis by interval breath hydrogen determination. J Pediatr 1978;93:17-22.
12. Waterlow JC. Lysine turnover in man measured by intravenous infusion of L-[U-14C]lysine. Clin Sci 1967;33:507-515.
13. van der Schoor SR, Reeds PJ, Stellaard F, Wattimena JD, Sauer PJ, Buller HA, van Goudoever JB. Lysine kinetics in preterm infants: the importance of enteral feeding. Gut 2004;53:38-43.
14. Steele R. Influences of glucose loading and of injected insulin on hepatic glucose output. Ann N Y Acad Sci 1959;82:420-430.
15. Tserng KY, Kalhan SC. Calculation of substrate turnover rate in stable isotope tracer studies. Am J Physiol 1983;245:E308-E311.
16. van Goudoever JB, Sulkers EJ, Kalhan SC, Sauer PJ. Glucose metabolism in a term infant with transient hyperinsulinism and high carbohydrate intake. Eur J Pediatr 1993;152:343-347.
17. Zuijdgeest-van Leeuwen SD, van den Berg JW, Wattimena JL, van der Gaast A, Swart GR, Wilson JH, Dagnelie PC. Lipolysis and lipid oxidation in weight-losing cancer patients and healthy subjects. Metabolism 2000;49:931-936.
18. Ford GC, Cheng KN, Halliday D. Analysis of (1-13C)leucine and (13C)KIC in plasma by capillary gas chromatography/mass spectrometry in protein turnover studies. Biomed Mass Spectrom 1985;12:432-436.
19. Kien CL, Horswill CA, Zipf WB, McCoy KS, Denne SC. Splanchnic uptake of leucine in healthy children and in children with cystic fibrosis. Pediatr Res 1999;45:680-683.
20. Souba WW, Pacitti AJ. How amino acids get into cells: mechanisms, models, menus, and mediators. JPEN J Parenter Enteral Nutr 1992;16:569-578.
21. Mailliard ME, Stevens BR, Mann GE. Amino acid transport by small intestinal, hepatic, and pancreatic epithelia. Gastroenterology 1995;108:888-910.

22. Iannoli P, Miller JH, Wang HT, Bode B, Souba WW, Avissar NE, Sax HC. Characterization of L-leucine transport system in brush border membranes from human and rabbit small intestine. Metabolism 1999;48:1432-1436.

23. Ganapathy V, Brandsch M, Leibach F. Intestinal transport of amino acids and peptides. Raven, New York, 1994; pp 1773-1794.

24. Tanaka H, Miyamoto KI, Morita K, Haga H, Segawa H, Shiraga T, Fujioka A, Kouda T, Taketani Y, Hisano S, Fukui Y, Kitagawa K, Takeda E. Regulation of the PepT1 peptide transporter in the rat small intestine in response to 5-fluorouracil-induced injury. Gastroenterology 1998;114:714-723.

25. Jebb SA, Osborne RJ, Maughan TS, Mohideen N, Mack P, Mort D, Shelley MD, Elia M. 5-fluorouracil and folinic acid-induced mucositis: no effect of oral glutamine supplementation. Br J Cancer 1994;70:732-735.

26. Klimberg VS, Nwokedi E, Hutchins LF, Pappas AA, Lang NP, Broadwater JR, Read RC, Westbrook KC. Glutamine facilitates chemotherapy while reducing toxicity. JPEN J Parenter Enteral Nutr 1992;16:83S-87S.

27. Blijlevens NM, Donnelly JP, Naber AH, Schattenberg AV, DePauw BE. A randomised, double-blinded, placebo-controlled, pilot study of parenteral glutamine for allogeneic stem cell transplant patients. Support Care Cancer 2005;13:790-796.

28. Kralovanszky J, Prajda N 1985 Biochemical changes of intestinal epithelial cells induced by cytostatic agents in rats. Arch Toxicol Suppl 1985;8:94-103.

29. Taminiau JA, Gall DG, Hamilton JR. Response of the rat small-intestine epithelium to methotrexate. Gut 1980;21:486-492.

30. Pollack MM, Ruttimann UE, Wiley JS. Nutritional depletions in critically ill children: associations with physiologic instability and increased quantity of care. JPEN J Parenter Enteral Nutr 1985;9:309-313.

31. den Broeder E, Lippens RJ, van't Hof MA Tolboom JJ, Sengers RC, van Staveren WA. Association between the change in nutritional status in response to tube feeding and the occurrence of infections in children with a solid tumor. Pediatr Hematol Oncol 2000;17:567-575.

32. Barr J, Hecht M, Flavin KE, Khorana A, Gould MK. Outcomes in critically ill patients before and after the implementation of an evidence-based nutritional management protocol. Chest 2004;125:1446-1457.

33. WHO. WHO handbook for reporting results of cancer treatment. World Health Organization, Geneva, 1979; pp 13.

8

PROTECTION AGAINST CHEMOTHERAPY INDUCED MUCOSITIS BY TGF-β_2 IN CHILDHOOD CANCER PATIENTS: RESULTS FROM A RANDOMIZED CROSS-OVER STUDY

Barbara A.E. de Koning, Bertine Philipsen-Geerling, Maarten Hoijer, Karel Hählen, Hans A. Büller, Rob Pieters.

Pediatric Blood and Cancer 48:532-539 (2007).

ABSTRACT

Mucositis is one of the most frequent and severe side-effect of chemotherapy in childhood-cancer patients for which there is no prophylaxis available. The efficacy and feasibility of a TGF-β_2-enriched feeding for preventing oral and gastro-intestinalmucositis in childhood-cancer patients were studied.

The study was designed as a two-period cross-over, randomized, double-blinded, placebo, controlled trial. Patients who had a high risk for developing mucositis and who would receive two comparable cycles of chemotherapy were eligible for the study. During one cycle of chemotherapy, TGF-β_2-enriched feeding was administered; during the other, a 'placebo' (not enriched) feeding was used. WHO toxicity scales of diarrhea, oral mucositis, fever, anal lesions and nausea/vomiting were scored daily. In addition, the incidence of occurrence of blood cultures, antibiotic therapy, and interventions or diagnostics related to mucositis were measured.

The feasibility of the study was good: 83% of the patients completed two cycles and 86% of the study-feeding was effectively consumed. Administration of TGF-β_2 was safe as serum TGF-β_2 did not increase, and renal and liver function were not affected during TGF-β_2 consumption compared to normal feeding. Differences in toxicity, scored during the whole observation period and the number of days with WHO 3/4 toxicity, were not significantly different between cycles with TGF-β_2 enriched and normal feeding.

TGFβ_2 administration via feeding is well tolerated and safe. Although this study might have had limitations to show potential benefit of TGF-β_2, it does not provide evidence that TGF-β_2 decreases the incidence or degree of mucositis induced by combination chemotherapy in childhood-cancer patients.

INTRODUCTION

Oral and gastrointestinal (GI) mucositis is one of the most frequent and severe side effects of chemotherapy. Depending on the dose and type of chemotherapy, up to 40% [1] of adult patients and more than 60% [2-5] of pediatric patients, experience oral and/or GI mucositis. Mucositis is associated with considerable oral and abdominal pain, diarrhea, and weight loss, which can severely impair quality of life.[6] Loss of intestinal integrity predisposes the patient to bacterial translocation, leading to life-threatening infections in the immune compromised patient.[7-9] These side effects can lead to reduction of chemotherapy intensity, thereby potentially reducing the efficacy of anti-cancer treatment.[1,7] Mucositis does not only imply clinical burden but also a financial burden due to increased resource utilization and days of hospitalization.[7,10] Despite a lot of effort, there is still no effective prophylaxis for mucositis available.

Mucositis research is mainly focused on adult cancer patients[11] and oral mucositis. This is in contrast with the fact that mucositis is more frequently observed in childhood-cancer patients in comparison to adult cancer patients[3,4,12] and with the observation that the risks of developing infection and bleeding are much more enhanced during GI mucositis[7] compared to oral mucositis. Therefore, this study is focused on the prevention or alleviation of oral and GI mucositis in childhood-cancer patients.

One of the main aspects of mucositis development is the damage induced directly to the highly proliferating progenitor cells in the crypts of Lieberkühn.[13] Different classes of cytostatic drugs affect cells of different hierarchical height in the proliferative compartment,[14,15] causing proliferation arrest and cell-death,[16-18] which leads to diminished cell renewal and finally ulceration. Previous studies focusing on growth factors hypothesized that protecting the highly vulnerable stem cells against chemotherapy leads to an increasing number of cells that survive chemotherapy, which could regenerate immediately after therapy and so, minimize the intestinal damage to the epithelium. TGF-β is a member of the transforming growth factor-β family of polypeptides, with three isoforms; TGF-β1, 2, 3.[19] TGF-β is a paracrine growth factor with a key role in cell proliferation and differentiation.[20] For epithelial cells, TGF-β is a negative growth factor, exposure to TGF-β leads to cell cycle arrest in the G1 phase in these cells,[20,21] which is reversible once TGF-β is removed.[22] *In vitro*, TGF-β_3 protects epithelial cells against chemotherapy, specifically against cell-cycle specific chemotherapy.[23] In animal models, TGF-β_3 was effective in protecting the oral epithelium against mucositis induced by 5-fluorouracil[24] and the intestinal epithelium against radiotherapy-induced mucositis.[25,26] In these rodent models, the decrease in mucositis was accompanied by decreased epithelial cell-proliferation, reduced weight loss, and increased survival. In humans, TGF-β_3 showed promising results as oral mucositis treatment in adult breast cancer patients,[27] the TGF-β_3-enriched mouthwash was well tolerated and appeared to be safe. TGF-β_2, originated from bovine milk,[28,29] showed *in vitro* the same inhibitory effect on epithelial cell proliferation and protection against chemotherapy, as the recombinant

TGF-β_3.[30] In a rodent model, TGF-β_2 appeared to be protective against methotrexate (MTX)-induced mucositis, rats treated with a TGF-β_2-enriched feeding encountered less weight loss and significantly reduced villus atrophy, compared to controls not treated with TGF-β_2.[30] No studies have been reported on prevention of mucositis with TGF-β_2 in children with cancer. The objective of the present study was to evaluate the efficacy and feasibility of a TGF-β_2-enriched feeding in childhood-cancer patients, with the objective of preventing or alleviating both oral and GI mucositis. The study was designed as a cross-over, randomized, double-blinded, placebo controlled trial.

PATIENTS AND METHODS

Participants

The study was conducted between October 2001 and June 2004, at the Department of Pediatric Oncology/Hematology of the ErasmusMC-Sophia Children's Hospital after approval from the institutional ethics committee. Informed consent was obtained from all patients and/or their guardians.

Eligible for the study were patients aged between 0 and 18 years, who were receiving two comparable cycles of chemotherapy in their drug regimen, for which the incidence of inducing severe intestinal side effects is predicted to be high. Patients diagnosed with AML/MDS, relapsed AML, B-NHL, and infant ALL fulfilled these criteria already at diagnosis. Patients diagnosed with other malignancies were eligible only after they had developed grade III/IV mucositis during previous chemotherapy cycles, provided they would receive another two identical consecutive cycles in their treatment schedule, as the one during which they experienced mucositis. The exclusion criteria were: (1) cow's milk allergy and (2) abdominal radiotherapy in their medical history.

Study design

A randomized, two-period cross-over, double-blinded, placebo-controlled design was chosen to control for therapy- and patient-specific variables. Randomization took place by opening a brown sealed envelope by the study-coordinator. These envelopes were made by an independent notary before tart of the study and contained the assigned order of the TGF-β_2-enriched and placebo feeding. Thereafter, the feeding was distributed in a double-blinded fashion. Patients were treated during two identical cycles of chemotherapy with study-feeding. During one chemotherapy cycle, patients received TGF-β_2-enriched study-feeding, during the other cycle they received study-feeding without TGF-β_2 enrichment (placebo). Patients, study personnel, and the sponsor were blinded as to whether an individual patient received first study-feeding or placebo and *visa versa*.

Sample size

For a cross-over study, a sample size of 25 will have a power of 80% to detect a difference in means of the WHO diarrhoea score of 0.5 with an estimated standard

deviation of differences of 0.6. Taken into account a drop-out rate of 20%, a total of 30 patients were included.

Intervention with TGF-β_2

From 2 days before start of the chemotherapy until one day after the last cytostatic drug infusion of the cycle, patients received a daily study-feeding. The first 16 patients received study-feeding enriched with direct active, unbound, TGF-β_2. Because of problems in the purification process, this direct active TGF-β_2 became no longer available. Therefore, patients 17 to 30 received study-feeding enriched with TGF-β_2, bound to its pro-protein Latency-associated peptide (LAP).[31] The direct active, unbound, TGF-β_2 was active already before consumption. The bound, indirect active TGF-β_2 was only active from the stomach on; here, the LAP degrades from the TGF-β_2 protein, leading to activation of TGF-β_2. Both forms of TGF-β_2, were obtained from bovine milk, the direct active TGF-β_2 as concentrated as described before,[30] the indirect active TGF-β_2 was also concentrated from the bovine whey by ion exchange chromatography and subsequent fractionation by hydrophobic interaction chromatography (DMV international). The bound TGF-β_2 is a more stable protein, present in bovine milk in a higher concentration and therefore, easier to obtain from bovine milk and to process in study-feeding. Digestion of the LAP from the TGF-β_2 protein was confirmed in an *in vitro* model for stomach digestion at pH 3 to 5 (data not shown).

Feeding

The TGF-β_2-enriched study-feeding and placebo study-feeding were formulated as a complete pediatric feeding (Tentrini, Nutricia, Zoetermeer) aromatized with banana flavor. Both, TGF-β_2-enriched and placebo feeding were identical in odor, taste, and appearance.

The total amount of TGF-β_2 a patient received each day in the TGF-β_2-enriched study-feeding was dependent on the weight of a patient at time of inclusion. Patients with a weight of less than 20 kg received 62 μg TGF-β_2/day, those with a weight between 20 and 40 kg received 124 μg TGF-β_2/day, and those with a weight of more than 40 kg received 186 μg TGF-β_2/day.

The feeding was packed in two alternatives for each different weight-group. There was a drink-feeding and a tube-feeding. For patients still capable of drinking a drink-feeding was packed in 60 ml vials of which two had to be taken each day in two to four portions during day time. Patients not capable of drinking received tube feeding, packed in 200 ml bottles of which one each day was administered. The total amount of TGF-β_2 (62 μg, 124 μg, or 186 μg/day) a patient received on one day was regardless of the type of feeding (drink or tube-feeding), because the concentration TGF-β_2/ml was adjusted to the total amount of milliliters.

Mouthwash

Patients receiving study-feeding via a gastric-tube were also treated twice daily with application of 10 ml mouthwash spraying or rinsing the oral cavity. The study-mouthwash consisted of TGF-β_2 dissolved in chloride-hexidine (1,550 μg/ml), but the placebo mouthwash consisted of chloride-hexidine only. During the entire study period, directly active TGF-β_2 was used in the preparation of study-mouthwash. The placebo mouthwash was identical to the study-feeding in odor, taste, and appearance. The mouthwash was prepared in large volumes for 10 - 15 patients at the same time; TGF-β_2 concentration was measured every 2 - 3 months, by ELISA analysis. The sponsor was responsible for study-feeding and mouthwash supply only. However, the sponsor was not responsible for study-design, or involved in data collection and data analysis.

Endpoints

The primary efficacy endpoint was diarrhea. The secondary endpoints were oral mucositis, fever, anal lesions, (abdominal) pain, and nausea, and/or vomiting, and were scored according to the World Health Organization (WHO) criteria.[32] Other secondary endpoints, not measured by WHO scale were: (1) use of analgesics (in days), for specific indication of anal-, abdominal-, or oral pain and scaled as, none = 0, paracetamol = 1, and opioid = 2 administration, (2) frequency of blood culture taken, (3) administration of antibiotic therapy for specific indication of fever with an intestinal or unknown source, (4) interventions or diagnostics necessary for abdominal problems, after consultation with the department of surgery: X-abdomen (suspicion of mucositis-related intestinal problems), prescription of special ''oligo-peptide'' tube-feeding which is more easy to digest, minimal enteral feeding, or no oral intake. Parameter (2) - (4) were all scaled as none = 0 and yes = 1. Assessment occurred daily by a small group of trained assessors. All patients were evaluated on all parameters, from 2 days before start of chemotherapy cycle until full recovery of patient's condition, characterized by a normalization of all assessed clinical features; WHO score 0, all other parameters scaled ''none.'' See for study time-line Figure 1.

Safety Parameters

Kidney and liver function were evaluated by β_2-microglobulin, creatinine, and ASAT/ALAT at Day -1 (1 day before start of chemotherapy), at Day 4 (the fourth day after start of chemotherapy), and at day +2 and +10 (2 and 10 days after the last cytostatic drug infusion). Serum TGF-β_2 was measured at the same time-points, blood was sampled in EDTA containing vials on ice, serum was collected and stored at -20 °C until analysis. Serum TGF-β_2 was measured by ELISA analysis (TGF-β_2 ELISA, R&D Systems, Minneapolis, MN). See for study time-line Figure 1.

Statistical Analyses

The trial design was cross-over so that for each toxicity parameter in each patient, two related values were obtained. The value for each parameter during each study-period was expressed as the area under the curve (AUC).

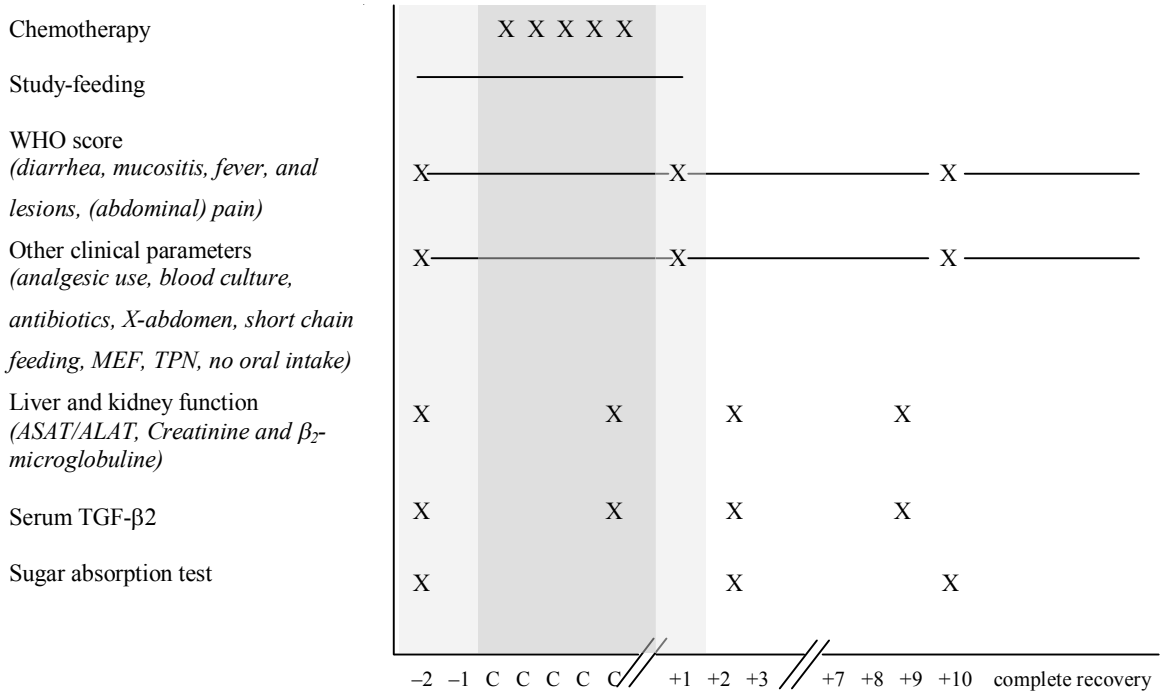

Figure 1 *Study time-line. The dark gray area indicates the chemotherapy-period whereas the light gray area indicates the study-feeding period, from 2 days before start of chemotherapy until one day after the last infusion of chemotherapy. On the y-axis, all clinical parameters are shown (WHO-scores and all other clinical scores), which are performed each day from start of study-feeding till full (clinical) recovery after the chemotherapy-period. The figure also points out the days laboratory analysis and sugar absorption tests are performed. The interrupted x-axis indicates a variable number of days of chemotherapy-period. The additive (-) or (+) to the days specifies the time period before (-) or after (+) chemotherapy.*

The AUC is the sum of the scores of an individual parameter (WHO 0 - 4, or analgesic use 0 - 2 or blood culture/antibiotic therapy/interventions and diagnostics 0 - 1) of all observed days. This way two AUC values per toxicity parameter were obtained; one of the TGF-β_2-enriched study-feeding period and one of the placebo study-feeding period. The distribution of the differences in direction and magnitude between the two related AUC-values were compared by Wilcoxon signed ranks tests. To compare effects on severe toxicity, the AUC for each individual parameter was calculated as the sum of days with WHO toxicity 3/4. The distribution of these values was compared by Wilcoxon signed ranks test. The distribution of the difference between TGF-β_2 concentrations measured before and after start of chemotherapy (at Day 4 after start of chemotherapy and at Day +2 and +10 after the last cytostatic infusion) measured during both study periods were also compared by Wilcoxon signed ranks test.

RESULTS

Patient and Study Characteristics

Of the 31 patients eligible for the study, only 1 patient did not give informed consent. Of the 30 included patients, 25 (83%) completed the two cycles of therapy with all study

assessments (Figure 2). Unfortunately, we could not collect data from patients who withdrew from the study because of logistical reasons.

Two patients withdrew 2 and 3 days, respectively, after inclusion because of the high burden they experienced participating in the study. The parents of these two patients did not agree to collect data after withdrawal. One patient who withdrew due to taste aversion became terminally ill shortly after withdrawal of the study and chemotherapy was stopped. Two patients dropped out from the study because they continued their therapy with other courses of chemotherapy, not comparable with the previous cycle.

The average age of all included patients was 8 years; 70% were boys. The included cases were 12 B-NHL(40%), 11 AML(37%), 4 ALL(13%), and 3 bone tumor(10%) patients. Table 1 shows the number of patients, chemotherapy cycles with the corresponding cytostatic drugs and treatment-protocol. Six patients were in the group of < 20 kg, 15 patients were in the group of 20 - 40 kg, and 9 patients were in the group of > 40 kg.

Among the 25 patients, who completed the whole study-period (patient characteristics Table 2), 11 patients first received TGF-β_2-enriched feeding, followed by placebo feeding, and for 14 patients the intervention periods were in the opposite direction. Sixty-nine percent of all study-feeding was administered as tube-feeding and 31% as drink-feeding; 94% of the tube-feeding was effectively consumed, for the drink-feeding, this was 73% (data not shown). The mean percentage of consumed feeding was identical for TGF-β_2-enriched feeding and placebo-feeding: 86% of the maximum possible amount of feeding (Table 2).

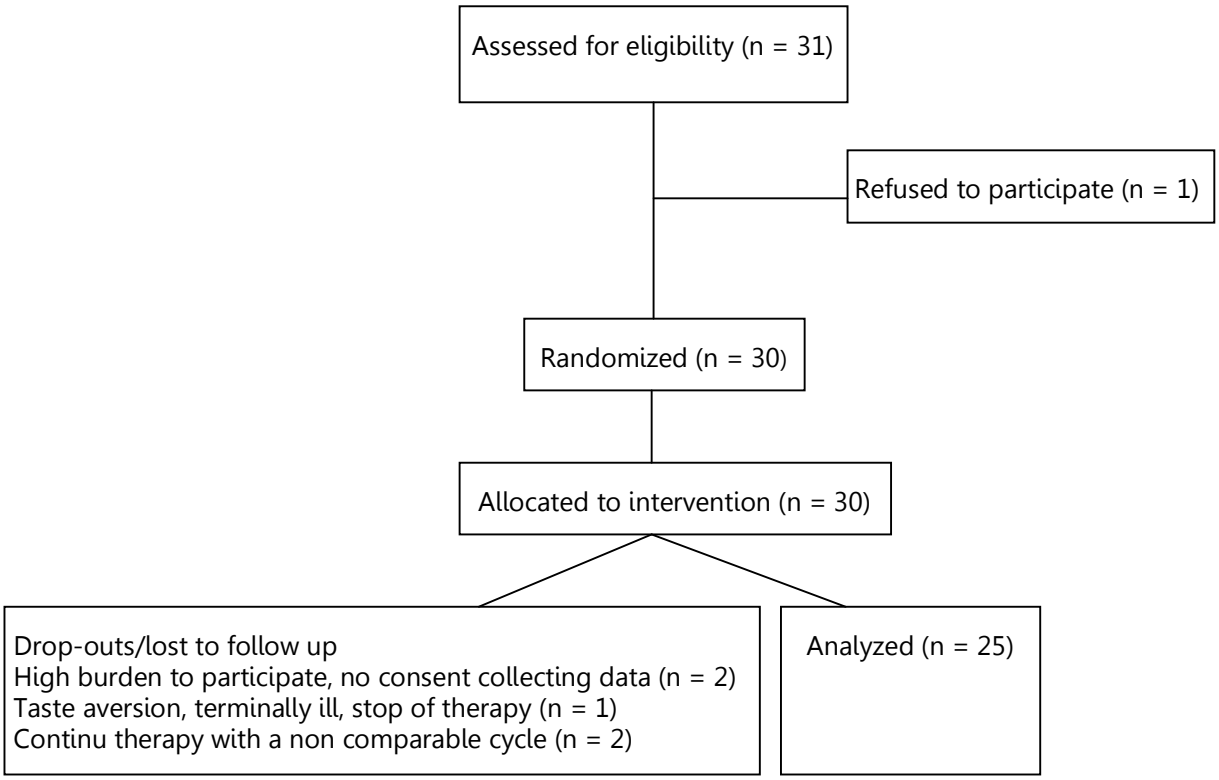

Figure 2 *Flow diagram of subject progress*

Table 1 Chemotherapy cycles

Number of patients (%)	Chemotherapy (treatment protocol)
10 (33%)	ADE: ara-C, daunorubicine and etoposide (MRC12/DCLSG-ANLL-97)
11 (37%)	COPADM: vincristine, cyclofosfamide, doxorubicine, high dose-methotrexate (DCLSG-NHL94)
1 (3%)	MAE: ara-C, mitox, etoposide (MRC12/ DCLSG-ANLL-97)
4 (13%)	MD-MTX: medium dose-MTX (DCLSG ALL 9)
2 (7%)	HD-MTX: high dose-MTX (DCLSG ALL 9)
1 (3%)	VIDE: vincristine, ifosfamide, daunorubicine, etoposide (EURO E.W.I.N.G. 99)
1 (3%)	CIA: 2-chloro-deoxy-adenosine, idarubicine, ara-C

Number of patients (%) subdivided according to the chemotherapy cycle they received during the study. MRC, UK Medical Research Council Adult and Children's Leukaemia Working Parties; DCLSG, Dutch Childhood Leukemia Study.

Safety measurement

Serum TGF-β_2 concentrations measured during the TGF-β_2 and placebo study period showed no significant difference. Aspartate-aminotransferase (ASAT) and Alanine–aminotransferase (ALAT) were assessed to reflect possible acute damage of TGF-β_2 to the liver. β_2-microglobulin and creatinine were assessed to measure the glomerular filtration. Previously, it was observed that high dose TGF-β_2 administered intravenously could cause a reversible decline of glomerular filtration.[33] However, all assessed parameters showed no difference between the TGF-β_2 and placebo study period.

Endpoints

Table 3 shows the WHO toxicity scores of all patients during the TGF-β_2 and placebo study period. The patients were assigned to the group of their highest toxicity score. Forty-eight percent of the patients in the TGF-β_2 period and 28% of the patients in the placebo period developed grade 1/2 diarrhea and only 16% and 24%, respectively, encountered grade 3/4 diarrhea. The type of severe toxicity that occurred most often was grade 3/4 mucositis: 40% of patients during TGF-β_2-treatment, versus 32% during placebo-treatment. More than 75% of patients encountered fever, but only 20% of the patients developed grade 3/4 fever after TGF-β_2 and 16% after placebo. The overall prevalence of anal lesions was low in both treatment groups. More than 40% of the patients suffered from (abdominal) pain of which only a very small percentage was grade 3/4. Grade 1/2 nausea/vomiting occurred in 52% of the patients in the TGF-β_2 period and 80% of the patients in the placebo period, grade 3/4 only in 8 and 4%, respectively. None of the observed differences proved to be significant.

Table 3 also shows the toxicity scores measured by other means than the WHO scale. During the placebo period, 48% of patients required opioids versus 40% during the TGF-β_2 period. From 60% of the patients, blood cultures were taken during the TGF-β_2 period and 48% of the patients received antibiotic treatment during the same period; this was 72% and 76%, respectively in the placebo period. The prevalence of intervention measures was very low in both groups, except for the administration of total parental nutrition (TPN): 24% of the patients received TPN during TGF-β_2 period and 40% during placebo period. However, none of the observed differences reached significance.

Table 2 WHO grading scale of primary and secondary endpoints

					Study-feeding	Diarrhea	Mucositis	Fever	Anal lesions	(Abdominal) pain	Nausea/vomiting
Pt	**Sex**	**Age**	**Dx**	**Chemo cycle**	**-/+**	**-/+**	**-/+**	**-/+**	**-/+**	**-/+**	**-/+**
1	M	1	ALL	MD-MTX	80/100	0/0	1/0	0/0	0/0	0/0	0/0
2	f	3	ALL	MD-MTX	80/60	0/1	1/1	2/2	0/0	0/0	1/0
3	f	7	ALL	MD-MTX	100/100	2/0	3/3	0/2	0/0	2/0	0/2
4	m	1	AML	MAE	66/95	0/1	0/0	2/3	0/0	1/0	2/3
5	m	2	AML	ADE	89/91	3/3	1/0	2/2	2/1	3/2	2/0
6	m	2	AML	ADE	76/100	2/1	2/0	3/2	0/0	1/0	2/2
7	m	6	AML	ADE	75/100	0/2	0/0	2/3	0/0	0/2	2/2
8	m	7	AML	MD-MTX	88/100	3/3	1/2	2/0	0/1	0/0	2/0
9	f	7	AML	ADE	93/94	2/2	1/1	2/2	0/0	0/0	2/2
10	f	8	AML	ADE	92/93	0/0	3/2	2/0	0/0	0/1	2/0
11	m	9	AML	ADE	86/93	3/0	1/0	2/0	0/0	1/0	0/0
12	m	13	AML	ADE	62/100	3/1	0/0	3/0	0/0	3/2	3/2
13	f	14	AML	ADE	100/32	3/3	1/2	2/3	0/0	0/0	1/1
14	m	4	B-NHL	COPADM	100/94	1/0	4/2	2/2	2/2	3/0	2/0
15	m	5	B-NHL	COPADM	100/91	1/0	2/3	2/2	0/2	2/0	2/2
16	m	6	B-NHL	COPADM	95/100	3/3	3/4	2/3	0/2	2/3	2/2
17	m	6	B-NHL	COPADM	75/27	0/2	2/3	2/2	0/0	1/2	2/2
18	f	6	B-NHL	COPADM	75/77	0/0	4/4	2/2	2/1	2/2	1/2
19	m	7	B-NHL	COPADM	100/81	0/0	3/4	3/3	2/0	1/2	2/3
20	m	8	B-NHL	COPADM	89/100	0/1	4/4	2/3	0/0	3/2	2/2
21	f	8	B-NHL	COPADM	89/89	2/2	3/4	2/2	0/3	0/0	2/2
22	f	13	B-NHL	COPADM	100/100	1/1	3/4	2/2	0/0	2/0	2/0
23	m	13	Bone tumor	HD-MTX	50/38	0/0	2/2	0/0	0/0	0/0	0/0
24	m	12	Bone tumor	HD-MTX	100/100	0/1	0/0	0/0	0/0	1/2	0/0
25	m	12	Bone tumor	VIDE	100/100	2/1	0/0	2/2	0/0	2/2	1/1

Table 3 Effect of TGF-β_2 versus placebo on the percentage of patients developing the assessed endpoints

	TGF-β_2			Placebo			
WHO	**0**	**1/2**	**3/4**	**0**	**1/2**	**3/4**	
Diarrhea	36	48	16	48	28	24	(% Affected patients)
Mucositis	32	28	40	24	44	32	
Fever	24	56	20	16	68	16	
Anal lesions	76	20	4	80	20	0	
(Abdomen) pain	56	36	8	44	44	12	
Nausea/vomiting	40	52	8	16	80	4	
Analgesic use							
Paracetamol		48			44		(% Affected patients)
Opioid		40			48		
Blood culture		60			72		
Antibiotics		48			76		
Intervention							
X-abdomen		12			16		
Oligo-peptide feeding		8			0		
Minimal enteral feeding		0			12		
Total parental nutrition		24			40		
No oral intake		12			12		

The first part of the table shows the percentages of patients scoring grade 0, grade 1 - 2, or 3 - 4 on the parameters assessed by WHO four-point scale. The first column was scored during TGF-β_2-treatment, the second during placebo-treatment. The bottom part of the table shows the clinical endpoints not assessed by WHO scale, also expressed in percentages of patients affected.

The cumulative toxicity for each WHO parameter during the observation time was expressed as AUC (Figure 3). For none of the assessed WHO parameters, a significant difference in AUC was found between the TGF-β_2 and placebo arm. In addition, for none of the other parameters (analgesic use, blood cultures, antibiotic therapy, and the interventions and/or diagnostics, scored each day during the observation period: no = 0 and yes = 1), a significant difference in AUC was found between TGF-β_2 and placebo cycles. The total number of days with WHO 3/4 toxicity did not differ between cycles with TGF-β_2 and placebo (Figure 4). We also subdivided patients into groups according to whether or not they received feeding enriched with the direct active (unbound) TGF-β_2 or with the indirectly active (bound) TGF-β_2, as explained in the patients and methods section. In short, the indirect active TGF-β_2 is bound to its pro-protein Latency-associated peptide (LAP) which is only activated after degrading LAP from the TGF-β_2 protein in the stomach. Furthermore, the group was subdivided for further analysis according to age, treatment regimen and diagnosis, percentage study-feeding consumed, and whether or not application of directly active TGF-β_2 to the mouth mucosa was successful. None of the stratified analyses showed a significant difference between the TGF-β_2 and placebo arm for any of the toxicity parameters.

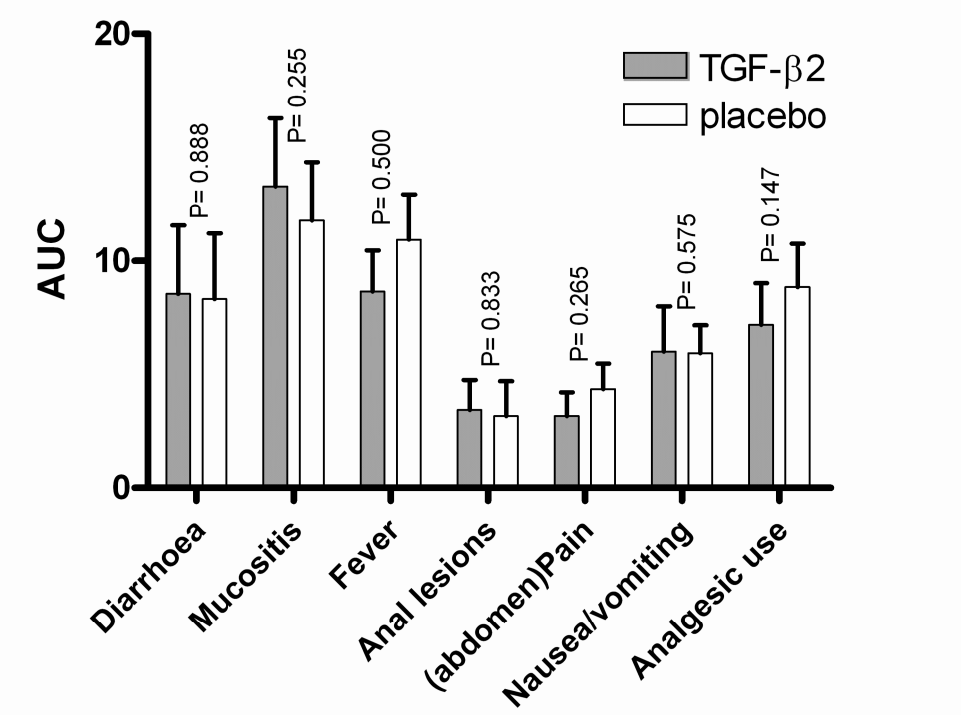

Figure 3 *The effect of TGF-β_2 on WHO toxicity. The area under the curve of the individual WHO scores during the TGF-β_2-enriched study period and during the placebo study period were compared by the Wilcoxon signed ranks test. There were no significant differences, as indicated above the bars by the P-value > 0.05. The bars are expressed as medians + SEM.*

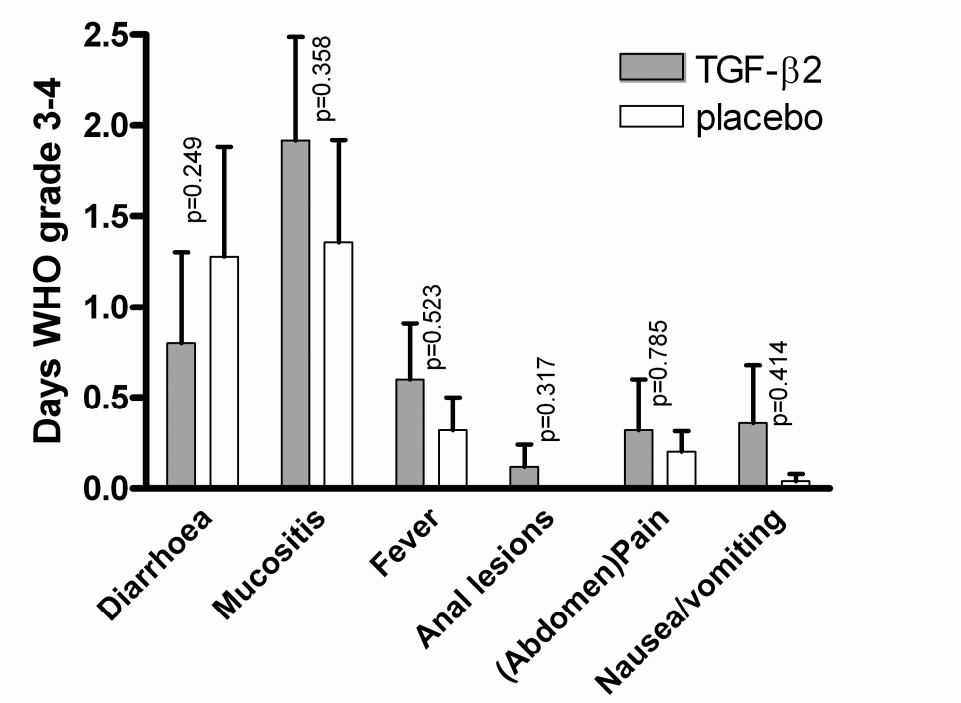

Figure 4 *The effect of TGF-β_2 on number of days with WHO grade 3 or 4. The distribution of the number of days patients suffered toxicity WHO grade 3 or 4 during the TGF-β_2 study period or the placebo study period were compared by the Wilcoxon signed ranks test. There were no significant differences, as indicated above the bars by the P-value > 0.05. The bars are expressed as medians + SEM.*

DISCUSSION

We evaluated the feasibility and efficacy of a TGF- β_2-enriched feeding versus a placebo. The feeding was well tolerated as only 3 of the 30 patients dropped out because of study burden or taste dislike. The compliance of consuming the study-feeding was very high, especially when tube feeding was administered. Patients diagnosed with AML predominantly caused the slightly decreased intake to 86% of the planned dose. Their chemotherapy cycle starts almost directly after diagnosis, which did not leave us enough time to start the study-feeding 2 days before chemotherapy infusion. The oral administration of TGF-β_2-enriched feeding appeared to be safe, as renal and liver function were not affected during TGF-β_2 administration in comparison to the placebo period. Furthermore, there were no indications of increased serum TGF-β_2 during or after TGF-β_2 supplementation.

We could not detect a significant effect of TGF-β_2-enriched study-feeding on the incidence of diarrhea, oral mucositis, anal lesions, fever, nausea and vomiting, or mucositis-related pain. Also, TGF-β_2 had no influence on reducing the severity of these symptoms; the number of days with WHO grade 3/4 toxicity was not significantly different in the TGF-β_2 treated-period compared to the placebo-period. The same was seen for the incidence in administration of opioids and antibiotics and the number of blood cultures and interventions. So, although the feasibility was good, this study showed no benefit of oral TGF-β_2 administration on the incidence or severity of mucositis.

Our findings are in contrast to the findings in the rodent model[30] in which TGF-β_2 supplementation reduced chemotherapy-induced mucositis. This discrepancy in findings between the animal model and the lack of efficacy in our study may be due to several reasons. First, it could simply be correct that TGF-β_2 does not protect against chemotherapy-induced mucositis in children with cancer. Important, however, is that in retrospect, our study might have been underpowered to detect a possible benefit of TGF-β_2 because the overall incidence of severe mucositis was low. Only about one-third of the patients showed grade 3/4 mucositis. Second, in the present study, a combination of chemotherapy was given during several consecutive days, whereas in the rodent model, only MTX was given as a single dose. In our study, only five patients were treated with MTX monotherapy, but none of them developed mucositis during the study periods, despite the fact they had severe mucositis during earlier MTX treatment. Third, the protective effect of TGF-β_2-enriched feeding in the rodent model was predominantly based on the preservation of villus length in the ileum.[30] Scoring symptoms and functional changes such as diarrhea and pain will not give specific information about which segment of the intestine is affected by chemotherapy.[1] On the other hand, clinical symptoms are ultimately the most important outcome parameters. Fourth, non-effectiveness of the TGF-β_2 could also be caused by a lack of knowledge about the required dose and timing of the TGF-β_2 supplementation, which has proven to be of

great importance in the effectiveness of TGF-β_3 protection of radiotherapy-induced mucositis.[26] Finally, research in the past few years (reviewed by Sonis *et al.*,)[34] revealed that mucositis is not solely the consequence of chemotherapy-induced damage to the progenitor cells in the crypts of Lieberkühn. It has a much more complex and dynamic pathophysiology, which includes damage of all mucosal cells.[34] Therefore, the approach of only decreasing the vulnerability of epithelial progenitors by TGF-β in order to prevent mucositis is, probably, not enough.

The lack of benefit of TGF-β_2 application to prevent oral mucositis in our study is in concordance with the finding that oral application of TGF-β_3 in adult patients[35] did not have any positive effect on oral mucositis incidence, onset, or duration. The same was seen for an other stem cell modifying factor flurbiprofen, which also protected the stem cells in an animal mucositis-model but showed no effect in adult cancer patients receiving radiotherapy in the head and neck region.[26,36,37] An exception is keratinocyte growth factor (KGF), which was found to have a clinically meaningful biologic effect in alleviating mucositis in adult colon cancer patients receiving chemotherapy, however, these data were obtained from a phase I trial.[38] More recently, the anti-mucositis effect of KGF was also demonstrated in adult hematologic cancer patients after intensive chemotherapy and radiotherapy for autologous stem-cell transplantation.[38,39] The protective mechanism of KGF is only partly elucidated; KGF increases stem cell numbers and/or the number of stem cells in S-phase,[40] and stimulates epithelial proliferation, thereby causing increased mucosal thickness.[41] KGF not only reduced the incidence and severity of oral mucositis but also reduced the sequential parameters of mucositis like infections, use of opioid analgesics, and parenteral nutrition.[39] Although the results are promising, the efficacy of KGF has yet to be proven in preventing chemotherapy-induced GI-mucositis in childhood-cancer patients.

We conclude that TGF-β_2-enriched feeding is well tolerated and safe in childhood-cancer patients. TGF-β_2, administered as in this study protocol, does not, however, decrease the incidence or degree of mucositis induced by combination chemotherapy in childhood-cancer patients. Because mucositis is one of the most important side effects of chemotherapy in children, more studies are warranted to investigate the possible beneficial role of TGF-β_2 and other products such as KGF.

ACKNOWLEDGMENT

The authors thank I. van der Vaart and E. Visser for their professional assistance, and W. Hop for his statistical advice. This work was performed in collaboration with Numico Research BV, Wageningen, The Netherlands.

REFERENCES

1. Sonis ST, Elting LS, Keefe D, et al. Perspectives on cancer therapy-induced mucosal injury: Pathogenesis, measurement, epidemiology, and consequences for patients. Cancer 2004;100:1995-2025.
2. Bonnaure-Mallet M, Bunetel L, Tricot-Doleux S, et al. Oral complications during treatment of malignant diseases in childhood: Effects of tooth brushing. Eur J Cancer 1998;34:1588-1591.
3. Childers NK, Stinnett EA, Wheeler P, et al. Oral complications in children with cancer. Oral Surg Oral Med Oral Pathol 1993;75:41-47.
4. Sonis ST, Sonis AL, Lieberman A. Oral complications in patients receiving treatment for malignancies other than of the head and neck. J Am Dent Assoc 1978;97:468-472.
5. Fayle SA, Curzon ME. Oral complications in pediatric oncology patients. Pediatr Dent 1991;13:289-295.
6. Bellm LA, Epstein JB, Rose-Ped A, et al. Patient reports of complications of bone marrow transplantation. Support Care Canc 2000;8:33-39.
7. Elting LS, Cooksley C, Chambers M, et al. The burdens of cancer therapy. Clinical and economic outcomes of chemotherapy-induced mucositis. Cancer 2003;98:1531-1539.
8. Ruescher TJ, Sodeifi A, Scrivani SJ, etal. The impact of mucositis on alpha-hemolytic streptococcal infection in patients undergoing autologous bone marrow transplantation for hematologic malignancies. Cancer 1998;82:2275-2281.
9. McGuire DB. Mucosal tissue injury in cancer therapy. More than muscositis and mouthwash. Cancer Pract 2002;10:179-191.
10. Sonis ST, Oster G, Fuchs H, et al. Oral mucositis and the clinical and economic outcomes of hematopoietic stem-cell transplantation. J Clin Oncol 2001;19:2201-2205.
11. Hockenberry M. Symptom management research in children with cancer. J Pediatr Oncol Nurs 2004;21:132-136.
12. Sonis S, Clark J. Prevention and management of oral mucositis induced by antineoplastic therapy. Oncology (Huntingt) 1991; 5:11-18; discussion 18-22.
13. Sonis ST. Mucositis as a biological process: A new hypothesis for the development of chemotherapy-induced stomatotoxicity. Oral Oncol 1998;34:39-43.
14. Ijiri K, Potten CS. Response of intestinal cells of differing topographical and hierarchical status to ten cytotoxic drugs and five sources of radiation. Br J Cancer 1983;47:175-185.
15. Ijiri K, Potten CS. Further studies on the response of intestinal crypt cells of different hierarchical status to eighteen different cytotoxic agents. Br J Cancer 1987;55:113-123.
16. Keefe DM, Brealey J, Goland GJ, et al. Chemotherapy for cancer causes apoptosis that precedes hypoplasia in crypts of the small intestine in humans. Gut 2000;47:632-637.
17. Harmon BV, Takano YS, Winterford CM, et al. Cell death induced by vincristine in the intestinal crypts of mice and in a human burkitt's lymphoma cell line. Cell Prolif 1992;25:523-536.
18. Anilkumar TV, Sarraf CE, Hunt T, et al. The nature of cytotoxic drug-induced cell death in murine intestinal crypts. Br J Cancer 1992;65:552-558.
19. Barnard JA, Lyons RM, Moses HL. The cell biology of transforming growth factor beta. Biochim Biophys Acta 1990;1032:79-87.
20. Massague J. The transforming growth factor-beta family. Annu Rev Cell Biol 1990;6:597-641.
21. Koff A, Ohtsuki M, Polyak K, et al. Negative regulation of g1 in mammalian cells: Inhibition of cycin e-dependent kinase by tgf-beta. Science 1993;260:536-539.
22. Roberts AB, Anzano MA, Wakefield LM, et al. Type beta transforming growth factor: A bifunctional regulator of cellular growth. Proc Natl Acad Sci USA 1985;82:119-123.

23. McCormack ES, Borzillo GV, Ambrosino C, et al. Transforming growth factor-beta3 protection of epithelial cells from cycle-selective chemotherapy in vitro. Biochem Pharmacol 1997;53:1149-1159.

24. Sonis ST, Van Vugt AG, BrienJP, et al. Transforming growth factor-beta 3 mediated modulation of cell cycling and attenuation of 5-fluorouracil induced oral mucositis. Oral Oncol 1997;33:47-54.

25. Potten CS, Booth D, Haley JD. Pretreatment with transforming growth factor beta-3 protects small intestinal stem cells against radiation damage in vivo. Br J Cancer 1997;75:1454-1459.

26. Booth D, Potten CS. Protection against mucosal injury by growth factors and cytokines. J Natl Cancer Inst Monogr 2001;29:16-20.

27. Wymenga AN, vander Graaf WT, Hofstra LS, et al. Phase i study of transforming growth factor-beta3 mouthwashes for prevention of chemotherapy-induced mucositis. Clin Cancer Res 1999;5:1363-1368.

28. Jin Y, Cox DA, Knecht R, et al. Separation, purification, and sequence identification of tgf-beta 1 and tgf-beta 2 from bovine milk. J Protein Chem 1991;10:565-575.

29. Rogers ML, Goddard C, Regester GO, et al. Transforming growth factor beta in bovine milk: Concentration, stability and molecular mass forms. J Endocrinol 1996;151:77-86.

30. van't Land B, Meijer HP, Frerichs J, et al. Transforming growth factor-beta2 protects the small intestine during methotrexate treatment in rats possibly by reducing stem cell cycling. Br J Cancer 2002;87:113-118.

31. Munger JS, Harpel JG, Gleizes PE, et al. Latent transforming growth factor-beta: Structural features and mechanisms of activation. Kidney Int 1997;51:1376-1382.

32. WHO. Who handbook for reporting results of cancer treatment. Geneva: World health Organization; 1979, 13p.

33. Calabresi PA, Fields NS, Maloni HW, et al. Phase 1 trial of transforming growth factor beta 2 in chronic progressive ms. Neurology 1998;51:289-292.

34. Sonis ST. The pathobiology of mucositis. Nat Rev Cancer 2004;4:277-284.

35. Foncuberta MC, Cagnoni PJ, Brandts CH, et al. Topical transforming growth factor-beta3 in the prevention or alleviation of chemotherapy-induced oral mucositis in patients with lymphomas or solid tumors. J Immunother 2001;24:384-388.

36. Stokman MA, Spijkervet FK, Burlage FR, et al. Clinical effects of flurbiprofen tooth patch on radiation-induced oral mucositis. A pilot study. Support Care Cancer 2005;13:42-48.

37. Antin JH, Lee SJ, Neuberg D, et al. A phase i/ii double-blind, placebo-controlled study of recombinant human interleukin-11 for mucositis and acute gvhd prevention in allogeneic stem cell transplantation. Bone Marrow Transplant 2002;29:373-377.

38. Meropol NJ, Somer RA, Gutheil J, et al. Randomized phase i trial of recombinant human keratinocyte growth factor plus chemotherapy: Potential role as mucosal protectant. J Clin Oncol 2003;21:1452-1458.

39. Spielberger R, Stiff P, Bensinger W, et al. Palifermin for oral mucositis after intensive therapy for hematologic cancers. N Engl J Med 2004;351:2590-2598.

40. Potten CS, O'Shea JA, Farrell CL, et al. The effects of repeated doses of keratinocyte growth factor on cell proliferation in the cellular hierarchy of the crypts of the murine small intestine. Cell Growth Differ 2001;12:265-275.

41. Farrell CL, Bready JV, Rex KL, et al. Keratinocyte growth factor protects mice from chemotherapy and radiation-induced gastrointestinal injury and mortality. Cancer Res 1998;58:933-939.

Part III

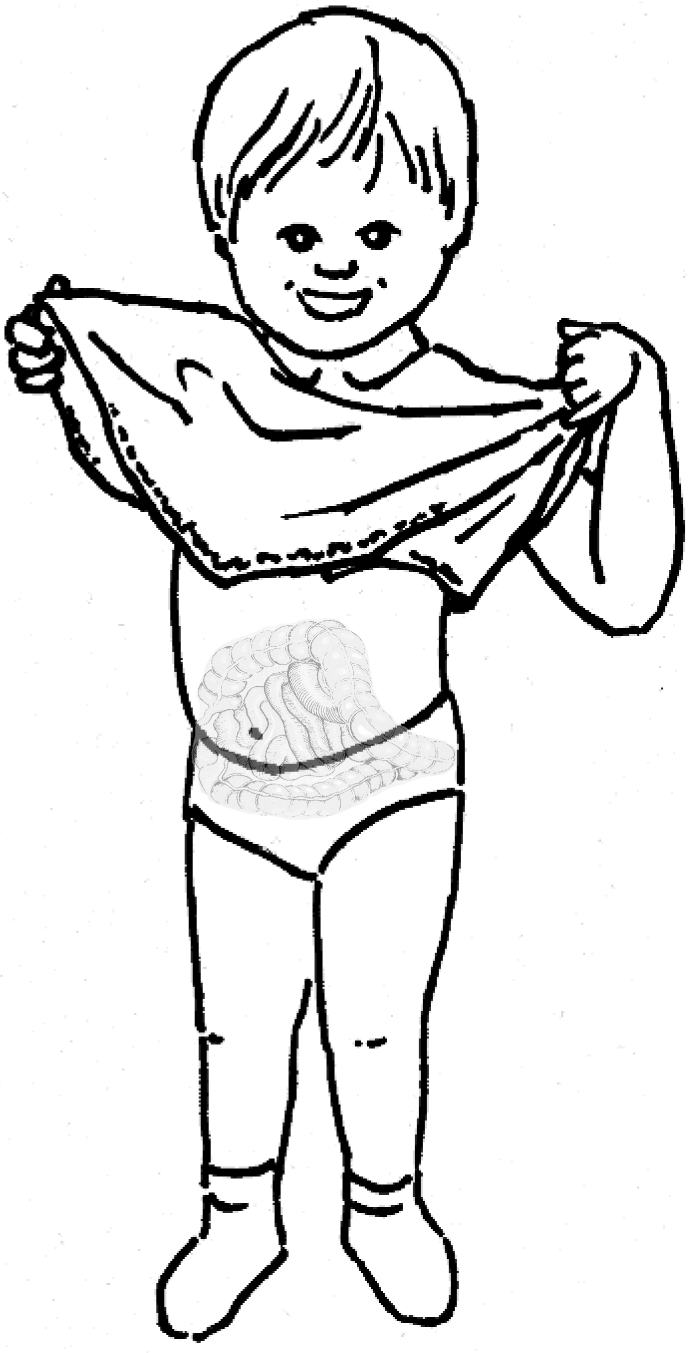

GENERAL DISCUSSION AND SUMMARY

9

GENERAL DISCUSSION

Until a few years ago, it was believed that mucositis arose solely from the effects of inhibited cell proliferation and renewal. However, recent studies have revealed that mucositis results from a dynamic cascade of events of which inhibition of epithelial proliferation is just one part. As such, various non-epithelial cells have been identified to serve as (unwanted) target of anti-cancer treatments.[1] Nevertheless, despite the expanding knowledge on the pathogenesis of mucositis, to date there is no effective treatment available.

The aim of this thesis was to extend our knowledge on the pathophysiology of chemotherapy induced-mucositis and thereby define factors influencing mucositis development in order to identify new targets for mucositis prophylaxis and/or treatment.

CYTOSTATIC DRUGS

Methotrexate versus doxorubicin

Although Methotrexate (MTX) and doxorubicin (DOX) work through different mechanisms, and the specific effects on various crypt-cells may differ,[2-4] the immune-histochemical characteristics upon mucositis induction were comparable (chapter 2). Both drugs affect both epithelial proliferation and differentiation, induce epithelial flattening, crypt loss, villus atrophy and finally epithelial ulceration. These findings confirmed earlier data on MTX induced mucositis[5,6] and 5′-Fluorouracil mucositis-murine-models.[7]

In both the MTX and DOX model increased proliferation was concomitant with a decrease in differentiation (chapter 2 and 3). This preferential state of hyper-proliferation during decreased epithelial differentiation is not only observed following chemotherapy treatment. The same is seen during severe epithelial damage in dextran sulfate sodium induced colitis[8,9] and in the active replicating phase of intestinal rota virus infection.[10] We hypothesize that this apparent paradoxical finding may represent an inborn mechanism of intestinal damage control. As proposed by others, increased proliferation could result from a feedback loop in which a loss of differentiated (villus) cells stimulates the crypt to increase proliferation.[11,12] This sheds new light on the discrepancy in timing of increased proliferation and decreased differentiation in the DOX (chapter 2) and MTX (chapter 3) animal models. In the MTX animal model, we found an increase in epithelial proliferation accompanied by a decrease in differentiation during severe histological damage (day 3). Similar observations were seen in the DOX model on day 1 but during severe histological damage on day 3 the opposite was observed (decreased epithelial proliferation, increased differentiation). These results suggest a more severe damage induced by DOX already at day 1, in comparison to day 3 in the MTX model, implying a prolonged period of epithelial regeneration after DOX-treatment.

PROLIFERATION AND DIFFERENTIATION

The role of proliferation in mucositis development and repair seems two-sided. Intestinal repair is the result of an increased epithelial proliferation after chemotherapy (chapter 2 and 3). Striking is however that, on the other side, increased proliferation prior to chemotherapy seems to be associated with less severe mucositis. Peyers' patch epithelium for example, exhibits an increased proliferation rate already at baseline conditions, showing mild mucositis after MTX-treatment compared to normal epithelium.[13] Recent clinical trials studying the effect of recombinant keratinocyte growth factor (KGF), revealed substantial efficacy in mucositis prevention when the drug was administered before start of chemotherapy. One of the mechanisms of action of KGF, is through an increase in epithelial proliferation rate.[14] Finally, normal microbial flora has a stimulating influence on intestinal cell proliferation, shown by a difference in epithelial proliferation between conventionally and germ-free kept mice.[15] This mechanism could play a role in the Muc-2 deficient mice, studied in chapter 4. These mice encounter an enhanced intestinal bacterial exposure due to absence of the intestinal mucus-layer. Although increase in proliferation could not be shown for 8-week-old Muc-2 deficient mice (as studied in chapter 4), this was shown for mice a few weeks older. Small changes in proliferation, could, in part, explain the observation that Muc-2 deficient mice experience less severe intestinal damage in comparison to wild type mice (chapter 4), as discussed later in this thesis. We hypothesize that continuous activation of NFκB signaling by commensal bacteria, may play a role in this enhanced cell proliferation.[16,17]

Signaling pathway

Intestinal proliferation and differentiation is associated with continuous cell-cell and epithelial-mesenchymal crosstalk.[18] These regulatory systems include the morphogenes BMP and the Wnt-signaling pathway. In this thesis we show that hyper-proliferation of the epithelium during DOX-induced mucositis is influenced by alterations in the BMP-4 - Wnt pathway (chapter 2). More specifically, during the first two days after DOX-treatment, TCF-4, a key player in the Wnt-signaling pathway, is distinctly up regulated while BMP-4 is concomitantly down regulated. This new balance results in a preference for epithelial proliferation over differentiation (chapter 2). Future studies are needed to elucidate the mechanisms by which BMP-4 and TCF-4 are regulated during intestinal damage and regeneration.

We could speculate that the Sonic hedgehog (Shh) signaling pathway regulates BMP-4 in reaction to chemotherapy induced intestinal damage. BMP-4 is one of the targets of Shh signalling.[19,20] Shh induces BMP-4 expression in the gut mesenchyme in early intestinal development.[21-23] Furthermore, an increased Shh expression enhances the proliferating activity of connective tissue cells as an epithelial signaling factor.[24] This hypothesis is supported by the observation that Shh expression is up-regulated in inflammatory bowel disease, suggesting an increase of intestinal stem proliferation in order to compensate for epithelial damage.[25] In this regard, a change in balance between Shh and BMP-4

could cause preference in epithelial proliferation (increased Shh expression) or differentiation (increased BMP-4 expression).

Transcription factors

During epithelial hyper-proliferation, differentiation seems actively down regulated, characterized by a decreased expression of sucrase–isomaltase (SI) and the SI transcription factors Cdx-2, GATA-4 and HNF-1α after MTX treatment (chapter 3). Decrease in BMP-4 expression, as discussed in chapter 2 may also, indirectly, cause the observed decrease in SI expression. This hypothesis is supported by data showing that inhibition of BMP-4 stimulates Wnt signaling, and that Wnt signaling itself induces SOX9 expression, which in turn is a negative regulator of Cdx2 expression.[26-28] Moreover, BMP-4 has shown to be directly involved in the expression of HNF-1α.[29] However, the dynamics of BMP-4 expression were not studied in the current MTX model and remain to be investigated. Another hypothesis is that the decreased expression of p21, a kinase inhibitor of cell proliferation,[30] is the cause of the increased proliferation observed, and thus, consequently leads to a decrease in Cdx2 expression. However, Gibson *et al.* recently presented data which disagree with this hypothesis, as they did not show any change in p21 expression following MTX-administration.[31]

Previous studies have also identified the intestinal mucin Muc-2 as a target gene for GATA-4[32] and Cdx-2,[33] just like SI. Both SI and Muc-2 mRNA expression are down-regulated after MTX-treatment.[5,6] However in contrast to SI protein expression which is concomitantly down-regulated, Muc-2 protein levels increase after chemotherapy.[5,6] This implies that post-translational factors influence protein expression, possibly in order to control further intestinal damage.

In general, almost all brush-border enzymes, involved in carbohydrate, sugar digestion and absorption are down-regulated during mucositis (chapter 3).[5,34,35] At the same time, goblet- and paneth cell function remain relatively intact after chemotherapy.[5,6] Of interest is to unravel whether these distinct differences in cellular function result directly from changes in cell fate.

Math1 has shown to be involved in intestinal cell fate decisions.[36] In case of an increased Math1 expression, cells differentiate into paneth-, goblet- or entero-endocrine cells. Low or absent levels of Math1 expression, on the other hand, lead to the differentiation of enterocytes and therefore may be regarded as a default pathway.[37] Math1 is a downstream target gene of the Notch signaling pathway, which is considered to be one of the critical regulators of intestinal differentiation and development, in addition to the Shh, Wnt and BMP signaling pathways.[38] Notch-Math1 interactions with Shh and BMP-4 have been described, although not in intestine, but in other organ systems.[36,39,40] Recent reports revealed that Cdx2 stimulates endogenous Math1 mRNA expression in intestinal crypts.[41] Furthermore Bosse *et al.* demonstrated an increased Math1 expression in GATA-

4 mutant mice.[42] These observations both suggest a regulatory role for Cdx-2 and GATA-4 on intestinal cell fate.

Intestinal metabolism

Despite induced hyper-proliferation and decreased differentiation, leucine metabolism is spared during mucositis (chapter 7). Especially, the unaffected first pass uptake of leucine is in contrast with our hypothesis which was deducted from earlier reports showing that the intestine is a 'selfish' organ; taking care of itself before passing nutrients to the systemic metabolism.[43] Leucine kinetic studies in intestinal infection models show an increased first pass uptake.[44] Our data on leucine metabolism, however, are in agreement with studies performed in animals suffering from short bowel syndrome, one week after intestinal resection.[45] In addition, the data from the leucine study reflect an acute loss of part of all absorptive (differentiated) enterocytes, suggesting that enterocyte function is not fully annulled, as whole intestinal metabolism is not influenced. Another hypothesis is that there is a hierarchical order in which down-regulation of intestinal differentiation takes place after epithelial damage. This hypothesis is supported by the discrepancy observed between SI and Muc-2 protein expression during MTX-treatment (chapter 3-4).

Previous studies show that the basic metabolic rate of children with a solid tumor is already increased at diagnosis and during the first phase of chemotherapy.[46] In agreement with this, in the study population as presented in chapter 7 almost all patients were shown to be in a catabolic state before start of their first cycle of chemotherapy. This indicates that children suffering from hematological malignancies are also at risk of being in a catabolic state, even before start of therapy. However, it is important to consider that leucine metabolism does not represent kinetics of all essential amino acids.[47] For example, animal studies have shown that oxidation resources change during low protein feeding from amino acid to glucose.[48] For our patient group however, catabolism was caused by a decreased protein intake, as a significant increase in leucine oxidation was not observed.

Recent studies show that tube feeding, especially rich of calories, can improve the nutritional state,[49,50] which is correlated to a reduction in infections in childhood cancer patients.[51] It remains to be elucidated if therefore tube feeding during periods of mucositis is best to consist of free amino acids (hydrolyzed feeding) or (small) peptides (non-hydrolyzed-feeding). Studies comparing the intestinal uptake of intrinsically labeled amino acids and proteins would give more information in this matter.

INTESTINAL BARRIER

Damage of the intestinal epithelium and lamina propria results from the cytotoxic actions of the pro-inflammatory tumor necrosis factor-α (TNF-α) (chapter 5). Earlier publications show a direct correlation between the level of TNF-α and mucositis severity.[52,53] Our

results, demonstrating an increased TNF-α expression after MTX-treatment, are in agreement with data established in a rat-mucositis-model, also showing increased TNF-α expression after MTX-treatment.[54] The increase in TNF-α expression is most likely caused by stimulation of the NFκB pathway.[1,54] Chemotherapy activates the NFκB directly or through the production of reactive oxygen species (ROS).[1,55] Recently, Logan and colleagues were the first to show increased NFκB expression in oral mucosa of patients following chemotherapy.[56]

In addition to TNF-α, INF-γ was shown to be released by effector-T cells (chapter 5) during mucositis. Both these cytokines in turn stimulate macrophages to additionally release TNF-α (chapter 5). This damage inducing cascade bares similarities with the etiology of Inflammatory Bowel Disease (IBD).[57] In chemotherapy induced mucositis as well as in IBD, macrophages release IL-6 and IL1b, pro-inflammatory cytokines associated with the pathogenesis.[1,57]

Besides chemotherapy, bacteria and their bacterial wall products stimulate the NFκB signaling pathway.[55] Particularly during the ulcerative phase of mucositis bacteria have free access to the lamina propria where they can amplify NFκB signaling. We therefore hypothesized that a deficiency of Muc-2, the structural component of the protective mucus barrier, would make the intestine more vulnerable to mucositis development due to an increased bacterial exposure (chapter 4). However, our results showed that the Muc-2 deficient mice were not more sensitive to MTX-treatment. Absence of Muc-2 may lead to a chronic microbial exposure. The immune system of the Muc-2 deficient mice therefore may have adapted to the situation of ongoing bacterial stimulation. Continuous stimulation of the NFκB-TNF-α axis, possibly, results in activation of pro- and anti-inflammatory cytokines, thereby preventing a rapid (unbalanced) pro-inflammatory activation by LPS, one of the main components of the bacterial wall, following chemotherapy. This hypothesis is supported by data showing that, under normal conditions, LPS, has an aggravating role in mucositis development (chapter 5)

We hypothesize that primary induction of TNF-α upon chemotherapy and microbial exposure play important roles in mucositis development under 'wild type' conditions. Moreover, bacterial products communicate with the intestinal epithelium through pattern-recognition receptors like Toll like receptor's (TLR). LPS communication is predominantly established via TLR-4 signalling.[58] TLR-4 could therefore play a role in mucositis development. In agreement, LPS unresponsive mice, carrying a defective TLR-4 gene[59] are less vulnerable to mucositis (chapter 5). TLR expression in Muc-2 mice has not been studied yet but could be the missing link in why Muc-2 mice are less vulnerable to mucositis in comparison to their WT littermates.

MUCOSITIS SCORING SYSTEMS

Scores for mucositis, diarrhea and pain formulated by the World health organization (WHO) classify damage induced by chemotherapy. These are widely used scoring systems, however they have shown to be influenced by pain medication,[60] and are not validated for childhood cancer patients. There are numerous validated mucositis scales for use in adults however not many for the use in childhood cancer patients.[61] Recently, the Oral Mucositis Assessment Scale (OMAS) is validated in children receiving chemotherapy,[62] the same has been done for the oral assessment guide (OAG), originally used for adult patients receiving chemotherapy or radiotherapy.[63] When used in combination with the WHO scale, these scales may reflect oral mucosa disruption and oral function objectively.

The small intestine is not incorporated in these scores. In addition to oral mucositis scores there is a need for non-invasive tools to evaluate gastro-intestinal-mucositis (GI-mucositis) prophylaxis even more since diarrhea and stomach ache do not fully correlate with GI-mucositis.[64] Preclinical studies show correlation between plasma level Glucagon-like peptide-2 and mucositis,[65] also noninvasive optical coherence tomography/optical Doppler tomography and intestinal histology after chemotherapy show promising association.[66] In the last two years two new clinical mucositis-monitoring tests have been published. One measures the concentration of serum citruline, directly reflecting the small intestinal cell mass.[67,68] In comparison to the sugar absorption test (SAT) measuring serum citruline shows higher sensitivity and specificity.[69] The second one is the (13) C-sucrose breath test, which uses the brush border enzyme sucrase as an indicator of intestinal absorptive function.[70] Like the serum citruline test, this breath test seems more sensitive in monitoring intestinal damage in children compared to the use of SAT.[71] These methods should be evaluated in forthcoming new mucositis prophylaxis studies.

Finally, quality of life scores as frequently used and developed for evaluation of the burden of mucositis in adult patients[72,73] are not available for childhood cancer patients. Besides the above-mentioned scoring systems these questionnaires also require our attention.

PROPHYLAXIS

Due to the complex pathobiology of mucositis many targets for prophylaxis could be identified. In this thesis we predominantly focused on epithelial proliferation and subsequent differentiation and epithelial barrier function. Knowledge of these processes together with the different time lines of induced damage (chapter 2 and 3) may eventually lead to tailored interventions at specific time schedules in relation to the administration of chemotherapy.

Transforming growth factor-β

We performed a randomized cross over study in children with cancer in which TGF-β was administered in order to reduce intestinal cell proliferation thereby reducing the vulnerability of epithelial cells against chemotherapy treatment. Unfortunately, TGF-β did not show to be of any value in mucositis prophylaxis (chapter 8).

One of the rare successes of growth factors in mucositis prophylaxis is keratinocyte growth factor (KGF)[74] or palifermin, recombinant human KGF. The anti-mucositis effect of KGF was successfully studied in adult patients with hematologic malignancies who received intensive chemotherapy and fractionated total-body irradiation before autologous stem-cell transplantation.[14,75] KGF not only reduced the incidence and severity of oral mucositis but also reduced the sequel of mucositis like infections, use of opioid analgesics, parenteral nutrition and costs of hospitalization.[14,76] Herewith, palifermin has been approved by the Food and Drug Administration to decrease the incidence and duration of severe oral mucositis in patients with hematological malignancies.

More recent clinical trials confirmed the beneficial effect of palifermin on oral mucositis reduction in the same patient population.[77,78] Other potential applications of KGF are being explored, thus far the use of palifermin in reduction of graft versus host disease in allogenic transplantation (GVHD) showed no convincing results.[78,79] However, palifermin in patients treated for metastatic colorectal cancer is safe and effective on oral mucositis reduction.[75,80] Pre-clinical data imply a potential for palifermin in reducing mucositis burden after radiation.[81,82] Surveys on the effect of KGF on GI-mucositis are not published yet but will be in the near future.

The stem cell protecting effect of KGF seem to be due to an (dose dependent) increased proliferation rate of the intestinal stem cells.[83,84] Herewith, KGF exhibits a trophic and regenerative effect of the intestinal epithelium, causing epithelial thickening characterized by increased crypt length and villus height of the small intestine.[85] The cytoprotective effect of KGF is only beneficial when administered before start of therapy.[86] Besides influencing proliferation, KGF up-regulates the protective intestinal trefoil factor 3 proteins (TFF3) in the goblet cells.[87,88] TFF3 has a major role in mucosal repair[89,90] and is spared during mucositis development, suggesting a protective role in mucositis pathobiology.[6] Finally, KGF induces detoxification of reactive oxygen species (ROS),[91] which are activators of NFκB signal transduction, involved in mucositis development.[1,55]

In contrast to KGF, TGF-β protects intestinal stem cells by arresting them in the G1 phase of the proliferation-cycle.[92,93] The consequence of prolonged TGF-β administration on crypt depth and villus height is not known. It could be speculated however, that villus atrophy might be induced following decreased proliferation. The positive effect of TFF3 on epithelial restitution is established in a TGF-β independent way.[94] However, it has

been shown that the TGF-β signaling pathway is involved in Muc-2 transcription,[95] but the role of Muc-2 is still unknown in mucositis pathobiology (chapter 4). TGF-β down regulates NFκB signaling by attenuating the pro-inflammatory cytokine release and enhancing IL-10 production,[96] favoring intestinal repair.

In conclusion, KGF and TGF-β show different effects on different levels of mucositis prophylaxis. Remarkable is the difference in their influence on stem cell proliferation. As discussed before proliferation remains an important target in mucositis prophylaxis. However, precautions' have to be made when bearing in mind the possible influence of proliferation stimulating agents on tumor growth.

MUCOSAL IMMUNOLOGY

Mucin-2 and Interleukine-10

In the described study control of further damage is predominantly regulated by the up-regulation of the anti-inflammatory cytokine IL-10. IL-10 can be released on activation of regulatory T-cells and macrophages (chapter 5). A role for IL-10 in the control of mucosal damage was established by showing an increase in mucositis severity in IL-10 deficient mice (chapter 5) and was further illustrated by the pre-existence of increased levels of IL-10 in the Muc-2 deficient mice (chapter 4). The mechanism of this damage limiting effect is not clear however. TNF-α was not shown to be down regulated, although IL-10 could possibly cause a limitation in TNF-α release (chapter 5). We hypothesize that the damage limiting effect of IL-10 is due to the ability of IL-10 to down-regulate NFκB thereby limiting the amplifying cascade between TNF-α and NFκB.[97] Even though, it remains questionable if the observed damage control by IL-10 is completely caused by IL-10 itself. From literature concerning colitis prevention it is known that regulatory T-cells produce IL-10 as well as TGF-β.[98,99] IL-10 deficient mice lack protective TGF-β/Smad signaling in comparison to wild-type mice and may therefore fail to inhibit the pro-inflammatory gene expression in the intestinal epithelium.[100] Earlier research showed that Peyers patches are protected against MTX induced mucositis.[13] This may also be the result of high IL-10 and/or TGF-β production seen in rodent peyers' patch.[101]

It is of interest that both total Muc-2 level and Muc-2 precursor synthesis are lower in the IL-10 deficient mice in comparison to wild-type mice.[102] These findings indicate that mucositis induced in IL-10 deficient mice, as described in chapter 5, could well be aggravated due to the combination of absence of IL-10 *and* decreased protein levels of Muc-2. In the absence of Muc-2, IL-10 up-regulation is highly important for intestinal homeostasis, and vice versa, as shown in mice lacking both a Muc-2 and IL-10 (Muc-2/IL-10 deficient mice) (van der Sluis *et al*. unpublished data). These double deficient mice show more pronounced spontaneous intestinal damage in comparison to both single Muc-2 or IL-10 deficient mice. These data suggest that Muc-2 has a damage controlling

effect in intestinal damage in unchallenged IL-10 deficient mice. The protective capacities of Muc-2 during MTX-treatment however, still remain to be investigated (chapter 4).

Because it is still not clear which role Muc-2 may play in mucositis development, a novel model should be developed. Most elegantly would be to silence the Muc-2 gene just before start of chemotherapy. In this novel model the intestinal mucosa and immune system would not already be unbalanced due to a pre-existing Muc-2 deficiency. By lack of these genetically modified mice, this problem could be addressed the other way around, hypothesizing that less mucositis would occur in the presence of an increased Muc-2 production. Muc-2 can be increased by administration of Muc-2 stimulating probiotics, lactobacillus casei GG (LGG),[103] lactobacillus plantarum 299v and lactobacillus rhamnosus GG.[104] *In vitro*, the last two inhibit Escherichia coli adherence to intestinal epithelial cells by their ability to increase expression of Muc-2. Furthermore it would be important to elucidate the role of the ability of Muc-2 in reducing bacterial translocation during mucositis. Especially as bacteraemia is one of the main concerns in these immune compromised patients.[105,106]

Previous experiments have demonstrated that IL-10 can locally be delivered to the intestine, when gut homing CD4+ lymphocytes are transduced with the retroviral vector containing IL-10.[107] The effect of lactococcus lactis secreting IL-10 on intestinal damage has been studied in both mouse and humans colitis models.[108,109] In humans, these genetically modified lactococcus lactis were proven to be safe and preliminary positive results in decreasing Crohn's disease activity were demonstrated.[110]

Apart from exogenously administered IL-10, we should consider the possibility of triggering the intestinal immune system to produce TNF-α and IL-10 in order to prepare the intestine for forthcoming damage analogous to the positive results of a triggered immune system as described in chapter 4. This could be done, for example, by the oral administration of low dose antigens which results in the generation of specific T-cells secreting TGF-β and IL-10.[111] Furthermore, Riehl *et al.* showed protective effects of LPS pre-treatment[112] stimulating the immune system before radiotherapy induced mucositis in a rodent model. These effects were ascribed to an induction of prostaglandin synthesis through cyclo-oxigenase-2 (COX-2) stimulation.

Increasing IL-10 and Muc-2 expression in the intestine by the use of pre- and probiotics, more specifically the lactobacillus strain, should be considered as mucositis prophylaxis. However, we should also bear in mind the immune compromised status of most cancer patients. This could partly be overcome by administration of only the DNA from the probiotic bacteria strain, however, this has only been proven to be sufficient to induce a delayed NFκB response in epithelial cells and an attenuation of epithelial pro-inflammatory TNF-α response.[113]

Nuclear factor-κB

The cascade of events that leads to the intricate balance between pro- and anti-inflammatory cytokines can be affected at various levels of signaling. NFκB for example, can be positively regulated by pro-inflammatory cytokines (*i.e.* TNF-α) and, in a feed-back loop, stimulates the release of TNF-α.[1] One of the most potent *in vivo* mechanisms inhibiting NFκB activation, is triggering of the peroxisome-proliferator-activated receptor-γ (PPAR-γ). PPAR-γ has an important anti-inflammatory function by inhibiting the NFκB signaling pathway, which is followed by a decreased production of pro-inflammatory cytokines.[114-118] For therapeutic use, Kelly *et al.* studied *Bifidus thetaiotaomicron* a prevalent anaerobe of the human intestine, which was found to target the active subunit of NFκB, RelA, in a PPAR-γ dependent way, by promoting its nuclear export and thereby block NFκB transcription.[119] Curcumin is a nutritional nutrient proven to inhibit NFκB.[120] Interestingly, Van 't Land and colleagues recently showed that curcumin diminishes chemotherapy induced epithelial damage[54] due to NFκB inhibition as NFκB is also involved in cell proliferation and survival.[121] It was shown that curcumin had a protective effect on MTX-induced villous atrophy, although this could not be linked to a reduction in pro-inflammatory cytokine production[54]

Directly reducing the bacterial load in order to down-regulate NFκB activities, has been shown to be effective, in the reduction of damage in acute pancreatitis and myocardial infarction.[122] In case of mucositis these treatments had contrasting results[123] as reviewed by Donnelly *et al.*,[124] strongly diminishing the clinical relevance of these interventions. These issues still remain very important to address, especially as prophylactic antibiotics show their efficacy in reducing bacteraemia and infection related mortality during neutropenic episodes in oncology patients.[125]

FUTURE PERSPECTIVES

In conclusion, the results described in this thesis give more insight in the pathobiology of mucositis and suggests new possible targets in mucositis prophylaxis. It is clear that a complex cascade of events results in mucositis. Prophylaxis will therefore not be found in one magic bullet, but must target different levels of intestinal homeostasis at the same time.

New (animal) studies are necessary to further elucidate the role of epithelial-mesenchymal signaling pathways in regulating epithelial (hyper) proliferation and decreased differentiation, specifically during intestinal damage. In addition, the role of Muc-2 should be identified in both mucosal protection and mucosal immunomodulation. Furthermore, the protective effect of increased IL-10 expression should be studied in a mouse model in combination with inhibition of TNF-α and NFκB. Cumulatively, these data would provide more insight in the effect of chemotherapy on the intestinal defense

mechanisms enabling us to develop a prophylactic drugs, aiming on different levels of the intestinal barrier.

In clinical practice we should attempt to increase the nutritional status of childhood cancer patients in an early stage of the disease in order to decrease their catabolic metabolism and thereby decrease chemotherapy induced morbidity. We should increase our knowledge on intestinal metabolism of different essential amino acids and study the intestinal absorption of intrinsically labeled hydrolyzed feeding. It is of utmost importance to implement new GI and oral mucositis scoring systems for childhood cancer patients, not only to optimize every day care but also as instruments to evaluate new mucositis prophylaxis agents in the near future. The efficacy of KGF, in mucositis prophylaxis, in childhood cancer patients, shall be the next agent to be tested in a clinical trial.

REFERENCES

1. Sonis ST. The pathobiology of mucositis. Nat Rev Cancer 2004;4:277-284.
2. Ijiri K, Potten CS. Response of intestinal cells of differing topographical and hierarchical status to ten cytotoxic drugs and five sources of radiation. Br J Cancer 1983;47:175-185.
3. Ijiri K, Potten CS. Further studies on the response of intestinal crypt cells of different hierarchical status to eighteen different cytotoxic agents. Br J Cancer 1987;55:113-123.
4. Moore JV. Clonogenic response of cells of murine intestinal crypts to 12 cytotoxic drugs. Cancer Chemother Pharmacol 1985;15:11-15.
5. Verburg M, Renes IB, Van Nispen DJ, Ferdinandusse S, Jorritsma M, Buller HA, Einerhand AW, Dekker J. Specific responses in rat small intestinal epithelial mRNA expression and protein levels during chemotherapeutic damage and regeneration. J Histochem Cytochem 2002;50:1525-1536.
6. Verburg M, Renes IB, Meijer HP, Taminiau JA, Buller HA, Einerhand AW, Dekker J. Selective sparing of goblet cells and paneth cells in the intestine of methotrexate-treated rats. Am J Physiol Gastrointest Liver Physiol 2000;279:G1037-1047.
7. Tanaka H, Miyamoto KI, Morita K, Haga H, Segawa H, Shiraga T, Fujioka A, Kouda T, Taketani Y, Hisano S, Fukui Y, Kitagawa K, et al. Regulation of the PepT1 peptide transporter in the rat small intestine in response to 5-fluorouracil-induced injury. Gastroenterology 1998;114:714-723.
8. Renes IB, Verburg M, Van Nispen DJ, Taminiau JA, Buller HA, Dekker J, Einerhand AW. Epithelial proliferation, cell death, and gene expression in experimental colitis: alterations in carbonic anhydrase I, mucin MUC2, and trefoil factor 3 expression. Int J Colorectal Dis 2002;17:317-326.
9. Renes IB, Verburg M, Van Nispen DJ, Buller HA, Dekker J, Einerhand AW. Distinct epithelial responses in experimental colitis: implications for ion uptake and mucosal protection. Am J Physiol Gastrointest Liver Physiol 2002;283:G169-179.
10. Boshuizen JA, Reimerink JH, Korteland-van Male AM, van Ham VJ, Koopmans MP, Buller HA, Dekker J, Einerhand AW. Changes in small intestinal homeostasis, morphology, and gene expression during rotavirus infection of infant mice. J Virol 2003;77:13005-13016.
11. Rijke RP, Hanson WR, Plaisier HM, Osborne JW. The effect of ischemic villus cell damage on crypt cell proliferation in the small intestine: evidence for a feedback control mechanism. Gastroenterology 1976;71:786-792.
12. Saxena SK, Thompson JS, Crouse DA, Sharp JG. Epithelial cell proliferation and uptake of radiolabeled urogastrone in the intestinal tissues following abdominal irradiation in the mouse. Radiat Res 1991;128:37-42.
13. Renes IB, Verburg M, Bulsing NP, Ferdinandusse S, Buller HA, Dekker J, Einerhand AW. Protection of the Peyer's patch-associated crypt and villus epithelium against methotrexate-induced damage is based on its distinct regulation of proliferation. J Pathol 2002;198:60-68.
14. Spielberger R, Stiff P, Bensinger W, Gentile T, Weisdorf D, Kewalramani T, Shea T, Yanovich S, Hansen K, Noga S, McCarty J, LeMaistre CF, et al. Palifermin for oral mucositis after intensive therapy for hematologic cancers. N Engl J Med 2004;351:2590-2598.
15. Nowacki MR. Cell proliferation in colonic crypts of germ-free and conventional mice--preliminary report. Folia Histochem Cytobiol 1993;31:77-81.
16. Wang W, Abbruzzese JL, Evans DB, Larry L, Cleary KR, Chiao PJ. The nuclear factor-kappa B RelA transcription factor is constitutively activated in human pancreatic adenocarcinoma cells. Clin Cancer Res 1999;5:119-127.
17. Ghosh S, May MJ, Kopp EB. NF-kappa B and Rel proteins: evolutionarily conserved mediators of immune responses. Annu Rev Immunol 1998;16:225-260.
18. Ishizuya-Oka A. Epithelial-connective tissue cross-talk is essential for regeneration of intestinal epithelium. J Nippon Med Sch 2005;72:13-18.
19. Perrimon N. Hedgehog and beyond. Cell 1995;80:517-520.

20. Ingham PW. Transducing Hedgehog: the story so far. Embo J 1998;17:3505-3511.

21. Roberts DJ, Johnson RL, Burke AC, Nelson CE, Morgan BA, Tabin C. Sonic hedgehog is an endodermal signal inducing Bmp-4 and Hox genes during induction and regionalization of the chick hindgut. Development 1995;121:3163-3174.

22. Roberts DJ, Smith DM, Goff DJ, Tabin CJ. Epithelial-mesenchymal signaling during the regionalization of the chick gut. Development 1998;125:2791-2801.

23. Sukegawa A, Narita T, Kameda T, Saitoh K, Nohno T, Iba H, Yasugi S, Fukuda K. The concentric structure of the developing gut is regulated by Sonic hedgehog derived from endodermal epithelium. Development 2000;127:1971-1980.

24. Ishizuya-Oka A, Ueda S, Inokuchi T, Amano T, Damjanovski S, Stolow M, Shi YB. Thyroid hormone-induced expression of sonic hedgehog correlates with adult epithelial development during remodeling of the Xenopus stomach and intestine. Differentiation 2001;69:27-37.

25. Nielsen CM, Williams J, van den Brink GR, Lauwers GY, Roberts DJ. Hh pathway expression in human gut tissues and in inflammatory gut diseases. Lab Invest 2004;84:1631-1642.

26. Blache P, van de Wetering M, Duluc I, Domon C, Berta P, Freund JN, Clevers H, Jay P. SOX9 is an intestine crypt transcription factor, is regulated by the Wnt pathway, and represses the CDX2 and MUC2 genes. J Cell Biol 2004;166:37-47.

27. He XC, Zhang J, Tong WG, Tawfik O, Ross J, Scoville DH, Tian Q, Zeng X, He X, Wiedemann LM, Mishina Y, Li L. BMP signaling inhibits intestinal stem cell self-renewal through suppression of Wnt-beta-catenin signaling. Nat Genet 2004;36:1117-1121.

28. Taylor JK, Boll W, Levy T, Suh E, Siang S, Mantei N, Traber PG. Comparison of intestinal phospholipase A/lysophospholipase and sucrase-isomaltase genes suggest a common structure for enterocyte-specific promoters. DNA Cell Biol 1997;16:1419-1428.

29. Nastos A, Pogge von Strandmann E, Weber H, Ryffel GU. The embryonic expression of the tissue-specific transcription factor HNF1alpha in Xenopus: rapid activation by HNF4 and delayed induction by mesoderm inducers. Nucleic Acids Res 1998;26:5602-5608.

30. Bilim V, Kawasaki T, Takahashi K, Tomita Y. Adriamycin induced G2/M cell cycle arrest in transitional cell cancer cells with wt p53 and p21(WAF1/CIP1) genes. J Exp Clin Cancer Res 2000;19:483-488.

31. Gibson RJ, Bowen JM, Cummins AG, Keefe DM. Relationship between dose of methotrexate, apoptosis, p53/p21 expression and intestinal crypt proliferation in the rat. Clin Exp Med 2005;4:188-195.

32. van der Sluis M, Melis MH, Jonckheere N, Ducourouble MP, Buller HA, Renes I, Einerhand AW, Van Seuningen I. The murine Muc2 mucin gene is transcriptionally regulated by the zinc-finger GATA-4 transcription factor in intestinal cells. Biochem Biophys Res Commun 2004;325:952-960.

33. Mesquita P, Jonckheere N, Almeida R, Ducourouble MP, Serpa J, Silva E, Pigny P, Silva FS, Reis C, Silberg D, Van Seuningen I, David L. Human MUC2 mucin gene is transcriptionally regulated by Cdx homeodomain proteins in gastrointestinal carcinoma cell lines. J Biol Chem 2003;278:51549-51556.

34. Kralovanszky J, Prajda N. Biochemical changes of intestinal epithelial cells induced by cytostatic agents in rats. Arch Toxicol Suppl 1985;8:94-103.

35. Taminiau JA, Gall DG, Hamilton JR. Response of the rat small-intestine epithelium to methotrexate. Gut 1980;21:486-492.

36. van Den Brink GR, de Santa Barbara P, Roberts DJ. Development. Epithelial cell differentiation--a Mather of choice. Science 2001;294:2115-2116.

37. Yang Q, Bermingham NA, Finegold MJ, Zoghbi HY. Requirement of Math1 for secretory cell lineage commitment in the mouse intestine. Science 2001;294:2155-2158.

38. Bjerknes M, Cheng H. Gastrointestinal stem cells. II. Intestinal stem cells. Am J Physiol Gastrointest Liver Physiol 2005;289:G381-387.

39. Alexandre C, Lecourtois M, Vincent J. Wingless and Hedgehog pattern Drosophila denticle belts by regulating the production of short-range signals. Development 1999;126:5689-5698.

40. Bermingham NA, Hassan BA, Wang VY, Fernandez M, Banfi S, Bellen HJ, Fritzsch B, Zoghbi HY. Proprioceptor pathway development is dependent on Math1. Neuron 2001;30:411-422.

41. Mutoh H, Sakamoto H, Hayakawa H, Arao Y, Satoh K, Nokubi M, Sugano K. The intestine-specific homeobox gene Cdx2 induces expression of the basic helix-loop-helix transcription factor Math1. Differentiation 2006;74:313-321.

42. Bosse T, Piaseckyj CM, Burghard E, Fialkovich JJ, Rajagopal S, Pu WT, Krasinski SD. Gata4 is essential for the maintenance of jejunal-ileal identities in the adult mouse small intestine. Mol Cell Biol 2006;26:9060-9070.

43. van Goudoever JB, van der Schoor SRD, Reeds PJ. De darm; een egoïstisch orgaan. Tijdschrift voor kindergeneeskunde 2001;69:193-200.

44. Yu F, Bruce LA, Calder AG, Milne E, Coop RL, Jackson F, Horgan GW, MacRae JC. Subclinical infection with the nematode Trichostrongylus colubriformis increases gastrointestinal tract leucine metabolism and reduces availability of leucine for other tissues. J Anim Sci 2000;78:380-390.

45. Sarac TP, Seydel AS, Ryan CK, Bessey PQ, Miller JH, Souba WW, Sax HC. Sequential alterations in gut mucosal amino acid and glucose transport after 70% small bowel resection. Surgery 1996;120:503-508.

46. den Broeder E, Oeseburg B, Lippens RJ, van Staveren WA, Sengers RC, van't Hof MA, Tolboom JJ. Basal metabolic rate in children with a solid tumour. Eur J Clin Nutr 2001;55:673-681.

47. Zello GA, Telch J, Clarke R, Ball RO, Pencharz PB. Reexamination of protein requirements in adult male humans by end-product measurements of leucine and lysine metabolism. J Nutr 1992;122:1000-1008.

48. van der Schoor SR, van Goudoever JB, Stoll B, Henry JF, Rosenberger JR, Burrin DG, Reeds PJ. The pattern of intestinal substrate oxidation is altered by protein restriction in pigs. Gastroenterology 2001;121:1167-1175.

49. den Broeder E, Lippens RJ, van 't Hof MA, Tolboom JJ, Sengers RC, van den Berg AM, van Houdt NB, Hofman Z, van Staveren WA. Nasogastric tube feeding in children with cancer: the effect of two different formulas on weight, body composition, and serum protein concentrations. JPEN J Parenter Enteral Nutr 2000;24:351-360.

50. den Broeder E, Lippens RJ, van't Hof MA, Tolboom JJ, van Staveren WA, Hofman Z, Sengers RC. Effects of naso-gastric tube feeding on the nutritional status of children with cancer. Eur J Clin Nutr 1998;52:494-500.

51. den Broeder E, Lippens RJ, van't Hof MA, Tolboom JJ, Sengers RC, van Staveren WA. Association between the change in nutritional status in response to tube feeding and the occurrence of infections in children with a solid tumor. Pediatr Hematol Oncol 2000;17:567-575.

52. Hall PD, Benko H, Hogan KR, Stuart RK. The influence of serum tumor necrosis factor-alpha and interleukin-6 concentrations on nonhematologic toxicity and hematologic recovery in patients with acute myelogenous leukemia. Exp Hematol 1995;23:1256-1260.

53. Sonis ST, Peterson RL, Edwards LJ, Lucey CA, Wang L, Mason L, Login G, Ymamkawa M, Moses G, Bouchard P, Hayes LL, Bedrosian C, et al. Defining mechanisms of action of interleukin-11 on the progression of radiation-induced oral mucositis in hamsters. Oral Oncol 2000;36:373-381.

54. van't Land B, Blijlevens NM, Marteijn J, Timal S, Donnelly JP, de Witte TJ, M'Rabet L. Role of curcumin and the inhibition of NF-kappaB in the onset of chemotherapy-induced mucosal barrier injury. Leukemia 2004;18:276-284.

55. Sonis ST. The biologic role for nuclear factor-kappaB in disease and its potential involvement in mucosal injury associated with anti-neoplastic therapy. Crit Rev Oral Biol Med 2002;13:380-389.

56. Logan RM, Gibson RJ, Sonis ST, Keefe DM. Nuclear factor-kappaB (NF-kappaB) and cyclooxygenase-2 (COX-2) expression in the oral mucosa following cancer chemotherapy. Oral Oncol 2006.

57. Bouma G, Strober W. The immunological and genetic basis of inflammatory bowel disease. Nat Rev Immunol 2003;3:521-533.

58. Bocker U, Yezerskyy O, Feick P, Manigold T, Panja A, Kalina U, Herweck F, Rossol S, Singer MV. Responsiveness of intestinal epithelial cell lines to lipopolysaccharide is correlated with Toll-like receptor 4 but not Toll-like receptor 2 or CD14 expression. Int J Colorectal Dis 2003;18:25-32.

59. Poltorak A, He X, Smirnova I, Liu MY, Van Huffel C, Du X, Birdwell D, Alejos E, Silva M, Galanos C, Freudenberg M, Ricciardi-Castagnoli P, et al. Defective LPS signaling in C3H/HeJ and C57BL/10ScCr mice: mutations in Tlr4 gene. Science 1998;282:2085-2088.

60. Sonis ST, Eilers JP, Epstein JB, LeVeque FG, Liggett WH, Jr., Mulagha MT, Peterson DE, Rose AH, Schubert MM, Spijkervet FK, Wittes JP. Validation of a new scoring system for the assessment of clinical trial research of oral mucositis induced by radiation or chemotherapy. Mucositis Study Group. Cancer 1999;85:2103-2113.

61. Tomlinson D, Judd P, Hendershot E, Maloney AM, Sung L. Measurement of oral mucositis in children: a review of the literature. Support Care Cancer 2007;15:1251-1258.

62. Sung L, Tomlinson GA, Greenberg ML, Koren G, Judd P, Ota S, Feldman BM. Validation of the oral mucositis assessment scale in pediatric cancer. Pediatr Blood Cancer 2006.

63. Gibson F, Cargill J, Allison J, Begent J, Cole S, Stone J, Lucas V. Establishing content validity of the oral assessment guide in children and young people. Eur J Cancer 2006;42:1817-1825.

64. Rapoport AP, Miller Watelet LF, Linder T, Eberly S, Raubertas RF, Lipp J, Duerst R, Abboud CN, Constine L, Andrews J, Etter MA, Spear L, et al. Analysis of factors that correlate with mucositis in recipients of autologous and allogeneic stem-cell transplants. J Clin Oncol 1999;17:2446-2453.

65. Hirotani Y, Yamamoto K, Ikeda K, Arakawa Y, Li J, Kitamura K, Kurokawa N, Tanaka K. Correlation between plasma glucagon-like peptide 2 levels and proliferative makers in small intestinal injury in rats induced by methotrexate administration. Biol Pharm Bull 2006;29:2327-2330.

66. Wilder-Smith P, Hammer-Wilson MJ, Zhang J, Wang Q, Osann K, Chen Z, Wigdor H, Schwartz J, Epstein J. In vivo imaging of oral mucositis in an animal model using optical coherence tomography and optical Doppler tomography. Clin Cancer Res 2007;13:2449-2454.

67. Blijlevens NM, Lutgens LC, Schattenberg AV, Donnelly JP. Citrulline: a potentially simple quantitative marker of intestinal epithelial damage following myeloablative therapy. Bone Marrow Transplant 2004;34:193-196.

68. Lutgens LC, Blijlevens NM, Deutz NE, Donnelly JP, Lambin P, de Pauw BE. Monitoring myeloablative therapy-induced small bowel toxicity by serum citrulline concentration: a comparison with sugar permeability tests. Cancer 2005;103:191-199.

69. Lutgens LC, Deutz N, Granzier-Peeters M, Beets-Tan R, De Ruysscher D, Gueulette J, Cleutjens J, Berger M, Wouters B, von Meyenfeldt M, Lambin P. Plasma citrulline concentration: a surrogate end point for radiation-induced mucosal atrophy of the small bowel. A feasibility study in 23 patients. Int J Radiat Oncol Biol Phys 2004;60:275-285.

70. Clarke JM, Pelton NC, Bajka BH, Howarth GS, Read LC, Butler RN. Use of the 13C-sucrose breath test to assess chemotherapy-induced small intestinal mucositis in the rat. Cancer Biol Ther 2006;5:34-38.

71. Tooley KL, Saxon BR, Webster J, Zacharakis B, McNeil Y, Davidson GP, Butler RN. A Novel Non-Invasive Biomarker for Assessment of Small Intestinal Mucositis in Children with Cancer Undergoing Chemotherapy. Cancer Biol Ther 2006;5.

72. Cheng KK, Leung SF, Thompson DR, Tai JW, Liang RH, Kan AS, Ying FW, Yeung RM. New measure of health-related quality of life for patients with oropharyngeal mucositis: development and preliminary psychometric evaluation. Cancer 2007;109:2590-2599.

73. Stiff PJ, Erder H, Bensinger WI, Emmanouilides C, Gentile T, Isitt J, Lu ZJ, Spielberger R. Reliability and validity of a patient self-administered daily questionnaire to assess impact of oral mucositis (OM) on pain and daily functioning in patients undergoing autologous hematopoietic stem cell transplantation (HSCT). Bone Marrow Transplant 2006;37:393-401.

74. von Bultzingslowen I, Brennan MT, Spijkervet FK, Logan R, Stringer A, Raber-Durlacher JE, Keefe D. Growth factors and cytokines in the prevention and treatment of oral and gastrointestinal mucositis. Support Care Cancer 2006;14:519-527.

75. Meropol NJ, Somer RA, Gutheil J, Pelley RJ, Modiano MR, Rowinsky EK, Rothenberg ML, Redding SW, Serdar CM, Yao B, Heard R, Rosen LS. Randomized phase I trial of recombinant human keratinocyte growth factor plus chemotherapy: potential role as mucosal protectant. J Clin Oncol 2003;21:1452-1458.

76. Elting LS, Shih YC, Stiff PJ, Bensinger W, Cantor SB, Cooksley C, Spielberger R, Emmanoulides C. Economic impact of palifermin on the costs of hospitalization for autologous hematopoietic stem-cell transplant: analysis of phase 3 trial results. Biol Blood Marrow Transplant 2007;13:806-813.

77. Horsley P, Bauer JD, Mazkowiack R, Gardner R, Bashford J. Palifermin improves severe mucositis, swallowing problems, nutrition impact symptoms, and length of stay in patients undergoing hematopoietic stem cell transplantation. Support Care Cancer 2007;15:105-109.

78. Nasilowska-Adamska B, Rzepecki P, Manko J, Czyz A, Markiewicz M, Federowicz I, Tomaszewska A, Piatkowska-Jakubas B, Wrzesien-Kus A, Bieniaszewska M, Duda D, Szydlo R, et al. The influence of palifermin (Kepivance) on oral mucositis and acute graft versus host disease in patients with hematological diseases undergoing hematopoietic stem cell transplant. Bone Marrow Transplant 2007.

79. Blazar BR, Weisdorf DJ, Defor T, Goldman A, Braun T, Silver S, Ferrara JL. Phase 1/2 randomized, placebo-control trial of palifermin to prevent graft-versus-host disease (GVHD) after allogeneic hematopoietic stem cell transplantation (HSCT). Blood 2006;108:3216-3222.

80. Rosen LS, Abdi E, Davis ID, Gutheil J, Schnell FM, Zalcberg J, Cesano A, Gayko U, Chen MG, Clarke S. Palifermin reduces the incidence of oral mucositis in patients with metastatic colorectal cancer treated with fluorouracil-based chemotherapy. J Clin Oncol 2006;24:5194-5200.

81. Kilic Y, Rajewski K, Dorr W. Effect of post-exposure administration of keratinocyte growth factor (Palifermin) on radiation effects in oral mucosa in mice. Radiat Environ Biophys 2007;46:13-19.

82. Lee SW, Jung KI, Kim YW, Jung HD, Kim HS, Hong JP. Effect of epidermal growth factor against radiotherapy-induced oral mucositis in rats. Int J Radiat Oncol Biol Phys 2007;67:1172-1178.

83. Potten CS, O'Shea JA, Farrell CL, Rex K, Booth C. The effects of repeated doses of keratinocyte growth factor on cell proliferation in the cellular hierarchy of the crypts of the murine small intestine. Cell Growth Differ 2001;12:265-275.

84. Zia-Amirhosseini P, Salfi M, Leese P, Yates W, Danilenko DM, Ring B, Cesano A, Sullivan JT. Pharmacokinetics, pharmacodynamics, and safety assessment of palifermin (rHuKGF) in healthy volunteers. Clin Pharmacol Ther 2006;79:558-569.

85. Farrell CL, Rex KL, Chen JN, Bready JV, DiPalma CR, Kaufman SA, Rattan A, Scully S, Lacey DL. The effects of keratinocyte growth factor in preclinical models of mucositis. Cell Prolif 2002;35 Suppl 1:78-85.

86. Farrell CL, Bready JV, Rex KL, Chen JN, DiPalma CR, Whitcomb KL, Yin S, Hill DC, Wiemann B, Starnes CO, Havill AM, Lu ZN, et al. Keratinocyte growth factor protects mice from chemotherapy and radiation-induced gastrointestinal injury and mortality. Cancer Res 1998;58:933-939.

87. Finch PW, Rubin JS. Keratinocyte growth factor/fibroblast growth factor 7, a homeostatic factor with therapeutic potential for epithelial protection and repair. Adv Cancer Res 2004;91:69-136.

88. Fernandez-Estivariz C, Gu LH, Gu L, Jonas CR, Wallace TM, Pascal RR, Devaney KL, Farrell CL, Jones DP, Podolsky DK, Ziegler TR. Trefoil peptide expression and goblet cell number in rat intestine: effects of KGF and fasting-refeeding. Am J Physiol Regul Integr Comp Physiol 2003;284:R564-573.

89. Mashimo H, Wu DC, Podolsky DK, Fishman MC. Impaired defense of intestinal mucosa in mice lacking intestinal trefoil factor. Science 1996;274:262-265.

90. Marchbank T, Cox HM, Goodlad RA, Giraud AS, Moss SF, Poulsom R, Wright NA, Jankowski J, Playford RJ. Effect of ectopic expression of rat trefoil factor family 3 (intestinal trefoil factor) in the jejunum of transgenic mice. J Biol Chem 2001;276:24088-24096.

91. Braun S, Hanselmann C, Gassmann MG, auf dem Keller U, Born-Berclaz C, Chan K, Kan YW, Werner S. Nrf2 transcription factor, a novel target of keratinocyte growth factor action which regulates gene expression and inflammation in the healing skin wound. Mol Cell Biol 2002;22:5492-5505.

92. Potten CS, Owen G, Hewitt D, Chadwick CA, Hendry H, Lord BI, Woolford LB. Stimulation and inhibition of proliferation in the small intestinal crypts of the mouse after in vivo administration of growth factors. Gut 1995;36:864-873.

93. Booth D, Haley JD, Bruskin AM, Potten CS. Transforming growth factor-B3 protects murine small intestinal crypt stem cells and animal survival after irradiation, possibly by reducing stem-cell cycling. Int J Cancer 2000;86:53-59.

94. Dignass A, Lynch-Devaney K, Kindon H, Thim L, Podolsky DK. Trefoil peptides promote epithelial migration through a transforming growth factor beta-independent pathway. J Clin Invest 1994;94:376-383.

95. Jono H, Shuto T, Xu H, Kai H, Lim DJ, Gum JR, Jr., Kim YS, Yamaoka S, Feng XH, Li JD. Transforming growth factor-beta -Smad signaling pathway cooperates with NF-kappa B to mediate nontypeable Haemophilus influenzae-induced MUC2 mucin transcription. J Biol Chem 2002;277:45547-45557.

96. Kitani A, Fuss IJ, Nakamura K, Schwartz OM, Usui T, Strober W. Treatment of experimental (Trinitrobenzene sulfonic acid) colitis by intranasal administration of transforming growth factor (TGF)-beta1 plasmid: TGF-beta1-mediated suppression of T helper cell type 1 response occurs by interleukin (IL)-10 induction and IL-12 receptor beta2 chain downregulation. J Exp Med 2000;192:41-52.

97. Schottelius AJ, Mayo MW, Sartor RB, Baldwin AS, Jr. Interleukin-10 signaling blocks inhibitor of kappaB kinase activity and nuclear factor kappaB DNA binding. J Biol Chem 1999;274:31868-31874.

98. Powrie F, Carlino J, Leach MW, Mauze S, Coffman RL. A critical role for transforming growth factor-beta but not interleukin 4 in the suppression of T helper type 1-mediated colitis by CD45RB(low) CD4+ T cells. J Exp Med 1996;183:2669-2674.

99. Asseman C, Mauze S, Leach MW, Coffman RL, Powrie F. An essential role for interleukin 10 in the function of regulatory T cells that inhibit intestinal inflammation. J Exp Med 1999;190:995-1004.

100. Ruiz PA, Shkoda A, Kim SC, Sartor RB, Haller D. IL-10 gene-deficient mice lack TGF-beta/Smad signaling and fail to inhibit proinflammatory gene expression in intestinal epithelial cells after the colonization with colitogenic Enterococcus faecalis. J Immunol 2005;174:2990-2999.

101. MacDonald TT, Monteleone G. IL-12 and Th1 immune responses in human Peyer's patches. Trends Immunol 2001;22:244-247.

102. Schwerbrock NM, Makkink MK, van der Sluis M, Buller HA, Einerhand AW, Sartor RB, Dekker J. Interleukin 10-deficient mice exhibit defective colonic Muc2 synthesis before and after induction of colitis by commensal bacteria. Inflamm Bowel Dis 2004;10:811-823.

103. Mattar AF, Teitelbaum DH, Drongowski RA, Yongyi F, Harmon CM, Coran AG. Probiotics up-regulate MUC-2 mucin gene expression in a Caco-2 cell-culture model. Pediatr Surg Int 2002;18:586-590.

104. Mack DR, Michail S, Wei S, McDougall L, Hollingsworth MA. Probiotics inhibit enteropathogenic E. coli adherence in vitro by inducing intestinal mucin gene expression. Am J Physiol 1999;276:G941-950.

105. Ruescher TJ, Sodeifi A, Scrivani SJ, Kaban LB, Sonis ST. The impact of mucositis on alpha-hemolytic streptococcal infection in patients undergoing autologous bone marrow transplantation for hematologic malignancies. Cancer 1998;82:2275-2281.

106. Gonzalez-Barca E, Fernandez-Sevilla A, Carratala J, Granena A, Gudiol F. Prospective study of 288 episodes of bacteremia in neutropenic cancer patients in a single institution. Eur J Clin Microbiol Infect Dis 1996;15:291-296.

107. Van Montfrans C, Hooijberg E, Rodriguez Pena MS, De Jong EC, Spits H, Te Velde AA, Van Deventer SJ. Generation of regulatory gut-homing human T lymphocytes using ex vivo interleukin 10 gene transfer. Gastroenterology 2002;123:1877-1888.

108. Steidler L, Hans W, Schotte L, Neirynck S, Obermeier F, Falk W, Fiers W, Remaut E. Treatment of murine colitis by Lactococcus lactis secreting interleukin-10. Science 2000;289:1352-1355.

109. Braat H, Rottiers P, Huyghebaart N, Zelinkova Z, Remaut E, Remon J, Van Deventer S, Neirynck S, Peppelenbosch M, Steidler L, Hommes D. Interleukin-10 producing *lactococcus lactis* for the treatment of Crohn's disease. Abstract Digestive Disease Week 2005, 685 2005.

110. Braat H, Rottiers P, Hommes DW, Huyghebaert N, Remaut E, Remon JP, van Deventer SJ, Neirynck S, Peppelenbosch MP, Steidler L. A phase I trial with transgenic bacteria expressing interleukin-10 in Crohn's disease. Clin Gastroenterol Hepatol 2006;4:754-759.

111. Chen Y, Kuchroo VK, Inobe J, Hafler DA, Weiner HL. Regulatory T cell clones induced by oral tolerance: suppression of autoimmune encephalomyelitis. Science 1994;265:1237-1240.

112. Riehl T, Cohn S, Tessner T, Schloemann S, Stenson WF. Lipopolysaccharide is radioprotective in the mouse intestine through a prostaglandin-mediated mechanism. Gastroenterology 2000;118:1106-1116.

113. Jijon H, Backer J, Diaz H, Yeung H, Thiel D, McKaigney C, De Simone C, Madsen K. DNA from probiotic bacteria modulates murine and human epithelial and immune function. Gastroenterology 2004;126:1358-1373.

114. Desreumaux P, Dubuquoy L, Nutten S, Peuchmaur M, Englaro W, Schoonjans K, Derijard B, Desvergne B, Wahli W, Chambon P, Leibowitz MD, Colombel JF, et al. Attenuation of colon inflammation through activators of the retinoid X receptor (RXR)/peroxisome proliferator-activated receptor gamma (PPARgamma) heterodimer. A basis for new therapeutic strategies. J Exp Med 2001;193:827-838.

115. Dubuquoy L, Bourdon C, Peuchmaur M, Leibowitz MD, Nutten S, Colombel JF, Auwerx J, Desreumaux P. [Peroxisome proliferator-activated receptor (PPAR) gamma: a new target for the treatment of inflammatory bowel disease]. Gastroenterol Clin Biol 2000;24:719-724.

116. Jiang C, Ting AT, Seed B. PPAR-gamma agonists inhibit production of monocyte inflammatory cytokines. Nature 1998;391:82-86.

117. Ricote M, Li AC, Willson TM, Kelly CJ, Glass CK. The peroxisome proliferator-activated receptor-gamma is a negative regulator of macrophage activation. Nature 1998;391:79-82.

118. Gelman L, Fruchart JC, Auwerx J. An update on the mechanisms of action of the peroxisome proliferator-activated receptors (PPARs) and their roles in inflammation and cancer. Cell Mol Life Sci 1999;55:932-943.

119. Kelly D, Campbell JI, King TP, Grant G, Jansson EA, Coutts AG, Pettersson S, Conway S. Commensal anaerobic gut bacteria attenuate inflammation by regulating nuclear-cytoplasmic shuttling of PPAR-gamma and RelA. Nat Immunol 2004;5:104-112.

120. Jobin C, Bradham CA, Russo MP, Juma B, Narula AS, Brenner DA, Sartor RB. Curcumin blocks cytokine-mediated NF-kappa B activation and proinflammatory gene expression by inhibiting inhibitory factor I-kappa B kinase activity. J Immunol 1999;163:3474-3483.

121. Karin M, Lin A. NF-kappaB at the crossroads of life and death. Nat Immunol 2002;3:221-227.

122. Gao Y, Lecker S, Post MJ, Hietaranta AJ, Li J, Volk R, Li M, Sato K, Saluja AK, Steer ML, Goldberg AL, Simons M. Inhibition of ubiquitin-proteasome pathway-mediated I kappa B alpha degradation by a naturally occurring antibacterial peptide. J Clin Invest 2000;106:439-448.

123. Loury D, Embree JR, Steinberg DA, Sonis ST, Fiddes JC. Effect of local application of the antimicrobial peptide IB-367 on the incidence and severity of oral mucositis in hamsters. Oral Surg Oral Med Oral Pathol Oral Radiol Endod 1999;87:544-551.

124. Donnelly JP, Bellm LA, Epstein JB, Sonis ST, Symonds RP. Antimicrobial therapy to prevent or treat oral mucositis. Lancet Infect Dis 2003;3:405-412.

125. van de Wetering MD, de Witte MA, Kremer LC, Offringa M, Scholten RJ, Caron HN. Efficacy of oral prophylactic antibiotics in neutropenic afebrile oncology patients: a systematic review of randomised controlled trials. Eur J Cancer 2005;41:1372-1382.

10

SUMMARY
SAMENVATTING

SUMMARY

Part 1 focuses primarily on the pathophysiology of mucositis, in order to gain more insight different experimental mouse models were used.

Chapter 2 describes mucositis induced by high dose doxorubicin (DOX)-treatment. DOX is a frequently used cytostatic drug in childhood cancer, often causing severe mucositis. DOX-induced mucositis closely resembles the characteristics of previously studied methotrexate (MTX)-induced mucositis. Both drugs induce severe damage to the epithelial morphology, characterized by severe villus atrophy, changes in epithelial proliferation and loss of epithelial differentiation. We did not expect these similarities in morphological damage as DOX attacks epithelial cells much closer to the stem cell than MTX does. DOX was suspected to have a more severe influence on intestinal homeostasis in comparison to MTX. The resemblance suggests a general mechanism in intestinal damage and repair. The time-line however, in which both drugs induced their damage to the intestine was different. DOX-treatment leads to immediate hyper-proliferation (day 1 and 2) with subsequent inhibition of proliferation during severe morphological damage (day 3). MTX causes proliferation inhibition within one day, followed by a period of hyper-proliferation during severe intestinal damage. Furthermore, we studied changes in epithelial-mesenchymal cross talk during DOX-induced mucositis. The expression of the intestinal morphogene and TCF4, the main Wnt pathway transcription factor in the intestinal epithelium were followed by immunohistochemistry during the different stages of DOX-induced mucositis. BMP4- and TCF4 expression appeared to be linked, shown by the fact that BMP signaling seem to suppress Wnt signaling and visa versa during mucositis development and regeneration. This suggests a balance between epithelial proliferation and subsequent intestinal differentiation.

Chapter 3 The objective of this study was to investigate the expression of the small intestinal transcription factors HNF-1α, Cdx2, GATA-4 in an experimental model of MTX-induced intestinal damage, and to correlate these alterations with histological damage, epithelial proliferation and differentiation. HNF-1α, Cdx2 and GATA-4 are critical transcription factors in epithelial differentiation, and in combination they act as promoting factors of the sucrase-isomaltase (SI) gene, an enterocyte-specific differentiation marker which is distinctly down regulated after MTX-treatment. Intestinal damage was most severe at day 3 and was associated with decreased expression of the transcriptional factors HNF-1α, Cdx2 and GATA-4, which correlated well with decreased expression of SI, and seemed inversely correlated with enhanced proliferation of epithelial crypt cells. During severe damage, the epithelium was preferentially concerned with proliferation rather than differentiation, most likely in order to restore the small intestinal barrier function rather than maintaining its absorptive function.

In **Chapter 4** we show that there were no major differences found in intestinal pathology or protein expression during MTX-induced mucositis in $Muc2^{+/+}$ mice in comparison to

MTX-induced mucositis in Muc2$^{-/-}$ mice. Mucositis regeneration however, could not be assessed in the absence of Muc2 as almost all mice died spontaneously 1 day prior to sacrifice for evaluation. Surprisingly, however, the intestine of the Muc2 deficient mice evaluated just a few days after MTX-treatment showed already increased regeneration compared to the wild type mice. In addressing this question it became clear that the cytokine production by the mucosal immune system of Muc2 deficient mice was different compared to wild type littermates. Both the pro-inflammatory cytokine TNF-α as the anti-inflammatory cytokine Il-10 was increased in naïve Muc2 deficient mice, indicating that Muc2 deficiency leads to induction of an inflammatory response. This suggests that MTX induced damage in the Muc2$^{-/-}$ mice may be tempered by triggering the immune system to release IL-10, an anti-inflammatory cytokine, prior to MTX-treatment.

Chapter 5 MTX is associated with severe damage of the intestinal epithelium. As a result, the mucosal immune cells become increasingly exposed to a vast amount of microbial stimuli. In this study we aimed at determining if and to what extent these cells are still functional during MTX treatment. Furthermore, we assessed whether activation of the mucosal immune system would play a role in the pathogenesis of mucositis.

The fact that the adaptive immune system contributes to mucositis was established by showing that lamina propria lymphocytes that were derived from MTX-treated mice responded by an enhanced production of various cytokines to *ex vivo* polyclonal (anti-CD3ε and anti-CD28 mAb)stimulation. Next, *in vitro* experiments revealed that macrophages, either a cell-line or cells isolated from the murine peritoneal cavity, were not affected by MTX in the capacity to produce TNF-α and IL-10 upon lipopolysaccharide (LPS) exposure. Moreover, *in vivo* experiments showed that peritoneal macrophages isolated from MTX treated mice produced more IL-10 and TNF-α upon LPS stimulation, compared to cells derived from control mice. These data indicate persistence of both innate and adaptive immune responses in this model. The clinical relevance of these findings was further established by the fact that LPS exposure prior to MTX treatment aggravated the course of mucositis. Furthermore, LPS responsive mice recovered more slowly compared to LPS unresponsive mice during MTX induced intestinal damage. Finally, we found an increase in weight loss and intestinal damage upon MTX treatment in IL-10 deficient mice in comparison to wild type (WT) controls, which suggests a protective role for IL-10 in mucositis.

Part 2 focuses on intestinal metabolism during mucositis and mucositis prophylaxis in childhood cancer patients.

In **Chapter 6** we validate a new method for collecting breath samples that simplifies the collection of breath samples in young children in order to use this method in studies described in chapter 7. Stable isotope tracers are used in clinical studies to measure (intestinal) metabolism of various substrates. Nowadays, the oxidation of [^{13}C] labeled substrates to $^{13}CO_2$ and the measurement of the appearance of excess $^{13}CO_2$ in expiratory

air is a common method. The collection of respiratory CO_2, occurs via trapping of CO_2 in sodium hydroxide (trapping method) sometimes in conjunction with indirect calorimetry. The aim of the present study was to determine the accuracy of direct nasal-pharyngeal sampling method for the collection of breath samples in preterm infants compared with the currently used trapping method. Seven pre-term infants were studied while receiving full enteral feeding. A primed constant 3-h intragastric infusion of [^{13}C] bicarbonate was given and breath samples were collected by means of direct nasal-pharyngeal sampling and by a sodium hydroxide trap simultaneously. Breath CO_2 isotopic enrichments rose rapidly to reach a plateau by 120 min with < 5% variation of plateau in both methods. $^{13}CO_2$ breath isotopic enrichments obtained by the direct nasal-pharyngeal sampling method correlated highly with the trapping method, showing that direct nasal-pharyngeal sampling for the collection of breath samples is as accurate as the trapping method.

Chapter 7 The aim of this study was to evaluate systemic availability of dietary amino acids (leucine) during chemotherapy-induced mucositis. We studied eight childhood cancer patients (age 1.5 to 16 years) on two days, i.e. the day before chemotherapy and 3-5 days after. Chemotherapy-induced oral mucositis and diarrhea were scored on a WHO toxicity scale. Stable isotope tracers were used to measure first-pass splanchnic leucine uptake and whole-body leucine kinetics. Patients showed increased mucositis and/or diarrhea toxicity scores after chemotherapy. Systemic availability of enterally administered leucine was not significantly affected by chemotherapy. Interestingly however was that most of the children were already catabolic prior to start of a new cycle of chemotherapy.

Therefore, all efforts should be directed at initiating enteral feeding even before start of chemotherapy in order to reduce catabolic state. Our data imply that this might be accomplished best by hydrolyzed formula.

In **Chapter 8** the efficacy and feasibility of a TGF-β_2-enriched feeding for preventing oral and gastro-intestinal mucositis in childhood cancer patients were studied. The study was designed as a 2-period crossover, randomized, double-blinded, placebo controlled trial. Patients who had a high risk for developing mucositis and who would receive two comparable cycles of chemotherapy were eligible to the study. During one cycle of chemotherapy TGF-β_2-enriched feeding was administered; during the other a 'placebo' (not enriched) feeding was used. WHO toxicity scales of diarrhea, oral mucositis, fever, anal lesions and nausea/vomiting were scored daily. In addition, the incidence of occurrence of blood cultures, antibiotic therapy and interventions or diagnostics related to mucositis were measured. The feasibility of the study was good: 83% of the patients completed two cycles and 86% of the study feeding was consumed. Administration of TGF-β_2 was safe, as serum TGF-β_2 did not increase and renal and liver function were not affected. The degree of toxicity, scored during the whole observation period and the number of days with WHO 3/4 toxicity did not significantly differ between cycles with

TGF-β_2 enriched and normal feeding. These studies do not provide evidence that TGF- decreases the incidence or degree of mucositis induced by combination therapy in childhood cancer-patients.

In **Part 3** all studies presented in this thesis are summarized, and new insights for future studies are discussed.

SAMENVATTING

Wat is mucositis?

Mucositis is schade aan de slijmvliezen van het spijsverteringskanaal, veroorzaakt door de behandeling van kanker. Het is een van de meest voorkomende en meest ernstige bijwerkingen van de behandeling met chemotherapie. Chemotherapie werkt volgens het principe dat de medicatie een verstorende invloed heeft op de sneldelende cellen in het lichaam. Omdat tumorcellen zich zeer snel delen, ondervinden zij schade van de behandeling met chemotherapie. Groot nadeel is dat ook andere sneldelende cellen in het lichaam erdoor beschadigd kunnen raken. Wanneer deze schade optreedt aan de slijmvliezen van het spijsverteringskanaal, is er sprake van mucositis.

Waarom gaat dit proefschrift over mucositis?

Mucositis wordt vaak door de patiënt ervaren als de ernstigste bijwerking van behandeling met chemotherapie. De schade aan de slijmvliezen veroorzaakt pijn, misselijkheid, infecties, diarree en ook vaak gewichtsverlies. Bovendien moet bij een patiënt die is behandeld met een dosis chemotherapie, de mucositis eerst hersteld zijn voordat een volgende dosis medicatie kan worden toegediend. Is de mucositis nog niet hersteld, dan moet de vervolgbehandeling worden uitgesteld. Dit betekent feitelijk dat de tumor niet optimaal kan worden behandeld, waardoor de genezingskansen van de patiënt verminderen. De noodzaak van het voorkomen van mucositis is daarmee evident. Ondanks dat er steeds meer onderzoek wordt gedaan, is er nog geen goede manier gevonden om mucositis te voorkomen.

Dit proefschrift gaat specifiek in op schade aan de dunnedarmslijmvliezen bij kinderen met kanker. Het meeste wetenschappelijk onderzoek naar mucositis concentreert zich op schade aan de mondslijmvliezen bij volwassenen. Minder onderzoek wordt gedaan naar schade aan de slijmvliezen van het maagdarmkanaal (gastro-intestinale mucositis), wat vooral bij de behandeling van kinderkanker een veelvoorkomende complicatie is.

De werking van het darmslijmvlies

De twee belangrijkste functies van de darm zijn enerzijds het verteren en absorberen van voedingsstoffen, en anderzijds het beschermen van het lichaam tegen allerlei vreemde stoffen. Dat proces vindt plaats aan de binnenzijde van de darm, die bestaat uit slijmvlies dat is bekleed met een laagje epitheel. Het slijmvlies aan de binnenzijde van de dunne darm (zie afbeelding) bestaat uit vingervormige uitstulpingen, die villi worden genoemd. Epitheelcellen in de darm hebben een specifieke rol in splitsen van en transporteren van koolhydraten, wat essentieel is voor het opnemen van voedsel door het lichaam. De enzymen en transporters die hiervoor nodig zijn, zitten op de buitenzijde van de epitheelcellen. Bovenop het epitheel bevindt zich nog een slijmlaag, die wordt geproduceerd vanuit slijmbekercellen die zich bevinden in het epitheel. Onder het epitheel bevindt zich het mesenchym, het steunweefsel van de darm, waarin ook het immuunsysteem van de darm huist. Samen met de slijmlaag heeft het immuunsysteem

een belangrijke rol in het beschermen van de darm en het lichaam tegen vreemde stoffen. Onderin de vingervormige uitstulpingen van het slijmvlies bevinden zich de crypten (holten) van waaruit de stamcellen zich vermenigvuldigen (proliferatie). De vermenigvuldigde cellen schuiven vervolgens omhoog de villus op, waar ze zich specifieker doorontwikkelen (differentiatie).

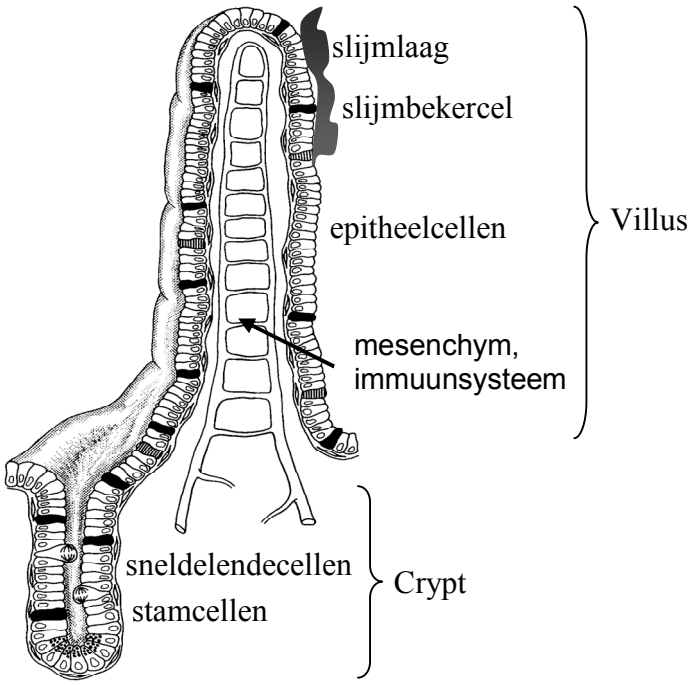

Schematische doorsnede van de dunnedarm

Symptomen van mucositis

Mucositis is vooral te herkennen aan roodheid en wondjes in de slijmvliezen van de mond en de anus. Hoe vaak gastro-intestinale mucositis voorkomt, is moeilijk te bepalen omdat dat minder zichtbaar is. Wel is aannemelijk dat patiënten met mucositis in de mond en anus, ook mucositis in het maagdarmkanaal hebben. Dat is vaak af te leiden uit symptomen zoals buikpijn en diaree. In welke mate patiënten mucositis krijgen, hangt nauw samen met de dosis en de combinatie van medicijnen die wordt gegeven. Bekend is dat circa tweederde van alle kinderen die chemotherapie krijgt, mucositis ontwikkelt in het mondslijmvlies. Hoe vaak gastro-intestinale mucositis bij kinderen voorkomt, is moeilijker te zeggen; eerdere onderzoeken onder kinderen rapporteren een incidentie tussen 0 en 50 procent.

Dit proefschrift bestaat uit drie delen. In **deel 1** van dit proefschrift wordt beschreven hoe mucositis ontstaat en welke factoren daarop mogelijk van invloed zijn. Hierbij is gebruik gemaakt van een onderzoeksmodel waarbij mucositis is veroorzaakt bij proefdieren (muizen) door toediening van methotrexate (MTX) en doxorubicine (DOX), twee veelgebruikte middelen bij de behandeling van kinderkanker.

Deel 2 van dit proefschrift beschrijft het onderzoek naar de effectiviteit van een mogelijke profylaxe, ter voorkoming van mucositis, bij een groep kinderen met kanker. Ook is in een groep kinderen gekeken naar mogelijke verschillen in de stofwisseling voor en na de behandeling met chemotherapie gedurende de aanwezigheid van mucositis.

In **deel 3** worden de verschillende hoofdstukken samengevat en bediscussieerd.

De opbouw van deel 1

In **hoofdstuk 2** is gekeken of er verschillen zijn tussen mucositis die is veroorzaakt door behandeling met MTX danwel DOX. Beide medicijnen hebben een bepaald aangrijpingspunt, waarbij de celdeling in de crypt wordt verstoord. De aanname was dat mucositis veroorzaakt door DOX een ernstiger vorm van celschade teweeg zou brengen dan MTX, omdat het aangrijpingspunt van DOX in de crypt dichter bij de stamcellen ligt dan bij MTX het geval is. Zowel DOX als MTX gaven echter dezelfde soort schade te zien, die op de derde dag van behandeling bij beide het grootst was.

Deze schade werd gekenmerkt door het kapot gaan van de villi, waarbij de overgebleven epitheelcellen hun vorm en functie verloren, daarnaast ging ook een deel van de crypten verloren. Verschil tussen beide medicijnen was er echter in de invloed van de medicatie op de proliferatie en differentiatie van de cellen in de loop van de tijd. MTX liet gedurende ernstige schade (op dag 3) een verhoogde proliferatie zien en een verlaagde differentiatie, terwijl DOX het tegenovergestelde liet zien gedurende ernstige schade (verlaagde proliferatie en verhoogde differentiatie). Beide medicijnen veroorzaken dus een zelfde soort mucositis; er ontstaat niet een ander soort mucositis bij een ander soort chemotherapie. Mogelijk is er sprake van een algemene reactie van de darm op darmschade en –herstel.

In dit onderzoek is verder gekeken naar de uitwisseling van signalen tussen cellen in het epitheel en cellen in het mesenchym. Normaal gesproken zorgen zulke signalen ervoor dat de opbouw en de functie van de crypten en villi bewaard blijft. Uit andere studies was gebleken dat mucositis niet alleen wordt veroorzaakt door schade aan de sneldelende epitheelcellen, maar dat ook verschillende cellen in het mesenchym daar een rol in spelen. Om dat nader te onderzoeken, zijn twee signaalpaden bestudeerd, die de namen BMP4- en Wnt-signalering dragen. Als het evenwicht tussen deze twee signaalpaden meer naar Bmp-4 ligt zullen de epitheel cellen zich meer doorontwikkelen (differentiatie), ligt de nadruk op Wnt-signalering dan is er meer vermenigvuldiging (proliferatie). Gedurende DOX-veroorzaakte mucositis lijkt het zo te zijn dat de twee signaalpaden zo worden beïnvloed dat een balans (homeostase) wordt behouden tussen vermenigvuldigen en doorontwikkelen van de epitheelcellen. Hierdoor kan de darm herstellen van mucositis.

In **hoofdstuk 3** wordt beschreven hoe een aantal darmspecifieke transcriptiefactoren zich gedraagt tijdens MTX-veroorzaakte mucositis. Transcriptiefactoren zijn eiwitten die

het proces kunnen starten van het vertalen van het erfelijk materiaal (op het DNA) naar de productie van eiwit. Transcriptiefactoren staan onder invloed van andere stoffen die in de cel aanwezig zijn en kunnen hierdoor wel of niet actief zijn. Hierdoor zijn bepaalde eiwitten al dan niet aanwezig.

Uit eerder onderzoek weten we dat verschillende functies van de darm, uitgevoerd door verschillende eiwitten, op bepaalde manier worden beïnvloed door MTX-mucositis. Sucrase-isomaltase (SI), verantwoordelijk voor een deel van de koolhydraatsplitsing, gaat kortdurend verloren terwijl Muc2, een belangrijk onderdeel van de slijmlaag, juist behouden blijft (zie verder hoofdstuk 4). Dit betekent dat SI een belangrijke differentiatie-marker is voor het darmepitheel tijdens schade. Als kan worden aangetoond dat SI aanwezig is, dan betekent dit dat darmcellen goed ontwikkeld zijn. Bij ernstige mucositis daarentegen, is er geen SI op het epitheel te vinden.

Drie belangrijke transcriptiefactoren in de darm zijn Cdx2, GATA-4 en HNF-1a. Zij hebben een belangrijke rol in de darmontwikkeling en zijn onafhankelijk van elkaar transcriptiefactor voor verschillende eiwitten in de darm. Bij elkaar vormen zij echter de transcriptiefactor voor SI.

Bij dit onderzoek is gebleken dat gedurende ernstige mucositis deze drie transcriptiefactoren verlaagd aanwezig zijn, terwijl de differentiatie is verlaagd en SI helemaal afwezigheid is. Dit wijst in de richting dat de transcriptiefactoren een rol spelen in verminderde differentiatie van cellen tijdens darmschade. Het evenwicht in de darm kan worden verschoven ten gunste van de proliferatie en daarmee kan het herstel van de darm bevorderd worden. Dit betekent dat de transcriptiefactoren een mogelijk aanknopingspunt zijn in het voorkomen van mucositis.

In **hoofdstuk 4** is specifieker gekeken naar de rol van de mucus-laag, de slijmlaag die op het epitheel ligt. De belangrijkste component van deze slijmlaag is het eiwit Muc2. Dit eiwit speelt een belangrijk rol bij het beschermen van de darm. Uit eerder onderzoek is bekend dat er gedurende mucositis meer Muc2 aanwezig is in de darm. De aanname dat Muc2 bij mucositis ook een beschermende rol zou kunnen spelen, is dan ook gerechtvaardigd. Om dit te onderzoeken is een vergelijkende studie uitgevoerd tussen proefdieren met en zonder Muc2 in de slijmlaag in de darm. Verrassend genoeg bleken de proefdieren zonder Muc2 niet gevoeliger te zijn voor de ontwikkeling van mucositis, dan de proefdieren met Muc2. Nader onderzoek wees uit de proefdieren zonder Muc2 zich daaraan bleken te hebben aangepast door de verhoogde aanmaak van de interleukine-10 (IL-10), een ontstekingsremmende afweerstof.

Uit dit onderzoek blijkt nog niet welke rol Muc2 heeft tijdens mucositis. Wel lijkt het erop dat het immuunsysteem een toegenomen taak heeft in het beschermen van de darm in de afwezigheid van Muc2. Daarnaast is dit een aanwijzing dat IL-10 de darm beschermt tijdens tegen mucositis.

In **hoofdstuk 5** wordt het immuunsysteem van de darm onderzocht tijdens mucositis. Onze eerste vraag is of het immuunsysteem nog werkt na chemotherapie, ondanks dat veel cellen in de darm beschadigd zijn. De tweede vraag is of het immuunsysteem een rol heeft in de ontwikkeling van mucositis? Uit experimenten met proefdieren blijkt dat zowel het aangeboren (innate) immuunsysteem als het op maat gemaakte (adaptive) immuunsysteem, nog kan functioneren. Beide systemen blijken te reageren op (onderdelen van) bacteriën die door de beschadigde darmwand in aanraking komen met de immuuncellen in het mesenchym-weefsel dat eronder ligt. Als reactie hierop maken de immuuncellen zowel ontstekingsactiverende stoffen aan (het pro-inflammatoire TNF-α) als ontstekingsremmende factoren (het anti-inflammtoire IL-10). Uit eerdere studies is bekend dat ontstekingsactiverende stoffen (TNF-α) een grote rol spelen bij mucositis. In een vergelijkende studie met proefdieren met IL-10 en zonder IL-10 blijkt de stof IL-10 de ernst van de mucositis te verminderen. Dit betekent dat IL-10 een aanknopingspunt zou kunnen zijn voor het voorkomen of verminderen van mucositis.

De opbouw van deel 2

In **hoofdstuk 6** wordt een onderzoek beschreven naar een eenvoudiger methode om de hoeveelheid koolstofdioxide (CO_2) te meten in de uitademinglucht bij jonge kinderen. Met de meting van de hoeveelheid CO_2 kan worden berekend hoe bij de patiënt de stofwisseling is van bepaalde eiwitten of bouwstenen van eiwitten (aminozuren). Oudere kinderen kunnen voor het opvangen van CO_2 door een rietje in een buisje blazen. Bij jonge kinderen die nog niet kunnen blazen, is voor deze studie een dun slangetje in de neus geplaatst waarmee de uitademinglucht wordt opgevangen. Gebleken is dat beide methoden voor het opvangen van CO_2 even goed werken.

Hoofdstuk 7 beschrijft een onderzoek naar de opname van het aminozuur leucine door de darmen van kinderen met mucositis. Aminozuren zijn de bouwstenen waaruit eiwitten zijn opgebouwd, en eiwitten zijn een belangrijk onderdeel van onze dagelijkse voeding. Het aminozuur leucine kun je alleen door middel van de voeding binnenkrijgen. Ook kan het lichaam zelf leucine vrijmaken door eiwitten af te breken waar bouwstenen leucine in zitten. Eerder onderzoek laat zien dat de darm een groot deel van de leucine uit de voeding opneemt. Een deel daarvan geeft de darm door aan het lichaam voor de stofwisseling, maar een groot deel van de opgenomen leucine gebruikt de darm zelf om in zijn eigen eiwitopbouw te voorzien. Voorafgaand aan dit onderzoek werd enerzijds gedacht dat de darm tijdens mucositis meer leucine voor zichzelf zou houden dan normaal om zichzelf weer op te bouwen. Anderzijds werd het ook mogelijk geacht dat de darm tijdens mucositis helemaal geen leucine zou kunnen opnemen, door ernstige beschadiging van het epitheel. Voor dit onderzoek is een groep kinderen bestudeerd, voor en na chemotherapie. Om de leucine in het lichaam te kunnen volgen, werd de leucine vooraf voorzien van een ‘vlaggetje’. Ontdekt werd dat de darm in beide perioden evenveel leucine opnam en dat ook de verwerking van leucine door het lichaam gelijk was. Opvallend was wel dat vrijwel alle kinderen al voor de start van de chemotherapie veel te weinig leucine binnenkregen via de voeding, waardoor ze veel eiwitten afbraken

om leucine in het lichaam te krijgen. Dit betekent dat kinderen met kanker al voor start van de chemotherapie ondervoed zijn.

Hoofdstuk 8 ten slotte beschrijft een onderzoek onder kinderen met kanker, naar een speciale voeding verrijkt met TGF-β, met als doel mucositis in de mond en het maagdarmkanaal te verminderen of te voorkomen. Eerder onderzoek liet zien dat TGF-β de sneldelende cellen in de crypt (zoals boven beschreven) kan beschermen door ze te stoppen in hun deling, vlak voordat de chemotherapie wordt gegeven. Op deze manier worden deze cellen ongevoelig voor de chemotherapie waardoor geen mucositis zou hoeven ontstaan. Dit bleek goed te werken in proefdieren, maar bij de kinderen in onze studie had TGF-β geen effect op het voorkomen van of de ernst van de mucositis.

Conclusies van dit onderzoek

Concluderend kan worden gezegd dat dit onderzoek meer inzicht geeft in het ontstaan van mucositis en de verschillende factoren die daarop van invloed zijn. Ook is - nog meer dan voorheen - duidelijk geworden dat mucositis niet alleen maar ontstaat als gevolg van beschadiging van de sneldelende cellen in de crypt; allerlei cellen door de gehele darm spelen hierbij een rol. Daarom zal een effectief medicijn ter voorkoming van mucositis moeten ingrijpen op verschillende cellen van de darm.

Voor verder onderzoek worden enkele aanbevelingen gedaan. Om erachter te komen hoe de deling en het verder ontwikkelen van de darmcellen precies geregeld worden, moeten nieuwe (dier)modellen worden bedacht om nader onderzoek te kunnen doen naar de signalen tussen het epitheel en het mesenchym en de signalen van de transcriptiefactoren tijdens mucositis. Daarnaast zal de rol van Muc2 bestudeerd moeten worden in een model waarin Muc2 bijvoorbeeld kortdurend verhoogd wordt of juist verlaagd word net voor chemotherapie, zodat de darm zich niet kan aanpassen aan de nieuwe situatie. Vervolgens zal het effect van verhoogde aanwezigheid van IL-10 verder onderzocht moeten worden, eventueel in combinatie met stoffen die de ontstekingsactiverende stoffen remmen.

In de kliniek moeten we proberen de kinderen in een betere voedingstoestand te krijgen al voor start van de chemotherapie. Daarnaast moet voor nieuwe studies naar middelen ter voorkoming van mucositis een beter systeem ontwikkeld worden om de ernst van gastro-intestinale mucositis te beoordelen. Ook zullen we verder kijken naar de stofwisseling van de darm tijdens mucositis door aminozuren en kleine eiwitten te labellen met vlaggetjes en zo inzicht te krijgen in de meest optimale voeding voor kinderen met kanker tijdens hun behandeling. Recente studies laten een goed beschermend effect van de stof KGF zien bij volwassen patiënten. Het effect van dit middel bij kinderen moet echter nog blijken.

Op grond van alle beschreven ontwikkelingen en onderzoek, kan mogelijk in de toekomst een optimaal middel worden samengesteld ter voorkoming van mucositis bij kinderen met kanker die behandeld worden met chemotherapie.

DANKWOORD

DANKWOORD

Kinderen - ouders.

Promotoren - copromotor - vertrekkende - nieuwe - extra begeleiders - enthousiast - rode draad - rots in de branding - op de achtergrond - goed commentaar - nieuw onderzoek - meer proeven - fantastisch!

Research team - CRF - GTST - movie with the girls.

Potjes voeding - inclusie - 2 Midden - 2 Zuid - oncologen - J & J.

Bubbelen met Sophie.

Laboratorium Kindergeneeskunde - specieel - isotopen - Hannover - Tokyo - NY.

Hulp in EDC.

Zitplek - spiegel - vrijdagmiddag - paters and maters laboratoria - kerstfeest.

Samenwerken - co-auteur - studenten - thee/koffie/lunch? - fenotypering - MTX - MTT - muizen - kleuringen - zeefjes - zo nauwkeurig - niet te remmen - statistiek - boys - Parijs - San Fransisco.

Paranimf - 3 musketiers - Rome - Besse-sûr-Issole.

Weekend - pruiken - Sint & Kerst - promoties - collega's - SKZ - Zuider.

Commissie - secure lay out - old fashion kaft - NL communicatie.

Supportive care - huisgenoot - bubbelbad - Peru - Leiden! - jongetjes & meisjes - shoe-shopping - wake up call - prachtig - schoon - huis - helpdesk.

Onwijs - bedankt.

Liefs

CURRICULUM VITAE

CURRICULUM VITAE

Barbara de Koning werd geboren op 1 mei 1973 te Delft. Na het behalen van haar VWO-diploma aan het St. Maartens College te Voorburg startte zij met de studie Geneeskunde aan de Rijksuniversiteit Leiden. Tijdens haar studie participeerde zij in een migraineonderzoek op de afdeling Neurologie van het LUMC (Leids Universitair Medisch Centrum). Aansluitend aan haar afstudeeronderzoek bij de afdeling Klinische Oncologie met als onderwerp 'Door chemotherapie geïnduceerde mucositis' volgde zij haar co-schappen, afgesloten met een keuze co-schap Kinderoncologie in het Erasmus MC-Sophia, het vroegere Sophia Kinderziekenhuis. Na het behalen van haar artsenexamen in juni 1999 werkte zij mee aan de ontwikkeling van een kinderoncologische database bij de afdeling Oncologie/Hematologie in het Erasmus MC-Sophia. In januari 2000 startte zij als artsonderzoeker een promotieonderzoek 'Door chemotherapie geïnduceerde mucositis", met als resultaat dit proefschrift. Deze studies voerde zij uit op de Medium care-afdeling van het Erasmus MC-Sophia en het laboratorium Kindergeneeskunde aldaar, onder begeleiding van prof. dr. R. Pieters, prof. dr. H.A. Büller, en dr. A.C.W. Einerhand. Gedurende de periode 2002 - 2004 was zij lid van de Medisch Ethische Toetsingscommissie. In juli 2005 startte zij als assistent (niet in opleiding) Kindergeneeskunde en vanaf januari 2006 is zij in opleiding tot kinderarts in het Erasmus MC-Sophia (opleiders, prof. dr. A.J. van der Heijden en dr. M. de Hoog).